

Universidade Federal de Minas Gerais
Instituto de Ciências Biológicas
Pós-Graduação em Bioquímica e Imunologia

Steve Peigneur

**Where spiders and cone snails meet – development of
novel sodium channel probes.**

Belo Horizonte – MG

Março / 2019

Universidade Federal de Minas Gerais
Instituto de Ciências Biológicas
Pós-Graduação em Bioquímica e Imunologia

Steve Peigneur

**Where spiders and cone snails meet – development of
novel sodium channel probes.**

Relatório Parcial apresentado à Universidade Federal de Minas Gerais-UFMG como parte das exigências do Programa de Pós-Graduação em Bioquímica e Imunologia para obtenção do título de doutor.

Orientador: Prof. Dr. Maria Elena de Lima
Coorientador: Prof. Dr. Jan Tytgat

Belo Horizonte – MG

Março/ 2019



Universidade Federal de Minas Gerais
 Curso de Pós-Graduação em Bioquímica e Imunologia ICB/UFMG
 Av. Antônio Carlos, 6627 – Pampulha
 31270-901 – Belo Horizonte – MG
 e-mail: pg-biq@icb.ufmg.br (31)3409-2615



ATA DA DEFESA DA TESE DE DOUTORADO DE STEVE PEIGNEUR. Aos vinte e um dias do mês de março de 2019 às 14:00 horas, reuniu-se no Instituto de Ciências Biológicas da Universidade Federal de Minas Gerais, a Comissão Examinadora da tese de Doutorado, indicada *ad referendum* do Colegiado do Curso, para julgar, em exame final, o trabalho intitulado ""Where spiders and cone snails meet - development of novel sodium channel probes"", requisito final para a obtenção do grau de Doutor em Ciências: Bioquímica. Abrindo a sessão, a Presidente da Comissão, Profa. Maria Elena de Lima Perez Garcia, da Universidade Federal de Minas Gerais, após dar a conhecer aos presentes o teor das Normas Regulamentares do Trabalho Final, passou a palavra ao candidato para apresentação de seu trabalho. Seguiu-se a arguição pelos examinadores, com a respectiva defesa do candidato. Logo após a Comissão se reuniu, sem a presença do candidato e do público, para julgamento e expedição do resultado final. Foram atribuídas as seguintes indicações: Dra. Russolina Benedeta Zingali (Universidade Federal do Rio de Janeiro), aprovado; Dr. Wamberto Antônio Varanda (Faculdade de Medicina de Ribeirão Preto), aprovado; Dr. Lucas Bleicher (Universidade Federal de Minas Gerais), aprovado; Dr. Paulo Sérgio Lacerda Beirão (Universidade Federal de Minas Gerais), aprovado; Dr. Jan Tytgat - Coorientador (The Katholieke Universiteit Leuven - Belgium), aprovado; Dr. Maria Elena de Lima Perez Garcia - Orientadora (Universidade Federal de Minas Gerais), aprovado. Pelas indicações o candidato foi considerado:

APROVADO
 REPROVADO

O resultado final foi comunicado publicamente ao candidato pela Presidente da Comissão. Nada mais havendo a tratar, a Presidente da Comissão encerrou a reunião e lavrou o presente Ata que será assinada por todos os membros participantes da Comissão Examinadora. Belo Horizonte, 21 de março de 2019.

R. B. Zingali

Dra. Russolina Benedeta Zingali (Universidade Federal do Rio de Janeiro)

Dr. Wamberto Antônio Varanda (Faculdade de Medicina de Ribeirão Preto)

Lucas Bleicher

Dr. Lucas Bleicher (UFMG)

Dr. Paulo Sérgio Lacerda Beirão (UFMG)

Dr. Jan Tytgat - Coorientador (The Katholieke Universiteit Leuven - Belgium)

Dr. Maria Elena de Lima Perez Garcia - Orientadora (UFMG)

Leda Quercia Vieira

Profª Leda Quercia Vieira
 Coordenadora do Curso de Pós Graduação
 em Bioquímica e Imunologia
 ICB - UFMG

Acknowledgments

I would like to thank my promotor, Professor Maria Elena de Lima for inspiring me to start the PhD at UFMG and for her advice and support throughout the duration of my PhD. I am very grateful to my co-promotor, Professor Jan Tytgat for all his support and help, not only during my PhD but also the many years that we are working together. I own many thanks to the people of LVTA for all the nice moments. Especially Edleusa I need to thank for all her help and translations during the classes of Base II. Furthermore, I am grateful to Pablo for all the funny moments, serious discussions and his help with translations and finding my way around UFMG. I thank Flavia, Cris and Professor Igor Dimitri for the help and expertise with the in vivo experiments and Orlando for helping me out with the many, many administrative issues. Ederson and Rogeria, quero agradecer-lhe por toda a ajuda e por fazer de sua casa a minha casa.

I am very grateful to my father and mother for all their advice and help during my PhD. Without their unconditional support, I would never have been able to walk the paths I have chosen in live. I truly need to thank my wife, Aninha, without whose infinite love, endless support, inexhaustible advice and aid, this thesis and PhD would not have been realized.

I am very grateful to all the jury members for excepting the invitation and for their valuable contributions.

I would like to thank CAPES for the financial support.

Summary

Voltage-gated sodium (Nav) channels play crucial roles in a range of (patho)physiological processes. Much interest has arisen within the pharmaceutical industry to pursue these channels as analgesic targets following the overwhelming evidence that Nav channel subtypes Nav1.7-Nav1.9 are involved in nociception (Ahern et al., 2016; Luiz and Wood, 2016). More recently, also Nav1.1, Nav1.3 and Nav1.6 have been identified to be involved in pain pathways. Venom-derived disulphide-rich peptide toxins (15–80 amino acids), isolated from spiders and cone snails, have been used extensively as probes to investigate these channels and have attracted much interest as drug leads for pharmaceutical development (Schroeder et al., 2012; Saez et al., 2010). However, few peptide drug leads have made it as drugs due to unfavourable physiochemical attributes including poor *in vivo* pharmacokinetics, rapid proteolytic cleavage and limited oral bioavailability. This project aims to bridge the gap in the development pipeline between *drug leads* and *drugs candidates* by downsizing these larger venom-derived Nav inhibitors into smaller, “drug-like” molecules.

As a first step, we searched the venom of the spider *Phoneutria nigriventer* for promising Nav channel ligands. A first toxin sparking our interest was the toxin PnTx2-1. Based on the *in vivo tests* in mice and the sequence identity with PnTx2-5 and PnTx2-6, this peptide is classified as a Nav channel toxin. However, it has never been tested on any Nav channel isoform. Therefore, in this study the Nav channel subtype selectivity and species specificity of PnTx2-1 are investigated. We performed an in-depth functional characterization of the Nav channel modulating properties of PnTx2-1. Furthermore, analysis of the activity of PnTx2-1 on Nav1.5 reveals that this *Phoneutria* toxin modulates the cardiac Nav channel in a bifunctional manner, resulting in an alteration of the inactivation process and a reduction of the sodium peak current. The obtained results allowed to conclude that PnTx2-1 is an interesting insecticidal peptide but

it does not represent a promising lead compound for the development of novel Nav channel ligands with therapeutic potential.

Another toxin potentially interesting as a Nav channel modulating ligand is the toxin PnTx1. PnTx1 was found to be the most interesting Nav channel toxin, considering its action in Navs related to pain (Silva et al., 2012a). Following identification of common sequence motifs from Nav inhibitors PnTx1 (Diniz et al., 2006a) (78 residues, 14 cysteine) and μ -conotoxin KIIIA (Bulaj et al., 2005) (16 residue, 6 cysteine) from cone snail *Conus kinoshitai*, we have produced the smallest cyclic peptide-based Nav channel inhibitor known to date (10 residues, 2 cysteines) with demonstrated subtype selectivity across Nav channel subtypes including Nav1.7 and Nav1.9 (Luiz and Wood, 2016). The methodology used in this project, involved a two-pronged approach that incorporates sophisticated peptide engineering carrying out several rounds of small cyclic peptide design to aid in the determination of what drives subtype selectivity and molecular interactions of these downsized inhibitors across Nav subtypes. This allowed us to design small, stable and novel Nav probes with high subtype selectivity and potency coupled with improved biopharmaceutical properties, rendering these peptides suitable as analgesic drug candidates.

Table of Contents

1. Introduction	8
1.1. The sodium channel structure and function	8
1.2. Neurotoxins and Na_v channel pharmacology	15
1.2.1. Neurotoxin Binding Site 1	18
1.2.2. Neurotoxin Binding Site 2	21
1.2.3. Neurotoxin Binding Site 3	22
1.2.4. Neurotoxin Binding Site 4	24
1.2.5. Neurotoxin Binding Site 5	25
1.2.6. Neurotoxin Binding Site 6	27
1.3. Na_v channels and pain	28
1.4. Cone snail venom as a source of drug discovery	31
1.4.1. Conotoxins acting on Na_v channels	35
1.4.2. μ-conotoxins	36
1.4.2.1. Muscle Na_v channel isoform preferring μ-conotoxins	37
1.4.2.2. Neuronal Na_v channel isoform preferring μ-conotoxins	42
1.5. Spider venom as a source of drug discovery	46
1.6. Phoneutria nigriventer	47
1.6.1. Nomenclature of Phoneutria nigriventer toxins	51
1.6.2. PhTx1	53
1.6.3. PhTx2	59
1.6.4. PhTx3	65
1.6.5. PhTx4	69
1.6.6. PhTx5	71
1.6.7. Non-protein P. nigriventer venom components	73
2. Hypothesis	74
3. Objectives	76
3.1. General Objective	76
3.2. Specific Objectives	76
4. Material & Methods	79
4.1. Animals	79
4.1.1. Mice	79

4.1.2.	<i>Xenopus laevis</i> frogs.....	79
4.2.	Algesimetric method.....	79
4.2.1.	Measurement of nociceptive threshold	79
4.2.2.	Drug Administration.....	80
4.2.3.	Experimental Protocol.....	80
4.2.4.	Statistical Analysis.....	81
4.3.	Peptide synthesis.....	81
4.4.	NMR spectroscopy.....	82
4.4.1.	Structural constraints	83
4.4.2.	Structure calculations.....	83
4.5.	Expression of voltage-gated ion channels in <i>Xenopus laevis</i> oocytes	84
4.6.	Electrophysiological recordings.....	84
4.7.	Serum-stability tests.....	86
5.	Results.....	88
5.1.	Chapter 1: Investigation of <i>P. nigriventer</i> venom peptide PnTx2-1	88
5.1.1.	Activity of PnTx2-1 on mammalian Na_v channels	89
5.1.2.	Activity of PnTx2-1 on insect Na_v channel currents	93
5.1.3.	Activity of PnTx2-6 on $Na_v1.5$ channel currents	94
5.1.4.	Discussion	95
5.2.	Chapter 2: Peptide engineering of the toxin PnTx1.....	99
5.2.1.	Design strategy	102
5.2.2.	Solution structure of Pn	102
5.2.3.	Electrophysiological characterization of Pn and mutants.....	105
5.2.4.	Serum stability test.....	112
5.2.5.	Fourth generation of Pn peptides: design of PnCs1 mutants	113
5.2.6.	Discussion	118
6.	General Discussion and Conclusion	123
6.1.	PnTx2-1	124
6.2.	PnTx1 & Pn peptides	125
7.	References	128
8.	Annex Publications.....	146

1. Introduction

1.1. The sodium channel structure and function

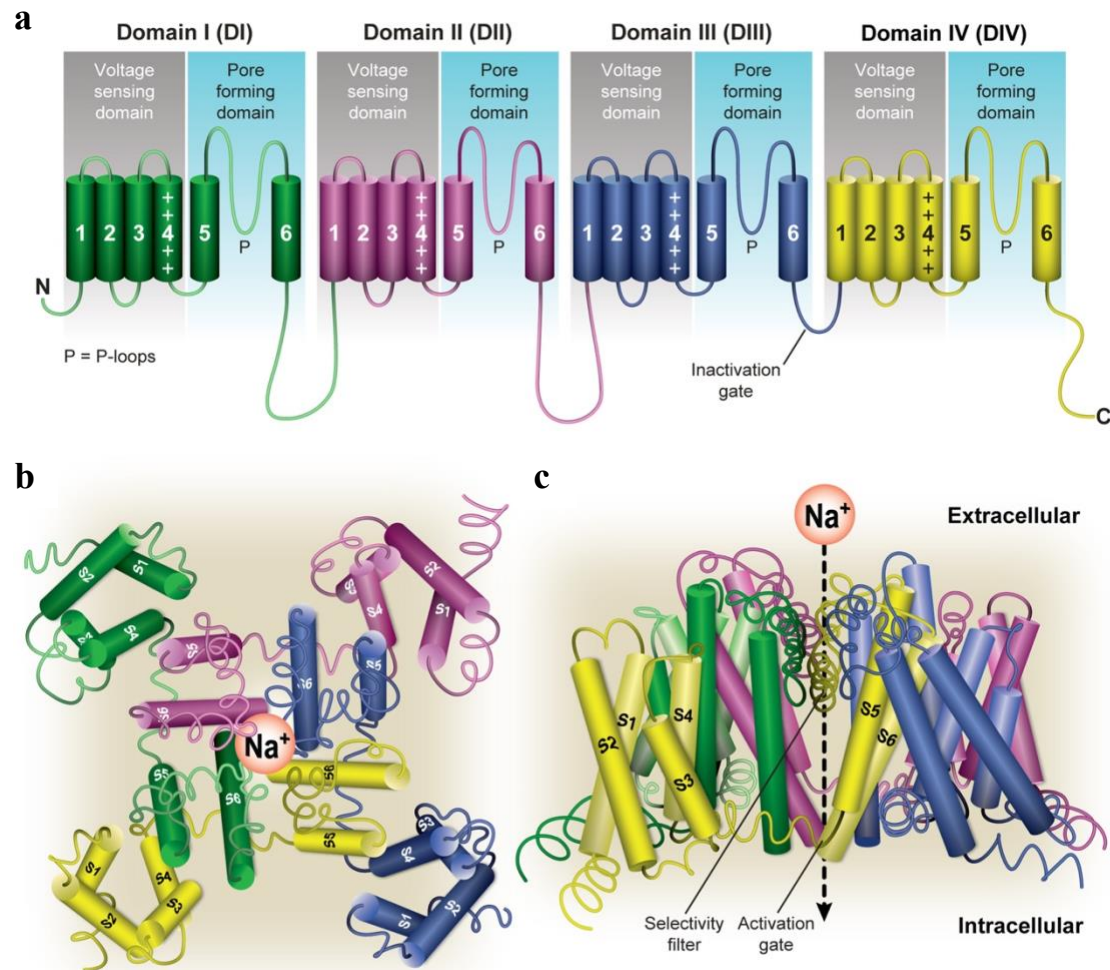


Figure 1. Schematic illustration of the sodium channel architecture. (a) Topology of the human Nav channel α subunits. These proteins consist of four homologous domains DI (green), DII (pink), DIII (blue), and DIV (yellow) connected by intracellular linkers. Each domain contains six transmembrane helical segments (S1–6). Segments S1–S4 form the voltage-sensing domain (VSD). Plus signs in S4 represent the positively charged voltage sensor (containing a number of arginine or lysine residues). Movement of S6 segments lead to channel opening in response to membrane depolarization. Segments S5, S6, and the connecting pore-loops (P-loops) form the channel pore. The intracellular loop connecting DIIIS6 and DIVS1 functions as an inactivation gate, closing the channel pore during fast inactivation. (b) Extracellular view of the open-channel conformation crystal structure of NavMs , a marine bacteria from *Magnetococcus sp.* Four identical domains are colored as in (A) to highlight parallels to the human Nav structure. (c) Side view of the open-channel conformation crystal structure of bacterial NavMs.12 Selectivity filter (SF) and activation gate are indicated at the centre and intracellular part of the channel pore, respectively. Figure adapted from (de Lera Ruiz and Kraus, 2015).

Nav channels are transmembrane protein complexes constituted of an α -subunit of approximately 260 kDa which can be associated with up to four auxiliary β -subunits (β 1-4) of 30 to 40 kDa. The pore-forming α -subunit alone is sufficient to obtain sodium current, however co-expression of β -subunits modifies expression level, kinetics and voltage dependence of channel gating (Yu and Catterall, 2003). It has been shown that the presence of β -subunits significantly affects the affinity of certain Nav channel modulators but it has little or no effect on the activity of small molecule inhibitors (Green and Olivera, 2016). The α -subunit is organized in four homologous domains (DI-IV). Each domain contains six putative transmembrane segments (S1-S6) connected by extracellular or intracellular loops (Figure 1). The S4 segments are the most conserved segments and they contain a basic residue, either lysine or arginine, in every third position. These positively charged S4 segments are believed to function as voltage sensors. They transport gating charges by moving outward upon membrane depolarization and as such initiating the voltage dependent activation which results in the opening of the channel (Figure 2).

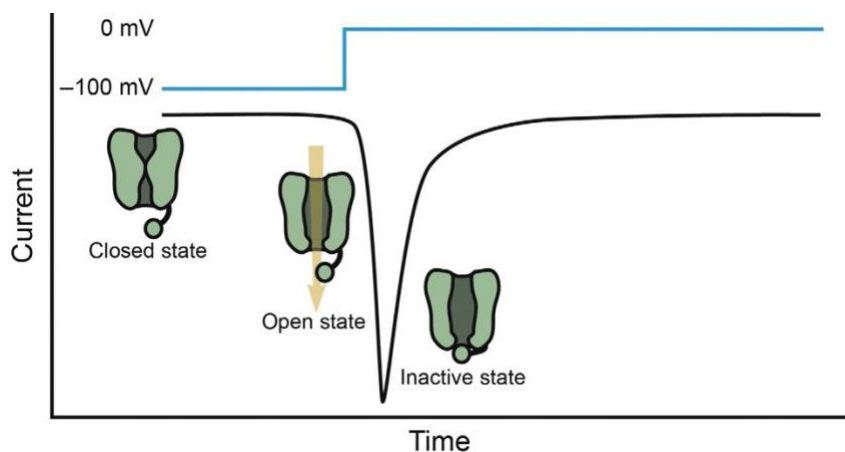


Figure 2. Upon depolarization of the cell membrane, the outward movement of the voltage-sensing S4 segment allows the Nav channels to transite from the closed or resting state to the open state which allows the permeation of Na⁺ ions through the pore. The process of fast inactivation leads to closure of the channel via occlusion of the pore by the inactivation particle or gate. After inactivation, channels will return to the closed state once membrane potentials are at resting levels. Figure was adapted from (Israel et al., 2017a).

The selectivity filter and pore are formed by the transmembrane segments S5 and S6 together with the re-entrant segments that are part of the loop that connects the S5 and S6 of each domain. Folding of the domains in a clockwise orientation, in which domain I and IV are in close proximity of each other, leads to the formation of the outer vestibule and the selectivity filter (Catterall, 2000; Chanda and Bezanilla, 2002). The short intracellular linker that connects the domains III and IV contains a highly conserved sequence of three hydrophobic residues (isoleucine, phenylalanine and methionine) or IFM motif. Sodium channel inactivation is mediated by this hydrophobic motif since it serves as an inactivation gate crucial for causing fast inactivation by binding to a receptor. This inactivation gate receptor is located near or within the intracellular mouth of the sodium channel pore. It has been shown that several residues in the intracellular loop that connects IIS4-S5 and in the loop connecting IVS4-S5 are contributing to the inactivation gate receptor (Dong, 2007; Yu and Catterall, 2003). Nine different mammalian sodium channel isoforms have been cloned, characterized and functionally expressed.

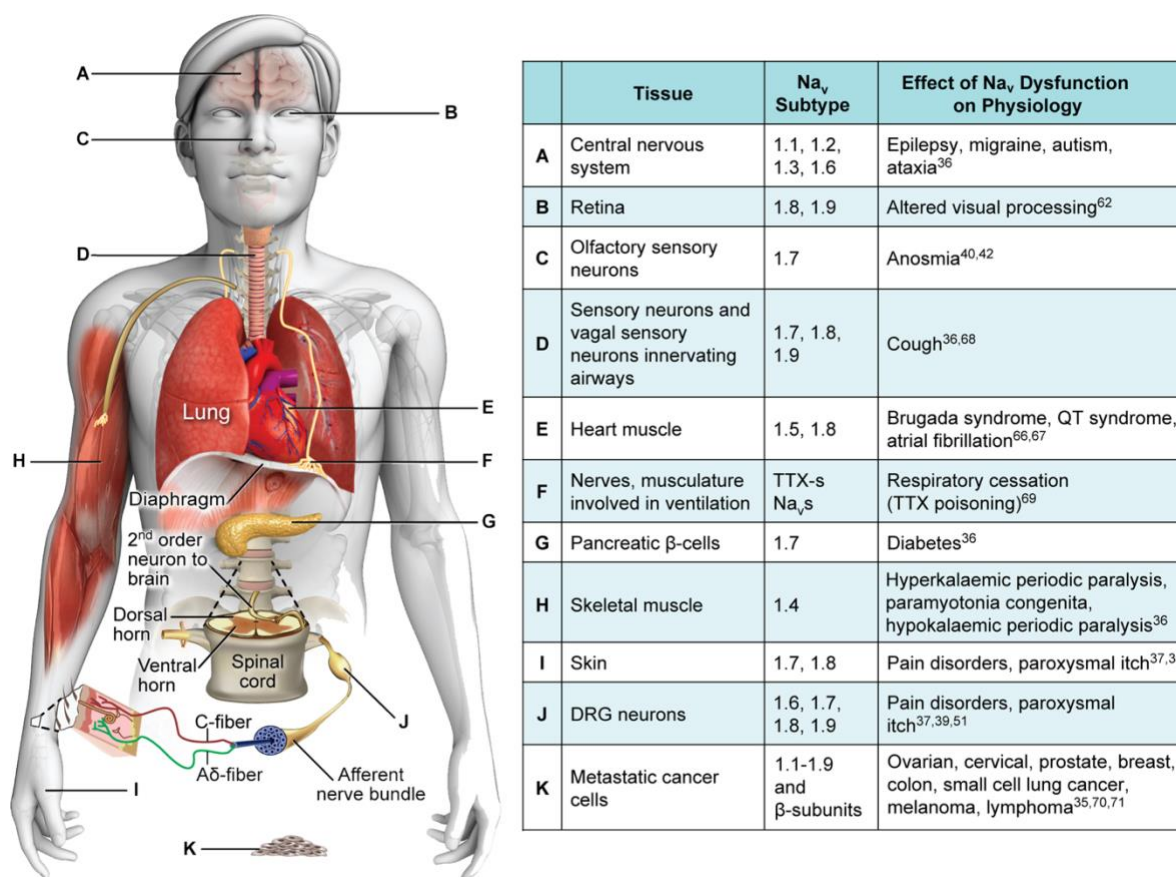


Figure 3. Tissue expression of Nav subtypes and effects of Nav dysfunction on physiology. Figure adapted from (de Lera Ruiz and Kraus, 2015).

These sodium channel isoforms exhibit distinct expression patterns in skeletal and cardiac muscle tissues and in the central and peripheral nervous systems (Figure 3) (Goldin, 1999). Nav1.1, Nav1.2, Nav1.3 and Nav1.6 are expressed in the central nervous system (CNS), whereas Nav1.7, Nav1.8 and Nav1.9 are predominantly expressed in the peripheral nervous system (PNS). Nav1.4 is expressed in skeletal muscles, while Nav1.5 is also known as the cardiac muscle isoform. The functional and pharmacological diversity of the mammalian Nav channels is primarily resulting from the expression of multiple genes (Goldin et al., 2000). The selective expression of different sodium channel genes mirrors the specialized function of sodium channels in various mammalian tissues and cell types (Yu and Catterall, 2003). Their specialized function results from the fact that each mammalian sodium channel α -subunit

isoform features distinct electrophysiological properties such as unique gating kinetics (Dong, 2007; Goldin, 2001).

Analysis of the human genome revealed that there are 143 ion channel proteins whose pore-forming segments are related to sodium channels, and they are associated with at least 10 distinct families of auxiliary subunits (Yu and Catterall, 2003). The voltage-gated ion channels and their molecular relatives are one of the largest superfamilies of signalling proteins and one of the most prominent targets for drugs used in the therapy of human diseases. The voltage-gated sodium channels were the founders of this large superfamily in terms of discovery of their function by Hodgkin and Huxley and the later discovery of the sodium channel protein itself. Surprisingly, the sodium channel family is ancient in evolution. The bacterial sodium channel NaChBac and several prokaryotic relatives are composed of homotetramers of a single subunit whose structure resembles one of the domains of a vertebrate sodium channel (Koishi et al., 2004; Ren et al., 2001). It is likely that these bacterial sodium channels are the evolutionary ancestors of the larger, four-domain sodium channels in eukaryotes (Catterall, 2012a, b).

For a long time, knowledge on the structure of Nav channels remained rather limited. Due to pseudosymmetry, heavy post-translational modifications, and medium molecular weight make Nav channels one of the most challenging targets for structure determination. The first information of sodium channel architecture was obtained by determination of the crystal structures of the bacterial sodium channels NavAb (Figure 4a) (Payandeh et al., 2012; Payandeh et al., 2011) and the NaChBac orthologue NavRh (Figure 4b) (Zhang et al., 2012). More recent, the technological breakthrough of electron microscopy (EM) allowed an impressive acceleration in elucidation of structures for many ion channels and receptors (Cheng, 2018). Recently, also of several eukaryotic Nav channels, the structure could be determined. The putative Nav channel from the American cockroach *Periplaneta Americana* (NavPas) was the first eukaryotic Nav channel to have its structure determined (Shen et al., 2018; Shen et al.,

2017). Next, the structure of a prototypical Nav channel from an electric eel in complex with the auxiliary subunit $\beta 1$, EeNav1.4- $\beta 1$, was resolved at a 4.0Å resolution (Figure 4c) (Yan et al., 2017). Interestingly, this EeNav1.4- $\beta 1$ complex revealed that the extracellular dome provides a docking site for β subunits, which might explain why the sensitivity of Nav channels to some peptide toxins is modulated by the presence of an accessory β subunit (Gajewiak et al., 2014; Wilson et al., 2011; Zhang et al., 2013).

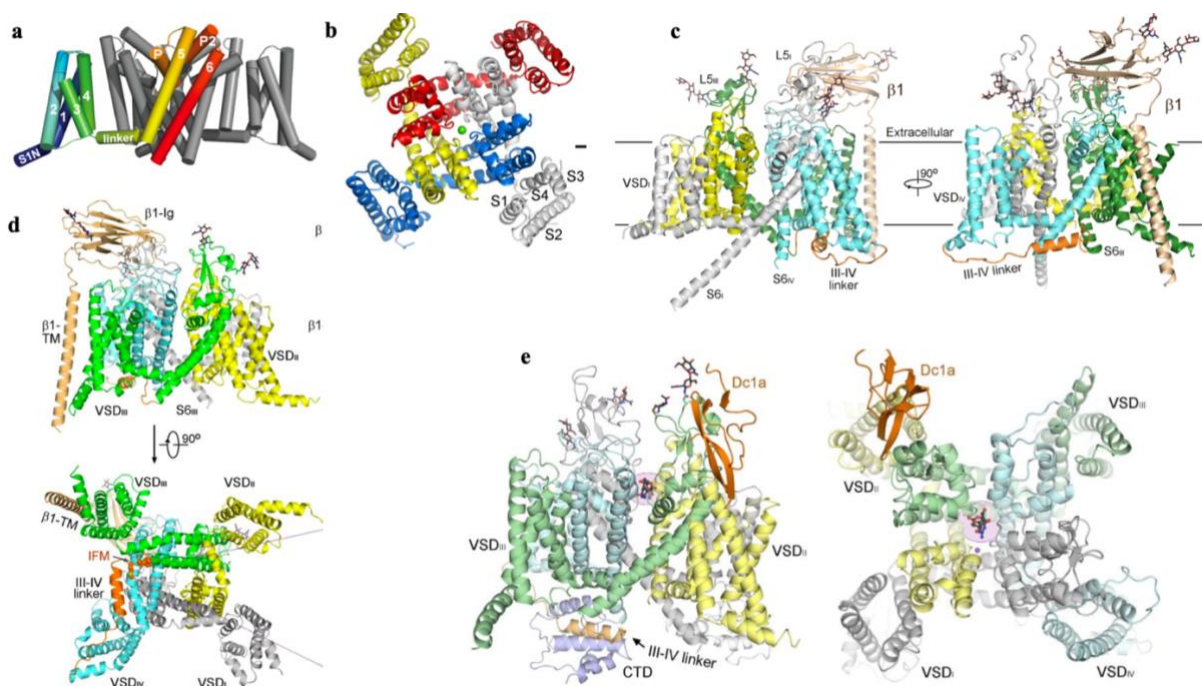


Figure 4. X-ray crystallography and cryo-microscopy structures of prokaryotic (a, b) and eukaryotic (c-e) Nav channels. (a) Main structural elements of NavAB. The nearest voltage-sensing domain and pore domain are removed for clarity. (b) Periplasmic view of the NavRh structure in a closed conformation. NavRh is crystallized as an asymmetric tetramer. The green sphere indicates the bound ion within the selectivity filter. (c) The overall structure of the EeNav1.4- $\beta 1$ complex. The α subunit is domain coloured, and the $\beta 1$ subunit is coloured wheat. The same colour scheme is applied throughout the manuscript. The glycosyl moieties are shown as black sticks. (d) *Upper panel* shows the structure of the human Nav1.4- $\beta 1$ complex. The extracellular and transmembrane regions of the Nav1.4- $\beta 1$ complex are clearly resolved. The structure is domain coloured. The glycosyl moieties are shown as sticks. *Bottom panel* illustrates that the intracellular gate of Nav1.4 is closed in this structure. The IFM fast inactivation motif is shown as spheres and the III-IV linker is coloured orange. (e) Structures of the NavPaS in complex with the peptide Dc1a with TTX. Side view and top view are shown. The four repeats in NavPaS are shown in different colours and Dc1a is coloured orange. The sugar moieties are shown as black sticks. TTX, shown as black ball-and-sticks, is highlighted by the pink shade. The putative Na⁺ ion is shown as purple sphere. Figures adopted from (Pan et al., 2018; Payandeh et al., 2012; Payandeh et al., 2011; Shen et al., 2018; Shen et al., 2017; Yan et al., 2017; Zhang et al., 2012).

Later on, the structure of NavPaS in complex with three natural toxins was reported. The elucidation of NavPaS bound by the well-characterized neurotoxin site 1 ligands tetrodotoxin (TTX) and Saxitoxin (STX) provided a molecular explanation for decades of functional studies using TTX or STX (Figure 4e) (Shen et al., 2018).

The structure determination of NavPaS in complex with the peptide toxin Dc1a shed light on the structural mechanism of action in which certain animal toxins modulate Nav channels. The spider toxin Dc1a, isolated from the desert bush spider *Diguetia canities*, promotes channel opening of insect Nav channels and is therefore classified as a gating modulating toxin (GMT) (Bende et al., 2014). Upon binding of Dc1a at the neurotoxin site 4, the channels will activate at more hyperpolarized membrane potentials, resulting in a leftward shift of the activation curve. Elucidation of the NavPaS channel in the presence of Dc1a confirmed the important role of VSDII in binding this GMT. However, it also revealed that the network of intermolecular interactions is much more complex than previously anticipated, with key interactions between the toxin and both the S5III pore-domain helix and the extracellular dome above the pore. Thus, one has to apply caution when using isolated Nav channel VSDs for drug discovery or for understanding the molecular basis of GMT action.

Although the structures of NavPas and EeNav1.4 displayed interesting conformational distinctions, no functional states could be defined for these two structures, mainly due to the absence of other reference structures. Furthermore, functional characterisation of these channels is hampered by the inability to measure NavPas- or EeNav1.4-mediated currents in heterologous expression systems (Pan et al., 2018). In order to obtain a well-defined model for structure-function relationship studies of Nav channels and their ligands, structural determination of a functional in depth characterized Nav channel was needed. This need was

fulfilled by the obtainment of the Cry-EM structure of human Nav1.4 channel in complex with $\beta 1$ at a 3.2Å resolution (Figure 4d) (Pan et al., 2018).

Together, all these remarkable Nav channels structures have revealed a wealth of new information about the structural basis for sodium selectivity and conductance, the mechanism of block of the channel by therapeutically important drugs, the mechanism of voltage-dependent gating, and hereby have provided a path towards mechanistic investigation of Nav channels and drug discovery for Nav channelopathies (Catterall, 2012a, b; Pan et al., 2018).

1.2. Neurotoxins and Nav channel pharmacology

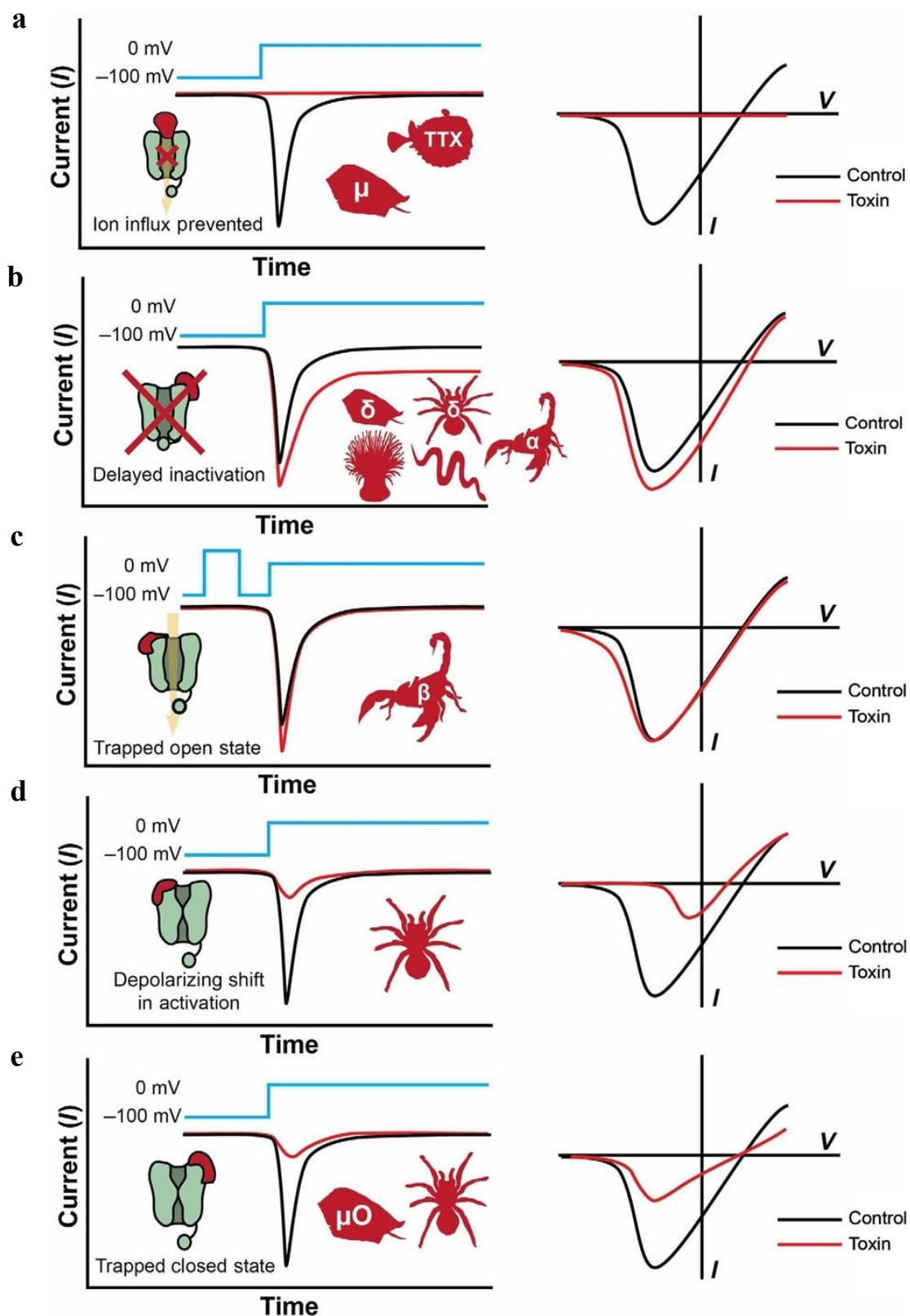


Figure 5. Overview of the common effects toxins have on the biophysical properties of Na_V channels. Left panels represent current–time plots. Right panels represent current–voltage (I – V) curves. Toxin effects are representative of an EC_{100} concentration. (a) Pore blockers, including the guanidinium neurotoxin TTX and the μ -conotoxins, inhibit Na^+ current by physically occluding the pore of Na_V channels. (b) Toxins that delay fast inactivation include δ -conotoxins, δ -spider toxins, sea anemone toxins, α -scorpion toxins,

and the new described snake toxin calliotoxin (δ -elapitoxin-Cb1a), all with differing effects on peak current. The schematic diagram illustrates the effect of the α -scorpion toxin OD1. (c) β -Scorpion toxins have different effects on peak current, but generally cause a hyperpolarizing shift in the voltage dependence of activation. The schematic diagram illustrates the effect of the β -scorpion toxin Css-IV. (d) Some spider peptides (including ProTx-II) inhibit peak current by shifting the voltage dependence of activation to more depolarized potentials, with some residual current at more depolarized potentials. (e) μ -conotoxins and some spider peptides are believed to trap the voltage sensors in the closed state, inhibiting peak current without shifting the voltage dependence of activation (Israel et al., 2017a).

To define the pharmacological activity of Nav channel targeting ligands such as peptide toxins and small molecules, a steadily increasing number of defined binding sites have been proposed (Israel et al., 2017a). However, it is becoming increasingly clear that there is significant overlap between sites and that the boundaries of these presumed distinct binding pockets are both poorly defined and can be occupied simultaneously by a single molecule. The interaction between neurotoxins and Nav channels can occur in two different ways. It results either in a pore block when the toxin physically occludes the pore and thereby inhibits the sodium conductance, or in a modification of the gating, which leads to altered gating kinetics and voltage-dependence of the channels. Toxins binding on site 1 use the first mechanism. The guanidinium toxins, TTX and saxitoxin STX are such site 1 pore blockers; they will form a plug in the outer vestibule of the pore (Figure 5a). This site is also recognized by μ -conotoxins, peptide toxins from Cone snail venom. Site 2 toxins like batrachotoxin and grayanotoxin will prevent inactivation and therefore persistently activate the channel. Scorpion α -toxins and sea anemone toxins are typical examples of site 3 toxins; they will slow or inhibit inactivation (Figure 5b). Scorpion β -toxins and β -spider toxins bind to site 4 and shift the voltage-dependence of activation toward more hyperpolarized potentials (Figure 5c). Site 5 neurotoxins like brevetoxins and ciguatoxins exhibit a real arsenal of effects upon Nav channel binding, e.g., inhibition of activation and a hyperpolarizing shift of the voltage-dependence of activation. δ -conotoxins acting on site 6 will cause similar effects as site 3 toxins by slowing or inhibiting inactivation (Figure 5b) (Stevens et al., 2011). The pyrethroid binding site or site 7 is the binding

site for some insecticidal agents like DDT and pyrethroids. Site 8 is recognized by the cone snail toxin $\mu\text{O}\delta$ -conotoxin GVIIJ from *Conus geographus* and upon toxin binding, a reduction in the sodium peak current is observed (Figure 5e) (Gajewiak et al., 2014). However, the exact mechanism in which this toxin acts on Nav channels remains non-elucidated. The binding site for local anaesthetics is also described as site 9 and is situated within the pore region. Small molecules, such as anticonvulsants and antiarrhythmics that bind in a use-dependent manner and act as pore blockers, bind this site.

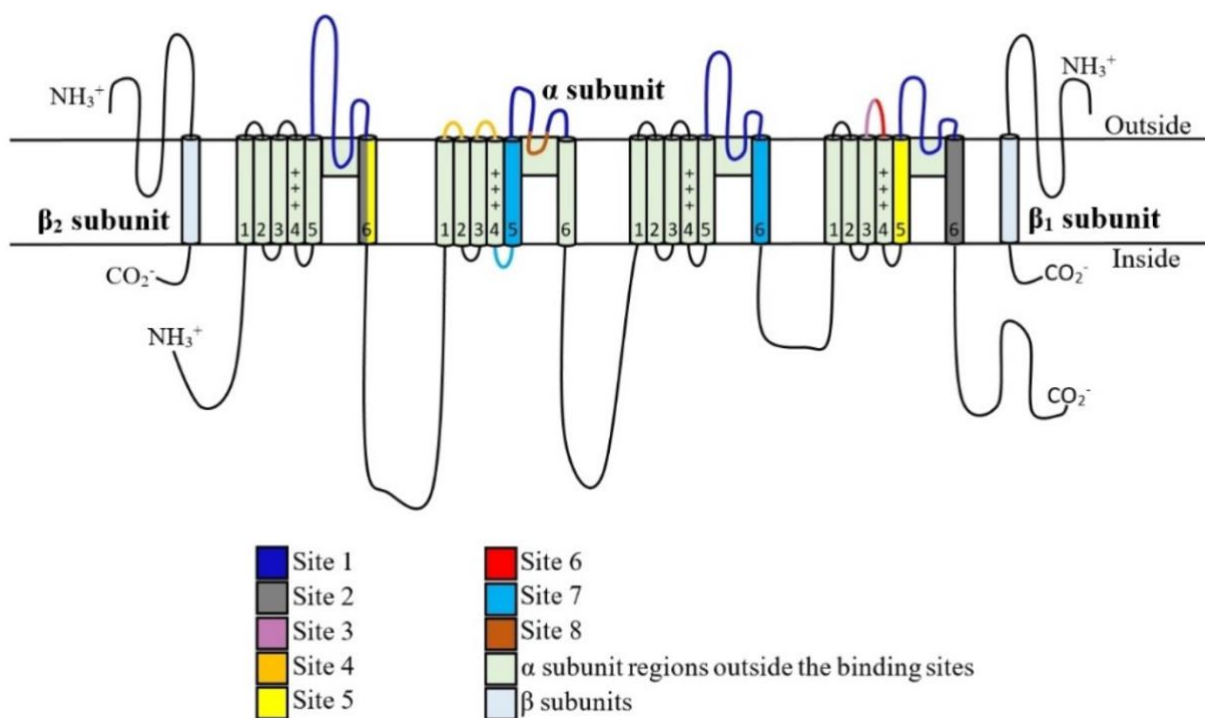


Figure 6. The binding sites on the voltage-gated sodium channel. Figure adapted from (Munasinghe and Christie, 2015).

The next text is partly based on the following publication: Neurotoxins and their binding areas on voltage-gated sodium channels. Stevens M, Peigneur S, Tytgat J. *Front Pharmacol.* 2011 Nov 9;2:71.

1.2.1. Neurotoxin Binding Site 1

Among all putative binding sites on Nav channels, site 1 is probably the best defined and most straightforward of all sites. It is composed by residues at the reentrant P-loops

connecting S5 and S6 of all four domains (Figure 6). The historical guanidinium molecules TTX and STX were the first neurotoxins shown to bind at this site. Upon their binding, Na⁺ conductance is blocked. They are produced by some bacteria and dinoflagellate species, respectively (Chau et al., 2011; Narahashi, 2008). Later on, the μ -conotoxins found in cone snails, also turned out to bind to this specific site and to cause the same effects. At first it was thought that both types of toxins would interact with exactly the same residues, but it seems to be a more complex interplay, as some mutations in Nav1.4 channels affecting TTX binding did only affect binding of a μ -conotoxin to a minor extent. Therefore, it was suggested that TTX and μ -conotoxins share an overlapping but non-identical binding site (Stephan et al., 1994). In this model, the core of the binding site is situated more in the inner side of the pore mouth and can be occupied by TTX or STX as well as μ -conotoxins, the latter interacting with some extra residues laying at the outer vestibule of the pore. (Zhang et al., 2009) first proposed the simultaneous binding of TTX and μ -KIIIA, a μ -conotoxin from *Conus kinoshitai*. Addition of both toxins to oocytes expressing Nav1.2 leads to the formation of a bi-liganded, ternary complex of Nav·TTX/alkaloid· μ -conotoxin. If μ -KIIIA binds first to the channel, this will slow the subsequent binding of TTX at its specific binding place, further down into the channel; and the other way around. But in another series of experiments done by the same group, this appeared not to be completely true for STX and its sulfated congener GTX2/3. Another, extended model was suggested, wherein the binary complex Nav· μ -conotoxin could flicker between a permissive state, in which the alkaloid can “sneak” by the μ -conotoxin, and an unpermissive state (French et al., 2010a; Zhang et al., 2010b). Because STX has an extra positive charge compared with TTX, this could lead to electrostatic repulsion. Docking of TTX and μ -KIIIA was consistent with their experimental results; both molecules do fit simultaneously in the vestibule (Lipkind and Fozzard, 2000).

The Nav channel homology models previously used turned out to be valuable to define the structure of the outer channel vestibule (Cervenka et al., 2010). Although the outer vestibule was long time believed to be a rigid structure, this does not correspond to the large amount of studies that predict a highly flexible P-loop that even might undergo conformational changes that are linked to gating transitions upon binding of TTX or μ -conotoxins. This can be deduced, amongst other things, from mutagenesis studies examining the effects of mutations in this region. Those mutations mostly correlated with alterations in gating kinetics and more specifically decreased (mutations in the P-loop of DI) or enhanced inactivation (mutations in the P-loop of DIV) (Cervenka et al., 2010). The latter can be explained by the proximity of DIV S6 to the P-loop of DIV, as DIV S6 plays an important role in the inactivation process. Moreover, this DIV S6 segment is supposed to enclose the binding site of LA, which on its turn connects site 1 and 6. The recent structure elucidation of NavPaS bound by both TTX and STX provided at last a detailed molecular structure conformation for the exact binding sites of TTX and STX (Shen et al., 2018).

Site 1 toxins such as μ -conotoxins can also influence the activation process by interacting with the voltage sensors. μ -Conotoxins such as μ -KIIIA and μ -GIIIA are strongly cationic peptides. Upon binding at site 1, these peptides electrostatically impede the outward movement of the positively charged residues in the S4 voltage sensor segments, which is a necessity for channel activation. The electrostatic repulsion, induced by binding of the toxin at site 1, most probably stabilizes the closed state, resulting in channels which will open at more depolarized membrane potentials (French et al., 2010a; Van Der Haegen et al., 2011).

Another neurotoxin believed to affect site 1 is PnTx1 from *Phoneutria nigriventer* (Martin-Moutot et al., 2006b). Though binding of labeled PnTx1 was not inhibited by TTX, it was inhibited by the μ -conotoxin μ -GIIIB (*Conus geographus*). Therefore, it was suggested that PnTx1, like TTX, binds to a micro site and that the binding site of μ -conotoxins overlaps the

micro sites of TTX and PnTx1. The toxin PnTx1 is discussed more in detail in the chapter on the venom of *Phoneutria nigriventer*. So far, only one other spider toxin is known to interact with binding site 1, that is Hainantoxin-I (HNTX-I) from *Ornithoctonus hainana* (Li and Tomaselli, 2004; Nicholson, 2007). Other spider toxins like Huwentoxin-IV (HWTX-IV) from *Ornithoctonus huwena* and some Hainantoxins (HNTX III-V) were at first considered to be potential site 1 neurotoxins as they inhibit Na⁺ conductance, an effect concerned to be typical for site 1 (Li and Tomaselli, 2004; Nicholson, 2007). The same is valid for μ O-conotoxins; but this hypothesis had to be adjusted as evidence occurred that these toxins do not bind to residues at site 1 but at residues in S3–S4 of DII (Leipold et al., 2006b). Intriguingly, these residues form part of what is generally determined as “site 4.”

1.2.2. Neurotoxin Binding Site 2

This site is targeted by a wide array of lipid-soluble toxins with greatly diverting chemical structures. Their structural non-relatedness is mirrored in their diverse source of origin as they can be found in plants, animals, and bacteria. Well-known examples of site 2 toxins from plants are alkaloids like veratridine (VTD; from *Liliaceae*) and aconitine (*Aconitum napellus*) and grayanotoxins (GTX) from *Ericaceae*. Batrachotoxin (BTX) and homologs are site 2 toxins produced by animals such as frogs (*Phyllobates* spp.) and birds (*Pitohui* and *Ifrita* spp.; (Dumbacher et al., 2000). Antillatoxin and hoiamide were isolated from some cyanobacteria (*Lyngbya majuscula*) and were found to bind to neurotoxin receptor site 2 (Cao et al., 2010; Pereira et al., 2009). Site 2 toxins are known as activators as they modulate sodium channels in such a way that the channels open more easily and stay open longer. Activators preferentially bind to channels in the open state and their binding leads to Nav channels with a unique and complex behavior. Several channel properties are altered upon site 2 binding: (i) the voltage-dependence of activation is shifted toward more negative potentials causing channels

to open at resting potentials; (ii) the inactivation is slowed down or inhibited resulting in sustained, non-inactivating currents; (iii) the sodium conductance through toxin-bound channels is reduced; (iv) the ion selectivity of modified channels is altered due to a decreased discrimination for permeating ions (Du et al., 2011; Tikhonov and Zhorov, 2005). Numerous studies have been conducted to map the neurotoxin site 2 and to provide a better understanding of the molecular determinants responsible for these intriguing channel gating alterations upon toxin binding (Figure 6).

1.2.3. Neurotoxin Binding Site 3

Neurotoxins binding to site 3 include members of different phyla of the kingdom of Animalia, among which major players are toxins from scorpions, sea anemones, and spiders. In fact, binding site 3 was first determined by radiolabeling and mutagenesis studies performed with α -scorpion and sea anemone toxins (Rogers et al., 1996; Tejedor and Catterall, 1988). Scorpion toxins affecting the gating of Nav channels are historically classified into α - and β -toxins according to the effects that they cause. β -Scorpion toxins cause a strong hyperpolarizing shift in the voltage-dependence of activation, which is linked to neurotoxin binding site 4 and will be discussed in the following chapter. α -Scorpion toxins are long polypeptides of 60–70 amino acids and can be further subdivided into three groups according to their phylogenetic specificity (Gordon et al., 1996; Hamon et al., 2002). Classical α -scorpion toxins or anti-mammalian toxins will inhibit inactivation of mammalian Nav channels and have low affinity for insect neuronal membranes. Well-known examples are AaH II (*Androctonus australis Hector*; (Jover et al., 1978) and Lqh II (*Leiurus quinquestriatus hebraeus*; (Sautiere et al., 1998). Anti-insect α -scorpion toxins like LqhaIT (Eitan et al., 1990) only show minor activity against mammalian brain preparations but do show significantly higher inhibition of insect Nav

channels. Finally, α -like scorpion toxins bind to both rat brain and insect Nav channels (Hamon et al., 2002; Sun et al., 2003).

The second class of toxins that are famous for inhibiting Nav inactivation is found in the venom of sea anemones. Sea anemone toxins targeting Nav channels are subdivided into several classes, but unlike α -scorpion toxins, this classification is not based on their phylogenetic preferences but on their amino acid sequences. (Norton, 1990) first proposed three classes to which a sea anemone toxin can belong. Type 1 and 2 toxins include larger peptides, composed of 46–49 amino acids and 3 disulfide bridges. Type 3 toxins are shorter peptides, composed of 27–30 amino acids only (Bosmans and Tytgat, 2007; Honma and Shiomi, 2006; Shiomi, 2009). Besides toxins from scorpions and sea anemones, site 3 is also targeted by toxins from other animals like spiders and wasps (de Lima et al., 2002a; Nicholson et al., 2004; Schiavon et al., 2010). Parts of the Nav channel that were first identified to be involved in the binding of site 3 neurotoxins were located in the extracellular loops between S5 and S6 in DI and DIV (Figure 6) (Thomsen and Catterall, 1989). Later on, residues in the extracellular loop between S3 and S4 in DIV also turned out to be involved in the binding of site 3 neurotoxins (Rogers et al., 1996). Fluorescence labeling studies indicated that site 3 neurotoxins stabilize the voltage sensor S4 of DIV in its deactivated position, thereby inhibiting its movement (Campos et al., 2008). As S4 of DIV is known to be involved in the voltage-dependent coupling between activation and fast inactivation (Chahine et al., 1994; Sheets and Hanck, 1995), it is logic that neurotoxin binding to this site causes an impairment of the fast inactivation. The inactivation can be slowed or even completely abolished, and these effects can be associated with a minor hyperpolarizing shift in the activation. Another important characteristic is the voltage-dependency of the binding of these neurotoxins, such that they bind to a lesser extent at more depolarizing potentials (Catterall, 2012b). Site 3 neurotoxins turned out to be interesting tools for the investigation of gating currents, which are small transient currents that occur by

movement of gating charges, mostly located on the S4 segments of the channel (Bezanilla, 2000).

1.2.4. Neurotoxin Binding Site 4

Receptor site 4 is recognized by the class of β -scorpion toxins targeting voltage-gated sodium channels (β NaScTxs) and by several spider toxins. These toxins exert their toxicity by acting as gating modifiers. Toxin binding at site 4 causes a shift in the voltage-dependence of activation toward more hyperpolarized membrane potentials and reduces the peak sodium current amplitude (Cestele et al., 2006; Vijverberg and Lazdunski, 1984). These alterations in channel gating are believed to be a direct result of toxin binding at site 4, hereby trapping the voltage sensor in its outward, activated position (Cestele et al., 2001; Cestele et al., 2006; Vijverberg and Lazdunski, 1984). Receptor site 4 has been primarily defined to specific residues in the extracellular loops connecting the S1–S2 and S3–S4 segments of DII (Figure 6) (Catterall et al., 2007). However, using the scorpion β -toxin Tz1 (*Tityus zuliaanus*) it was shown that three residues in the pore-loop of DIII are determining for the specificity of β -toxin for different sodium channel isoforms (Leipold et al., 2006b). Toxins belonging to the class of β NaScTxs are long chain peptides composed of 58–76 amino acids, cross-linked by four disulfide bridges. They belong to the structural superfamily of cysteine stabilized α/β motif containing proteins. This spatially conserved scaffold provides β NaScTxs with a high stability and a strong resistance against mutations in their sequence (de la Vega and Possani, 2007; Gurevitz et al., 2007; Possani et al., 1999). β NaScTxs are, similar to their α NaScTxs counterparts, classified into three groups according to their pharmacological properties exemplified by their preference for mammalian or insect sodium channels: mammalian-selective, β -like or insect-selective. (i) Mammalian-selective β -toxins such as Css4 (*Centruroides suffusus suffusus*) are highly toxic to mammals (Martin et al., 1987). (ii) β -like

toxins are capable of competing for binding sites on both insect and mammalian Nav channels. Ts γ , also known as Ts1 or Ts VII (*Tityus serrulatus*) and Lqh β 1 (*Leiurus quinquestriatus hebraeus*) are well-studied examples of such β NaScTxS acting on both insects and mammals (De Lima et al., 1986) (Gordon and Gurevitz, 2003; Martin-Eauclaire et al., 2018). (iii) Insect-selective β -toxins fail to exert any affinity whatsoever for mammalian sodium channels, even in very high concentrations (de Dianous et al., 1987). Exactly this complete lack of mammal activity combined with their strong insect specificity and potency makes these insect-selective β NaScTxS interesting lead compounds in the design of new insecticides (Gurevitz et al., 2007).

The insect-selective β -toxins can be further subdivided into excitatory and depressant toxins according to the symptoms they evoke in vivo. Injection of excitatory toxins induces a fast and repetitive activity of motor nerves that results in a reversible contraction paralysis. These excitatory toxins differ from the other β -toxins as one disulfide bridge is located differently and furthermore, they display extra secondary structural elements. The depressant toxins cause a transient contraction followed by a slow depressant and flaccid paralysis (Karbat et al., 2007; Zlotkin et al., 1991). Current-clamp experiments have shown that peptides belonging to this group suppress the evoked action potentials as a result of strong depolarization of the membrane (Strugatsky et al., 2005). Remarkably, when mammalian channels are excited by a long, preconditioning and depolarizing prepulse, insect-selective depressant β -toxins are given the opportunity to affect those channels. The same phenomenon is observed in the case of simultaneous binding of an α -toxin to site 3 (Cohen et al., 2007). As such, it can be seen that the presence of depressant β -toxins in the scorpion venom may still contribute significantly to the toxicity toward mammals.

1.2.5. Neurotoxin Binding Site 5

Marine dinoflagellates produce highly lipophilic, cyclic polyether compounds which target the neurotoxin receptor site 5. Brevetoxins (*Karenia brevis*) and ciguatoxins (*Gambierdiscus toxicus*) are such multi-ring polyether ladder toxins acting at site 5. Brevetoxins (PbTx) consist of 11 transfused rings, 23 stereocenters and an overall linear low-energy conformation (Jeglitsch et al., 1998). PbTx-1 and PbTx-2 are two most potent brevetoxins and they are considered to be the parent toxins. Up to date at least 14 brevetoxins have been described. The two most potent brevetoxins are PbTx-1 and PbTx-2 that slightly differ from each other in their backbone structure. PbTx-1 and PbTx-2 are considered parent toxins since all other brevetoxins can be seen as derivatives from one of these two structural backbones. All PbTx possess a lactone in the A-ring and a strictly rigid region that forms a ladder structure, and which is separated from the A-ring by a spacer region with limited flexibility (Gawley et al., 1995). Furthermore, they all possess a side chain that allows modification at the molecules' termini (Baden et al., 2005). PbTx interact with Nav channels by intercalating in the membrane in a head-down orientation. Several studies have indicated that these toxins position themselves across the plasma membrane, parallel with the transmembrane segments, with the A-ring toward the intracellular side and the tail end of the molecule facing the extracellular side (Figure 6) (Jeglitsch et al., 1998; Trainer et al., 1994). Experiments, in which a photoreactive PbTx-3 derivative was used as probe, could identify S6 of DI and S5 of DIV to participate in the formation of neurotoxin receptor 5 (Trainer et al., 1994). However, the key residues involved in brevetoxin activity still remain unknown. PbTx binding at site 5 leads to distinct alteration in channel gating: (i) the activation potential is shifted toward hyperpolarized potentials; (ii) channels remain longer in the open configuration which results in a longer mean open time; (iii) the inactivation is slowed down or inhibited; and (iv) brevetoxins have, among all known voltage-gated sodium channel modifying toxins, the unique capability to stabilize more than one conductance level. As such brevetoxin binding induces distinct sodium ion subconductance

states in addition to the normal 21 pS rate (Baden et al., 2005; Jeglitsch et al., 1998; Schreibmayer and Jeglitsch, 1992). It is believed that the terminal, rigid four ring system is involved in channel binding while the functional lactone A-ring is responsible for the alterations in channel inactivation and prolongation of the mean open time (Jeglitsch et al., 1998; Purkerson-Parker et al., 2000).

1.2.6. Neurotoxin Binding Site 6

Among all sites, site 6 still is the most speculative and yet undefined site. A first proposal for this site arose when TxVIA and GmVIA, δ -conotoxins from the cone snails *Conus textile* and *Conus gloriamaris* respectively, were characterized (Fainzilber et al., 1994; Shon et al., 1994). As they turned out to slow down Nav channel inactivation without the typical voltage-dependency that is seen with classical site 3 toxins, it was suggested that they bind to a novel, unidentified site (Fainzilber et al., 1994). To date, 35 δ -conotoxins sequences can be found in the ConoServer database (Kaas et al., 2010; Kaas et al., 2012), but for none of them the exact binding site has been reported. Their pharmacology has not been extensively studied because their highly hydrophobic character makes them difficult targets for chemical synthesis (Peigneur et al., 2014a). Only for δ -SVIE an interaction with conserved residues in the linker between S3–S4 of DIV was shown (Leipold et al., 2011). This indicates that at least the S3–S4 of DIV is involved in the interaction of the toxin and Nav channel (Figure 6). It remains to be determined whether this is a general phenomenon and if δ -SVIE is a good representative of all δ -conotoxins, or if a difference exists between the two distinct groups that exist in δ -conotoxins. Those two groups or “clades” are based on the prey targeted by the according cone snail: namely the fish-hunting clade and the mollusk-hunting clade, as structural differences can be recognized between both groups (Bulaj et al., 2001). However, data on δ -conotoxins are still very limited and further studies are needed to elucidate the exact binding site(s) and mechanism

of action of δ -conotoxins and to determine if other toxins apart from δ -conotoxins bind to this site.

1.3. Nav channels and pain

Tissue damage is experienced as a distressing sensory perception upon which our natural defence mechanism triggers pain or noxious sensation (Cardoso and Lewis, 2018). Nav channels, together with other ion channels and receptors, are important in pain pathways. Interestingly, Nav channels are involved in both acute pain pathways and in chronic pain. Chronic pain is considered a major burden for human society and is defined as lasting more than 3 months, excessive to the degree of injury and often not or poorly treatable (Treede et al., 2015). Chronic pain can be classified in two distinct categories, nociceptive pain and neuropathic pain.

The first category is nociceptive pain that is related to tissue damage and inflammatory pain such as joint inflammation or skin burn injury. Injury of tissue leads to local inflammation and the accumulation of multiple inflammatory mediators that will trigger the release of secondary mediators. Nociceptive pain is hereby a consequence of the increase in excitability of afferent neurons innervating the damaged tissue (Cardoso and Lewis, 2018).

The second category of chronic pain is neuropathic pain which is a consequence of nerve damage or disorders of the nervous system. Neuropathic pain is associated by significant changes in both the peripheral and central nervous system. These changes in the nervous systems can induce re-expression of Nav channels. Furthermore, alteration of the synthesis and transport of Nav channels results in changed axonal trafficking and altered nodal composition (Bennett et al., 2019; Cardoso and Lewis, 2018). Specific Nav channel isoforms are involved in nociceptive signalling. Since the Nav channel isoforms all have differing kinetics and distinct expression patterns, each isoform contributes to different pain disorders (Figure 7).

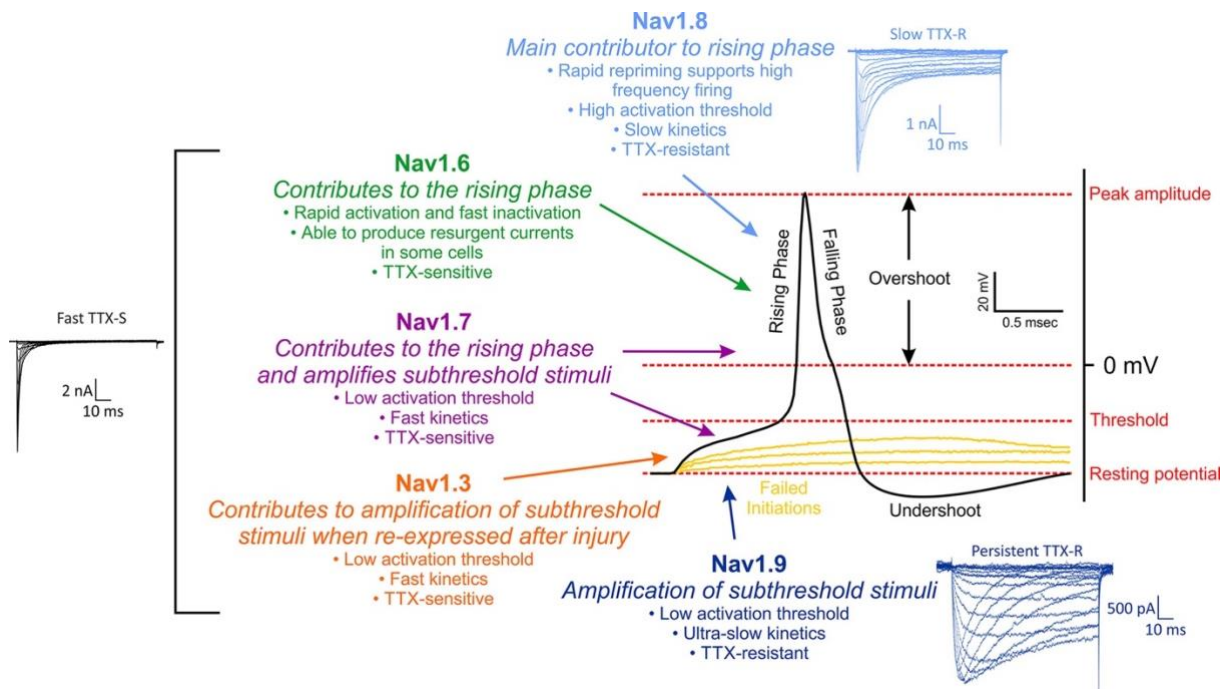


Figure 7. Overview on the distinct contribution of the different Nav channel isoforms to the rising phase of the action potential. Representative action potential waveform recorded from a small-diameter nociceptive dorsal root ganglia neuron, excited by a depolarizing current step of 200 pA is shown. Inset: representative current traces of fast TTX-S (sensitive) currents from Nav1.3, Nav1.6, or Nav1.7; slow TTX-R (resistant) currents from Nav1.8, and persistent TTX-R currents from Nav1.9. Figure was adapted from (Bennett et al., 2019).

Nav1.1 channels were found to be important in mechanical but not thermal pain (Osteen et al., 2016). Using 2 spider venom derived toxins, it was shown that the selective activation of Nav1.1 channel leads to pain and mechanical hypersensitivity. Nav1.3 expression is high during development but nearly undetectable in adulthood (Waxman et al., 1994). Nevertheless, Nav1.3 expression is strongly upregulated upon nerve injury and demyelination (Bennett et al., 2019; Garry et al., 2005). Neuropathic pain states, including thermal pain, are linked to Nav1.6 channels (Bennett et al., 2019; Cardoso and Lewis, 2018). The nodes of Ranvier in myelinated sensory afferents display a dense expression of Nav1.6 channels. Following nerve damage, the expression of Nav1.6 channels increases in the nodes of Ranvier (Caldwell et al., 2000). Nav1.6 channels generate resurgent currents that facilitate repetitive firing and hereby contributes to persistent pain sensation (Figure 7) (Tanaka et al., 2016). Inflammatory mediators have been reported to mediate the upregulation of Nav1.7 channels in inflammatory and visceral pain

models (Black et al., 2004). In the last decade, Nav1.7 has emerged as a key target for inflammatory pain therapeutics. Given its crucial role in pain perception, numerous studies have been devoted to the development of selective inhibitors of this Nav channel. Besides small molecules, several venom-derived peptide toxins are being developed as potential Nav1.7 targeting therapeutics (Table 1). The expression of Nav1.7 channels is mostly limited to the peripheral nervous system and therefore, one can hope that selective inhibitors of Nav1.7 will be efficient analgesics with fewer side effects than the currently available analgesics (Bennett et al., 2019).

Toxin	Organism Species	Nav subtypes targeted	Preclinical/clinical studies showing therapeutic efficacy	Reference
TTX	Puffer fish Family <i>Tetraodontidae</i>	Nav1.1–Nav1.4, Nav1.6 and Nav1.7	Inflammatory and neuropathic muscle mechanical hyperalgesia Inflammatory thermal and mechanical pain Inflammatory, visceral and neuropathic pain Burn-associated neuropathic pain Chemotherapy-induced neuropathic pain (clinical trials)	Alvarez and Levine (2015) Beloil <i>et al.</i> (2006) Marcil <i>et al.</i> (2006) Salas <i>et al.</i> (2015) Wex Pharmaceutical Inc.
Neosaxitoxin	Dinoflagellates	Nav _s	Bladder pain syndrome (clinical trials)	Manriquez <i>et al.</i> (2015)
Gonyautoxin	Dinoflagellates	Nav _s	Chronic tension-type headache (clinical trials)	Lattes <i>et al.</i> (2009)
ProTx-II	Spider <i>T. pruriens</i>	Nav1.7	Painful diabetic neuropathy Inflammatory pain	Tanaka <i>et al.</i> (2015) Flinspach <i>et al.</i> (2017), Patent US20150099705 A1
HnTX-IV	Spider <i>H. haianum</i>	Nav1.2, Nav1.3 and Nav1.7	SNI-induced neuropathic pain and formalin-induced inflammatory pain	Liu <i>et al.</i> (2014a)
μ-TRTX-HI1a	Spider <i>H. lividium</i>	Nav1.8	Inflammatory and neuropathic pain	Meng <i>et al.</i> (2016)
HwTx-IV	Spider <i>O. huwena</i>	Nav1.7	Inflammatory pain and SNI-induced neuropathic pain	Liu <i>et al.</i> (2014b)
μ-TRTX-Pn3a	Spider <i>P. nigricolor</i>	Nav1.7	Inflammatory pain, co-administrated with opioid	Deuis <i>et al.</i> (2017)
μO-MrVIB	Cone snail <i>C. marmoreus</i>	Nav1.8	Allodynia and hyperalgesia associate to neuropathic and chronic inflammatory pain Post-incision allodynia	Ekberg <i>et al.</i> (2006) Bulaj <i>et al.</i> (2006)
μO-MfVIA	Cone snail <i>C. magnificus</i>	Nav1.4 and Nav1.8	Inflammatory pain (analogue E5K and E8K MfVIA)	Deuis <i>et al.</i> (2016a)
μ-KIIIA	Cone snail <i>C. kinoshitai</i>	Nav1.2, Nav1.4, Nav1.6 and Nav1.7	Inflammatory pain	Zhang <i>et al.</i> (2007) and Han <i>et al.</i> (2009)
μ-SIIIA	Cone snail <i>C. striatus</i>	Nav1.2, Nav1.4 and Nav1.6	Inflammatory pain	Green <i>et al.</i> (2007)

Table 1. Currently ongoing preclinical and clinical trials with venom-derived peptide toxins. Figure adapted from (Cardoso and Lewis, 2018).

Nav1.8 channels are involved in both nociception and chronic pain since these channels have a critical role in repetitive firing (Figure 7). Moreover, Nav1.8 channels are expressed in free

nerve endings, where external stimuli are detected, and action potentials are generated (Bennett et al., 2019). In inflammatory pain, the inflammation-induced mediators change Nav1.8 expression levels which contribute significantly to pain (Hucho and Levine, 2007). In neuropathic pain, a complex phenotype of Nav1.8 expression is reported. Following axonal damage, the expression levels of Nav1.8 channels is strongly reduced in both small and large DRG neurons (Sleeper et al., 2000). Contradictorily, Nav1.8 upregulation is observed in uninjured neurons after spinal nerve ligation, suggesting that Nav1.8 channel redistribution occurs to axons of undamaged unmyelinated afferents (Bennett et al., 2019; Gold et al., 2003). Biophysical and pharmacological characterisation of Nav1.9 has been limited compared to the other Nav channels. This was due to difficulties in studying Nav1.9 in neurons and the lack of functional expression of this channel in heterologous expression systems. It is only till recent years that progress has been made in efficient expression systems for Nav1.9 channels, allowing a more comprehensive understanding of the unique properties of Nav1.9 channels and their contribution in generation of action potentials (Figure 7). Nav1.9 has been implicated in cold, visceral and bone cancer pain (Lolignier et al., 2015; Qiu et al., 2012). Furthermore, this channel is suggested to be involved in inflammatory pain as well (Priest et al., 2005). Nevertheless, more research is still needed to elucidate more details on the normal physiological role and involvement in pathological conditions for Nav1.9 channels.

1.4. Cone snail venom as a source of drug discovery

Contrary to popular belief, a majority of medicine used today in the western society is derived of natural sources (Newman and Cragg, 2016). Animal venoms represent one of the natural sources of potential drugs that has received more and more attention in the last decades (Robinson et al., 2017). Marine gastropods known as cone snails (*Conus*) are one of the largest single genus of living marine invertebrates. All cone snails are venomous predators and possess

a very complex venom apparatus. They use their venom for capturing prey as well as to defend themselves. Based on their prey, cone snails can be divided into three groups: vermivorous (worm-hunting), piscivorous (fish-hunting), and molluscivorous (mollusc-hunting) cone snails (Figure 8) (Prashanth et al., 2017).

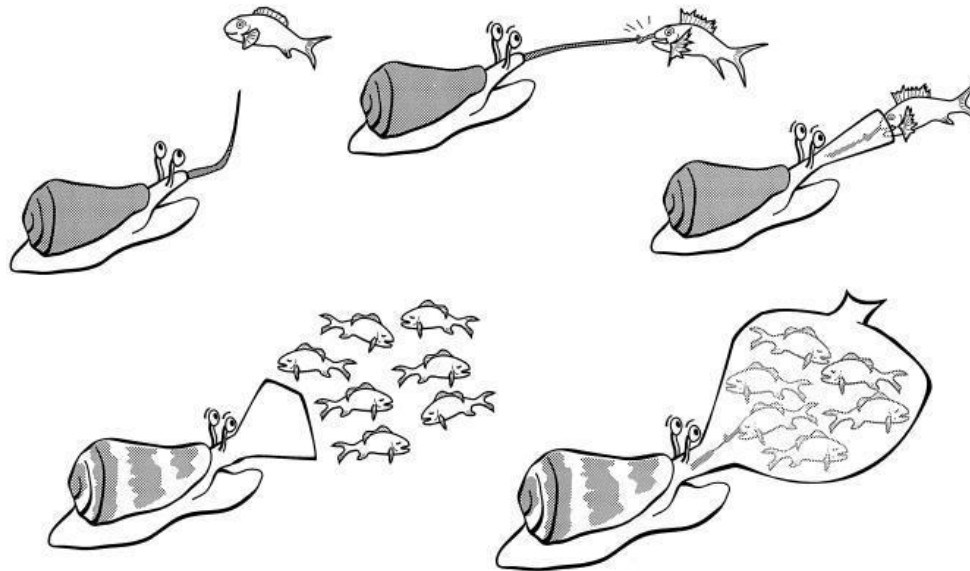


Figure 8. A cartoon showing the different fish-hunting strategies. (*top three*) ‘Hook-and-line-fishing’ strategy, where the snails use their long proboscis to sting their prey with the harpoon-like teeth. (*bottom two*) ‘Net-fishing’ strategy where the prey is engulfed with a large distensible mouth before stinging. Figure adapted from (Olivera, 1997).

More than 800 different cone snail species are known today, and each species produces an unprecedented molecular diversity of up to 1000 distinct pharmacologically active components. The venom of each different *Conus* species has a different set of peptides, resulting in an estimated array of more than 800,000 peptides. Cone snail venoms can be seen as an untapped cocktail of biologically active compounds that are increasingly recognized as an emerging source of peptide-based therapeutics. Each conopeptide is encoded by a single messenger ribonucleic acid (mRNA) and translated as a prepropeptide precursor that is proteolytically cleaved at specific sites to yield the mature toxin. Although hypermutation of peptide sequences is the main cause for conopeptide diversity, post-translational modifications provide an

overlying level of diversity (Green and Olivera, 2016; Prashanth et al., 2017). Conopeptides can be classified into two major groups: the disulfide-poor and the disulfide-rich conopeptides, the latter also called conotoxins. These are classified into superfamilies, based on a conserved signal sequence found in the precursor peptide and in their cysteine framework, and subsequently into pharmacological families based on the targets they interact with (Figure 9). Up to date, 26 cysteine frameworks have been identified. These frameworks can be classified in 27 gene superfamilies and 12 different pharmacological families (Kaas et al., 2012; Karbat et al., 2007).

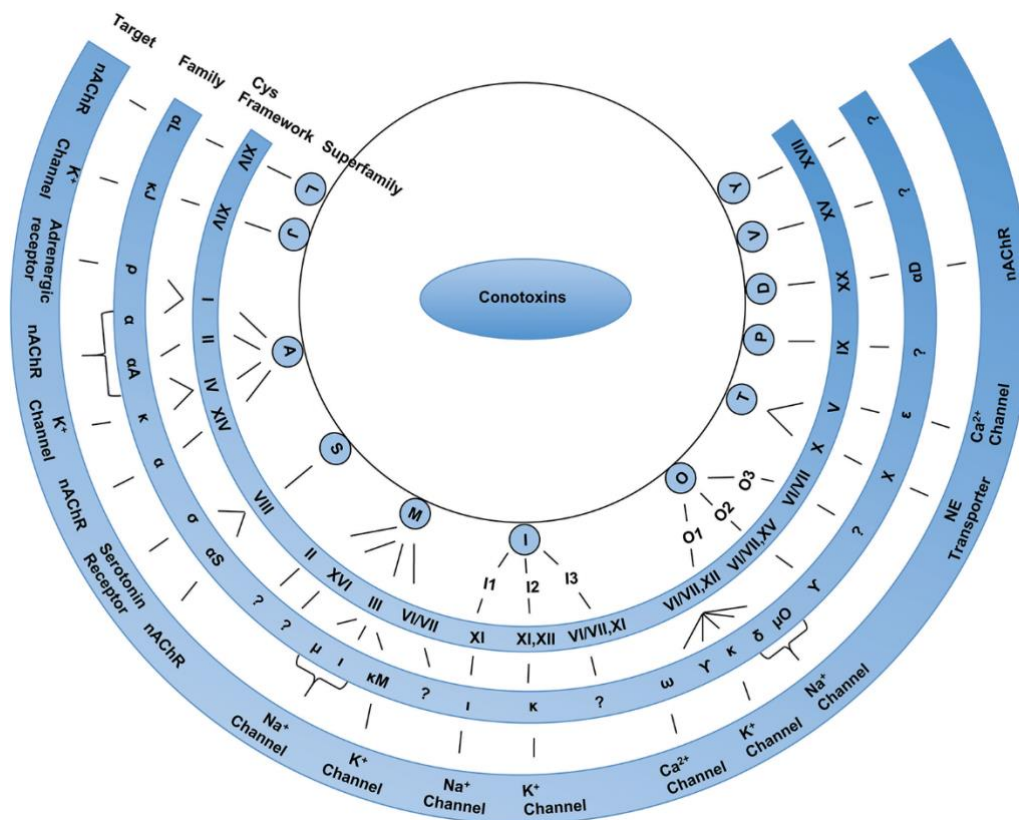


Figure 9. Classification of conotoxins into gene superfamilies (based on their conserved signal sequence homology), cysteine framework and pharmacological families (based on their target receptor). Target receptors for the conotoxin families, which do not have a specified receptor shown in this figure, are yet to be identified. NE = norepinephrine; nAChR = nicotinic acetylcholine receptor. Figure adapted from (Akondi et al., 2014b).

To date, only 0.1% out of potentially 800,000 venom components has been functionally and structurally investigated. Nevertheless, the consideration of *Conus* venoms as gold mines for the discovery of new therapeutics is validated by the knowledge that, out of the limited number of studied conopeptides, at least ten peptides have reached human clinical trials, and one (Ziconotide, Prialt®) was approved as an analgesic in 2004 (Safavi-Hemami et al., 2018; Webster, 2015) (Table 2). The toxins of *Conus* sp. are usually potent, selective and small (typically <5 kDa) which is an advantage for cost-effective synthesis and makes them ideal pharmacological probes (Lewis et al., 2012; Safavi-Hemami et al., 2018).

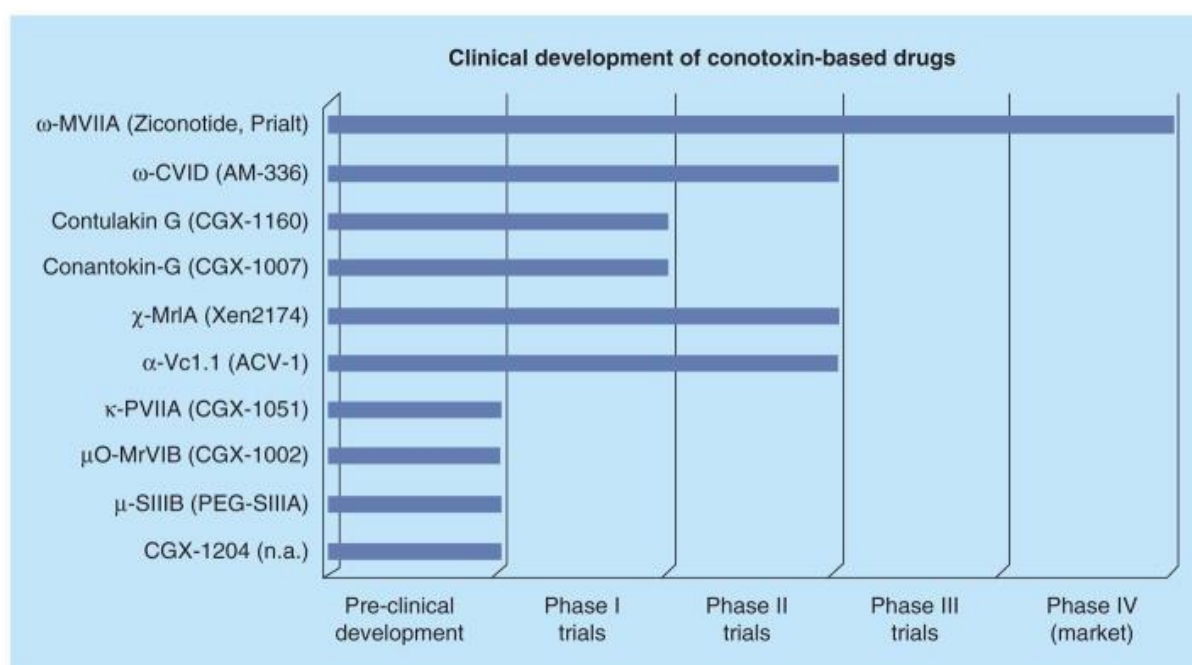


Table 2. Conotoxins at various stages of preclinical and clinical development. Figure adopted from (Green et al., 2014).

The ω -conotoxin ω -MVIIA, later on called Ziconotide, is a 25 amino acid peptide characterized from the venom of the cone snail *Conus magus*. It is a potent and selective inhibitor of N-type calcium channels and more specific Cav2.2 channels. Therefore, it represented an analgesic therapy for neuropathic pain related to several disorders such as multiple sclerosis, cancer, nerve damage, stroke and diabetes (Anand et al., 2015). The synthetic version of ω -MVIIA,

marketed as **Prialt**[®] (the ‘**Primary Alternative**’ to Morphine) was the first cone snail peptide to gain FDA approval in 2004 for the treatment of neuropathic pain. The success of Prialt[®] can be explained by the fact that it is a non-opioid analgesic that thus not exert the unwarranted side effects as observed with opioids such as respiratory depression and withdrawal phenomenon. However, application of the Prialt[®] is limited due to inefficient systemic delivery methods, a hurdle shared with most peptide-based drugs. Prialt[®] does not cross the blood brain barrier and therefore needs to be administered by means of an intrathecal drug delivery system which allows the peptide to be directly delivered to the cerebrospinal fluid (Safavi-Hemami et al., 2018, 2019). Moreover, Prialt[®] induces psychomotor side effects such as mild to more debilitating ataxia, auditory hallucinations and psychosis (Safavi-Hemami et al., 2018, 2019). Although these side effects can be mostly avoided by careful dosing, the very narrow therapeutic window does represent limitations on the application of this analgesic (McDowell and Pope, 2016). Nevertheless, the introduction of Prialt[®] onto the market not only demonstrated the therapeutic potential of conotoxins but also stimulated more interest from biotechnology companies into conotoxin research (Akondi et al., 2014a; Pope and Deer, 2013).

1.4.1. Conotoxins acting on Nav channels

Five families of conotoxins target Nav channels (Figure 9). These are categorized according to either their functional agonistic or antagonistic effects. δ -Conotoxins and ι -conotoxins produce agonistic effects, whereas μ O-conotoxins, μ O \S -conotoxins and μ -conotoxins exert antagonistic effects (Green and Olivera, 2016; Israel et al., 2017a; Lewis et al., 2012). μ -conotoxins physically and electrostatically occlude the pore, whereas μ O-conotoxins prevent activation by binding on the voltage-sensing domain on the extra-cellular surface of the channel. The toxin family relevant for this thesis are the μ -conotoxins. They display a typical folding pattern called framework III. In this conformation, three conserved disulphide bridges are formed between

Cys1-Cys4, Cys2-Cys5, and Cys3-Cys6 (Cys residues are numbered according to their order in the total sequence) (Green et al., 2014; Green and Olivera, 2016; Israel et al., 2017a; Lewis et al., 2012). Binding experiments have shown that μ -conotoxins compete with TTX and saxitoxin for binding to site1, located in the outer part of the ion-conducting pore of the channel (Figure 1 & 6). However, their binding site is not identical, but overlapping. Other contact points on the outer channel vestibule are possibly also essential with respect to their binding (French et al., 2010a; Green and Olivera, 2016). It is their high potency as well as small size (16–26 AAs) and selectivity that render μ -conotoxins very promising as novel ligands with therapeutic potential (French et al., 2010a; Green and Olivera, 2016).

1.4.2. μ -conotoxins

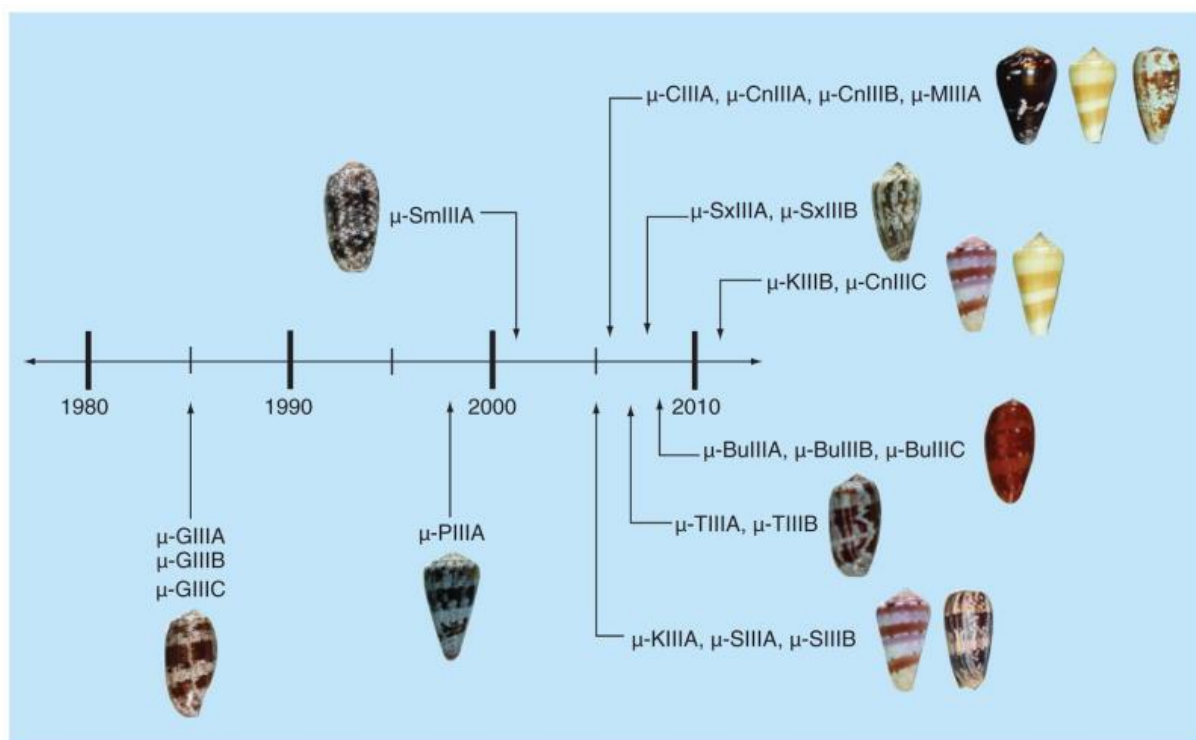


Figure 10. The timeline illustrates the chronological discovery of the μ -conotoxins. Figure adapted from (Green and Olivera, 2016).

The class of μ -conotoxins are increasingly recognized as interesting Nav channel inhibiting peptides. Ample research in the last decade has demonstrated that the μ -conotoxins are very well suited for peptide engineering involving structure modifications and amino acid replacements which allow to fine-tune the selectivity profile of these peptides and to optimize their pharmacological properties (Green et al., 2014; Green and Olivera, 2016). The first μ -conotoxins were discovered more than three decades ago (Figure 10). In 1985, the first three μ -conotoxins, μ -GIIIA, μ -GIIIB and μ -GIIIC, were isolated from the venom of *Conus geographus* (Cruz et al., 1985). Later on, μ -conotoxins were isolated from other *Conus* species such as *C. purpurascens*, *C. stercusmuscarum*, *C. striolatus*, *C. tulipa*, *C. kinoshitai*, *C. striatus*, *C. catus*, *C. magus* and *C. bullatus* (Tosti et al., 2017). Up to date, approximately 32 cone snail venom derived peptides have been suggested to be μ -conotoxins. However, several of these peptides still await their functional characterization. Nevertheless, for 21 peptides it was experimentally shown that these peptides inhibit Nav channels (Green et al., 2014). The sequences of the best-characterized μ -conotoxins are shown in figure 11. The μ -conotoxin family can be further divided in a m4 and m5 branch based on the preference for muscle versus neuronal Nav channel isoforms, respectively (Figure 11) (Green et al., 2014). All μ -conotoxins are characterized by a type III framework in which three disulfide bridges are formed between six cysteine residues (Figure 11 & 12) (Green and Olivera, 2016). These disulfide bridges provide an important stabilization of the overall structure of conotoxins in general and μ -conotoxins specifically. In general, the μ -conotoxins are rich in basic amino acids, which are responsible for the interaction with the acidic residues of the outer vestibule within the ion-conducting pore region of the Nav channels. Indeed, it has been shown for several μ -conotoxins that the substitution of a single basic residue already can result in a complete loss of Nav channel binding (Green and Olivera, 2016; Lipkind and Fozzard, 2000).

1.4.2.1. Muscle Nav channel isoform preferring μ -conotoxins

The 3 μ -conotoxins isolated from *C. geographus*, μ -GIIIA, μ -GIIIB and μ -GIIC, have been characterized as potent Nav channel inhibitors, which show a strong preference for muscle over nerve Nav channels (Cruz et al., 1985). In fact, the experiments with μ -GIIIA were among the first studies to show that discrete Nav channel isoforms exist within different excitatory tissues (Green et al., 2014; Moczydlowski et al., 1986). Ala-scanning experiments, together with solution structure determination of μ -GIIIA, revealed that the amino acid residues that are important for interaction with the Nav channels are almost all located in the C-terminal part of the peptide (Figure 12). The Arg13, Lys16, Arg19 and Hyp17 are orientated on the same molecular surface and thus it can be assumed that this region of the peptide interacts with Nav channel (Moczydlowski et al., 1986; Sato et al., 1991). Furthermore, it is interesting to note that the solution structure of μ -GIIIA showed that the hydroxyl group of Hyp17 is in close proximity of the guanidine group of Arg13. This observation founded the hypothesis that μ -conotoxins might interact with Nav channels in way, similar as the guanidinium toxins, which block Nav channels by binding at site 1 (Figure 1). Indeed, later on, in competitive binding experiments using labeled TTX and μ -GIIIA, it was shown that the μ -conotoxin and guanidinium toxins compete for binding at Nav channels (Green et al., 2014; Yanagawa et al., 1987).

	ER Signal sequence	Propeptide sequence	Mature toxin	Toxin name
m4 branch	MSKLGVLLTICLLLFPLTA	LPMDGDEPANRPVERMQDNISSEQYPLFEKR	RDCC ¹ TOOKK-CKDR ² QC ³ KOQR-CCA	μ -GIIIA
			RDCC ¹ TOORK-CKDR ² RCKOMK-CCA	μ -GIIIB
			RDCC ¹ TOOKK-CKDR ² RCKOLK-CCA	μ -GIIC
			RHG ¹ CCKGOKG-CSS ² RE ³ CROQH-CC	μ -TIIIA
			ZRL ¹ CGFOKS-CRS ² RQCKOHR-CC	μ -PIIIA
			RCCTGKKGSCSG ² RACKNLK-CCA	μ -SxIIIA
			ZKCC ¹ TGKKGSCSG ² RACKNLK-CCA	μ -SxIIIB
m5 branch	MSKLGVLLTICLLLFPLTA	LPMDEDQPADQLED ² RMQDDISSEQYPSFVRR	ZNCC-NG--G ¹ CSK ² WCRDHARCC	μ -SIIIA
			ZNCC-NG--G ¹ CSK ² WCKGHARCC	μ -SIIIB
			CC-N-----C ¹ SSK ² WCRDHSRCC	μ -KIIIA
			NGCC-N-----C ¹ SSK ² WCRDHSRCC	μ -KIIIB
			ZRCC-NGRRG ¹ CSS ² RWCRDHSRCC	μ -SmIIIA
			VTDR ¹ CCKNGKRGCG- ² RWCRDHSRCC	μ -BuIIIA
			VGER ¹ CCKNGKRGCG- ² RWCRDHSRCC	μ -BuIIIB
			GRCC-EGPNG ¹ CSS ² RWCKDHARCC	μ -CIIIA
			GRCC-DVPNA ¹ CSS ² RWCRDHAQCC	μ -CnIIIA
			ZGCC-GEPNL ¹ CFT ² RWCRN ³ NARCC ⁴ RQQ	μ -CnIIIB
			ZGCC-NGPKG ¹ CSS ² WCRDHARCC	μ -CnIIIC
ZGCC-NVPNG ¹ CSS ² RWCRDHAQCC	μ -MIIIA			

Figure 11. Summary of identified μ -conotoxins from m4 and m5 branches of the M-superfamily. ER signal and propeptide sequences for μ -GIIIA and μ -SIIIA are illustrated as examples. ‘O’ denotes hydroxyproline; ‘Z’ denotes pyroglutamic acid. Arg13 in μ -GIIIA, or the residue in the equivalent position, is underlined to illustrate the sequence differences among conotoxins that preferentially block muscle versus neuronal subtypes. ER: Endoplasmic reticulum. Figure adapted from (Green et al., 2014).

From the venom of *C. purpurascens*, the μ -conotoxin μ -PIIIA was isolated (Shon et al., 1998). This 22-residue peptide also displayed a strong preference for muscle type Nav channel isoforms. μ -PIIIA inhibits Nav channels irreversibly. The solution structure of this peptide provided further evidence that μ -conotoxins interact with the Nav channel in a similar manner as the guanidinium toxins. As was seen for μ -GIIIA, the hydroxyl group of Hyp18 is oriented close to the guanidine group of Arg14 (Nielsen et al., 2002). Structure-function studies on μ -PIIIA have shown that the basic residues are the key residues for the recognition and binding of this peptide to the Nav channels (Li and Tomaselli, 2004).

Another interesting μ -conotoxin was characterized from the venom *C. tulipa* (Figure 11 & 12). μ -TIIIA inhibits Nav1.2 and Nav1.4 channels at lower nM concentrations (Lewis et al., 2007; Wilson et al., 2011). Ala-scanning experiments demonstrated that substitution of Lys6, Lys9, Arg17 and His20 decreases the activity while replacing His2, Glu15 and Gln19 enhances the potency of μ -TIIIA (Figure 12). Furthermore, mutating Glu15 into an Ala results in increased channel inhibition and alters the preference of μ -TIIIA towards neuronal Nav channel isoforms. It thus seems that the presence of a negative charge at position 15 can be considered as unfavorable for interaction with the Nav channel (Schroeder et al., 2012).

μ -SmIIIA has been identified from the cDNA library of the venom of *C. stercusmuscarum* (West et al., 2002). Within the family of μ -conotoxins, this peptide is rather an outsider. Besides the cysteine pattern, μ -SmIIIA shares little sequence identity with the other μ -conotoxins (Figure 11 & 12). This is further indicated by the solution structure of μ -SmIIIA which display significant differences in the orientation of specific amino acid residues and

overall topology. It is suggested that these differences in sequence and structure are related to the potent activity of μ -SmIII A on TTX-resistant Nav channels. In fact, its strong affinity for the TTX-resistant cardiac Nav1.5 channel deprives μ -SmIII A of any consideration for therapeutic application (Wilson et al., 2011).

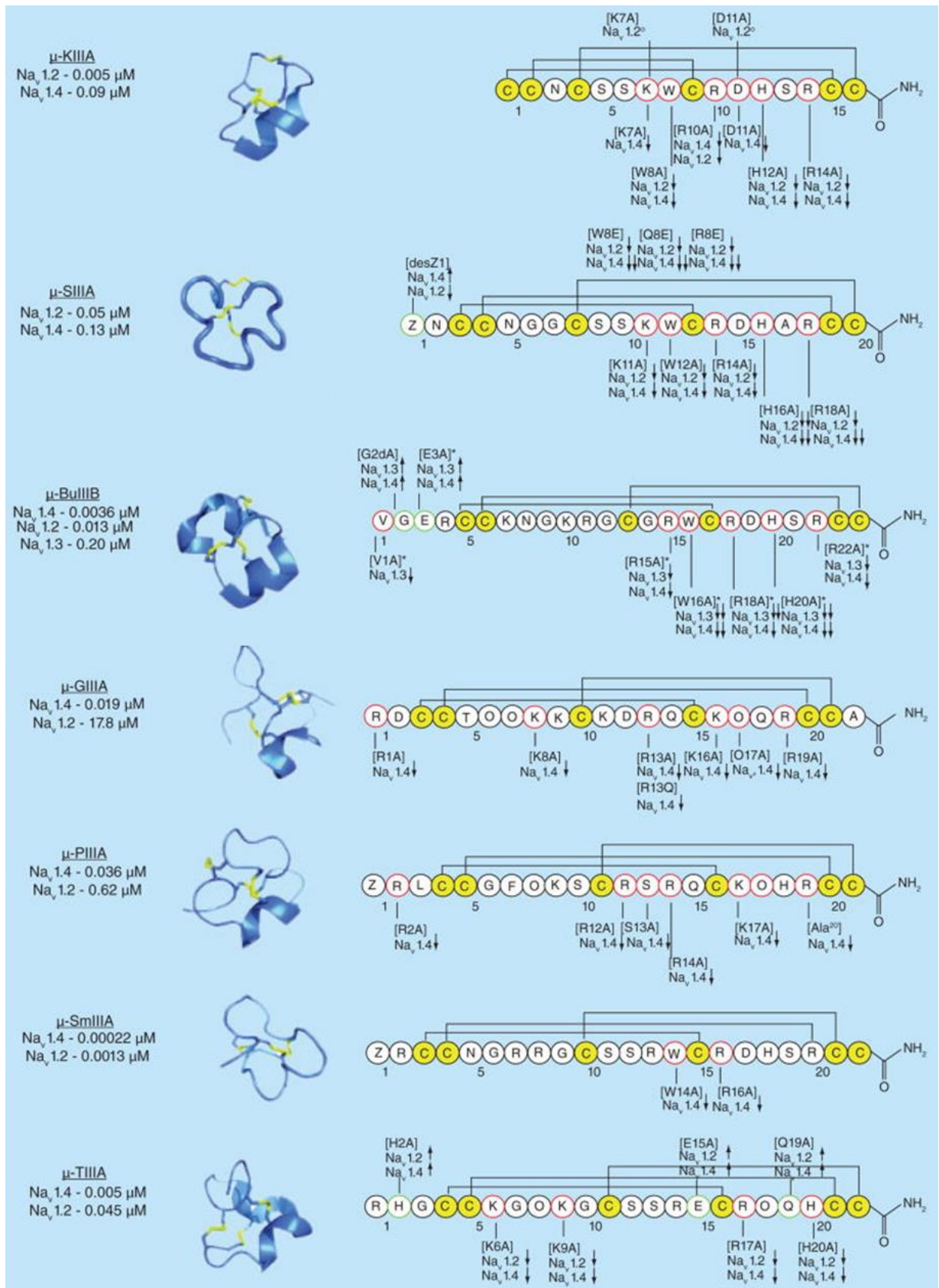


Figure 12. Structure–activity characterization of μ -conotoxins (cont.). Potencies of characterized μ -conotoxins against skeletal ($Na_v1.4$) and neuronal ($Na_v1.2$) subtypes. Solution structures showing the folded peptide structures with disulfide connectivity. PDB ID: 1TCK (μ -

GIIIA), 1R9I (μ -PIIIA), 1Q2J (μ -SmIIIA), 2LXG (μ -KIIIA) and 2LO9 (μ -BuIIIB). BMRB Entry# 20024 (μ -TIIIA) and 20023 (μ -SIIIA). The resultant of individual amino acid replacements on Nav channel subtype affinity are shown. (\uparrow) indicates mutations that improve potency against Nav channel subtypes, (\downarrow) denotes decreased potency. (desZ1) indicates deletion of pyroglutamic acid in position 1 of μ -SIIIA. Figure adapted from (Green et al., 2014).

1.4.2.2. Neuronal Nav channel isoform preferring μ -conotoxins

Investigation of the venom of *C. striatus* resulted into the discovery of 2 μ -conotoxins which differ from each other by two residues (Figure 11) (Lewis et al., 2007). μ -SIIIA exhibits a threefold selectivity for Nav1.2 over Nav1.4 channels. This selectivity is even enhanced by the removal of the N-terminal pyroglutamate since deletion of this residue increased the potency for Nav1.2 and at the same time decreased the activity for Nav1.4 (Wilson et al., 2011). μ -SIIIA was also subjected to Ala-scanning experiments which demonstrated that, in concordance with studies on other μ -conotoxins, the C-terminal is determining for Nav channel recognition and binding (Figure 12) (Bulaj et al., 2005). Substitution of Lys 11, Trp12, Arg14, His16 and Arg18 resulted in the most significant alterations of Nav channel inhibition (Bulaj et al., 2005). Interesting to note is that the Ala replacement of His16 resulted in a decreased binding affinity for both neuronal and muscle Nav channel isoforms, indicating that this residue is involved in general binding of Nav channels. The structure-function data on μ -SIIIA aided in a better understanding of the structural differences within the μ -conotoxin family. μ -conotoxins that exert a preference for neuronal Nav channel isoforms share a high sequence identity at the C-terminus but differ from the C-termini of the μ -conotoxins that preferably bind to muscle Nav channel isoforms (Yao et al., 2008). ^{13}C NMR relaxation experiments with μ -SIIIA demonstrated that the N-terminus is very flexible while the C-terminus is rather rigid (Yao et al., 2008). This observation, together with the results of the structure-function experiments, allowed to suggest a general hypothesis on the structural properties of μ -conotoxins in which the N-terminus of the peptides contributes to the Nav channel isoform selectivity while the C-

terminus is mainly important for recognition and interaction with neuronal Nav channel isoforms.

Three μ -conotoxins have been purified from the venom of *C bullatus* (Holford et al., 2009). These three peptides, μ -BuIIIA, μ -BuIIIB and μ -BuIIIC, all have extended N-termini compared to the other μ -conotoxins (Figure 11). Selectivity profile determination of μ -BuIIIA and μ -BuIIIB indicated that both toxins show the strongest affinity for Nav1.2 and Nav1.4 channels (Wilson et al., 2011). Interestingly, μ -BuIIIB also potently inhibits Nav1.3 channels (Wilson et al., 2011). An Ala-walk of μ -BuIIIB showed that the residues in the N-terminal part of the peptide are contributing to the potency but not the selectivity of μ -BuIIIB (Figure 12). Interestingly, Ala substitution of Gly2 or Glu3 resulted in an increased Nav1.3 potency (Zhang et al., 2007).



Figure 13. *Conus kinoshitai* occurs in the South China Sea, the Pacific Ocean and Indian Ocean (Puillandre et al., 2015).

μ -KIIIA, from *Conus kinoshitai*, has only 16 amino acid residues, which makes it the smallest μ -conotoxin described so far (Figure 12) (Bulaj et al., 2005). Interestingly, and in contrast to the other μ -conotoxins described here above, μ -KIIIA blocks preferentially neuronal Nav channel isoforms (Bulaj et al., 2005). Indeed, μ -KIIIA displays a 20 fold higher affinity for neuronal over muscle type Nav channel isoforms (Zhang et al., 2007). μ -KIIIA shows potent activity on TTX-sensitive mammalian sodium channels. Structure–activity studies and an Ala-walk have shown that the residues on the α -helix in the C-terminal part (Lys7, Trp8, Arg10, Asp11, His12 and Arg14) are functionally important (Figure 12). Moreover, replacement of Lys7, Trp8 and Asp11, single or in combination, yields more selective blockers, discriminating between neuronal and skeletal sodium channels (McArthur et al., 2011; Stevens et al., 2012; Van Der Haegen et al., 2011). For example, Trp8, Arg10, His12 and Arg14 are determining residues for Nav1.2 preference of μ -KIIIA (Zhang et al., 2007). The Lys7 of μ -KIIIA can be considered as a key epitope for both efficacy and potency of μ -KIIIA inhibition. Substitution of this basic residue with a neutral Ala resulted in a decreased activity on Nav1.4 channels while the activity on Nav1.2 remained unchanged and thus hereby creating an increased selectivity window (Zhang et al., 2007). The Trp8 was found to be important for the ability of μ -KIIIA to distinguish between neuronal and muscle Nav channel isoforms. Remarkably, substitution of this residue with an Ala resulted in a reduced maximal inhibition with 50% and 20% for Nav1.2 and Nav1.4 channels, respectively (Zhang et al., 2007). This substitution also altered the kinetics of inhibition for Nav1.2 channels but not Nav1.4 channels. In concordance herewith, it was demonstrated that replacing Trp8 with an amino acid residue of a less hydrophobic nature, enhanced the reversibility of channel inhibition (Van Der Haegen et al., 2011). Importantly, mutating Trp8 contributes to reduced Nav1.4 potency and thus creates opportunities to engineer μ -KIIIA towards peptides with an increased selectivity for neuronal Nav channel isoforms. Ala replacement of His12 also resulted in an increased affinity for Nav1.2 and Nav1.7 channels and

a decreased Nav1.4 channel inhibition (McArthur et al., 2011). Similar, mutations of Arg14 allows shifting of the preference towards Nav channel isoforms of the peripheral nervous system (McArthur et al., 2011). It is believed that the Arg14 of μ -KIIIA forms tight interactions with the Asp1241 of domain III of the outer ring of the P-loop of Nav1.2 and Nav1.4. It is believed that this strong interaction, at least in part, is responsible for the strong binding affinity of μ -KIIIA on Nav1.2 and Nav1.4 channels. Interestingly, Nav1.7 channels display an Ile residue at the corresponding position within the P-loop of the outer vestibule. This indicates that peptide engineering of μ -KIIIA might result in peptides selectively targeting for instance pain related Nav channels such as Nav1.7 (McArthur et al., 2011) (Green et al., 2014). Several derivatives of μ -KIIIA have been synthesized and tested for their ability to block Nav channels. The obtained data provided interesting structure-function data (Figure 12 & 13) (Khoo et al., 2011b). For example, it was shown that the CysII-CysV and CysIII-CysVI disulphide bridges are required for overall structure stability and activity. However, the μ -KIIIA analogues with the CysI-CysIV removed retained the same potent biological activity as the wild type peptide. This can be explained by the fact that the removal of this disulphide bridge results in a greater flexibility of the N-terminal region but does not affect the α -helical region at the C-terminus, which is crucial for Nav channel interaction (Khoo et al., 2011b). Synergistic and antagonistic interactions between μ -KIIIA and TTX in the blocking of sodium channels have been described as well (French et al., 2010a; Green et al., 2014; Green and Olivera, 2016; Israel et al., 2017a; Lewis et al., 2012). *In vivo* experiments, using mice, demonstrated that upon systemic administration of μ -KIIIA a decrease in the frequency of paw licking without impairment of the motor performance. These experiments suggest for μ -KIIIA a possible therapeutic application as an anti-inflammatory analgesic. Overall, the results obtained from the structure-function studies and *in vivo* experiments on μ -KIIIA renders this peptide as an in-depth characterised template for further peptide engineering.

Figure 14 provides an overview of all data available in the literature on Nav channel selectivity profiling and structure-function studies performed with μ -conotoxins. This figure confirms that specific changes in amino acid composition allow altering the Nav channel isoform selectivity. Furthermore, it can be concluded that μ -conotoxins represent interesting scaffolds to be used as templates for peptide engineering. Their high potency and the intrinsic specificity towards Nav channels combined with the amenability to chemical modification renders μ -conotoxins as attractive alternatives of currently used low molecular weight inhibitors of Nav channels.

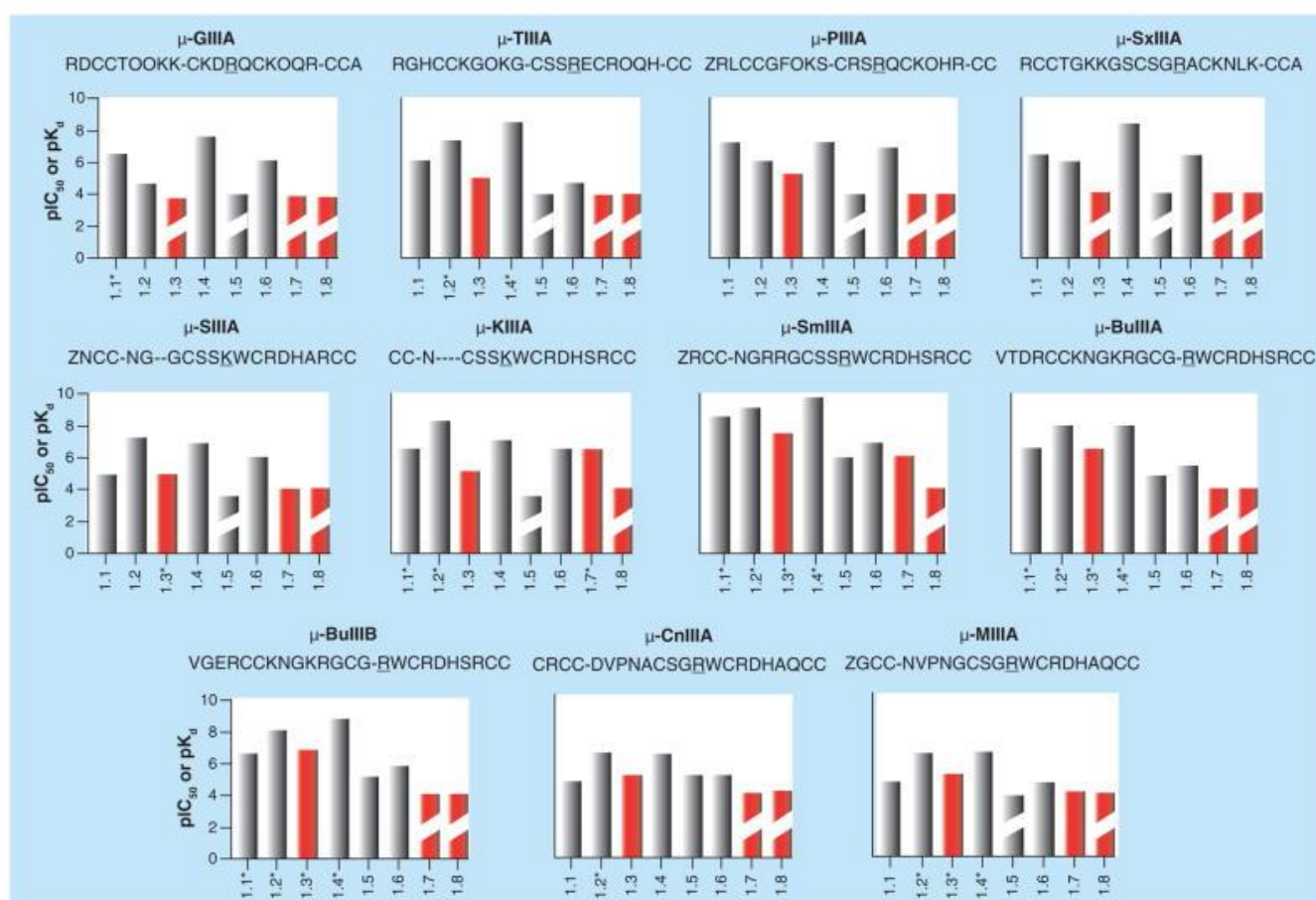


Figure 14. Selectivity profiles of μ -conotoxins against Nav1-subtypes. Data were obtained from reported IC_{50} values; *represents data obtained from pK_d values (Wilson et al., 2011). Pain-relevant subtypes are highlighted in red. Broken bars represent values greater than 100 μ M. Figure adapted from (Green et al., 2014).

1.5. Spider venom as a source of drug discovery

Spiders can be considered as one of the most successful venomous animals ever to inhabit the planet. So far over 47000 species have been characterised (Pineda et al., 2014). According to ArachnoServer, approximately the venom of 100 species of spiders has been studied. This has resulted in 1427 characterized spider venom peptides (Herzig et al., 2011; Pineda et al., 2018). Since it is believed that spider venoms contain over 10 million biologically active peptides, no more than 0.01% of spider peptides have thus been studied so far (Escoubas, 2006; Klint et al., 2012). Therefore, spider venom can be considered as an untapped treasure of biological active compounds that are potentially interesting for drug discovery as well as for the development of bio-insecticides to control pests. To date, no spider peptide-based drug has been approved by the Food and Drug Administration. However, one should take into account the small number of spider venom peptides investigated so far. This is a significant lower number compared for instance with scorpion or snake venom components. Several spider venom peptides have been characterized as insecticidal peptides with a strong preference for insect over mammalian targets. Illustrative hereof is the spider toxin ω/κ -HXTV-Hv1a. This peptide, isolated from the venom of *Hadronyche versuta*, is a potent inhibitor of insect voltage-gated calcium (Cav) channels devoid of activity on mammalian Cav channels. A modified synthetic version of this toxin is the basis of the approved insecticidal agent SPEAR[®] (Fitches et al., 2012; Herzig and King, 2015; King and Hardy, 2013). Recently, exciting research has also highlighted the potential of spider venom-based drug discovery. H11a, a toxin isolated from the Australian funnel-web spider *Hadronyche infensa*, was found to be highly neuroprotective in acid-mediated neuronal injuries. This toxin inhibits acid-sensing ion channel 1a and hereby strongly attenuates for instance brain damage after stroke (Chassagnon et al., 2017). H11a is thus considered as a lead for development of therapeutics to protect the brain from ischemic injury.

1.6. Phoneutria nigriventer

This chapter is based on the following publication with minor changes: *Phoneutria nigriventer* venom: A pharmacological treasure. Peigneur S, de Lima ME, Tytgat J. *Toxicon*. 2018 Sep 1;151:96-110.



Figure 15. *Phoneutria nigriventer*. The right picture shows the *Phoneutria* in the typical defence position, standing on his hind legs while raising four frontal legs up high. Left picture was taken by Daniel Santos at Fundação Ezequiel Dias. Left picture was adapted from (Peigneur et al., 2018).

The spiders of the genus *Phoneutria* are members of the family Ctenidae, suborder Labidognatha, and order Araneidae. They inhabit forests of the neotropical region from Southern Central America (Costa Rica) throughout South America, from the East of the Andes to the North of Argentina. The *Phoneutria* spiders are also known as the “armed spider” because of the characteristic posture they adopt when threatened. When in defence position, the *Phoneutria* will stand on his hind legs while typically raising four frontal legs up high, resulting in an “armed position” (Figure 15, right picture). Another popular name is the “banana spider” which relates to their preference for hiding in banana bunches. The genus *Phoneutria* belongs to the Retrolateral Tibial Apophysis (RTA) clade, whose adaptive and evolutionary process is associated with the loss of cribellate silk and prey-capture webs. They only use silk for the

production of the sacs in which the eggs hatch or for nursery webs. These are wandering spiders with nocturnal habits. They are active hunters, relying on their fast acting and efficient venom for prey capture and defence. Their natural preys are insects although there are reports of *Phoneutria* hunting on other spiders and small rodents as well (de Lima, 2016; Herzig et al., 2002).

Phoneutria nigriventer are very aggressive, solitary spiders. They are synanthropic species, explaining the high number of human accidents occurring with this spider. Human envenomation involving *Phoneutria* spiders occur mainly in Brazil, but there are reports of sporadic cases in Central America and in neighbouring countries (de Lima, 2016). More recently, the export of bananas to Europe has resulted in certain cases of *Phoneutria* envenomation in countries such as the United Kingdom and the Netherlands. Most accidents involving humans are mild with only up to 0.5% of severe cases (Hauke and Herzig, 2017). Despite the venom being highly neurotoxic, the amount inoculated through the bite is usually too small to induce lethal effects. However, fatal envenomation usually occurs after a bite by female specimens. It is reported that females inject a larger amount of venom compared to males. Furthermore, as with most venomous animals, intersexual differences in venom composition have been demonstrated (Herzig et al., 2002). The clinical manifestations of severe systemic intoxication are usually seen in elderly and children. In such cases, the penile erection or priapism is one of the most noted signs of phoneutrism. Other clinical manifestations often reported after a *Phoneutria* bite are convulsions, agitation, somnolence, nausea, profuse sweating and vomiting, lacrimation, excessive salivation, hypertension, tachycardia, tachypnea, tremors and spastic paralysis (de Lima, 2016; Raposo et al., 2016). Cases of systemic poisoning in adults are uncommon but may happen. The venom of *P. nigriventer* is considered as a pharmacological treasure for drug discovery for over 60 years now. Indeed, this venom is a complex mixture of proteins and peptides, including neurotoxins, acting on ion channels and

chemical receptors of the nervous and muscular systems of insects and mammals (Richardson et al., 2006b). Notwithstanding that no *Phoneutria* venom-derived peptide has made it to the drug market, the potential pharmacological applicability of these peptides is evidenced by the ample research studies using these peptides, not only as potent ligands for specific targets, but also as tools to have a better understanding of their physiological function and their involvement in diseases and channelopathies.

The first studies on *P. nigriventer* venom, report the presence of biologically active proteins such as peptides, proteases, and hyaluronidase. Furthermore, other active compounds such as histamine serotonin and some free amino acids were also identified (de Lima, 2016; Gomez et al., 2002). Early work indicated that the whole venom exhibits a pronounced neurotoxic activity. Injection of whole or partially fractionized venom caused a myriad of excitatory symptoms in experimental animals (Bucherl, 1953, 1969; Schenberg and Lima, 1966). These observations in animals corroborated well by the reports on human envenomation (Bucarechi et al., 2008; Diniz et al., 1990a). The very first biochemical and pharmacological characterization of an isolated *Phoneutria nigriventer* toxin was performed in 1990s by Dr. Diniz and colleagues at Fundação Ezequiel Dias (Belo Horizonte, MG, Brazil). Almost 30 years before, Diniz has been the pioneer in studying this venom (Diniz, 1963). Nowadays *P. nigriventer* venom has been extensively studied making it one of the most studied spider venoms in the world. Besides some non-protein low-molecular-mass compounds, 41 neurotoxins have been identified from the crude venom up to date (Herzig et al., 2011; Pineda et al., 2017). A recent study, which combines transcriptomic and proteomic techniques, has revealed a wealth of new information on *P. nigriventer* venom (Diniz et al., 2018). The constructed cDNA library resulted in the characterisation of 29 unique cysteine-rich peptide toxins. Several of these sequences corresponded to already described *P. nigriventer* toxins. However, many isoforms of already described toxins and novel sequences were identified as

well (Diniz et al., 2018). The latter underlines that the *P. nigriventer* venom still contains many peptide toxins worthwhile to investigate.

1.6.1. Nomenclature of *Phoneutria nigriventer* toxins

The nomenclature of *Phoneutria nigriventer* toxins is rather confusing and problematic. Over time, often several names have been given to the same peptide. Historically, the *Phoneutria* toxins are annotated based on their occurrence in the venom when following the venom purification methods used in the first studies (Diniz et al., 1990a), i.e. based on a particular chromatographic step and in the order of elution of the toxin, in this step. In an attempt to solve the confusing nomenclature of peptides of spiders and of other animal venoms, (King et al., 2008) have proposed a rational nomenclature, which considers the molecular target (including sub-types) of the toxin and also the family, genus and species of the animal from which the toxin was obtained. As an example, the toxin originally named Tx2-6/PnTx2-6 from *P.nigriventer*, is also annotated, following the new nomenclature as: δ -CNTX-Pn2a (delta meaning its modulating activity on Nav inactivation, CNTX = Ctenitoxin from Ctenidae family; Pn = *Phoneutria nigriventer*, = isoform). Some efforts have been done to adopt the new nomenclature of King. However, in general with *Phoneutria* venom peptides, the name given to the toxin in the first publication has become the commonly used name of the toxin. Therefore, in this review we adopted the name as found in the respective publications. The corresponding names suggested by King's nomenclature can be consulted in ArachoServer. Since the venom is a complex mixture, an efficient purification method was needed. Therefore, an activity-guided purification and fractionation procedure, using gel filtration and reversed-phase chromatography had to be developed (Diniz et al., 1990a).

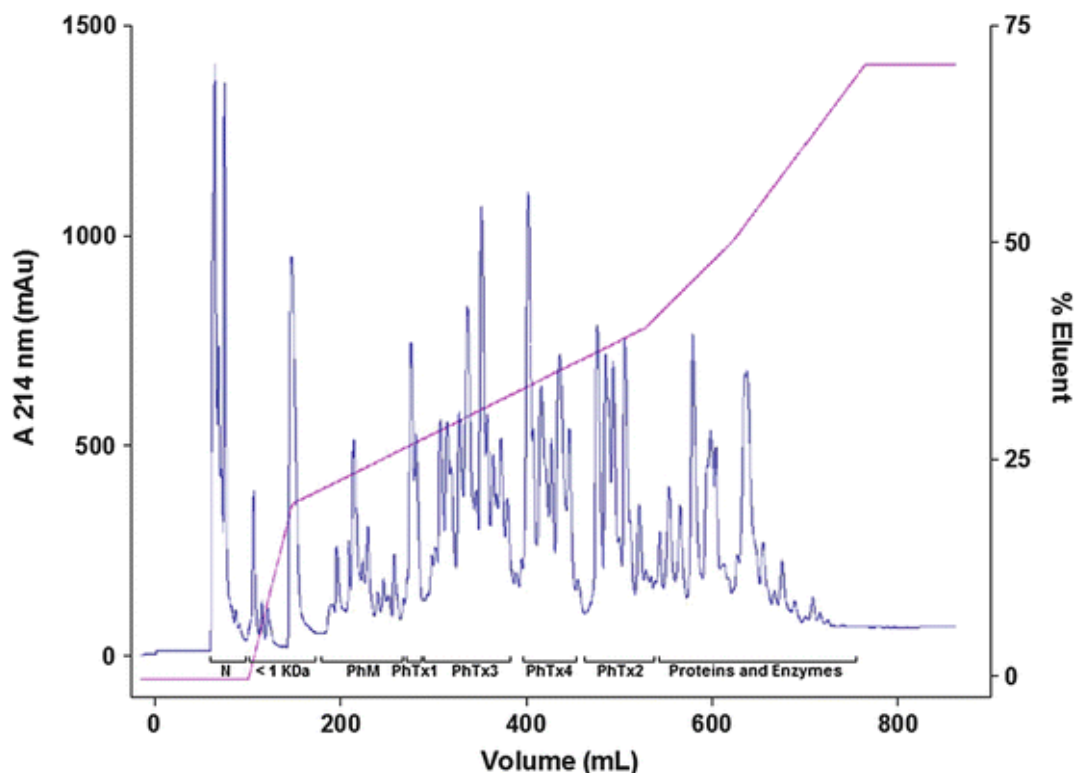
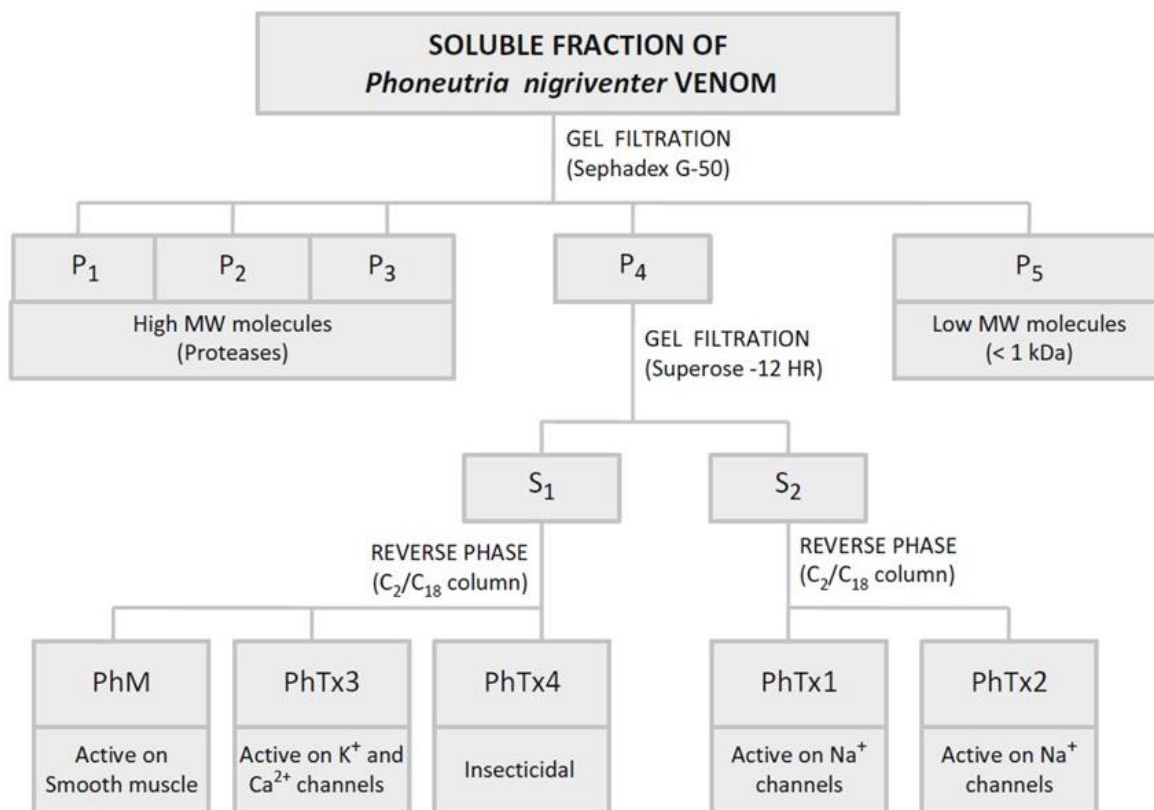


Figure 16. *Upper panel:* Flowchart showing the purification procedure of *Phoneutria nigriventer* venom fractions. Adapted from de Lima et al., 2016). *Lower panel:* Elution profile of reversed-phase (RP-HPLC) fractionation of *Phoneutria nigriventer* venom. Venom sample was loaded on a preparative Vydac C4 column (2.2 × 25 cm). Column was

eluted at a flow rate of 5 mL/min, monitored at 214 nm, under a gradient of acetonitrile . The solid bars indicate the eluted fractions and (N) nigriventrine. Figure adapted from (Peigneur et al., 2018).

Following this procedure typically generated five distinct venom fractions. Each fraction showed different activity when assayed in mammals and/or insects, suggesting the presence of toxins with different pharmacological properties (Figueiredo et al., 1995; Rezende Junior et al., 1991). For most of the initial studies, toxicity was evaluated *in vivo* by intracerebral (i.c.) or intrathoracic injections in mice and insects, respectively, and *in vitro* by smooth muscle assays using guinea pig ileum, besides some assays in synaptosomes from rat brain. Using this activity guided purification method, four distinct venom fractions, named PhTx1, PhTx2, PhTx3, and PhTx4 were identified. PhTx1, PhTx2, and PhTx3 are active on mammals and differ in their lethality and effects in mice (Rezende Junior et al., 1991). PhTx4 produces marked stimulatory effects in insects and is more toxic to insects than to mammals (Figueiredo et al., 1995). It was shown that some toxins from the PhTx4 fraction, besides acting on insect sodium channels (de Lima et al., 2002a), also can act on mammal sodium channels (Paiva et al., 2016; Silva et al., 2015b), although no apparent toxicity was observed when injecting (i.c.) these molecules in rat brain. The fifth fraction (PhM), apparently not toxic to mammals, is active on smooth muscle, causing contraction (Pimenta et al., 2005a; Richardson et al., 2006a). The average LD50 by i.c. injection in mice for the whole venom, PhTx1, PhTx2, PhTx3, and PhTx4, was 47, 45, 1.7, 137, and 480 µg/kg, respectively (Rezende Junior et al., 1991). PhTx2 is the fraction which displayed the strongest neurotoxic activity while PhTx5 or PhM (15 mg/kg, i.v. injection) has no lethal effect in mice (Rezende Junior et al., 1991). Figure 16, *upper panel* shows a flow diagram describing the purification of *Phoneutria nigriventer* venom fractions.

1.6.2. PhTx1

The fraction PhTx1 is constituted by just one peptide, initially called Toxin 1 or Tx1. Afterwards, it was given the name *Phoneutria nigriventer* Toxin 1 or PnTx1. This peptide represents 0.45% of the whole venom protein content and it was the first purified and sequenced neurotoxin from *P. nigriventer* venom (Diniz et al., 1990a). PnTx1 has a molecular mass of 8594.6 Da and is constituted of 78 amino acid residues, 14 of which are cysteines (Figure 17). It is thus a fairly large peptide with a complex disulfide bridge pattern that remains undetermined till today.

1 10 20 30 40 50 60 70
 AELTSCFPVGH^CCDGDASN^{CN}CCGDDVY^{CG}CGWGRWN^{CK}CKKVADQSYAYGI^{CK}DKVNC^{PNRHLWPAKV^CKKPCRRN^CGG}

Figure 17. Sequence of PnTx1. Cysteines are indicated in red.

Early research indicated that PnTx1 induces excitation and spastic paralysis in mice upon i.c. injection (Rezende Junior et al., 1991). PnTx1 is lethal to rodents and has an astonishing LD₅₀ of 5.5 pmol/g in mice (Diniz et al., 1993; Diniz et al., 2006b; Klint et al., 2012). Nevertheless, the exact molecular target of this toxin remained unknown for many years. Initially, it was suggested that PnTx1 could act on calcium channels because radio-iodinated ¹²⁵I-PnTx1 showed partial competition with the fraction PhTx3, which contains several calcium channel modulating peptides. However, labeled PnTx1 did not compete with ω-conotoxin GVIA, a calcium channel inhibiting toxin isolated from cone snail venom (Santos et al., 1999). This rather contrary result was later attributed to the presence of a small contamination with PnTx3-3. PnTx3-3 is a well-characterized toxin that potently inhibits high-voltage-activated Cav channels, but not low-voltage-activated Cav channels (Leao et al., 2000). This contamination could explain the partial competition for Cav channel inhibition (Martin-Moutot et al., 2006a). However, the question whether or not PnTx1 interacts with Cav channels can still not be answered unambiguously. Experiments using a highly purified PnTx1 showed that this toxin

partially displaced the calcium-antagonist dihydropyridine derivative 3H-PN200-110 in GH3 cell membranes. Furthermore, a 50% inhibition of the calcium influx in GH3 cells was observed after application of 1 μ M PnTx1 (Santos et al., 1999). On the other hand, experiments with the recombinant PnTx1 (rPnTx1) showed no modification in the calcium currents of dorsal root ganglia (DRG) neurons (Silva et al., 2012b). One explanation for these seeming contradictorily observations could be that PnTx1 does interact with Cav channels but only selectively with a certain specific subtype of Cav channels. Nonetheless, PnTx1 awaits further investigation in order to elucidate its Cav channel interaction.

Using similar competitive binding experiments it was shown that 125 I-PnTx1 partially blocked the PhTx2 induced activity in myenteric plexus-longitudinal muscle preparations (Santos et al., 1999). Since PhTX2 is the fraction that contains mainly sodium channel toxins, this observation hinted towards an activity of PnTx1 on Nav channels. Interestingly, 125 I-PnTx1 did not compete with PnTx2-6, a toxin that modulates the inactivation process of Nav channels (Silva et al., 2015b). The authors consequently concluded that PnTx1 might be interacting with Nav channels via another binding site on the Nav channel (Santos et al., 1999). Later on, these conclusions were shown to be correct when it was demonstrated that PnTx1 competes with μ -conotoxin μ -GIIIA (Martin-Moutot et al., 2006a). It is interesting to note that PnTx1 competes with μ -conotoxins for site 1 but not with the small compound Nav channel inhibitor TTX. Using the patch-clamp technique and Chinese hamster ovary cells expressing Nav1.2 channels, PnTx1 was characterized as a state-dependent channel inhibitor, preferring to interact with the Nav channels in the open state (Martin-Moutot et al., 2006a).

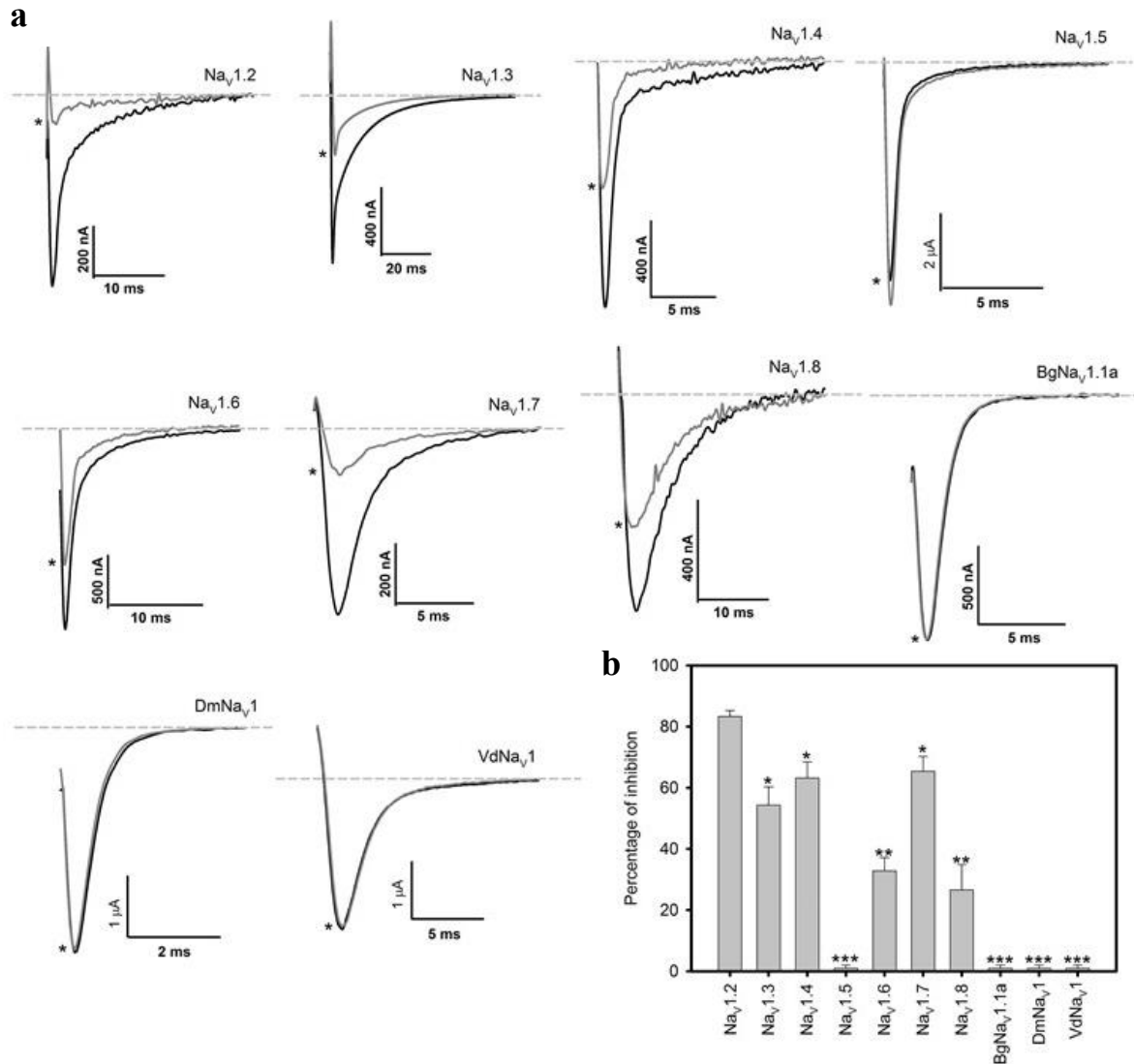


Figure 17. Effect of rPnTx1 on different subtypes of sodium channels expressed in oocytes. (a) Representative records of Na⁺ currents before (black line) and after (gray line*) the addition of 1 μM rPnTx1. Dashed line is the baseline. Holding potential: -90 mV. Test potential: 0 mV. (b) Average percentage of Na⁺ current inhibition by rPnTx1 (1 μM) of different sodium channel subtypes expressed in oocytes. Na_v1.2 inhibition was significantly higher when compared with Na_v1.3, Na_v1.4 and Na_v1.7 and these were higher when compared with Na_v1.6 and Na_v1.8. No effect was observed with Na_v1.5 and with the arthropod isoforms (DmNa_v1, BgNa_v1.1a and VdNa_v1). The symbols (*), (**) and (***) denote the isoforms on which the toxin effects were not statistically different. Figure adapted from (Silva et al., 2012a).

The recombinant PnTx1 was expressed in a bacterial heterologous system and inhibited a variety of sodium channel isoforms expressed in *Xenopus laevis* oocytes (Figure 19a) and native sodium channels in DRG neurons (Silva et al., 2012b). Surprisingly, recombinant toxin displayed a 3-fold lower IC₅₀ value compared to native peptide. This could possibly be

explained by the presence of three additional amino acids in the sequence of the recombinant produced toxin, namely alanine and methionine at the N-terminus and a glycine at the C-terminus. The recombinant toxin, rPnTx1, inhibited mammalian Nav channel isoforms with the following order of potency: rNav1.2 > rNav1.7 rNav1.4 rNav1.3 > mNav1.6 hNav1.8 with no effect on Nav1.5 (Figure 19b) (Silva et al., 2012b). Accordingly, rPnTx1 was less effective on TTX-resistant sodium channels in DRG neurons (Silva et al., 2012b). From a drug development point of view, it is interesting to note that PnTx1 does not inhibit the cardiac isoform Nav1.5. Indeed, such a significant selectivity towards neuronal sodium channels is considered appealing as this avoids unwanted cardiovascular side effects. Inhibition of Nav channels occurred without modification of the biophysical properties of the channels since no alterations of the voltage dependence of activation and steady-state inactivation were noted (Martin-Moutot et al., 2006a; Silva et al., 2012b). Competitive binding studies have shown that PnTx1 does not compete with toxins acting on site 2, 3, 4, 5. Nor does PnTx1 bind to the interaction site for local anesthetics or for pyrethroids (Martin-Moutot et al., 2006a). Furthermore, using mutated Nav1.2 channels devoid of fast inactivation, it was shown that PnTx1 does not stabilize the channels in the inactivated state (Silva et al., 2012b). It thus can be concluded that the PnTx1 induced sodium current inhibition is not a result of modified gating and open time probability but rather from a physical obstruction of the sodium ion pathway through the Nav channel. The result of PnTx1 binding is thus a reduction of the single channel conductance.

PnTx1 does not inhibit insect Nav channels. Even at higher concentrations, PnTx1 failed to decrease the current peak amplitude of arthropod Nav channel isoforms such as from the fruit fly *Drosophila melanogaster* (DmNav1), the cockroach *Blattella germanica* (BgNav1.1) and the mite *Varroa destructor* (VdNav1). This inactivity on arthropod Nav channels corroborates well previous studies showing a lack of insecticidal activity of venom fraction PhTx1, when injected in insects (Santos et al., 1999).

Curiously, both native and recombinant toxins were not able to block 100% of the Nav1.2 currents, reaching a maximal inhibition of approximately 85% of the sodium peak current, even at saturating conditions. Subsequent addition of TTX results in completely inhibited sodium channels indicating that TTX can still reach and bind its site of interaction, independent of the presence of PnTx1 (Silva et al., 2012b). Since these experiments were performed in *Xenopus* oocytes heterologously expressing Nav channels it was concluded that PnTx1 incompletely inhibits the sodium conductance through the channel, a phenomenon shared with the μ -conotoxins (French et al., 2010b; Silva et al., 2012b).

Moreover, an interesting sequence comparison can be made between a central segment of PnTx1 and μ -conotoxins such as GIIIA and μ -KIIIA. In this way, the amino acids W33, R35 and K39 of PnTx1 can be aligned with the similar amino acids W8, R10 and R14, present in the μ -conotoxin μ -KIIIA (Khoo et al., 2011a; Silva et al., 2012b; Zhang et al., 2010a). Single mutations can alter significantly the selectivity of a toxin. The substitution of tryptophan at position 8 by arginine decreased affinity of μ -conotoxin μ -KIIIA for Nav1.2 subtype, making it more selective to Nav1.4 (Van Der Haegen et al., 2011). There are three basic amino acids conserved in μ -conotoxin μ -GIIIA that are putative key residues for the interaction with Nav channels: R13, K16, and K19. PnTx1 has basic residues in two correspondent positions, R35 (instead K16) and K39 (corresponding to K19). However, PnTx1 lacks the first arginine (R13) and has a glycine (G32) in the corresponding position. Arginine-13 was postulated to be a general residue for μ -conotoxins to interact with the receptor site of sodium channels. This residue is particularly critical, since it is believed to compete with the guanidinium group of TTX or STX for the binding site 1. The toxin binding sites of sodium channels were classified based on their ability to compete with other toxins in binding experiments. Site 1 is the binding site of TTX and STX and toxins that can displace them, such as μ -conotoxin μ -GIIIA. Since

PnTx1 competes with μ -conotoxin μ -GIIIA but not with TTX, it would be more appropriate to consider it as a macro site 1 instead (de Lima, 2016).

Based on all information to date, one hypothesis is a mechanism of action where PnTx1 binds to the outer mouth of the channel pore, at a site similar or at least partially overlapping with the μ -conotoxin binding site within neurotoxin binding site 1. Upon binding, PnTx1 hinders the flow of sodium ions. Presumably, the inhibition is a result of both physical occlusion and repulsion of positive charges, similar to what has been proposed for the μ -conotoxins (French et al., 2010a). Therefore, the likely mechanism of action of PnTx1 would be the reduction of the unitary conductance of the channel, similarly to what is seen for the mutated toxin μ -conotoxin μ -GIIIA (R13Q) (Becker et al., 1992).

Spider venom peptides targeting Nav channels (NaSpTxS) have been divided into 12 families based on sequence identity and intercysteine spacing (Klint et al., 2012). PnTx1 is the representative of family 8, which constitutes the family of the longest NaSpTxS. So far, no structure, or even disulfide bridge pattern for that matter, has been determined for this structural family. Moreover, none of the *Phoneutria nigriventer* peptides has its structure determined so far, emphasizing the challenges, and herewith the opportunities from a structural point of view, to be found in the *Phoneutria* venom. This is mainly due to peptide scarcity since only small amounts can be isolated from the venom and due to the peptide size and complexity. Therefore, many structure-function questions about PnTx1 remain open, which makes it an attractive object for future studies. Elucidation of the structure of PnTx1 would greatly enhance the understanding on how this toxin exerts its interesting pharmacology.

1.6.3. PhTx2

The fraction PhTx2 was found to be toxic to both mice and insects (Figueiredo et al., 1995). Intracerebral injection in mice resulted in priapism, salivation, convulsions and spastic

paralysis of the anterior and posterior limbs among other manifestations (Rezende Junior et al., 1991). Using a frog skeletal muscle preparation, it was shown that fraction PhTx2 alters the Nav channel kinetics. PhTx2 caused a shift in the activation and steady-state inactivation curves, a slowing down of the channel inactivation and a partial inhibition of the sodium peak current. The same experiments indicated that PhTx2 does not affect the potassium current (Araujo et al., 1993).

	1	10	20	30	40	50
PnTx2-1	ATCAGQDKPCKETCDCCGERGECVCA LSYEGKYRCICRQGNFLIAWHKLASCK					
PnTx2-5	ATCAGQDQTCKVTCDCCGERGECVCGGPCI CRQGNFLIAWYKLASCKK					
PnTx2-6	ATCAGQDQPCKETCDCCGERGECVCGGPCI CRQGYFWIAWYKLANCKK					
PnTx2-9	SFCIPFKPCKSDEN CCKKFKCKTTGIVKLCRW					

Figure 20. Sequences of the toxins identified in *Phoneutria nigriventer* venom fraction 2.

Purification of fraction PhTx2 resulted in 9 peptides which were named PnTx2-1 till PnTx2-9 (Cordeiro et al., 1992). All peptides were investigated for their toxicity by i.c. injection in mice. PnTx2-2, PnTx2-3, PnTx2-4, PnTx2-7, and PnTx2-8 showed low toxicity and these peptides still await justification for their classification as neurotoxin. PnTx2-1, PnTx2-5, and PnTx2-6 share up to 77% identity with each other (Figure 20) and all 3 toxins elicit neurotoxic effects when injected into mice (Cordeiro et al., 1992). Pruritus, lacrimation, increased salivation, sweating, and agitation followed by spastic paralysis of the limbs was observed. PnTx2-9, was much less toxic to mice, causing pruritus, reduction in motility and tail erection. PnTx2-9 differs in sequence from the other peptides of PhTx2. It is a rather short peptide of 32 residues with 3 disulfide bridges. Although annotated as a Nav channel toxin, no functional data is available to justify this classification.

PnTx2-1 remains scarcely studied. The *in vivo* tests in mice and based on the sequence identity with PnTx2-5 and PnTx2-6, it can be assumed that this peptide also targets Nav

channels. However, functional studies are required to investigate the subtype selectivity and species specificity of PnTx2-1 (Richardson et al., 2006b).

Among all the polypeptides purified from PhTx2 fraction, PnTx2-5 and PnTx2-6 are the most studied toxins. They have high sequence identity, differing only in five amino acid residues (Cordeiro et al., 1992). Both toxins were shown to modulate sodium channel kinetics by slowing down the inactivation process and by shifting the voltage dependence of activation towards more hyperpolarized potentials. Both peptides were found to induce a painful and persistent penile erection, also known as priapism which is a common clinical manifestation upon *Phoneutria nigriventer* envenomation. Interestingly, despite the high identity between both peptides, significant differences in potency have been reported. PnTx2-5 displayed an approximately 6-fold lower potency than PnTx2-6 in electrophysiological assays (Matavel et al., 2002b; Matavel et al., 2009; Nunes et al., 2010b).

Using frog skeletal muscle, an in-depth characterization of PnTx2-6 on a molecular level was performed. PnTx2-6 induces a plethora of modifications of channel kinetics. PnTx2-6 reduces the sodium peak current, slows down the time constant for fast inactivation and causes a hyperpolarizing shift of the voltage dependence of both the activation and steady-state inactivation curves (Matavel et al., 2002b). The diversity of channel modulations is intriguing from a biophysical point of view. The slowing down of the inactivation process is similar to the activity of certain scorpion, sea anemone and other spider toxins such as the β/δ -agatoxins (Cardoso and Lewis, 2017; Deuis et al., 2017; Israel et al., 2017b; Nicholson, 2007; Wanke et al., 2009). The subtype selectivity for mammalian Nav channel isoforms was determined for PnTx2-6 (Figure 20) (Silva et al., 2015a). These toxins have been characterized to bind to the so called neurotoxin binding site 3 Nav channels (Catterall et al., 2007). These site 3 toxins slow down sodium channel inactivation and in many cases they induce other channel gating modifications as well (Cardoso and Lewis, 2017; Peigneur et al., 2012; Zhu et al., 2012).

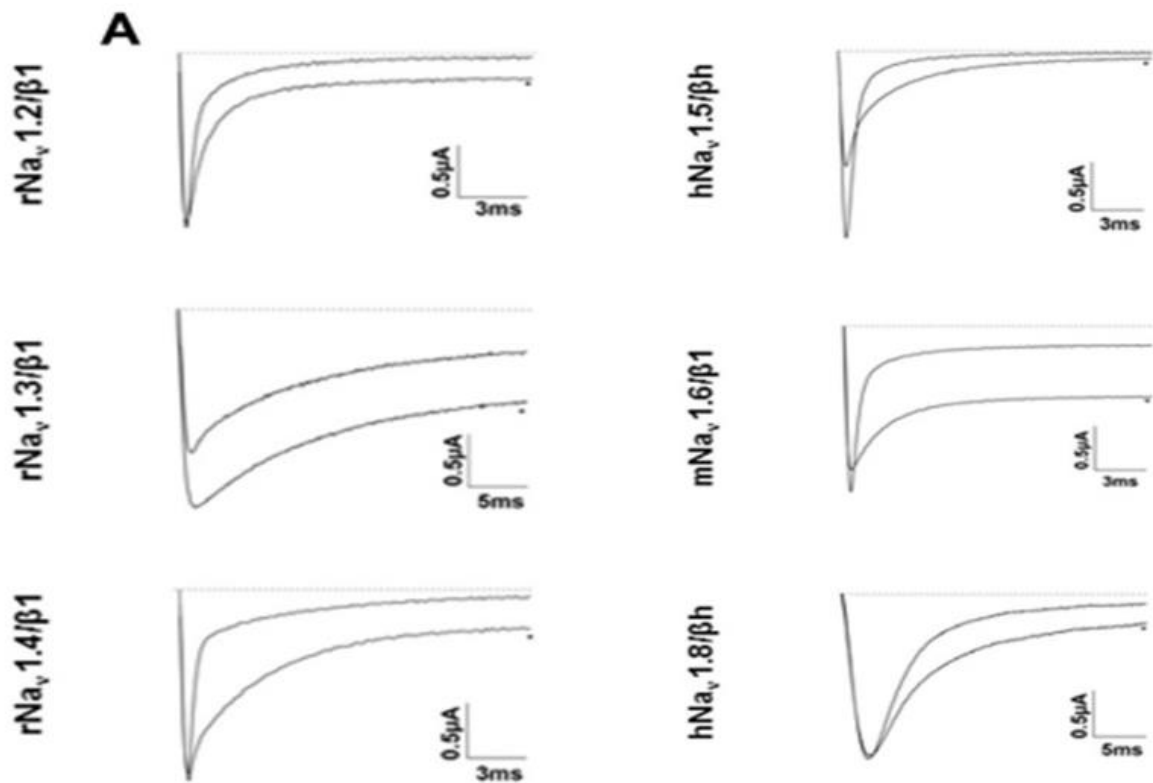


Figure 20. Representative traces of Na_v channel isoforms expressed in *Xenopus* oocytes in control situation and after the application of 3 μM PnTx2-6. Dotted line indicates zero current level. Asterisk indicates steady state current traces after toxin application. Figure adapted from (Silva et al., 2015a).

Binding experiments in brain synaptosomes showed that PnTx2-6 partially competes with the typical α -scorpion toxin AaHII (from *Androctonus australis Hector*) (Matavel et al., 2009). A shift of the midpoint of activation potential toward more negative potentials together with a reduction in sodium peak current are characteristics of gating alterations often observed for β -scorpion toxins and certain spider toxins (Leipold et al., 2006a; Nicholson et al., 2004; Peigneur et al., 2015). However, it was shown that PnTx2-6 does not compete with the β -scorpion toxin CssIV (from *Centruroides suffusus suffusus*) and it thus seems unlikely that PnTx2-6 binds to same site as β -scorpion toxin (Matavel et al., 2009). As such, structure-function studies are required to pinpoint which toxin-channel interactions are responsible for the PnTx2-6 induced channel modulations.

The effect of PnTx2-6 on spontaneous penile erection is remarkable and opens perspectives for clinical applications. In a first step to further investigate the exact role of PnTx2-6 in erectile function, the toxin was expressed recombinantly in *E. coli* cells (Torres et al., 2010b). The recombinant toxin was able to produce erection, similar to native toxin (Torres et al., 2010b). The mechanism of action through which PnTx2-5 and PnTx2-6 promote cavernosal relaxation and enhance erectile function is not completely clarified (Nunes et al., 2010b; Nunes et al., 2012a; Yonamine et al., 2004). However, intensive research in recent years has provided a better understanding on how these toxins influence erectile function (Nunes et al., 2012b). It is suggested that PnTx2-6 intervenes in the nitric oxide (NO)/cyclic GMP pathway by increasing the release of NO in the corpus cavernosum tissue (Nunes et al., 2008). The release of NO from penile endothelial cells or nitrenergic nerves is a key regulator in erectile function. Increased NO concentrations, triggered by sexual stimulation, induces relaxation of penile smooth muscle. This relaxation results in an increased blood flow and intracavernosal pressure which leads to penile erection. The PnTx2-6 induced relaxation is neuronal nitric oxide synthase (nNOS) depended (Nunes et al., 2012b). The activation of nNOS by PnTx2-6 is most likely indirect. Since PnTx2-6 is characterized as a modulator of Nav channel inactivation, the binding of PnTx2-6 to Nav channels will result in an increased sodium influx. This will trigger a cascade of cellular reactions, eventually resulting in an activation of nNOS and consequently stimulation of NO release. This mechanism of action was supported by the observation that ω -conotoxin GVIA, an inhibitor of N-type calcium channels, could block the relaxation induced by PnTx2-6. Additionally, it was shown that the cavernosal relaxation provoked by PnTx2-6 is not dependent on phosphodiesterase-5 (PDE5) inhibition (Nunes et al., 2012b). Furthermore, it was shown that PnTx2-6 induces priapism in mice even after cavernosal denervation, indicating that the toxin might not depend on cavernosal nerves integrity (Ravelli et al., 2017). Investigating the gene expression in mice erectile tissue showed overexpressing of two genes

potentially related to PnTx2-6 induced priapism (Villanova et al., 2009). One of these genes is directly involved in the activation of the NO/cGMP pathway.

PnTx2-5 has been less investigated, compared to PnTx2-6, but the results that are available do suggest that this toxin is involved in penile potentiation similar to PnTx2-6 (Villanova et al., 2009). PnTx2-5 also caused penile erection when injected intraperitoneal in male mice. These effects are completely abolished by the nNOS-selective inhibitor 7-nitroindazole, indicating an important involvement of nNOS in this effect as well (Yonamine et al., 2004). Both toxins, PhTx2-5 and PhTx2-6, represent interesting pharmacological tools to study erectile dysfunction. A 19 residues peptide, devoid of disulfide bridges but comprising the pharmacophore of PnTx2-6 was designed. This PnTx2-6-derived peptide, named PnPP-19, was no longer active on Nav channels. The abolishment of Nav channel activity can be considered as an important amenity since this strongly reduces the peptide toxicity and hereby unwanted side effects. Interestingly however, PnPP-19 potentiates penile erection with a similar activity as PnTx2-6 (Silva et al., 2015b). Therefore, PnPP-19 can be considered as an exciting lead compound for drug development related to the treatment of erectile dysfunction. Moreover, PnPP-19 has also been investigated for its role in both peripheral and central antinociception (Freitas et al., 2016). It was shown that PnPP-19 inhibits neutral endopeptidase and activates receptors involved in pain pathways such as the cannabinoid receptor 1 and the μ - and δ -opioid receptors (da Fonseca Pacheco et al., 2016; Freitas et al., 2016). Furthermore, the peripheral antinociceptive effect induced by PnPP-19 is resulting from an activation of the NO-cGMP- K_{ATP} pathway. Hereby, an activation of both endothelial nitric oxide synthase (eNOS) and nNOS by PnPP-19 occurs in rat paw Freitas et al., 2017. PnPP-19 selectively activates μ -opioid receptors inducing indirectly inhibition of calcium channels and hereby impairing calcium influx in dorsal root ganglion (DRG) neurons. Interestingly, notwithstanding the activation of opioid receptors, PnPP-19 does not induce β -arrestin2 recruitment. PnPP-19 is the first spider

toxin derivative that, among opioid receptors, selectively activates μ -opioid receptors. The observed lack of β -arrestin2 recruitment highlights the potential of this peptide for the design of new improved opioid agonists (Freitas et al., 2018). One of the very serious and life-threatening conditions developed following the use of the usual opioid agonist medicines is respiratory paralysis. It has been demonstrated that the induction of respiratory paralysis, as well as other side effects, after the use of opioids may be linked with the recruitment of the β -arrestin pathway, which is stimulated downstream following activation of μ -opioid receptor. Since opioid receptors are still one of the most relevant targets for pain treatment, great effort is being put in the development of new opioid agonists that elicit fewer negative side effects. In this way, the lack of β -arrestin2 recruitment by PnPP-19 underlines the potential of this peptide as a possible lead compound in the development of improved opioid agonists (Freitas et al., 2018).

1.6.4. *PhTx3*

Injection in mice of fraction PhTx3 results in a progressive flaccid paralysis of all legs (Kushmerick et al., 1999; Prado et al., 1996; Rezende Junior et al., 1991). Of all venom fractions, PhTx3 must be the most studied and best characterized fraction. This is a consequence of the pharmacological potential present in this fraction. All of the PhTx3 peptides were found to target voltage-gated calcium (Cav) channels or K_v channels. It is remarkable that up to date only one voltage-gated potassium channel targeting peptide (KSpTxS) has been characterized from *Phoneutria* venom while other spiders are known to produce potent and pharmacological interesting KSpTxS (Priest et al., 2005).

	1	10	20	30	40	50	60	70																																																																			
PnTx3-1	A	E	C	A	A	V	Y	E	R	C	G	K	G	Y	K	R	C	E	E	R	P	C	K	C	N	I	V	M	D	N	C	T	C	K	K	F	I	S	E	L																																			
PnTx3-2	-	A	C	A	G	L	Y	K	K	C	G	K	G	A	S	P	C	E	D	R	P	C	K	C	D	L	A	M	G	N	C	I	C	K	K	F	I	E	F	F	G	G	G	K																															
PnTx3-3	G	C	A	N	A	Y	K	S	C	N	G	P	H	T	C	C	W	G	Y	N	G	Y	K	K	A	C	I	C	S	G	X	N	W	K																																									
PnTx3-4	S	C	I	N	V	G	D	F	C	D	G	K	K	D	C	Q	C	C	R	D	N	A	F	C	S	C	S	V	I	F	G	Y	K	T	N	C	R	C	E	V	G	T	T	A	T	S	Y	G	I	C	M	A	K	H	K	C	G	R	Q	T	T	C	T	K	P	C	L	S	K	R	C	K	N	H	G
PnTx3-5	G	C	I	G	R	N	E	S	C	K	F	D	R	H	G	C	C	W	P	W	S	C	S	C	W	N	K	E	G	Q	P	E	S	D	V	W	C	E	C	S	L	K	I	G	K																														
PnTx3-6	A	C	I	P	R	G	E	I	C	T	D	D	C	E	C	C	G	C	D	N	Q	C	Y	C	P	P	G	S	S	L	G	I	F	K	C	S	C	A	H	A	N	K	Y	F	C	N	R	K	K	E	K	C	K	K																					

Figure 21. Sequences of the toxins identified in *Phoneutria nigriventer* venom fraction 3.

From this fraction six toxins, named PnTx3-1 to PnTx3-6, have been characterized (Figure 21). PhTx3 is the venom fraction composed of the most heterogeneous group of toxins. The peptides found in PhTx3 share little sequence identity, and therefore, display a wide array of differing pharmacological activities when injected *in vivo*. For example, PnTx3-1, PnTx3-5, and PnTx3-6 induce paralysis of the posterior limbs. PnTx3-2 induces immediate clockwise gyration and flaccid paralysis. PnTx3-3 and PnTx3-4 are the most toxic: at 5 µg/mouse they reproduce the fast flaccid paralysis followed by death observed for the whole PhTx3 fraction (Cordeiro et al., 1993; de Lima, 2016). PnTx3-6 also induces analgesia models pain in rodents (Souza et al., 2008).

It was shown that PnTx3-1 increases calcium oscillation in GH3 cells, presumably by blocking potassium currents (Kushmerick et al., 1999). Whole-cell patch clamp experiments showed that PnTx3-1 reversibly and selectively inhibits type-A potassium current (IA) without affecting the delayed or the inward rectifying potassium current. PnTx3-1 has no effect on large conductance calcium sensitive potassium channels. Furthermore, this toxin does not interact with T- and L-type Cav channels. The inhibition of IA favors cell depolarization and Cav channel activation, increasing the frequency of calcium oscillation (Kushmerick et al., 1999). It is important to note that these patch clamp experiments in GH3 cells do not rule out that the observed effects on oscillation frequency are following upon interaction of PnTx3-1 with an

unknown target. Further research is required to verify that Tx3-1 is indeed a potassium channel toxin and to determine which potassium channel isoforms this peptide is targeting. In the heart, PnTx3-1 had an anti-arrhythmogenic effect, decreasing the ACh-mediated heart rate by doubling the frequency of spontaneous miniature end plate potential protecting ischemia/reperfusion heart against arrhythmia (Almeida et al., 2011; de Lima, 2016). More recently, it was shown that PnTx3-1 causes an antinociception by interfering with the choline esterase activating cholinergic system (Rigo et al., 2017).

PnTx3-2 is characterized as a selective inhibitor of L-type Cav channels (Kalapothakis et al., 1998). PnTx3-2 does not show affinity for N- or P/Q-type Cav channels since the presence of this toxin did not modify the KCl-evoked glutamate release nor the rise of intracellular calcium in synaptosomes (Prado et al., 1996).

PnTx3-3 is considered as the most potent toxin from the venom fraction PhTx3. Many of the toxic properties of fraction PhTx3 are produced by this toxin (Guatimosim et al., 1997; Prado et al., 1996). PnTx3-3 inhibits P/Q- and R-type Cav channels with high affinity. At higher concentrations, PnTx3-3 also inhibits L- and N-type Cav channels (Leao et al., 2000). Interestingly, PnTx3-3 induces a different profile of behavioral effects compared to the well characterized ω -conotoxin MVIIC which is also an inhibitor of P/Q-type Cav channels. Ample ω -conotoxins have been identified from cone snail venom (Prashanth et al., 2014). Using *in vivo* electrophysiological recordings, it was shown that PnTx3-3 exerts a prevalent antinociceptive effect mainly by inhibiting R-type Cav channels (Dalmolin et al., 2017).

PnTx3-4 affects the neurotransmission by blocking presynaptic calcium channels associated with exocytosis in mammals, lower vertebrates and arthropods (de Lima, 2016; Troncone et al., 2003). PnTx3-4 potently inhibits high-voltage-activated Cav channels in the sensory neurons of dorsal root. No activity was observed on low-voltage-activated Cav

channels (Cassola et al., 1998). Moreover, PnTx3-4 is suggested to act on P/Q-type Cav channels (Miranda et al., 2001). Using heterologous expressed channels in HEK293 cells, it was shown that PnTx3-4 produced a potent and almost irreversible inhibition of P/Q-type Cav2.1 channels and N-type Cav2.2. Only a partial and reversible inhibition of R-type Cav2.3 channels was observed (Dos Santos et al., 2002).

The least studied toxin of the venom fraction PhTx3 is the toxin PnTx3-5. However, this peptide is known to potently block L-type Cav channels (Leao et al., 2000). PnTx3-5 demonstrated promising antinociceptive activity in clinically relevant pain models of postoperative, neuropathic and cancer-related pain (Oliveira et al., 2016). Interesting to note is that PnTx3-5 also displayed efficacy in opioid tolerant animals. Indeed, the clinical applicability potential of L-type, as well as N-type, Cav channel inhibitors such as PnTx3-5, can be found in their apparent synergism with morphine.

The toxin PnTx3-6 (also known as Ph α 1b) binds to a broad range of high-voltage-activated Cav channels. It inhibits N-, R- and P/Q-type Cav channels with a comparable affinity. At higher concentrations, this toxin also blocks L-type Cav channels. However, PnTx3-6 has no activity on T-type Cav channels (Vieira et al., 2005). More recent, it was discovered that the analgesic activity of PnTx3-6 results, besides of the inhibition of Cav channels, from the interaction with TRPA1 receptors. PnTx3-6 is a potent TRPA1 antagonist while having no affinity for TRPV1 or TRPV4 receptors (Tonello et al., 2017). PnTx3-6 has been investigated for its analgesic proprieties. PnTx3-6 was effective in potentiating the analgesic effect of morphine in mice. Furthermore, the same study showed that this peptide reduced the hyperalgesia, tolerance, constipation and withdrawal syndrome induced by repeated morphine injection (Tonello et al., 2014). Similar, PnTx3-6 also potentiates the analgesic action of TRPV1 blockers, underlining the potential of Cav channel inhibitors as adjuvant analgesic agents (Palhares et al., 2017).

1.6.5. PhTx4

PhTx4 is historically referred to as the insecticidal fraction. It earned this reference based on its high toxicity and lethality toward insects while displaying a minor toxicity when injected in mice. This fraction causes hyperactivity such as cramps, quivering, jerking of the limbs, and violent trembling of the body and the legs, leading to muscle fatigue and therefore causing paralysis in insects (de Lima, 2016; Figueiredo et al., 1995). It is suggested that PhTx4 acts on the glutamatergic system of both insects and mammals. Three toxins have been characterized from the venom fraction PhTx4 (Figure 22). They were named PnTx4(6-1), PnTx4(5-5), and PnTx4(4-3) (de Figueiredo et al., 2001; Figueiredo et al., 1995; Oliveira et al., 2003). These 3 insecticidal toxins share high sequence identity and as such are believed to exhibit similar pharmacological properties.

	1	10	20	30	40
PnTx4-3	CGDINAACKED	CDCCGYTTACD	CYWSSSCK	CREAAIVIY	TAPKKKLTTC
PnTx4 (5-5)	CADINGACKSD	CDCCGDSVT	CDYWSDSCK	CRESNFKI	GMAIRKKF-C
PnTx4 (6-1)	CGDINAACKED	CDCCGYTTACD	CYWSSSCK	CREAAIVIY	TAPKKKLTTC

Figure 22. Sequences of the toxins identified in *Phoneutria nigriventer* venom fraction 4.

PnTx4(4-3) is not very well studied compared to the other toxins in this venom fraction. However, this toxin induces excitatory effects when injected in houseflies and cockroaches. Furthermore, it inhibits the glutamate uptake in rat brain synaptosomes (Oliveira et al., 2003).

PnTx4(6-1) and PnTx4(5-5) act on insect sodium channels (De Lima et al., 2007; de Lima et al., 2002b). Despite their apparent lack of toxicity to mammals, they have been shown to inhibit glutamate uptake in the mammalian central nervous system and to modulate the inactivation process of mammalian Nav channels (Mafra et al., 1999; Oliveira et al., 2003; Paiva et al., 2016). It was evidenced that PnTx4(5-5) is a reversible antagonist of NMDA ionotropic glutamate receptor in rat brain neurons (de Figueiredo et al., 2001). The activity of PnTx4(5-5)

on insect and mammalian Nav channels was characterized in depth (Paiva et al., 2016). The subtype selectivity among mammalian Nav channels was determined using the *Xenopus* oocyte expression system and recombinant produced PnTx4(5-5). Among mammalian Nav channels, the toxin caused a delay in the channel inactivation and a reduction of the sodium peak current. This reduction in peak current is the result of a toxin induced shift of the channel activation towards more depolarized membrane potentials. PnTx4(5-5) has the most pronounced effect on insect Nav channels. Using the cockroach Nav channel BgNav1, it was illustrated that PnTx4(5-5) has a devastating modulatory effect on these channels (Figure 23 a & b). Upon binding, this toxin causes a complete inhibition of the inactivation of the channel and an increase of the sodium peak amplitude. However, contrary to what was observed for mammalian Nav channels, no shift in the midpoint of activation was noted for insect Nav channels (Figure 23 c) (Paiva et al., 2016).

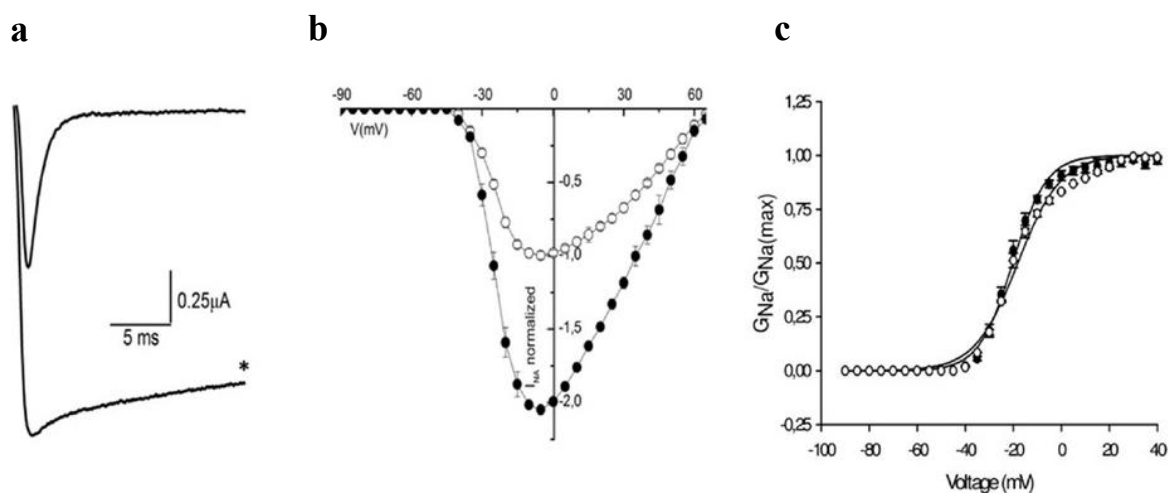


Figure 23. Effects of PnTx4(5-5) on the cockroach *B. germanica* sodium channel (BgNav1) expressed in *X. leavis* oocytes. (a) Representative whole-cell current traces in control and in presence of 1 μM PnTx4(5-5) (*). (b) Current–voltage ($I \times V$) relationships in control (\circ) and in presence of 1 μM PnTx4(5-5) (\bullet). (c) Activation of the conductance in control (\circ) and in presence of 1 μM PnTx4(5-5) (\bullet), fitted with the Boltzmann equation. Figure adapted from (Paiva et al., 2016).

The most active toxin of this fraction is the anti-insect neurotoxin PnTx4(6-1). Tests performed in a voltage-clamp configuration showed that both PnTx4(6-1) and PnTx4(5-5) prolonged the

axonal sodium current in a manner similar to toxins binding to neurotoxin site 3 of Nav channels. Similar tests in *Xenopus* oocytes indicated that PnTx4(6-1) has no effect on Nav1.2 and Nav1.4 channels (de Lima, 2016; de Lima et al., 2002b). However, in DUM cells, PnTx4(6-1) changed the regular spontaneous firing pattern of action potential generation into an irregular activity, evidencing its activity on insect Nav channels. The results obtained with electrophysiological experiments suggested that PnTx4(6-1) is most likely binding to the neurotoxin binding site 3 of Nav channels. This was later on confirmed with binding assays using Bom IV, an α -like scorpion toxin that binds to receptor site 3 on insect sodium channels. Bom IV was displaced by PnTx4(6-1) (Figueiredo et al., 1995). More recently, it was found that PnTx4(6-1) induces antinociception in inflammatory, neuropathic and acute pain models in rats. It is suggested that this antinociceptive effect involves the cannabinoid system, through cannabinoid receptor 1, and the opioid system, through the μ - and δ - opioid subtype receptors (Emerich et al., 2016).

1.6.6. *PhTx5*

	1	10
PnTkP-I	Q	KKDKKD
PnTkP-II	Q	KKDKKDK
PnTkP-III	Q	KKDKKDR
PnTkP-IV	Q	KKDKKDKF
PnTkP-V	Q	KKDKKDRF
PnTkP-VI	Q	KKDRFLGLM
PnTkP-VII	Q	KKDRFLGLF
PnTkP-VIII	Q	KKDKKDRFY
PnTkP-IX	Q	KKDKDRFYGLM
PnTkP-X	Q	KKDKKDKFYGLM
PnTkP-XI	Q	KNDKKDRFYGLM
PnTkP-XII	Q	KKDKKDKFYGLF
PnTkP-XIII	Q	KKDKKDRFYGLM
PnTkP-XIV	Q	KKDKKDRFYGLF
PnTkP-XV	Q	KKDKKDRFPNGLV

Figure 24. Amino acid sequences of the tachykinin family identified in the *Phoneutria nigriventer* venom.

The fifth *Phoneutria* venom fraction is also known as fraction PhM (Figure 16). An improved purification method of *P. nigriventer* venom combined with mass spectrometry analysis contributed for the identification of the fraction PhM (Pimenta et al., 2005b; Richardson et al., 2006b). This fraction was characterized for its activity on smooth muscle. However, the previous described purification method did not allow identification of these peptides because of their low levels in the whole venom and because their N-termini were somehow blocked which prevented sequencing by Edman degradation. It is also probable that some of these small molecules do not represent mature peptides, but are result of precursor processing and/or degradation of mature toxins (Pimenta et al., 2005a). PhM consists of a pool of similar isoforms of smaller (<2 kDa) peptides. The amino acid sequences of 15 of these isoforms (Figure 24) were determined by mass spectrometry (Pimenta et al., 2005b). These muscle-active peptides contain 7–14 amino acid residues and have a common scaffold

composed of basic and acid amino acids (PyrKKDKKD_x), where x can be either K or R. Since all of these molecules are structurally related to the tachykinin family of neurohormone peptides, which possess N-terminal pyroglutamate residues, they were named *Phoneutria nigriventer* tachykinin peptides PnTkPs (Pimenta et al., 2005b). The PnTkPs display a variation of post-translational modifications such as proteolysis, C-terminal amidation, and cyclization (Pimenta et al., 2005b).

1.6.7. Non-protein *P. nigriventer* venom components

In addition, a novel non-protein low-molecular-mass neurotoxin named nigriventrine was isolated from the hydrophilic fractions obtained from the venom by RP-HPLC purifications (Gomes et al., 2011b). Nigriventrine, a piperidine derivative, has neuroactive properties and causes convulsion when injected in mice, intracerebrally or peripherally by intravenous injection (i.v.). Its structure was determined and it was characterized as a hydroxyl-hydrazylidioxopiperidine (Figure 25) (Gomes et al., 2011b).

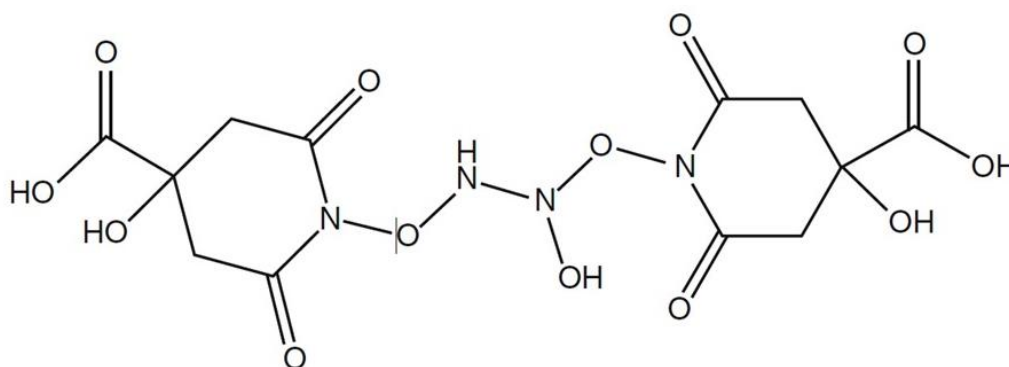


Figure 25. Proposed structure of nigriventrine (Gomes et al., 2011a).

It is estimated that venom of *P. nigriventer* is complex cocktail of more than 150 peptides/protein components (Richardson et al., 2006b). Considering that only about 41 toxins were pharmacologically and/or chemically characterized so far, a wide diversity of new

molecules, with possible different biological targets and activities, remains to be discovered in this venom. The studies conducted with *P. nigriventer* venom revealed several toxins acting on sodium, calcium, and TRPA channels, while other showed interesting activity on NMDA, cannabinoid or opioid receptors. Some of them have shown biotechnological and therapeutic potential, for example, by enhancing erectile function, acting as analgesics or insecticides. Although much of the richness and diversity of active peptides of *Phoneutria nigriventer* venom has been revealed many more remains to be discovered. For instance, since not a single structure of a *Phoneutria* venom peptide has been elucidated many structural questions remain unanswered. Determination of the structures is a requisite for careful designed mutagenesis studies. Therefore, further exploration of the characterized *Phoneutria* toxins necessitate advancing on the structural knowledge of these peptides. It is interesting that up to now, the venom of *Phoneutria nigriventer* has been intensively investigated for drug discovery but only few studies have focussed on the insecticidal properties of the venom components. It can be anticipated that also within the venom of *Phoneutria nigriventer* peptides can be found with a potential as lead for the development of novel insecticidal agents. It is clear that the complex biochemical and pharmacological diversity of this venom has not yet been unravelled to the fullest and thus it can be expected in the years to come that many new peptides will be characterized as promising pharmacological tools, as lead compounds for drug development and as novel insecticidal agents.

2. Hypothesis

Our hypothesis is that elucidation of the Nav binding site and the structure-activity relationship of our downsized chimeric peptide probes, coupled with the introduction of molecular features that improve oral availability, will allow further rational design of small cyclic peptides with desirable biopharmaceutical properties that show greatly improved

selectivity for Nav channels of therapeutic interest. Our goal is to modify venom-derived disulphide-rich Nav inhibitors into more “drug-like” molecules that display improved Nav channel selectivity and potency.

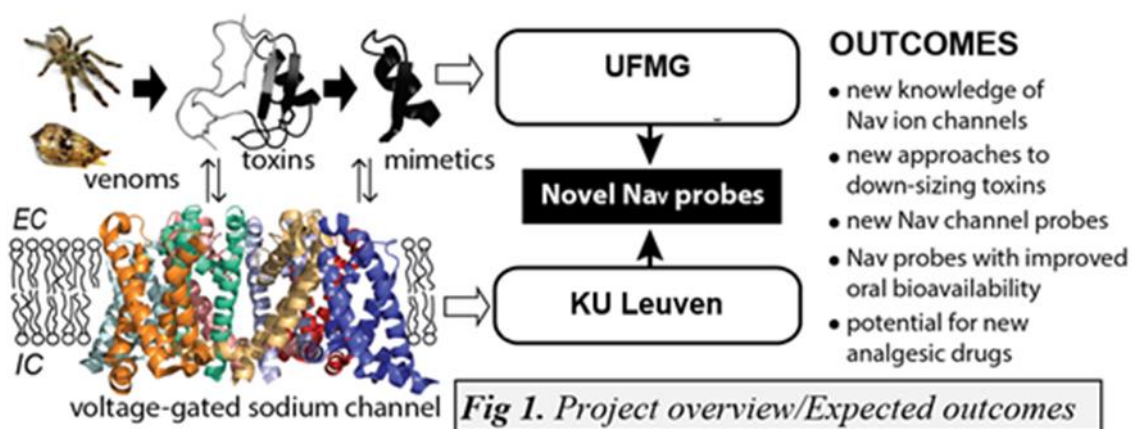


Figure 26. Project hypothesis.

There is a general perception that peptides, including disulfide-rich toxins, make good drug leads, but poor drug candidates due to unfavorable physiochemical attributes, including poor *in vivo* pharmacokinetics, rapid proteolytic cleavage and low oral bioavailability. These issues can be overcome by downsizing the toxin peptides, by improving their structural stability and by incorporating elements known to improve oral bioavailability. Downsizing approaches such as described for the chimeric peptide Pn allow better Nav subtype selective targeting by reducing cross-subtype reactivity. Structural stabilization also allows tighter control of Nav binding interactions and can be achieved by chemical modification of the disulfide bond whereas oral bioavailability can be improved by backbone cyclisation (Wang and Donald, 2004). These methods will play an important role in future development of toxin-based peptide drugs, and exploration of these methods will be incorporated in to our engineering strategy when designing our novel Nav channel probes with improved physiochemical properties. In order to take the next step and turn our novel peptide probes into analgesic drug candidates, we need to delineate what drives oral bioavailability of peptides and the research intended in this

project will address whether a rational method can be incorporated into peptide design to achieve this goal.

This project will advance the knowledge in the field of ion channel probe design, as it will fill a major gap in our understanding of the molecular requirements that drive subtype selective regulation of Nav channels pore inhibitors. The pain research industry has made a considered judgment that ion channels are key pharmaceutical targets and that venom-derived toxins are a largely untapped source of molecules with potent actions on a range of ion channels. However, due to the sequence and structural similarities between different Nav channel subtypes, it is imperative to tease out the molecular basis for selective inhibition, thereby minimising the side effects of off-target binding.

3. Objectives

3.1. General Objective

This project aims to identify peptides from the venom of *P. nigriventer* as Nav channel ligands with potential towards pharmaceutical application.

3.2. Specific Objectives

In order to achieve this, we aim at two strategies; **(i)** investigation of *P. nigriventer* venom peptide **PnTx2-1** which still lack an in-depth characterisation of their activity on Nav channels and **(ii)** peptide engineering of the already well-characterized toxin **PnTx1**.

(i) PnTx2-1

Aim 1: In-depth characterization of PnTx2-1 as a Nav channel ligand and evaluation of its therapeutic potential.

Aim 2: Peptide engineering of PnTx2-1 if positively evaluated as a lead compound following aim 1.

Outcomes: Characterization of PnTx2-1 as a Nav channel ligand. Depending on the obtained pharmacological profile, PnTx2-1 will be evaluated for its therapeutic potential. Upon positive evaluation, this peptide will be subjected to peptide engineering in order to improve its bioavailability and to determine the key residues for interaction with its targets.

(ii) PnTx1

Aim 1: Subtype selectivity determination of second and third generation Pn mutants.

Aim 2: Design and evaluation of activity and Nav subtype selectivity of novel Nav probes.

Design of fourth generation Nav probes

Following the identification of PnCS1 as a promising scaffold for further Nav1.7 and Nav1.9 inhibitor design, we will carry out a fourth round of structure-activity relationship studies using Multiple Attribute Positional Scanning (MAPS). This method systematically replaces every non-cysteine residue with an amino acid possessing a variety of chemical attributes. To cover a broad range of chemical space, we will replace each amino acid with alanine, lysine or glutamic acid, and also replace tryptophan residues with tyrosines. This design cycle will result in a second series of 28 cyclic peptides which will be synthesised at IMB and that will undergo pharmacological evaluation at KU Leuven and UFMG.

Pharmacological evaluation Nav probes

Nav subtype activity for each of the analogues will be evaluated using electrophysiology assays (at KU Leuven). *Xenopus laevis* oocytes injected with mRNAs encoding Nav channel subtype genes (Nav1.1-Nav1.9_C4) will be used in two-electrode voltage clamp experiments. Current-voltage relationships, voltage-dependence of activation and inactivation, as well as voltage-

dependent Na⁺ conductance will be determined and used to describe Nav channel inhibition by control toxins compared to the novel probes.

Stability of novel Nav probes

We will determine the stability of Nav probe analogues with promising binding and/or activity profile in serum monitoring the loss of peptide integrity using RP-HPLC and MS (Huang et al., 2015).

Outcomes: The third generation of small cyclic Nav probes will provide extensive structure-activity relationship data across therapeutically relevant Nav channels, including Nav1.7 and Nav1.9, crucial for taking these peptides into the next phase of delineating peptide-Nav channel interactions and incorporating features to improve oral bioavailability.

Aim 2: In vivo evaluation of the role of selected novel Nav probes in the nociceptive pathway

Algesimetric method

We intended to investigate the role of selected novel Nav probes in the nociceptive pathway using the algesimetric method.

Outcomes: 4 selected Nav probe analogues, with a promising subtype selectivity towards pain pathway related Nav subtypes, will be used to validate the role of these molecules in the nociceptive pathway. These unique probes will be excellently positioned to provide the next generation of Nav channel neuroscience tools and drug candidates for the treatment of pain.

4. Material & Methods

4.1. Animals

4.1.1. Mice

All animal care and experimental protocols are approved by the local Ethics Committee on Animal Experimentation (CETEA) of UFMG and are in accordance with ARRIVE guidelines (Kilkenny et al., 2010; McGrath and Lilley, 2015). Efforts were made to minimize suffering and reduce the number of animals used in the experiments. Male Swiss mice, weighing between 30 g and 40 g, from the Bioterism Center of Federal University of Minas Gerais (CEBIO-ICB/UFMG, Brazil), were used in all experiments. The animals were placed in standard cages, with free access to water and food. They were housed in a temperature-controlled room ($24^{\circ}\text{C} \pm 2^{\circ}\text{C}$) with a 12-hour light/dark cycle. After the experimental procedures, the animals were euthanized with 300 mg/kg of ketamine and 15 mg/kg of xylazine, both Sigma-Aldrich, USA.

4.1.2. Xenopus laevis frogs

The use of the frogs was in accordance with the license number LA1210239 of the Laboratory of Toxicology & Pharmacology, University of Leuven. All animal care and experimental procedures agreed with the guidelines of ‘European convention for the protection of vertebrate animals used for experimental and other scientific purposes’ (Strasbourg, 18.III.1986).

4.2. Algesimetric method

4.2.1. Measurement of nociceptive threshold

Hyperalgesia was induced using subcutaneous injection of prostaglandin E2 (PGE₂; 2 µg) into the plantar surface of the hind paw (intraplantar injection). The nociceptive threshold

was measured according to Randall and Selitto (Randall and Selitto, 1957) and adapted to mice by Kawabata et al. (Kawabata et al., 1992), using the mechanical paw pressure test. An analgesia-meter was used (UgoBasile, Italy) with a cone-shaped paw-presser with a rounded tip, which applies a linearly increasing force to the hind paw. The weight in grams (g) required to elicit the nociceptive response of paw withdrawal was determined as the nociceptive threshold. The nociceptive threshold was expressed in grams and it was determined in the right hind paw according to the average of 3 consecutive measures recorded before (0 time) and after PGE2 injection (3 hours). A cut-off value of 160 g was used to reduce the possibility of damage to the paws.

4.2.2. Drug Administration

Prostaglandin E2 (PGE2; Sigma, EUA) was diluted in ethanol 10% whereas the peptides PnCs1, PnCs1[W4K], PnCs1[R6E] and PnCs1[W7Y] were dissolved in sterile physiological solution (saline). All these drugs were injected into the right plantar surface of the paw in a volume of 20 μ L per paw.

4.2.3. Experimental Protocol

To evaluate the temporal development of the dose response curve, PGE2 (2 μ g) was injected into the right hind paw of the animals and the peptides were given 180 minutes after the local injection of PGE2 (peak of PGE2 hyperalgesia). The nociceptive threshold measurements were recorded every 5 minutes, from 180 to 240 minutes. To exclude systemic effect, PGE2 was injected into both hind paws, whereas each peptide was injected only into the right paw 150 minutes after PGE2 injection. The contralateral paw received vehicle (saline). Nociceptive threshold was measured in both hind paws in two moments, before any injection

(zero time) and at 180 min after PGE2 injection. The difference between these values was expressed as Δ of the nociceptive threshold.

4.2.4. *Statistical Analysis*

The results were shown as the mean \pm S.E.M. and the data were statistically analyzed using analysis of variance followed by Bonferroni test. Statistically significance was set at $p < 0.05$.

4.3. Peptide synthesis

Pn and PnM1-PnM9 were purchased from GenicBio Limited[®]. PnCS1-PnCS4 and Pn-Ala/Lys/Glu scanning peptides were chemically synthesized using standard Fmoc solid-phase synthesis protocols on a Symphony peptide synthesizer (Protein Technologies Inc). PnCS1 and PnCS2 were assembled on rink-amide resin at 0.25 mmol scale to produce an amidated C terminus whereas PnCS3 and PnCS4 were assembled on 2-chlorotrityl (2-CTC) resin at 0.25 mmol scale. Amino-acid protecting groups used were Cys(Trt), Asp(tBu), Lys[Boc, #307], Asn(Trt), Arg(Pbf), Trp(Boc), Lys(Alloc) and Asp(Allyl). For PnCS1, the peptide was released from the resin and amino acid side chain simultaneously deprotected by incubation with triisopropylsilane (TIPS):H₂O:trifluoroacetic acid (TFA) (2:2:96, v/v/v) for 2.5 h at room temperature. TFA was evaporated under vacuum, and the peptide precipitated with ice-cold diethyl ether. PnCS1 was dissolved in 50% acetonitrile (ACN) (0.05% TFA) and lyophilized. The crude linear peptide was purified using reversed phase high-performance liquid chromatography (RP-HPLC) (0–80% B over 80 min, flow rate 8 mL/min, solvent A; 0.05% TFA, solvent B 90% ACN/0.045% TFA on a Shimadzu instrument) and its molecular mass determined using electrospray mass spectrometry (ESI-MS). Purified PnCS1 was oxidized at room temperature in 0.1 M ammonium bicarbonate buffer at pH 8.3 over 24 h. Peptides were

>95% pure, as determined using analytical-HPLC, and 1D and 2D NMR ^1H spectroscopy was used to confirm the presence of one isomer. The PnCS2's lactam bridge was formed by cleaving the Allyl and Alloc groups off with 3 eq. of $\text{Pd}(\text{Ph}_3\text{P})_4$ in chloroform/acetic acid/*N*-methylmorpholine (37:2:1) for 2 h under argon. The resin was then consecutively washed with 0.5% *N,N*-diisopropylethylamine (DIPEA) in *N,N*-dimethylformamide (DMF) and sodium diethyldithiocarbamate (0.5% w/w) in DMF to remove the catalyst. The bond was then formed by coupling the two free side chains with 2 eq. of (benzotriazol-1-yloxy)tris(dimethylamino)phosphonium hexafluorophosphate (BOP) and 4 eq. of DIPEA in DMF overnight. The resin was washed with DMF and then dichloromethane (DCM) before being dried under N_2 . The peptide was then worked up as previously described for PnCS1. For PnCS3 and PnCS4, the peptides were released from the resin by treatment of 1% TFA in DCM for 10 x 5 min leaving the protecting groups attached. PnCS3 and PnCS4 were cyclized protected in solution by addition of (1-[bis(dimethylamino)methylene]-1H1,2,3-triazolo[4,5b]pyridinium3-oxidhexafluorophosphate) (HATU) and DIPEA to peptide (ratio 5:10:1) in DMF for 3 h. The protecting groups were subsequently removed using the conditions described for cleavage of PnCS1 and PnCS2. PnCS4 was oxidized as previously described and both PnCS3 and PnCS4 were purified and characterized as described above.

4.4. NMR spectroscopy

1D and 2D NMR spectra of Pn were recorded on a 600 MHz or 500 MHz Bruker Avance II NMR spectrometer equipped with a cryoprobe. Peptide samples were prepared in 90% $\text{H}_2\text{O}/10\% \text{D}_2\text{O}$ or 100% D_2O (Sigma-Aldrich) at ~ 5 mM and pH ~ 4 . Water suppression was achieved using excitation sculpting gradients (Hwang and Shaka, 1998). Spectra recorded were 1D ^1H and 2D TOCSY (mixing time 80 ms), NOESY (mixing time 200 and 300 ms) and DQF-COSY. In the processing of two-dimensional spectra, data were apodized with a shifted sine-

bell square function in both dimensions. All spectra were processed by using Topspin 2.1 (Bruker Biospin) and analyzed using CARA program (version 1.8.4). Proton chemical shifts were calibrated by using residual water (HOD) signal as a reference (4.97 ppm at 293 K). Natural abundance ^1H - ^{13}C HSQC spectra in D_2O were recorded with sensitivity enhancement and gradient coherence selection, optimized for selection of aliphatic CH groups ($J_{\text{CH}} = 135$ Hz) using 64 scans, 1024/2048 complex data points, and 12072/7210 Hz spectral widths in t_1 and t_2 respectively.

4.4.1. Structural constraints

Distance restraints were derived from cross-peak volumes of the NOESY spectrum recorded with 200 ms mixing time. Average cross-peak volume of the geminal methylene proton pairs was used as reference volume, which corresponds to the fixed reference distance of 1.8 \AA . The $^3J_{\text{HN-H}\alpha}$ coupling constants were measured from the one-dimensional proton spectrum recorded in H_2O and then should be converted to dihedral restraints as follows: $^3J_{\text{HN-H}\alpha} > 8 \text{ Hz}$, $\varphi = -120 \pm 30^\circ$; $^3J_{\text{HN-H}\alpha} < 5.5 \text{ Hz} = -60 \pm 30^\circ$. However, all $^3J_{\text{HN-H}\alpha}$ were between 5.5 and 8 Hz, therefore no dihedral restraints were applied in the structure calculation.

4.4.2. Structure calculations

All structure calculations were performed by using Xplor-NIH program, version 2.25. A set of 100 structures was generated by torsion angle molecular dynamics, starting from an extended strand and by using NMR-derived NOE restraints and two disulfide (C1-C11, C3-C13) bond restraints. Following torsion angle molecular dynamics, the majority of the structures had no NOE or dihedral violations. Twenty lowest energy structures were used for further refinement during a “gentle molecular dynamics” round in explicit water (Spronk et al., 2002). A box of water was constructed and optimized around selected structures obtained from the previous

torsion angle dynamics step. The final stage of refinement commenced with a 20-ps constant temperature molecular dynamics simulation at 300 K (20,000 steps of 0.001 ps) and was followed by a 200-step conjugate gradient energy minimization of the average structure of the last 10 ps of the 20 ps simulation. Structures were analyzed by using PROCHECK. Visual representations of the molecule were created by using UCSF Chimera program (version 1.8rc).

4.5. Expression of voltage-gated ion channels in *Xenopus laevis* oocytes

For the expression of Nav channels (hNav1.1, rNav1.2, rNav1.3, rNav1.4, hNav1.5, mNav1.6, rNav1.7, rNav1.8, hNav1.9_C4, the invertebrate channels DmNav1, BgNav1.1, VdNav1 and the auxiliary subunits β 1, β 1 and TipE) in *Xenopus* oocytes, the linearized plasmids were transcribed using the T7 or SP6 mMESSAGE-mMACHINE transcription kit (Ambion®, Carlsbad, California, USA). The construction of Nav1.9_C4 was described previously (Goral et al., 2015). Stage V–VI *Xenopus laevis* oocytes were isolated by partial ovariectomy. The animals were anesthetized by a 15 min submersion in 0.1% tricaine methane sulfonate (Sigma®) solution (pH 7.0). Isolated oocytes were defolliculated with 1.5 mg/mL collagenase. Defolliculated oocytes were injected with with 50 nL of cRNA at a concentration of 1 ng/nL using a micro-injector (Drummond Scientific®, Broomall, Pennsylvania, USA). The oocytes were incubated in a solution containing (in mM): NaCl, 96; KCl, 2; CaCl₂, 1.8; MgCl₂, 2 and HEPES, 5 (pH 7.4), supplemented with 50 mg/L gentamycin sulfate.

4.6. Electrophysiological recordings

Two-electrode voltage-clamp recordings were performed at room temperature (18–22 °C) using a Geneclamp 500 amplifier (Molecular Devices®, Downingtown, Pennsylvania, USA) controlled by a pClamp data acquisition system (Axon Instruments®, Union City, California, USA). Whole-cell currents from oocytes were recorded 1–4 days after mRNA injection. Bath

solution composition was (in mM): NaCl, 96; KCl, 2; CaCl₂, 1.8; MgCl₂, 2 and HEPES, 5 (pH 7.4). Voltage and current electrodes were filled with 3 M KCl. Resistances of both electrodes were kept between 0.8 and 1.5 MΩ. The elicited currents were filtered at 1 kHz and sampled at 20 kHz using a four-pole low-pass Bessel filter. Leak subtraction was performed using a -P/4 protocol. In order to avoid overestimation of a potential toxin-induced shift in the current–voltage relationships of inadequate voltage control when measuring large Na⁺ currents in oocytes, only data obtained from cells exhibiting currents with peak amplitude below 2 μA were considered for analysis. For the electrophysiological analysis of toxins, a number of protocols were applied from a holding potential of –90 mV with a start-to-start interval of 0.2 Hz. Na⁺ current traces were evoked by 100-ms depolarizations to V_{max} (the voltage corresponding to maximal Na⁺ current in control conditions). The current–voltage relationships were determined by 50-ms step depolarizations between –90 and 70 mV, using 5-mV increments. The Na⁺ conductance (g_{Na}) was calculated from the currents according to Ohm's law: $g_{Na} = I_{Na}/(V - V_{rev})$, where I_{Na} represents the Na⁺ current peak amplitude at a given test potential V, and V_{rev} is the reversal potential. The values of g_{Na} were plotted as a function of voltage and fitted using the Boltzmann function: $g_{Na}/g_{max} = [1+(\exp(V_g - V)/k)]^{-1}$, where g_{max} represents maximal g_{Na}, V_g is the voltage corresponding to half-maximal conductance and k is the slope factor. Toxin-induced effects on the steady-state inactivation were investigated using a standard two-step protocol. In this protocol, 100-ms conditioning 5-mV step prepulses ranging from –90 to 70 mV were followed by a 50-ms test pulse to –30 or –10 mV. Data were normalized to the maximal Na⁺ current amplitude, plotted against prepulse potential and fitted using the Boltzmann function: $I_{Na}/I_{max} = [(1-C)/(1+\exp((V-V_h)/k))] + C$, where I_{max} is the maximal I_{Na}, V_h is the voltage corresponding to half-maximal inactivation, V is the test voltage, k is the slope factor, and C is a constant representing a non-inactivating persistent fraction (close to zero in control). The time constants (τ) of the Nav channel fast inactivation were measured directly

from the decay phase of the recorded Na⁺ current using a single-exponential fit. To assess the concentration–response relationships, data were fitted with the Hill equation: $y = 100/[1+(EC_{50}/[toxin])^h]$, where y is the amplitude of the toxin-induced effect, EC_{50} is the toxin concentration at half maximal efficacy, $[toxin]$ is the toxin concentration and h is the Hill coefficient. All data are presented as mean \pm standard error (S.E.M.) of at least 5 independent experiments ($n \geq 5$). All data were tested for normality using a D'Agostino Pearson omnibus normality test. All data were tested for variance using Bonferroni test or Dunn's test. Data following a Gaussian distribution were analyzed for significance using one-way ANOVA. Non-parametric data were analyzed for significance using the Kruskal–Wallis test. Differences were considered significant if the probability that their difference stemmed from chance was 55% ($p < 0.05$). All data was analyzed using pClamp Clampfit 10.0 (Molecular Devices®, Downingtown, Pennsylvania, USA) and Origin 7.5 software (Originlab®, Northampton, Massachusetts, USA).

4.7. Serum-stability tests

The stability of peptides in human serum was examined using a protocol reported previously (Chan et al., 2011). Briefly, stock solutions of peptides (300 μ M) were diluted 10 times with pre-warmed 100% human serum isolated from male AB plasma (Sigma-Aldrich) and incubated at 37 °C for 0, 1, 2, 3, 5, 8, 12 and 24 h. Controls with peptides in ND96 were included. The reaction was stopped by denaturing the serum proteins with urea at a final concentration of 3 M at 4 °C for 10 min, followed by precipitation of serum proteins with trichloroacetic acid at a final concentration of 7% (v/v) (4 °C, 10 min) and centrifugation (17,000 g, 10 min). The supernatant of each sample was recovered and run on an analytical column using a linear gradient of 0–40% solvent B (acetonitrile 100% (v/v) with 0.085% (v/v) TFA in H₂O) in solvent A (0.1% (v/v) TFA in H₂O) over 40 min at a flow rate of 0.5 mL/min with monitoring at 214

nm. The elution profile of each peptide was identified by the ND96 sample from 0 time point. The percentage of peptide remaining in serum-treated samples was determined by comparing the height of the peptide peak obtained at each time point with that of the peptide peak obtained at 0 time point. Each experiment was done in triplicate.

5. Results

5.1. Chapter 1: Investigation of *P. nigriventer* venom peptide PnTx2-1

This chapter is based on the following publication with minor changes: Peigneur S, Paiva ALB, Cordeiro MN, Borges MH, Diniz MRV, de Lima ME, Tytgat J. Toxins (Basel). 2018 Aug 21;10(9).

Historically, the *Phoneutria* toxins are annotated based on their occurrence in the venom when following the venom purification methods used in the first studies (Diniz et al., 1990b), i.e. based on a particular chromatographic step and in the order of elution of the toxin, in this step. However, a new nomenclature has been proposed based on the genus of the spider, the target of the toxin, the isoform, etc (King et al., 2008). According to this nomenclature, PnTx2-1 is also called δ -Ctenitoxin-Pn1a and it can be accessed in Archnoserver databank (<http://www.archnoserver.org>) (Pineda et al., 2018). The fraction PhTx2 was found to be toxic to both mice and insects (Figueiredo et al., 1995). Purification of fraction PhTx2 resulted in 9 peptides which were named PnTx2-1 till PnTx2-9 PnTx2-1, PnTx2-5 and PnTx2-6 showed higher toxicity after i.c. injection in mice (Cordeiro Mdo et al., 1992). Both PnTx2-5 and PnTx2-6 have been characterized as modulators of the inactivation of voltage gated sodium (Nav) channels (Matavel et al., 2002a; Matavel et al., 2009).

Toxin PnTx2-1(5838.8 Da) shares up to 77% identity with PnTx2-5 and PnTx2-6 (Figure 27) (Cordeiro Mdo et al., 1992). When injected *in vivo*, PnTx2-1 causes pruritus, lacrimation, increased salivation, sweating, and agitation followed by spastic paralysis of the limbs (Figueiredo et al., 1995). However, PnTx2-1 remains scarcely studied. A recent transcriptomic and proteomic investigation of *P. nigriventer* venom showed that PnTx2-1 altogether with its isoforms is among the most expressed toxins in this venom (Diniz et al., 2018). This suggests that this toxin may play an important role in the envenoming of natural preys. Based on the *in*

in vivo tests in mice and the sequence identity with PnTx2-5 and PnTx2-6, this peptide is classified as a Nav channel toxin. However, it has never been tested on any Nav channel isoform. Therefore, in this study the Nav channel subtype selectivity and species specificity of PnTx2-1 are investigated. Furthermore, comparison of the activity of both PnTx2-1 and PnTx2-6 on Nav1.5 reveals that this family of *Phoneutria* toxins modulates the cardiac Nav channel in a bifunctional manner, resulting in an alteration of the inactivation process and a reduction of the sodium peak current.

	1	10	20	30	40	50
PnTx2-1	ATCAGQDKPCKETCDCCGERGECV	CALSYEGKYRCICRQGNFLIAWHK	LASCK-			
PnTx2-5	ATCAGQDQTCKVTCDCCGERGECV	CGG-----PCICRQGNFLIAWYK	LASCKK			
PnTx2-6	ATCAGQDQPCKETCDCCGERGECV	CGG-----PCICRQGYFWIAWYK	LANSCKK			

Figure 27. Sequence alignment of PnTx2-1 with Nav_s channel toxins from *Phoneutria nigriventer* venom fraction 2.

5.1.1. Activity of PnTx2-1 on mammalian Nav channels

PnTx2-1 was screened against a panel of 7 mammalian Nav channel isoforms (Nav1.1-Nav1.6 and Nav1.8), 1 insect from the cockroach *Blattella germanica* (BgNav1) and 1 arachnid channel from the mite *Varroa destructor* (VdNav1) (Figure 28).

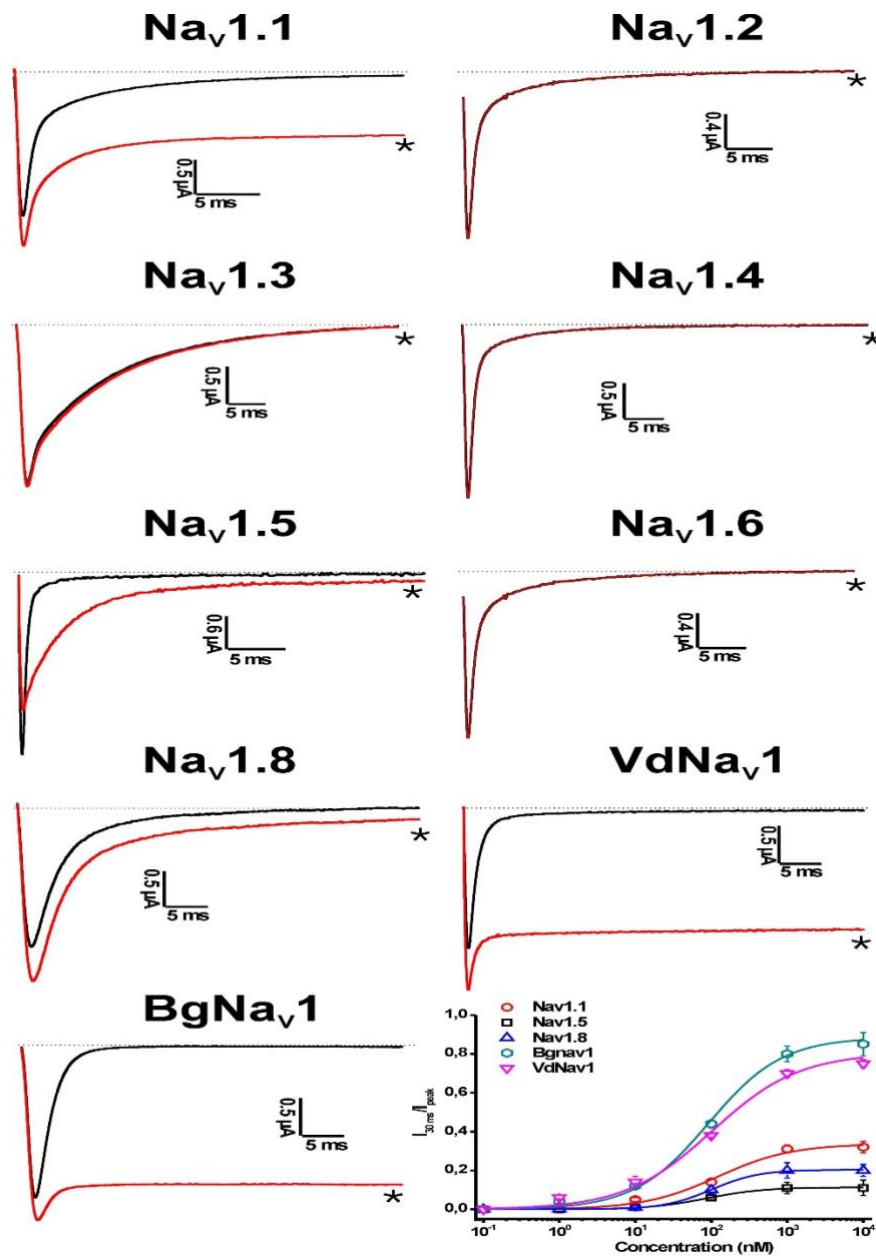


Figure 28. Electrophysiological profile of PnTx2-1 on Navs. Panels show superimposed current traces. The dotted line indicates zero current level. Black; current trace in control conditions, red, current trace in toxin situation. The asterisk marks steady-state current trace after application of 1 μM peptide. The bottom right panel shows the concentration-response curves for PnTx2-1 on mammalian Nav channel isoforms.

Among the mammalian isoforms, 1 μM PnTx2-1 slowed the inactivation of Nav1.1, Nav1.5 and Nav1.8. Nav1.2, Nav1.3, Nav1.4, Nav1.6 were not affected by PnTx2-1. Interestingly, PnTx2-1 had a profound effect on the inactivation of the insect channel BgNav_v1 and the arachnid channel VdNav_v1. PnTx2-1 almost completely inhibited inactivation of BgNav_v1 channels, resulting in a small percentage of

inactivating channels remaining (<5% of the whole cell current). Concentration response curves were constructed to determine the values at which half of the channels were modulated by PnTx2-1. Among the mammalian isoforms, the EC₅₀ values yielded 122.1 ± 34.6 nM, 87.0 ± 7.5 nM and 101.1 ± 5.1 nM for Nav1.1, Nav1.5 and Nav1.8, respectively. Activation and steady-state inactivation curves were constructed for Nav1.1, Nav1.5 and Nav1.8 channels (Figure 29a-c, Table 3). In the presence of 1 μM toxin, a significant modulation of gating kinetics was observed for Nav1.1 and Nav1.5 (Figure 29a & b). For both Nav1.1 and Nav1.5 channels, the midpoint of activation shifted towards more depolarized potentials (Table 3). At the same time, the steady-state inactivation curves shifted towards more hyperpolarized membrane potentials. The resultant for both Nav1.1 and Nav1.5 is an increased window of open probability. No relevant modulation of the gating kinetics was observed for Nav1.8 channel isoforms since no significant shift in V_{1/2} values was noted (Figure 29c, Table 3). No significant change in the reversal potential was observed in the presence of toxin which indicates that the ion selectivity of Nav channels is not altered. 1 μM PnTx2-1 strongly enhanced the recovery from inactivation for Nav1.5 channels with τ = 50.2 ± 3.0 ms in control conditions and τ = 22.8 ± 3.2 ms in the presence of the toxin (Figure 29d). To verify whether PnTx2-1 binds to neurotoxin site 1, competitive binding experiments were performed. Application of TTX at its half-maximal inhibitory concentration (IC₅₀) resulted in a blockage of half of the expressed Nav1.5 channels, as a 50% decrease of the sodium current peak amplitude was observed. Subsequent and additional application of PnTx2-1 at its EC₅₀ did result in an additional reduction of the peak amplitude (n = 6) (Figure 29e).

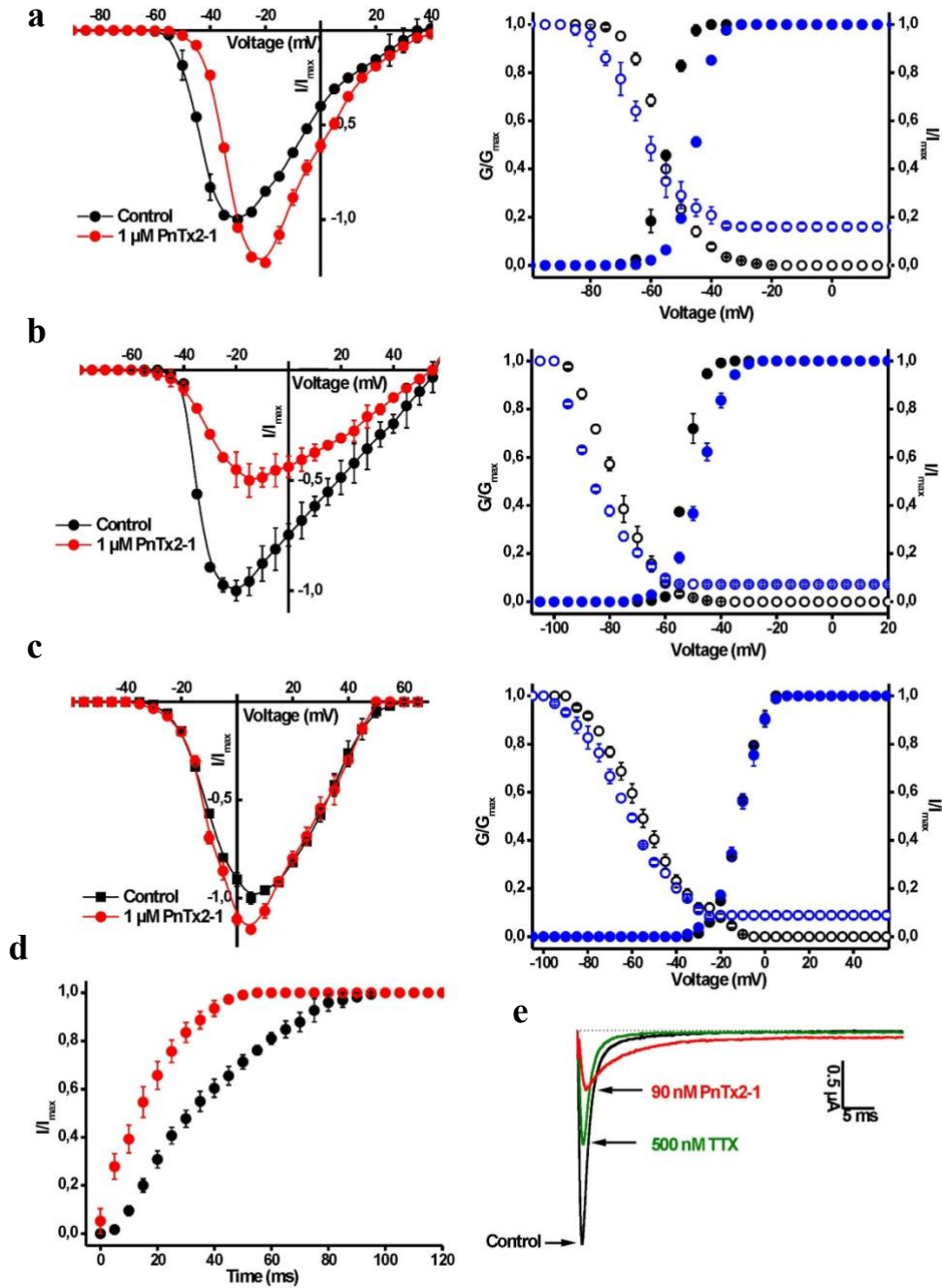


Figure 29. Electrophysiological characterization of PnTx2-1 on mammalian Nav channels. Left panels show the current voltage relationships and the right panels show the steady-state activation (closed symbols) and inactivation (open symbols) curves in control (black) and toxin conditions (1 μ M PnTx2-1, blue) for Nav1.1 (a), Nav1.5 (b) and Nav1.8 (c). (d) Recovery from inactivation in control (black symbols) and in the presence of 1 μ M PnTx2-1 (red symbols). (e) Competitive experiments to indicate that PnTx2-1 does not bind at site 1. Representative traces are shown in control; after application of 500 nM TTX and after subsequently addition of 90 nM PnTx2-1.

$V_{1/2}$ (mV)	Activation		Inactivation	
	Control	PnTx2-1 (1 μ M)	Control	PnTx2-1 (1 μ M)
Nav1.1	-56.4 \pm 0.2	-63.4 \pm 0.1	-54.7 \pm 0.1	-45.3 \pm 0.1
Nav1.5	-53.1 \pm 0.1	-45.3 \pm 0.1	-78.4 \pm 0.2	-87.5 \pm 0.7
Nav1.8	-11.5 \pm 0.1	-11.4 \pm 0.1	-55.8 \pm 0.4	-63.9 \pm 0.4
BgNav1	-38.1 \pm 0.1	-45.8 \pm 0.3	-63.3 \pm 0.3	-70.7 \pm 0.13

Table 3. $V_{1/2}$ values for the activation and steady state inactivation curves obtained for Nav1.1, Nav1.5, Nav1.8 and BgNav1.

5.1.2. Activity of PnTx2-1 on insect Nav channel currents

The EC_{50} values for BgNav1 and VdNav1 were determined at 91.9 ± 17.0 nM and 101.8 ± 14.7 nM, respectively. The most toxin-sensitive isoform, the insect Nav channel BgNav1, was used to further investigate the characteristics of PnTx2.1 in inducing modulation of channel gating (Figure 30a). A shift in the midpoint of activation and in the voltage dependence of steady-state inactivation was observed (Table 3). From Figure 28, it can be seen that the steady-state inactivation became incomplete after toxin addition. A $62.3 \pm 3.2\%$ non-inactivating current component of steady-state inactivation can be seen. In addition, we examined the recovery from fast inactivation in the absence or presence of PnTx2-1 and found that 1 μ M does not influence the recovery from fast inactivation in BgNav1 (Figure 30b). To determine whether inhibition occurs during the closed or open state of the channel, 1 μ M toxin was applied to the bath solution with oocytes clamped at -90 mV, allowing interaction with the membrane for 2 min without depolarizing the membrane. After 2 min, currents were elicited by a depolarizing pulse to 0 mV. The obtained currents in presence of toxin were normalized to the currents obtained in the same cells in control conditions. A significant slowing down of inactivation was observed when PnTx2-1 was applied to the oocytes without applying depolarizing pulses (Figure 30c). This indicates that there is toxin interaction with the channel in the closed state and suggests that membrane depolarization and hence most likely channel opening is not required to allow the toxin to bind.

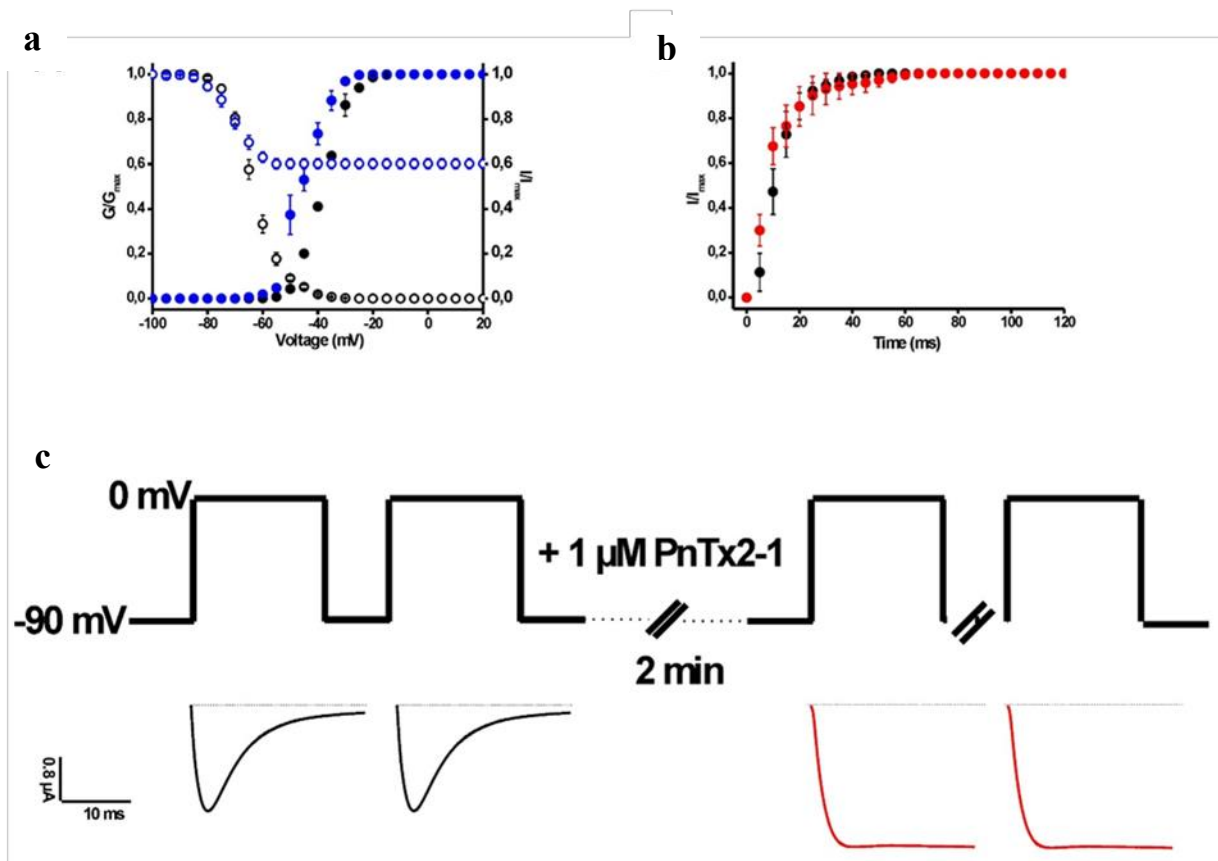


Figure 30. Electrophysiological characterization of PnTx2-1 on insect Nav channels. (a) Steady-state activation (closed symbols) and inactivation (open symbols) curves in control (black) and toxin conditions (1 μ M PnTx2-1, blue) for BgNav1.1. (b) Recovery from inactivation in control (black symbols) and in the presence of 1 μ M PnTx2-1 (red symbols). (c) Investigation of the state-dependence of indicating that an expected degree of channel inactivation inhibition was observed after the 2 min incubation, indicating that the open state is not required for toxin interaction with the channel.

5.1.3. Activity of PnTx2-6 on $Nav1.5$ channel currents

The pharmacological phenotype induced on $Nav1.5$ channels by PnTx2-1 is very similar to what has been reported previously for PnTx2-6. Therefore, we performed further characterisation of PnTx2-6 on $Nav1.5$ channels. In the presence of 1 μ M PnTx2-6, an inhibition of the sodium peak current and a delay of the inactivation was observed (Figure 31a). The slowing down of inactivation was characterized by an EC_{50} value of 22.3 ± 3.1 nM (Figure 31b). The voltage-current relationship shows a reduction of the sodium current with $21.3 \pm$

2.8% (Figure 31c). Construction of the activation and steady-state inactivation curves indicated that no significant modification of gating processes occurs (Figure 31d).

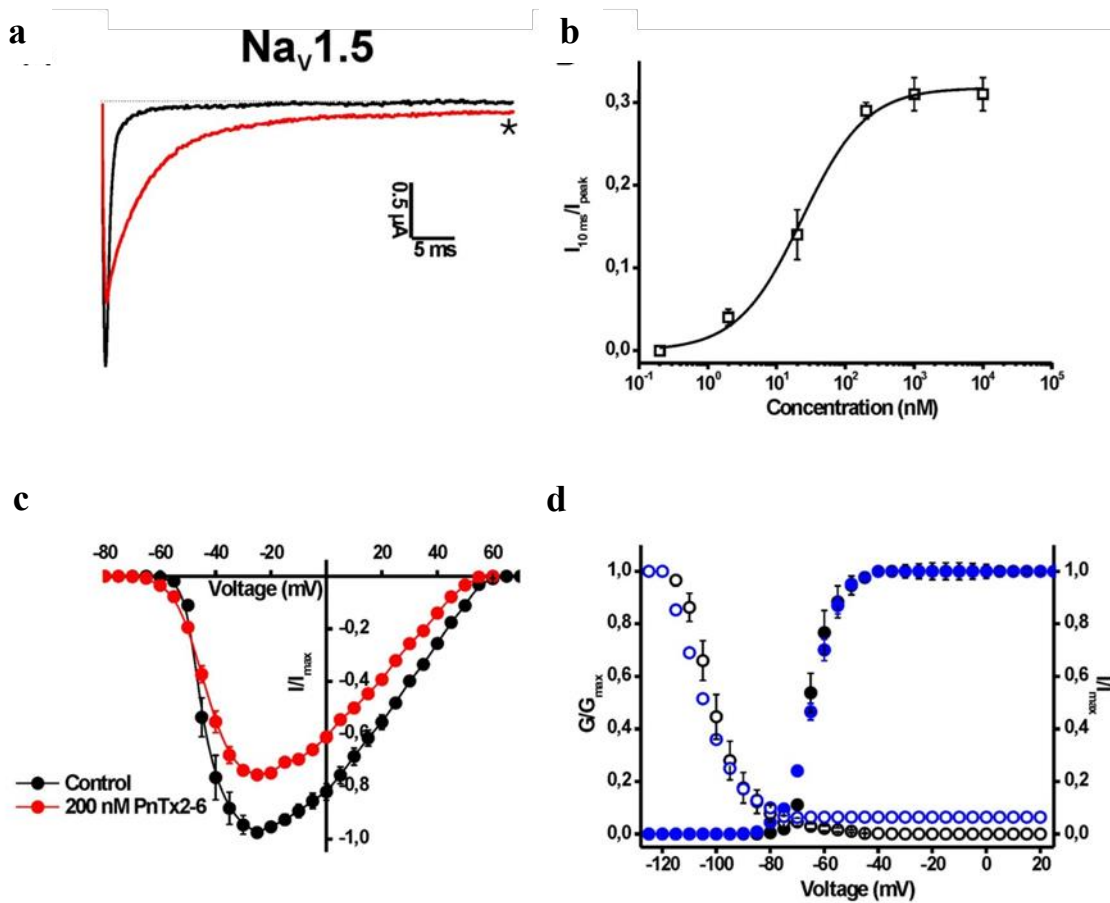


Figure 31. Electrophysiological characterization of PnTx2-6 on Nav1.5. (a) Representative whole-cell current trace in control (black) and toxin (red) conditions are shown. The dotted line indicates the zero-current level. The asterisk marks steady-state current trace after application of 1 μ M peptide. (b) Concentration-response curve for PnTx2-6 on Nav1.5. (c) Current voltage relationship. (d) Steady-state activation (closed symbols) and inactivation (open symbols) curves in control (black) and toxin conditions (1 μ M PnTx2-6, blue) for Nav1.5 channels.

5.1.4. Discussion

PnTx2-1 shares the highest sequence identity with PnTx2-5 and PnTx2-6, which are also isolated from the *Phoneutria nigriventer* venom fraction 2 (Cordeiro Mdo et al., 1992). Among all the polypeptides purified from PhTx2 fraction, PnTx2-5 and PnTx2-6 are the most studied toxins. They have high sequence identity, differing only in five amino acid residues

(Figure 27). PnTx2-5 and PnTx2-6 were found to induce a painful and persistent penile erection, also known as priapism, a common clinical manifestation upon *Phoneutria nigriventer* envenomation (Nunes et al., 2010a; Nunes et al., 2013). Both toxins were shown to modulate sodium channel kinetics by slowing down the inactivation process and by shifting the voltage dependence of activation towards more hyperpolarized potentials (Matavel et al., 2002a; Matavel et al., 2009). Interestingly, despite the high identity between both peptides, significant differences in potency have been reported. PnTx2-5 displayed an approximately 6-fold lower potency than PnTx2-6 in electrophysiological assays. It has been suggested that Tyr41 and Trp43 in PnTx2-6 are involved in the higher potency compared to PnTx2-5 (Matavel et al., 2009). Interestingly, these residues are also not conserved in PnTx2-1 (Figure 27). Nevertheless, similar EC₅₀ values were found for PnTx2-1 and PnTx2-6 on Nav1.5 channels. While PnTx2-6 exerts a strong affinity for Nav1.2-Nav1.4 and Nav1.6 channels (Silva et al., 2015a), PnTx2-1 shows no activity on these channels, even at concentrations up to 5 μM. It is well established that even minor differences in amino acid composition of peptide toxins can influence the Nav channel isoform selectivity. Binding experiments in brain synaptosomes showed that PnTx2-6 partially competes with the typical α-scorpion toxin AaHIII (from *Androctonus australis Hector*) (Matavel et al., 2009). It thus can be assumed that PnTx2-1 also acts by binding to a site similar as PnTx2-6 and the typical α-scorpion toxins. A shift of the midpoint of activation potential toward more negative potentials together with a reduction in sodium peak current are characteristics of gating alterations often observed for β-scorpion toxins and certain spider toxins (Leipold et al., 2006b; Nicholson et al., 2004; Peigneur et al., 2015). However, it was shown that PnTx2-6 does not compete with the β-scorpion toxin CssiV (from *Centruroides suffusus suffusus*) and it thus seems unlikely that PnTx2-6 binds to same site as β-scorpion toxin (Matavel et al., 2009). However, it can be assumed that the PnTx2-1 and PnTx2-6 induced inhibition of the sodium peak current results from gating modification,

rather than physical obstruction of the ion pathway. Scorpion toxins such as Ts1 and Tz1 induce a similar pharmacological phenotype activity on Nav1.5 channels as observed for PnTx2-1 (Leipold et al., 2012; Leipold et al., 2006b; Peigneur et al., 2015). For these toxins, it was evidenced that by trapping the voltage sensor in the inward position, channels are prevented from opening, which is seen as an inhibition of the sodium current for Nav1.5 channels (Catterall et al., 2007; Leipold et al., 2012; Leipold et al., 2006b; Peigneur et al., 2015). Specific residues within the voltage sensor of each Nav channel isoform together with the electrical activity of the exposed cell will determine whether a toxin exerts an excitatory, depressant or combinational pharmacological phenotype activity.

δ -Atracotoxins (δ -ACTX) are a family of Nav channel targeting toxins isolated from the venom of Australian funnel-web spiders (Nicholson et al., 2004). They are peptides of 42 amino acid residues including 8 conserved cysteine residues which form four disulfide bridges in an inhibitor cysteine-knot (ICK) motif (Nicholson et al., 2004; Rash et al., 2000). Although very low sequence identity (>25%) can be found between PnTx2-1 and these funnel web spider toxins, they do seem to interact with the Nav channels in a similar way. δ -Atracotoxins produce a selective slowing of Nav current inactivation and a reduction in peak sodium current. Moreover, they cause a hyperpolarizing shift in the midpoint of activation and an increased recovery from inactivation was seen for toxin-bound channels (Alewood et al., 2003; Gunning et al., 2003; Nicholson et al., 1996; Nicholson et al., 1994). Radiolabeled binding assays have determined that the δ -ACTX bind to the neurotoxin site 3 (Gilles et al., 2002). Several residues have been suggested to be important for the interaction of δ -ACTX with the Nav channels. However, this family still awaits structure-activity data to elucidate the exact key residues (Klint et al., 2012; Nicholson et al., 2004). It thus seems that PnTx2-1 and the δ -ACTX exert a comparable complex voltage-dependent modulation of Nav channel gating. Further structure-

function studies are required to pinpoint which toxin-channel interactions are responsible for the PnTx2-1 induced Nav1.5 channel modulations.

Although both toxins were insecticidal to the larval and adult forms of the housefly (Cordeiro Mdo et al., 1992), PnTx2-5 and PnTx2-6 have never been evaluated for their insecticidal activity towards insect Nav channels. In fact, it was always believed that *Phoneutria nigriventer* venom fraction 4 (PhTx4) was the venom fraction with the highest and most specific insecticidal activity. However, here we show that peptides of PhTx2 fraction have a similar insecticidal potential, at least regarding Nav channels. PnTx2-1 is the first member of this spider toxin family to be characterized in depth for its activity on insect Nav channels. The weak species selectivity of PnTx2-1 makes difficult the suitability of this peptide for the development of novel insecticidal agents. However, seen the low sequence identity with other spider toxins, PnTx2-1 might be a valuable tool for further characterization of possible interaction sites for bio insecticides on the insect Nav channel.

5.2. Chapter 2: Peptide engineering of the toxin PnTx1.

This chapter is based on the following publication with minor changes: Where cone snails and spiders meet: design of small cyclic sodium-channel inhibitors. Peigneur S, Cheneval O, Maiti M, Leipold E, Heinemann SH, Lescrinier E, Herdewijn P, De Lima ME, Craik DJ, Schroeder CI, Tytgat J. FASEB J. 2018 Dec 3:fj201801909R.

Voltage-gated sodium channels (Nav) are integral membrane glycoproteins responsible for generation and propagation of action potentials in excitable cells. Mutations in genes encoding these channels can lead to a variety of severe illnesses. Nav channels are considered as potential drug targets for diseases including pain syndromes, cardiac disorders and epilepsy (Abdelsayed and Sokolov, 2013). asking for potent and selective Nav channel inhibitors. *Phoneutria nigriventer*, also known as the Brazilian wandering spider, produces a potent venom, which is accountable for many of South Brazil's most severe envenomations in humans (De Marco Almeida et al., 2015; Peigneur et al., 2018). *Phoneutria nigriventer* toxin 1 (PnTx1 or Mucitenitoxin-Pn1a following the nomenclature suggested by King and colleagues (King et al., 2008)) is a 78-amino acids residue peptide, comprising 14 cysteine residues (Figure 32). It has been characterized as a Nav channel blocker with nM affinities for subtype Nav1.2 (Diniz et al., 1993; Diniz et al., 2006a; Martin-Moutot et al., 2006b). Recombinantly produced PnTx1 (rPnTx1) features selectivity toward neuronal Nav channels with the following rank: Nav1.2 > Nav1.7 ~ Nav1.4 > Nav1.3 > Nav1.6 > Nav1.8 (Silva et al., 2012a). No significant effect was observed for the cardiac isoform (Nav1.5) and invertebrate channels (Silva et al., 2012a). PnTx1's inhibitory activity for Nav1.7 channels is particularly important because of this Nav channel subtype is essential for the transmission of acute and inflammatory pain signals (King and Vetter, 2014; Liu and Wood, 2011; Silva et al., 2012a). Despite its interesting pharmacological profile, PnTx1 has never been explored for its therapeutically potential. Most likely this is because of large peptides are hard to administer and normally highly immunogenic.

Compared with these spider toxins, μ -conotoxins from predatory cone snails appear to have better properties: they have a small molecular size (<3 kDa), are readily synthesized, and display high selectivity for various Nav channel subtypes (Tietze et al., 2012). The μ -conotoxins possess an inhibitory cysteine knot structure containing three disulfide bridges (Figure 32).

As described in the introduction, μ -KIIIA targets a variety of Nav channel subtypes with high affinity (5-300 nM half-blocking concentrations) and its structure-function relationship is well characterized (Zhang et al., 2007). μ -KIIIA competes with the prototypic Nav channel blocker TTX, which inhibits the Na⁺ flow through the channel by binding to the outer vestibule of the ion-conducting pore (Figure 1). Interestingly, alanine replacement of K7, W8 and D11 yields more selective blockers, discriminating between neuronal (Nav1.2) and skeletal (Nav1.4) Nav channels (Leao et al., 2000; Torres et al., 2010a). Comparing the sequence of both toxins, one can observe similarities between the functionally important segment of the 16-residue conotoxin μ -KIIIA with a central segment of the 78-residue spider toxin PnTx1 (Figure 32d). This apparent homology raises the question whether it is possible to confer pharmacological properties of the large spider toxins to the scaffold of a miniaturized cone snail toxin.

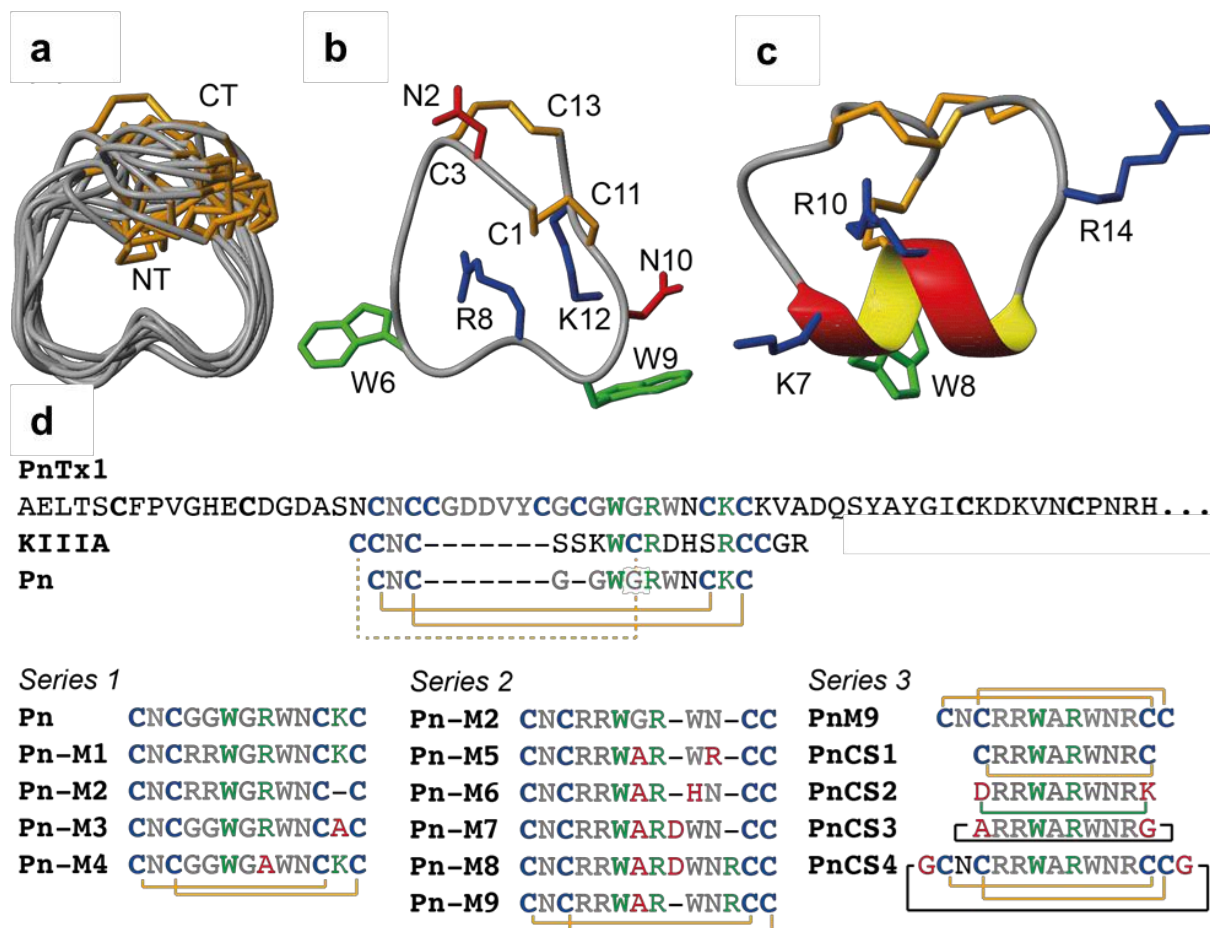


Figure 32. Structure and sequence comparison of Pn. (a) Superimposition of ten of the lowest energy structures. Superimposed across heavy backbone atoms for residues 4–12. Disulfide bonds (C1-C11 and C3-C13) are shown. (b) Ribbon structure of a Pn representative structure showing all the side chains. (c) Ribbon structure of μ -KIIIA (PDB ID: 2LXG) highlighting pharmacophore residues. Positively charged residues are shown in blue, negatively charged residues are shown in red, hydrophobic residues are in green and disulfide bonds in orange. (d) Sequence alignment and design strategy. Key residues for Na_v channel inhibition (green), PnTx1 and μ -KIIIA cysteines included in the design are shown in blue, and PnTx1 cysteines not included in the design strategy are highlighted in bold. PnM1-PnM9 (Series 1 and 2) include sequence variations compared to Pn, with mutations shown in red. PnCS1-PnCS4 (Series 3) peptides are cyclic variations of PnM9; mutations introduced for cyclisation purposes are shown in red. Disulphide bonds are shown in orange, dashed disulphide bond highlights the additional disulphide bond present in μ -KIIIA compared to Pn. Backbone cyclisation is depicted with black lines, lactam-bond is shown in green and amidated C terminus is shown by *.

We subsequently designed a 13-amino acids residue peptide with two disulfide bridges incorporating residues from the central segment of PnTx1 and known pharmacophore residues from μ -KIIIA (Figure 32b). This hybrid peptide, Pn, showed an interesting selectivity pattern when screened against a panel of Na_v channel subtypes. A first series of Pn mutants (PnM1-

PnM4) and a subsequent second series (PnM5-PnM9) allowed us to pinpoint the key residues important for activity. The remarkable ribbon-shaped and cysteine-stabilized conformation inspired the design of a third series of cyclic peptides incorporating various cyclisation strategies, including backbone, lactam bridge and disulfide bond cyclisation, with retained potent activity. These cyclized Nav channel inhibitor peptides are the smallest cyclic peptides reported to inhibit Nav channel to date and represent promising templates for further development of toxin-based therapeutics with improved physiochemical properties.

5.2.1. Design strategy

In this study, we aimed to design minimized hybrid peptides inhibiting Nav channels, benefiting from features known to be important for Nav inhibition of two toxins, μ -KIIIA and PnTx1. Alignment of PnTx1 and μ -KIIIA shows that the spacing of key residues of μ -KIIIA (W8, R10 and R14) is conserved in PnTx1 (W33, R35 and K39) (Figure 32d). Previous work has illustrated that the first disulfide bridge between Cys1 and Cys9 in μ -KIIIA is removable, almost without affecting the peptides inhibitory potency on Nav1.2 and Nav1.4 (Han et al., 2009; Stevens et al., 2011). Hence, in order to simplify peptide synthesis, the first disulfide bridge was excluded in our hybrid peptide. This resulted in the design of a thirteen amino acids residue peptide with two disulfide bridges possessing the central segment of PnTx1 while simultaneously incorporating key residues from μ -KIIIA grafted onto the scaffold of a minimized μ -KIIIA peptide.

5.2.2. Solution structure of Pn

Analysis of one-dimensional (1D) and two-dimensional (2D) TOCSY, NOESY, DQF-COSY and ^1H - ^{13}C HSQC NMR spectra shows the formation of a predominant single set of sharp resonances for the Pn peptide, indicating that it adopts a single conformation in solution.

However, additional NOEs were observed for the HE1 protons of the W6 and W9 side chains in the NOESY and TOCSY spectra, albeit with lower intensity, suggesting tryptophan side chain flexibility and the presence of a minor side chain conformation. Resonance assignment was performed using homonuclear 2D TOCSY, NOESY and DQF-COSY spectra by following standard assignment protocols as outlined by (Kline and Wuthrich, 1986). Assignment of ^1H - ^{13}C HSQC spectra further reconfirmed the homonuclear proton assignments. The geminal methylene protons were not assigned stereospecifically, and the NOE distance restraints involving these protons were used ambiguously during structure calculation in the Xplor-NIH program. The solution structure of Pn was calculated using 124 distance (78 intra-residue and 46 inter-residue) restraints derived from NOESY spectra including two disulfide (C1–C11, C3–C13) bond restraints. All $^3J_{\text{HN-H}\alpha}$ coupling constant values were in between 5.5 and 8 Hz, indicating angular averaging across the Φ dihedrals reflecting flexibility in the peptide backbone. Therefore, no dihedral restraints were included during structure calculation. Moreover, temperature coefficients ($\Delta\delta/\Delta T$) derived from the chemical shifts of backbone amide protons were -3 to -8 ppb/K, with only one exception being residue C11 with a value of -1 ppb/K. Typically, residues with temperature coefficients <-4.6 ppb/K are considered shielded and potentially involved in a hydrogen bond. No hydrogen bond acceptors were identified during structure calculations and, therefore, no hydrogen bond restraints were included in the structure calculations. Statistical analysis was carried out on the final ensemble of 20 lowest energy structures (Figure 32a, Table 4) of synthetic peptide Pn. The final 20 structures are very flexible with backbone and heavy atom RMSD of 2.89 ± 1.16 and 4.35 ± 1.15 , respectively, calculated using Molmol. Evaluation of the structure with PROCHECK showed no bad non-bonded contacts and the majority of the backbone dihedral angles were within the allowed regions of the Ramachandran plot (3.1% in the disallowed region). A closer look into the structures of Pn reveals that the peptide backbone adopts a flexible, cyclic ribbon-

shaped conformation (Figure 32a), having a main disordered loop that is closed by two disulfide bonds (C1–C11 and C3–C13). The structure is devoid of any α -helical or β -turn secondary structural elements. Side-chain orientations for all residues vary considerably within different defined domains.

PnCS1-PnCS4 peptides were analyzed using 1D ^1H and 2D TOCSY and NOESY spectra. All peptides displayed one single conformation evident from one set of resonances present for each peptide.

Distance restraints	
Intra residue	78
Inter residue	46
Total	124
Dihedral angle restraints	
	0 (Not restrained)
Atomic RMSD (\AA) ^a	
Mean global backbone (1–13)	2.89 ± 1.16
Mean global heavy (1–13)	4.35 ± 1.15
Mean global backbone (4–9)	1.41 ± 0.41
Mean global heavy (4–9)	3.31 ± 0.89
MolProbity Statistics ^b	
Clash score ($>0.4 \text{ \AA} / 1000$ atoms)	1.61 ± 2.53
Poor Rotamers	0.3 ± 0.47

Ramachandran Outliers (%)	11.82 ± 7.86
Ramachandran Favoured (%)	54.09 ± 11.61
MolProbity Score	1.91 ± 0.53
MolProbity Percentile ^c	75.60 ± 24.16

Table 4. Structural statistics for the 20 Pn structures with best MolProbity scores. ^aRMSD (Koradi et al., 1996). ^bMolProbity (Davis et al., 2007). ^c100th percentile is the best among structures of comparable resolution; 0th is the worst.

5.2.3. Electrophysiological characterization of Pn and mutants

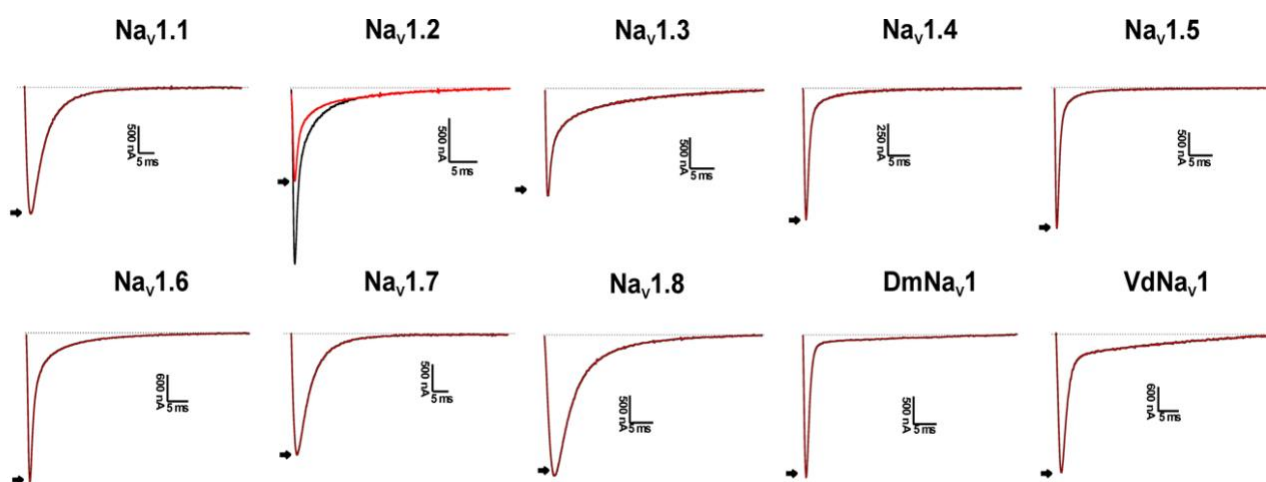


Figure 33: Electrophysiological profile of Pn on Navs. Superimposed current traces for the indicated Nav isoforms before (black) and after application of 50 μM Pn. Currents were elicited by depolarizing pulses to 0 mV. The arrow indicates the peak current level in the presence of toxin; the dotted line indicates zero current level.

When screened against a panel of ten different Nav channel isoforms (Nav1.1–1.8, and Nav insect channels BgNav1.1, VdNav1), we found that 50 μM of Pn selectively inhibited 44.6 ± 2.4% (n≥9) of the Nav1.2 channel (Figure 33) and a concentration-response curve produced an IC₅₀ value of 53.7 ± 3.2 μM (Figure 34b). No shift in the voltage dependence of activation or steady-state inactivation was observed after addition of 50 μM Pn (Figure 34a). To verify that Pn does bind to neurotoxin site 1, competitive binding experiments were performed using both

mother molecules, μ -KIIIA or PnTx1, as competitors. Application of PnTx1 at its IC_{50} value of 35 nM (Silva et al., 2012a) resulted in $48.7 \pm 4.3\%$ ($n \geq 8$) inhibition of the Na^+ peak current. Subsequent addition of IC_{50} concentrations of Pn did not result in further inhibition (Figure 34b). Similar experiments, in which first IC_{50} concentration of μ -KIIIA (60 nM, (Van Der Haegen et al., 2011)) was applied, followed by subsequently addition of IC_{50} of Pn, also did not result in additional current reduction (data not shown), indicating that Pn binds to site 1, like its parent peptides PnTx1 and μ -KIIIA.

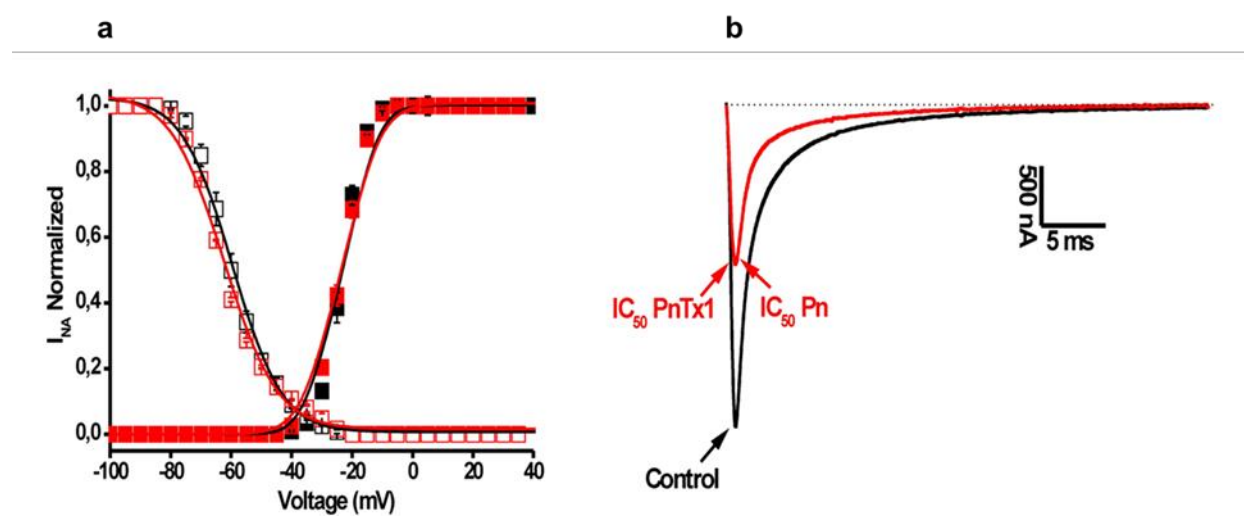


Figure 34. Electrophysiological characterization of Pn on Nav1.2 channels. (a) Steady-state activation and inactivation curves in control (closed symbols) and toxin conditions (50 μ M Pn, open symbols). (b) Competitive experiments to indicate that Pn does bind at site 1. Representative traces are shown in control (1); after application of 35 nM PnTx1 and after subsequently addition of 50 μ M Pn.

In order to improve potency of Pn, we designed a first series of mutants (Series 1) using data available from structure-function studies on μ -KIIIA and other μ -conotoxins (Figure 32d) (Brady et al., 2013; Han et al., 2009; Khoo et al., 2009; Khoo et al., 2012; Schroeder et al., 2012; Zhang et al., 2007). From this first series of mutants, PnM2 showed the most promising increase in activity when tested on Nav1.2-Nav1.6 (Table 5). Compared to Pn, PnM2 has the G4 and G5 replaced by arginine residues, and the lysine between the two last cysteines has been

removed, shortening the peptide by one residue. The second series of mutants (Series 2, Figure 32d) was designed based on the PnM2 sequence. Of these mutants, PnM9 was the most potent displaying an IC₅₀ value for Nav1.2 channels of 312.4 ± 12.8 nM (Figure 35b, Table 5).

IC ₅₀ in μM	Nav1.2	Nav1.4	Nav1.5	Nav1.6
Pn	53.7 ± 3.2	n.a.	n.a.	n.a.
PnM1	6.4 ± 0.2	> 100	5.3 ± 0,6	2.2 ± 1.1
PnM2	1.8 ± 0.5	n.a.	10.4 ± 2.1	12.3 ± 1.8
PnM3	n.a.	n.a.	n.a.	n.a.
PnM4	n.a.	n.a.	n.a.	n.a.
PnM5	4.2 ± 0.4	8.3 ± 0.8	9.8 ± 1.1	27.4 ± 0.6
PnM6	31.7 ± 2.1	32.4 ± 2.1	> 100	> 100
PnM7	7.2 ± 0.1	3.1 ± 0.2	8.3 ± 2.1	n.d.
PnM8	3.7 ± 0.2	2.4 ± 0.1	> 100	n.d.
PnM9	0.3 ± 0.1	0.3 ± 0.1	> 100	56.3 ± 4.6

Table 5. IC₅₀ values of series 1 & 2 mutants on several Nav channel isoforms. n.d. = not determined, n.a. = no activity (at 100 μM), > 100 = IC₅₀ value estimated above 100 μM.

In PnM9, Gly7 was replaced by an alanine since it has been reported that a glycine at this position is unfavorable for Nav channel activity (Nav1.1-Nav1.7) (Lebbe et al., 2014). Furthermore, an extra positive charge in form of Arg11, was introduced prior to the C-terminal cysteine. Although PnM9 increased in potency at Nav1.2 compared to Pn and PnM2, it was less selective and also inhibited the current through Nav1.4 channels, while being inactive against Nav1.5 and less active against Nav1.6 channels (Figure 35a, Table 5).

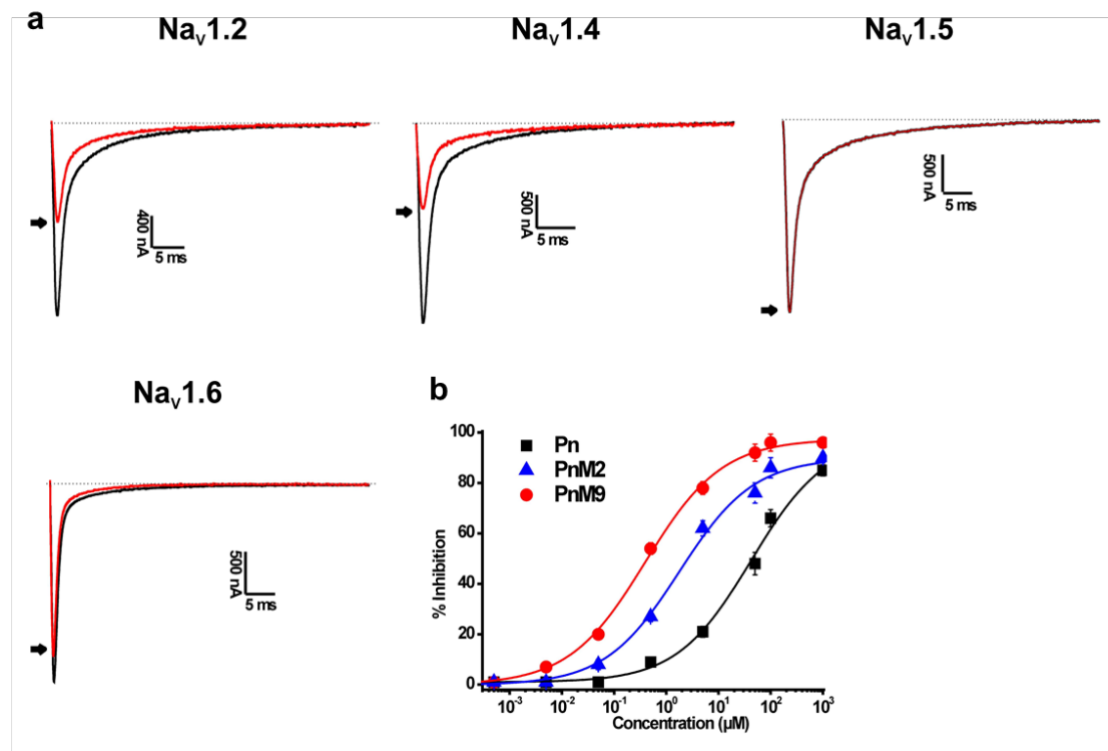


Figure 35. Electrophysiological characterization of PnM9. (a) Activity profile of PnM9 on Nav channel isoforms. Representative whole-cell current traces in control and toxin conditions are shown. The dotted line indicates the zero-current level. The arrow marks steady-state current traces after application of 400 nM peptide. (b) Concentration-response curves for Nav_v1.2 channels indicating the concentration dependence of the Pn, PnM2 and PnM9-induced decrease of the Na⁺ peak current.

Considering the close proximity of the N and the C terminus in the NMR structure of Pn (Figure 32a), and the improved potency of PnM9 compared to Pn, a third series of peptides, PnCS1-PnCS4 was designed (Series 3, Figure 32d). In PnCS1, the second disulfide bond was removed and the peptide was cyclized via its N- and C-terminal Cys residues, resulting in a ten-amino acid residue peptide. In PnCS2, the peptide was also shortened with respect to PnM9 and the N- and C-terminal Cys residues were replaced with an Asp and a Lys residue, respectively, and cyclized via a lactam bridge, resulting in a ten-amino acid residue peptide. Both PnCS1 and PnCS2 included a C-terminal amidation. PnCS3 was backbone cyclized following the replacement of the N- and C-terminal Cys residues with Ala and Gly, respectively, again leading to a ten-residue peptide, whereas in PnCS4 an additional Gly was introduced in both

the N- and the C-terminal and the peptide was backbone cyclized via an amide bond, resulting in a 15-residue peptide. Peptides, PnCS1-PnCS4, were tested for their activity against nine vertebrate Nav channels (Nav1.1-Nav1.9_C4) and three invertebrate Nav channel subtypes (BgNav1.1, VdNav1 and DmNav1) (Figure 36).

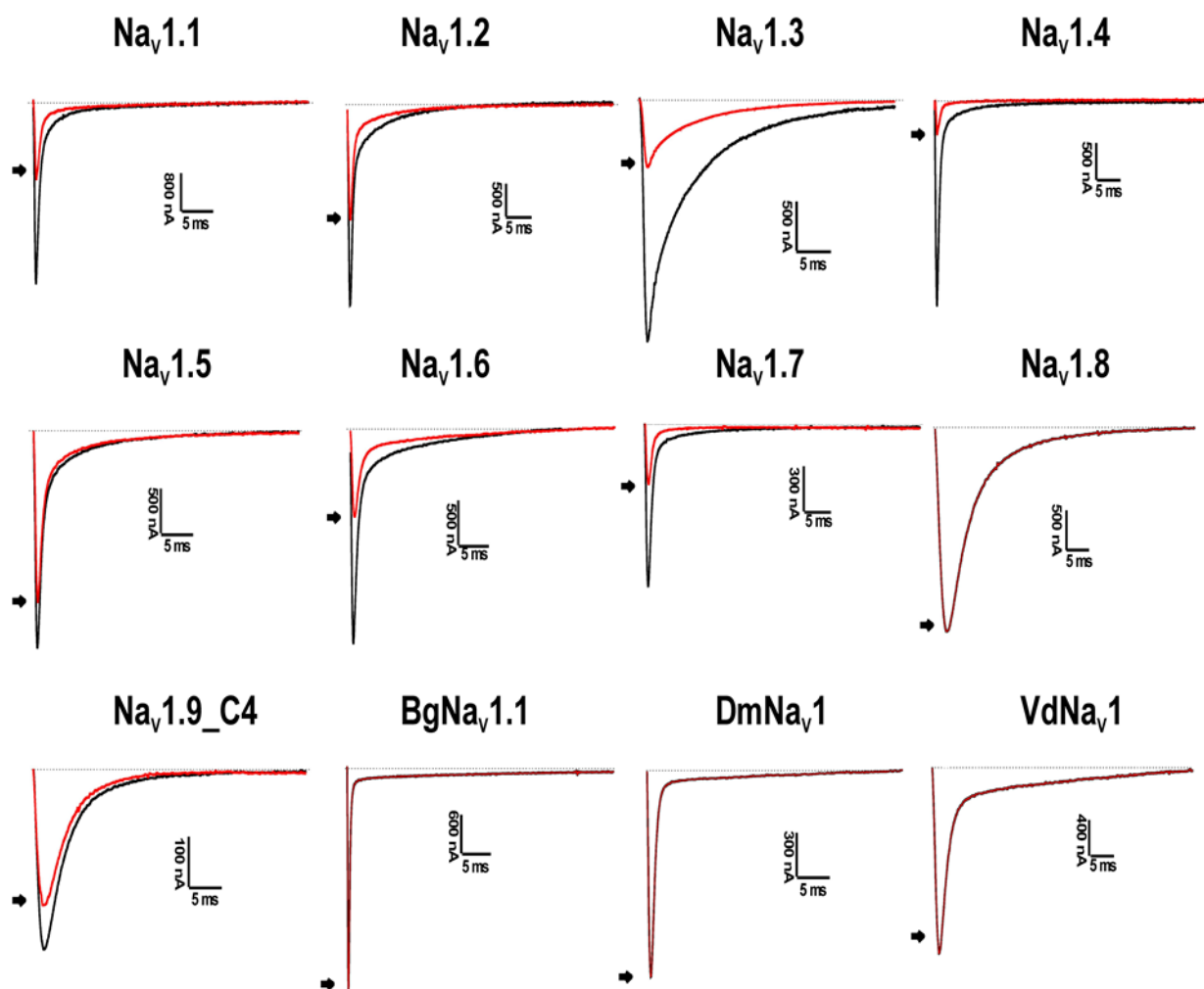


Figure 36: Electrophysiological characterization of PnCS peptides. Activity profile of PnCS1 on Nav channels. Representative whole-cell current traces in control and toxin conditions are shown. The dotted line indicates the zero-current level. The arrow marks steady-state current traces after application of 1 μ M peptide. Black; current trace in control conditions, red, current trace in toxin situation.

The concentration-dependence inhibitory effect of the PnCS peptides on Nav channels and IC_{50} values for the four cyclic variants are shown in Table 6. Both PnCS2 and PnCS3 showed a strong reduction in potency, while PnCS1 and PnCS4 were active with IC_{50} values in an approximately 3-fold higher range (Table 6).

	PnCS1	PnCS2	PnCS3	PnCS4
Nav1.1	0.8 ± 0.1	> 100	4.9 ± 0.4	1.1 ± 0.2
Nav1.2	1.0 ± 0.1	> 100	5.3 ± 0.3	0.8 ± 0.1
Nav1.3	1.1 ± 0.2	23 ± 1.6	5.4 ± 0.1	2.1 ± 0.6
Nav1.4	0.6 ± 0.2	14.3 ± 1.4	10.7 ± 0.7	0.9 ± 0.2
Nav1.5	2.8 ± 0.6	> 100	30.4 ± 4.5	4.5 ± 0.4
Nav1.6	0.7 ± 0.2	> 100	4.5 ± 0.7	4.1 ± 0.6
Nav1.7	0.9 ± 0.1	> 100	5.7 ± 0.2	3.1 ± 0.2
Nav1.8	> 100	> 100	> 100	> 100
Nav1.9_C4	4.5 ± 0.4	> 100	23.8 ± 3.5	6.3 ± 0.4
BgNav1.1	n.a.	n.a.	n.a.	n.a.
VdNav1	n.a.	n.a.	n.a.	n.a.
DmNav1	n.a.	n.a.	n.a.	n.a.

Table 6. Table with IC₅₀ values in μM obtained for PnCS1-4 (3th generation peptides) on Nav channel isoforms included in this study. n.a.; not active.

PnCS1 was used to further investigate the mechanism in which these cyclic peptides interact with their target. PnCS1, at a concentration of 1 μM, significantly inhibited the current through TTX-sensitive channels (Nav1.1-Nav1.4, Nav1.6 and Nav1.7), while the TTX-resistant isoforms were less (Nav1.5 and Nav1.9_C4) or not sensitive (Nav1.8) (Figure 36). Nav1.9_C4 is a chimera of Nav1.9 harboring the C-terminus of Nav1.4. Previous work has shown that the C-terminal structure of Nav1.9 is limiting the heterologous expression in host cells, thus

replacing the C-terminus with the corresponding segment of the Nav1.4 channel allows for functional expression in oocytes (Goral et al., 2015). Interestingly, this chimera retains the same sensitivity for site-1 blockers as Nav1.9 channels (Goral et al., 2015). Nav1.4 channels were used to further characterize the interaction of 1 μM PnCS1 with the channel.

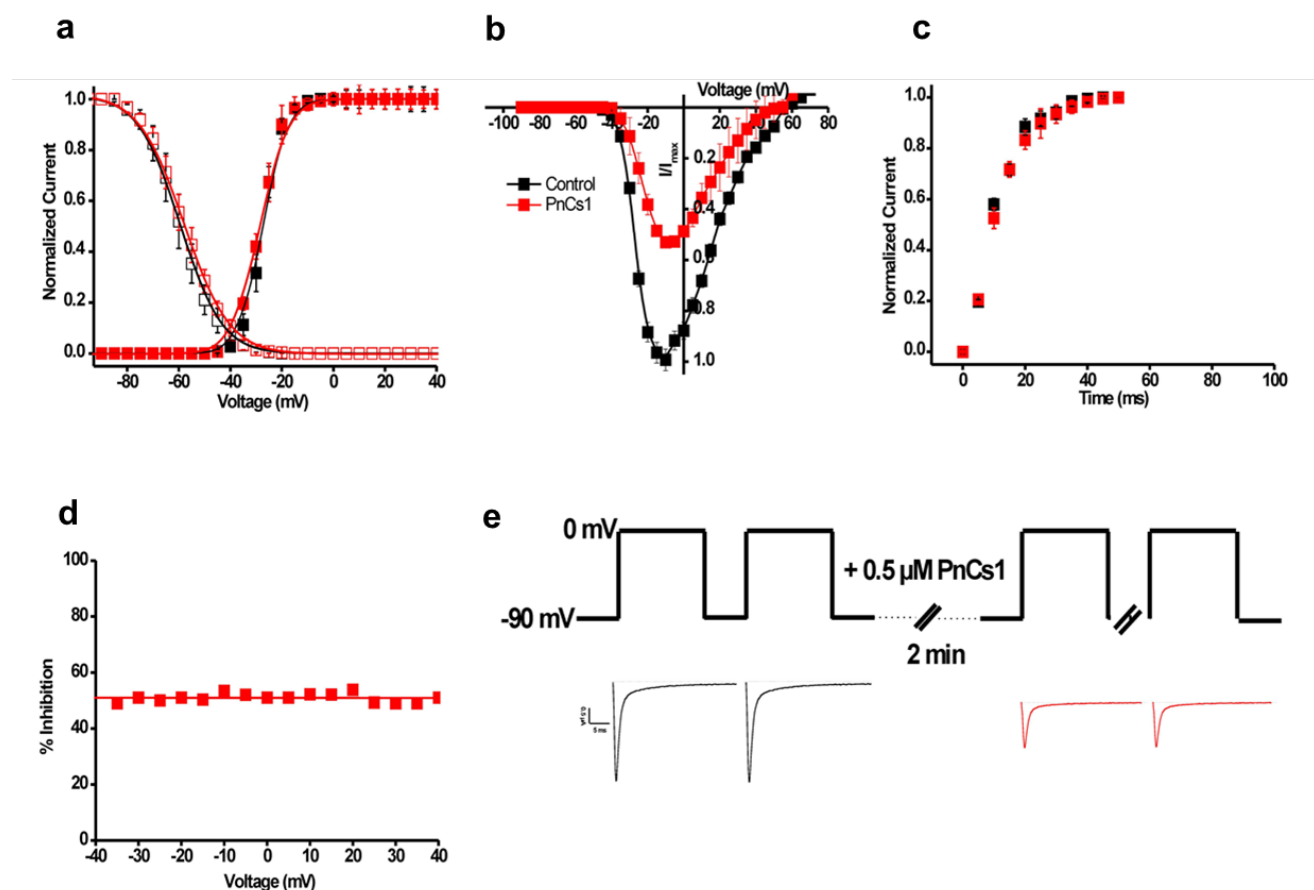


Figure 37. Electrophysiological characterization of PnCS1 on Nav1.4 channels. (a) Steady-state activation and inactivation curves in control (black symbols) and toxin conditions (0.5 μM PnCS1, red symbols). No significant alteration of activation was noted. (b) Normalized voltage-current relationship. (c) Recovery from inactivation in control (closed symbols) and in the presence of 0.5 μM PnCS1 (open symbols). (d) Voltage dependence of PnCS1 inhibition. No difference in the degree of inhibition was observed over a range of test potentials. (e) Investigation of the state-dependence of inhibition was carried out and an expected degree of inhibition was observed after the 2 min incubation, indicating that the open state is not required for toxin interaction with the channel.

Steady-state activation and inactivation curves show that no modulation of Nav channels occurs upon peptide binding (Figure 37a,b). The midpoint of activation for Nav1.4 did not shift significantly since the $V_{1/2}$ values of activation yielded -27.4 ± 0.1 mV in control and $-28.6 \pm$

0.3 mV in the presence of PnCS1. For the inactivation curves, the $V_{1/2}$ shifted from -59.4 ± 0.6 mV to -57.9 ± 1.4 mV in control and toxin situation, respectively. PnCS1 did not significantly enhance the recovery from inactivation (Figure 37c). PnCS1 inhibition was found to be voltage independent since no difference in the degree of inhibition was observed over a range of test potentials (Figure 37d). To investigate the state-dependence of inhibition, the following protocol was used. As control, a series of depolarizing pulses was applied to an oocyte expressing Nav1.4 channels. Thereafter, 0.5 μ M PnCS1 was added and no pulsing performed for 2 min. This was followed by a similar series of pulses. A strong degree of delay of inactivation was observed after the 2 min incubation, indicating that the open state is not required for toxin interaction with the channel (Figure 37e).

5.2.4. Serum stability test

To evaluate whether the designed cyclic peptides acquire increased stability compared to the non-cyclized peptides, linear and folded non-cyclic peptides (Pn, PnM9) and cyclic peptides (PnCS1-4) were incubated in human serum and the remaining peptide was quantified by analytical-HPLC (Figure 39). Linear Pn and PnM9 were fully degraded by proteases in serum within 1 h. The oxidized peptides showed higher stability than linear peptides. Nevertheless, after 24 h folded Pn was completely degraded whereas only 16% of PnM9 remained. In contrast, the cyclic peptides PnCS1-CS4 were stable in human serum with 100% of peptide remaining after 24 h.

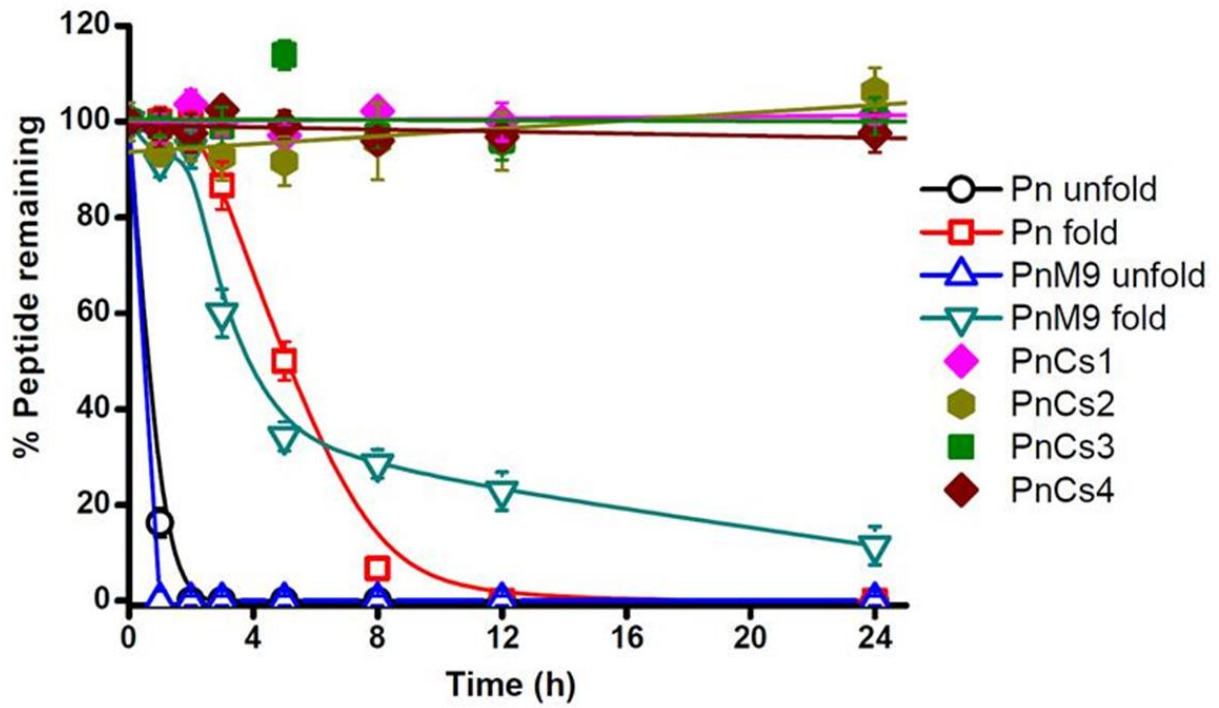


Figure 39. Serum-stability assay results. Percentage of peptide remaining in human serum in function of incubation time is shown.

5.2.5. Fourth generation of Pn peptides: design of PnCs1 mutants

Ala mutants

PnCsl [R2A] CARWARWNRC*
 PnCsl [R3A] CRAWARWNRC*
 PnCsl [W4A] CRRAARWNRC*
 PnCsl [R6A] CRRWAAWNRC*
 PnCsl [W7A] CRRWARANRC*
 PnCsl [N8A] CRRWARWARC*
 PnCsl [R9A] CRRWARWNAC*

Lys mutants

PnCsl [R2K] CKRWARWNRC*
 PnCsl [R3K] CRKWARWNRC*
 PnCsl [W4K] CRRKARWNRC*
 PnCsl [A5K] CRRWKRWNRC*
 PnCsl [R6K] CRRWAKWNRC*
 PnCsl [W7K] CRRWARKNRC*
 PnCsl [N8K] CRRWARWKRC*
 PnCsl [R9K] CRRWARWNKC*

Glu mutants

PnCsl [R2E] CERWARWNRC*
 PnCsl [R3E] CREWARWNRC*
 PnCsl [W4E] CRREARWNRC*
 PnCsl [A5E] CRRWERWNRC*
 PnCsl [R6E] CRRWAEWNRC*
 PnCsl [W7E] CRRWARENRC*
 PnCsl [N8E] CRRWARWERC*
 PnCsl [R9E] CRRWARWNEC*

Tyr mutants

PnCsl [W4Y] CRRYARWNRC*
 PnCsl [W7Y] CRRWARYNRC*

Free C-terminal

PnCslDeAm CRRWARWNRC

Acetylation of N-terminal

PnCslAcAm Ac-CRRWARWNRC*

Acetylation of N-terminal and Free C-terminal

PnCslAc Ac-CRRWARWNRC

Figure 40. Fourth generation of mutants based on PnCS1.

The obtained results justify the consideration of PnCsl as a lead compound for further studies. In a next step, a thirds generation of mutants, based on PnCsl have been generated. Figure 40 shows a series of 28 cyclic peptides, representing an Alanine scan, a Lysine scan and a Glutamate scan. In addition, Tyrosine mutants and peptides with or without N-terminal acetylation or C-terminal amidation have been synthesised. Table 7 shows the obtained IC₅₀ values for several Nav channel subtypes. Table 6 shows the maximum inhibition at a concentration of 100 µM observed for each peptide on the different Nav channel isoforms tested. In order to obtain a complete selectivity profile and to elucidate the key residues determining Nav channel subtype selectivity, the IC₅₀ values of these peptides for Nav1.1, Nav1.3, Nav1.7 & Nav1.8 needs to be determined.

IC50	Nav1.2	Nav1.4	Nav1.5	Nav1.6	Nav1.8
PnCs1[R2A]	2.9 ± 0.2	1.4 ± 0.1	1.7 ± 0.5	1.6 ± 0.2	>100
PnCs1[R3A]	1.8 ± 0.1	1.6 ± 0.3	>100	1.9 ± 0.1	>100
PnCs1[W4A]	0.8 ± 0.1	0.7 ± 0.2	3.4 ± 0.1	1.2 ± 0.2	>100
PnCs1[R6A]	9.2 ± 0.4	0.5 ± 0.1	7.6 ± 1.4	0.9 ± 0.1	>100
PnCs1[W7A]	0.8 ± 0.1	1.1 ± 0.2	6.8 ± 0.5	11.4 ± 2.8	>100
PnCs1[N8A]	0.9 ± 0.2	0.9 ± 0.3	2.2 ± 0.4	0.8 ± 0.2	>100
PnCs1[R9A]	6.7 ± 0.3	1.1 ± 0.2	9.2 ± 1.7	0.9 ± 0.3	>100
PnCs1[R2K]	1.1 ± 0.4	0.8 ± 0.1	2.5 ± 0.2	0.6 ± 0.1	>100
PnCs1[R3K]	0.8 ± 0.1	0.6 ± 0.2	2.7 ± 0.3	0.8 ± 0.1	>100
PnCs1[W4K]	0.5 ± 0.3	0.7 ± 0.3	2.7 ± 0.2	0.7 ± 0.2	>100
PnCs1[A5K]	1.2 ± 0.3	1.9 ± 0.3	2.1 ± 0.1	0.7 ± 0.2	>100
PnCs1[R6K]	8.7 ± 1.7	0.6 ± 0.2	3.3 ± 0.3	0.9 ± 0.2	>100
PnCs1[W7K]	2.8 ± 0.3	1.7 ± 0.4	3.0 ± 0.3	8.2 ± 0.1	>100
PnCs1[N8K]	4.4 ± 0.2	0.9 ± 0.2	2.8 ± 0.1	0.5 ± 0.1	>100
PnCs1[R9K]	10.2 ± 2.1	6.1 ± 1.4	9.2 ± 0.2	6.7 ± 0.6	>100
PnCs1[R2E]	>100	>100	>100	>100	>100
PnCs1[R3E]	>100	>100	>100	>100	>100
PnCs1[W4E]	13.2 ± 3.2	12.8 ± 2.1	>100	14.8 ± 2.2	>100
PnCs1[A5E]	1.4 ± 0.1	>100	8.8 ± 2.8	1.8 ± 0.4	>100
PnCs1[R6E]	>100	>100	>100	>100	>100
PnCs1[W7E]	>100	>100	>100	>100	>100
PnCs1[N8E]	>100	>100	>100	>100	>100
PnCs1[R9E]	>100	>100	>100	>100	>100
PnCs1[W4Y]	>100	>100	>100	>100	>100
PnCs1[W7Y]	7.4 ± 2.6	7.8 ± 2.2	11.7 ± 3.4	0.7 ± 0.2	>100
PnCs1AcAm	/	/	/	/	>100
PnCs1DeAm	>100	>100	>100	>100	>100
PnCs1Ac	>100	>100	>100	>100	>100

Table 7. IC₅₀ values of 4th generation peptides.

Max Inhibition (100 μM)	Nav1.2	Nav1.4	Nav1.5	Nav1.6	Nav1.8
PnCs1[R2A]	84	96	68	71	0
PnCs1[R3A]	86	89	51	87	0
PnCs1[W4A]	89	95	82	76	0
PnCs1[R6A]	73	90	78	96	0
PnCs1[W7A]	92	96	78	57	0
PnCs1[N8A]	96	94	92	89	0
PnCs1[R9A]	80	86	72	79	0
PnCs1[R2K]	92	93	82	85	0
PnCs1[R3K]	96	92	94	86	0
PnCs1[W4K]	75	94	89	92	0
PnCs1[A5K]	84	91	92	93	0
PnCs1[R6K]	67	94	89	88	0
PnCs1[W7K]	71	87	90	82	0
PnCs1[N8K]	81	96	86	92	0
PnCs1[R9K]	62	66	67	72	0
PnCs1[R2E]	41	11	27	5	0
PnCs1[R3E]	52	36	21	24	0
PnCs1[W4E]	72	59	34	67	0
PnCs1[A5E]	81	35	73	82	0
PnCs1[R6E]	49	0	19	41	0
PnCs1[W7E]	21	42	33	27	0
PnCs1[N8E]	47	53	44	27	0
PnCs1[R9E]	42	0	40	11	0
PnCs1[W4Y]	39	33	43	42	0
PnCs1[W7Y]	76	73	75	93	0
PnCs1AcAm	/	/	/	/	0
PnCs1DeAm	34	43	10	24	0
PnCs1Ac	0	0	0	0	0

Table 8. Maximum percentage of inhibition for 4th generation peptides at 100 μ M concentration.

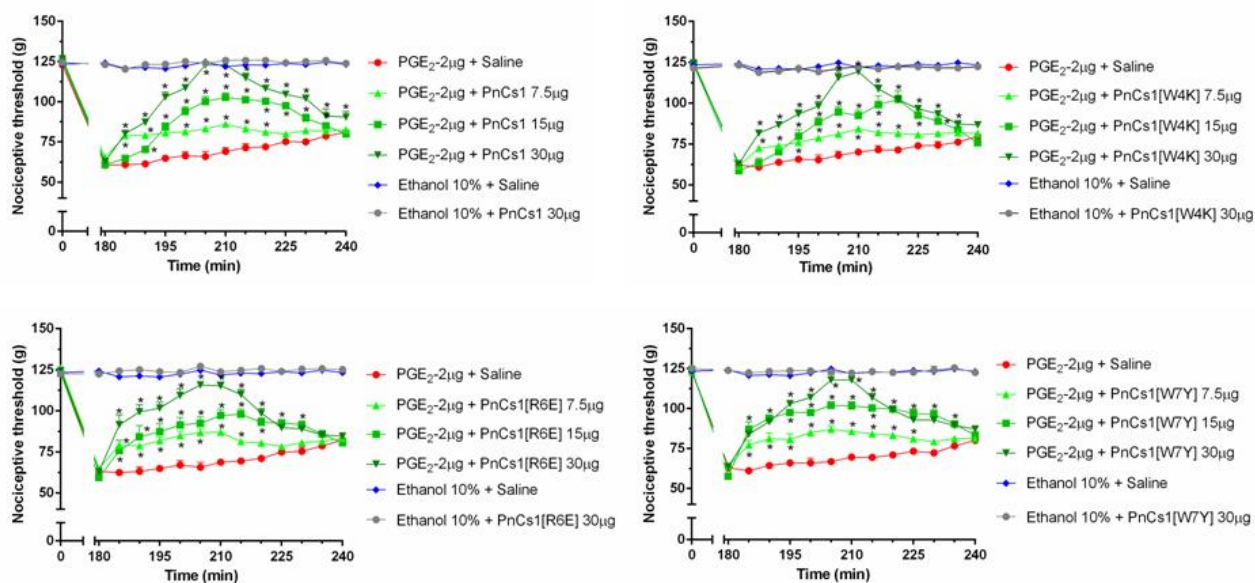


Figure 40. Antinociceptive effect of PnCs1, PnCs1[W4K], PnCs1[R6E] and PnCs1[W7Y] upon intraplantar injection in mice.

The PnCs1, PnCs1[W4K], PnCs1[R6E] and PnCs1[W7Y] were evaluated separately, however, similar results were observed for the four different peptidic types. The intraplantar injection of the four peptides, at the doses of 30 µg/paw, 15 µg/paw and 7.5 µg/paw, at the third hour after injection of PGE₂ (2 µg/paw), induced a significant antinociceptive effect when compared to the control group (ethanol 10%). Increase in the nociceptive threshold was observed 5 minutes after peptide injection and the peak of action was noticed 30 minutes following (Figures 40a-d). An intermediary antinociception was observed with the 15 µg/paw and 7.5 µg/paw doses and a maximum antinociception was noticed with the 30 µg/paw dose. When compared to the group treated only with prostaglandin (PGE₂), no nociception was observed with the intraplantar injection of ethanol 10% (vehicle of prostaglandin) and saline (peptide vehicle). One hour following to the peptide injection, the peptide treated and control groups presented similar nociceptive thresholds.

In order to exclude a possible systemic effect, PGE₂ (2 µg/paw) was injected, at time zero, into both hind paws, whereas the peptides (30 µg/paw) were given, at 150-minute time,

only in the right hind paw and the vehicle (saline) was injected just in the left hind paw. Nociceptive threshold measurements of both hind paws were made before and 180 minutes after injection of prostaglandin. The difference between the averages of these measurements was calculated (Δ nociceptive threshold). These assessments showed that the four peptides, at a dose of 30 μ g/paw, induced antinociception restricted to the paw treated, while the contralateral paw presented nociceptive threshold without significant difference when compared to the prostaglandin-induced hyperalgesia (Figures 41a-d).

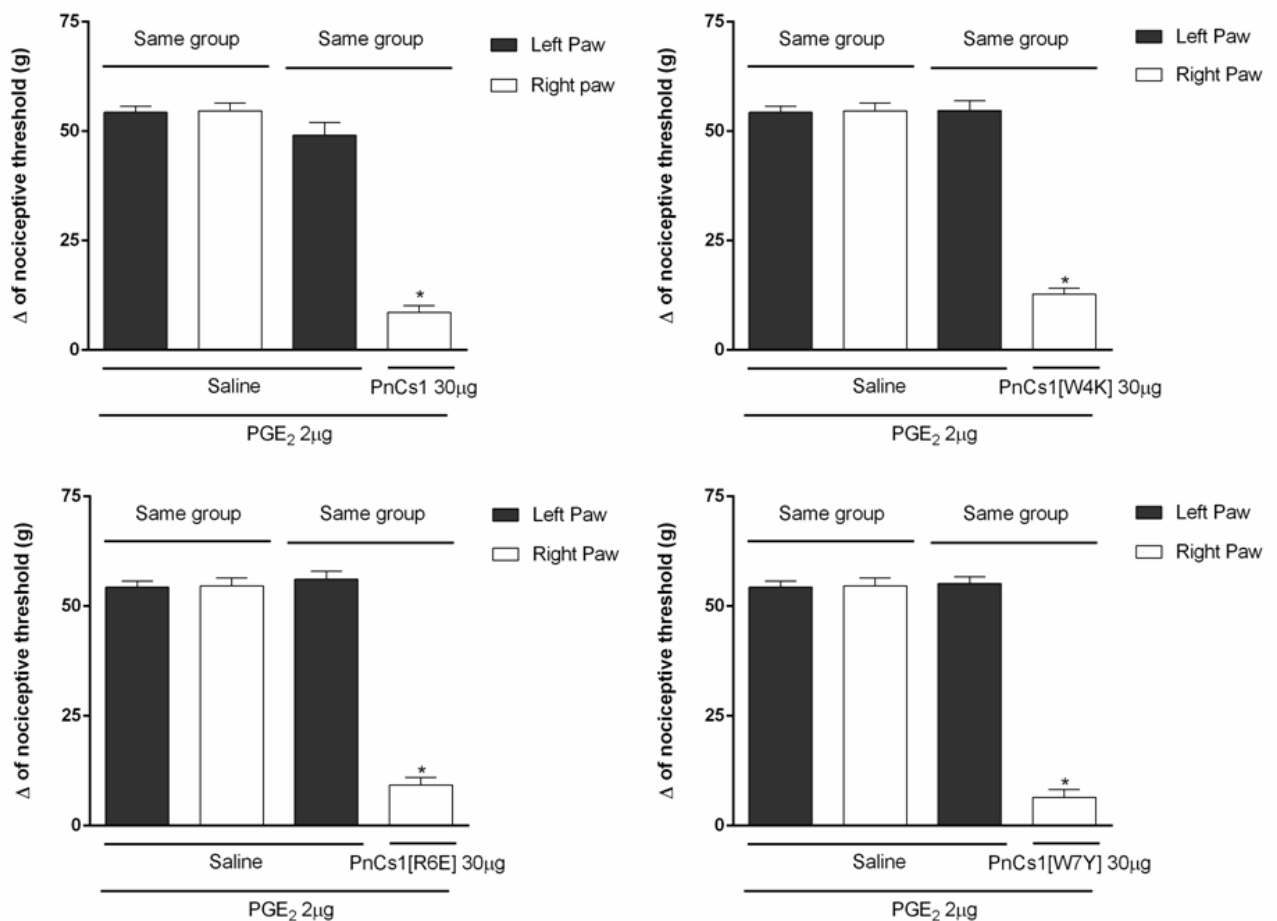


Figure 41. Exclusion of a possible systemic effect of PnCs1, PnCs1[W4K], PnCs1[R6E] and PnCs1[W7Y].

5.2.6. Discussion

The initial goal of this study was to identify small cyclic inhibitors for Nav subtypes. Therefore, we grafted the proposed pharmacophore of PnTx1, a potent Nav channel inhibitor peptide toxin from the Brazilian wandering spider, into the scaffold of μ -KIIIA, a potent Nav channel inhibiting peptide isolated from the venom of a cone snail. The resulting peptide, Pn, was investigated for Nav channel inhibition. Competitive binding experiments suggest that Pn competes with its parent peptides, PnTx1 and μ -KIIIA, for the same binding site on the Nav channel. It can thus be assumed that Pn and analogs obstruct the ion flow by binding at the extracellular channel vestibule rather than acting as voltage-sensor modifiers. These results corroborate previous studies indicating that PnTx1 and μ -conotoxins compete for the same site as well (Martin-Moutot et al., 2006b). The solution structure of the Pn peptide was determined using NMR displaying a highly flexible backbone and a minor set of peaks were observed for the HE1 protons of both Trp residues in the 1D proton NMR spectra suggesting the presence of a minor conformation.

Next, two series of peptide mutants were designed in order to increase the potency of Pn, resulting first in PnM2 and subsequently in PnM9, the latter displaying nM inhibition at Nav channel subtypes Nav1.2 and Nav1.4. A third series of peptides was designed with the aim to further minimize the peptide scaffold as well as introduce improved stability of the peptides through various methods of cyclisation including disulfide and lactam bond as well as backbone cyclisation. Within the third series of peptides, PnCS1 retained inhibition at submicromolar potency while losing selectivity for Nav1.2. Cyclization of PnCS1-PnCS4 rendered these peptides highly stable towards degradation when incubated in human serum, compared to linear or oxidized, but not cyclized peptides in this study, indicating a great improvement in their biopharmaceutical properties. However, due to the lack of selectivity for this series of peptides, future structure-function studies are required to obtain peptides with a Nav channel subtype selective activity. Interestingly, PnCS1, PnCS3 and PnCS4 showed inhibition of Nav1.9_C4,

albeit in low μM range, an understudied Nav channel due to difficulties relating to heterologous expression as well as the lack of potent and selective inhibitors. Nav1.9 is of particular interest due to its links to inflammatory mediated gut pain present in Chron's disease and irritable bowls syndrome (IBD) (Dib-Hajj et al., 2015).

Considerable effort has been made in elucidating the molecular determinants for the subtype specificity of peptide toxins towards specific Nav channel subtypes. More specific, many studies have focused on the key residues responsible for subtype selectivity among μ -conotoxins (Akondi et al., 2014a; Akondi et al., 2014b; Green et al., 2014; Leipold et al., 2012; Leipold et al., 2011; Lewis et al., 2012; Zhang et al., 2007). These studies paved the way for the rational design of selective Nav channel antagonists and will assist in further peptide engineering of the PnCS scaffold with the aim to design small, cyclic, selective and potent Nav channel inhibitors for therapeutically relevant Nav subtypes. In a fourth series of peptides, we tried to determine the key residues of the PnCs1 peptide. Furthermore, we aim to elucidate the amino acid positions tunable towards Nav channel subtype selectivity. Although this is still a work in progress, the results obtained so far clearly indicate that changes in subtype selectivity can be achieved by altering specific residues.

Besides PnCs1, 3 peptides from the 4th generation were tested for their activity *in vivo* by intraplantar injection three hours after injection of PGE₂. PnCs1[W4K], PnCs1[R6E] and PnCs1[W7Y] were chosen based on the initial electrophysiological data indicating interesting activity for these peptides on the tested Nav channels. It was found that of all four peptides induced a significant antinociceptive effect that lasted up to 1 hour. Furthermore, the experiments indicated that a systemic effect can be excluded. It is well documented that PGE₂ has important cell signaling activities in neurons and hereby influences the pain threshold by increasing the excitability of afferent neurons innervating the area of inflammation (Cardoso and Lewis, 2018). PGE₂ lowers the pain threshold in thermal, chemical and mechanical stimuli.

Inflammatory mediators such as PGE₂ are important contributors to the pain induced by local inflammation after tissue damage (Aley and Levine, 1999; Fitzgerald et al., 1999). In fact, secondary mediators, activated by inflammatory mediators like PGE₂ act directly on specific Nav channels related to nociception (Cardoso and Lewis, 2018). For example, it has been reported that inflammatory regulators mediate an up-regulation of Nav1.3 and Nav1.7 channels in DRGs (Black et al., 2004). In axotomized DRGs, the mediator glial-derived neurotrophic factor or GDNF, enhances the expression of the TTX-resistant current which largely consists of Nav1.8 and Nav1.9 current (Cummins et al., 2000). Elevated PGE₂ concentrations induces a kinase, PKC, which in turn will also increase the TTX-resistant currents (Gold et al., 1998). It has been shown that adenosine and bradykinin cause a Nav channel mediated alteration of the excitability of sensory neurons (Cardoso and Lewis, 2018) (Binshtok et al., 2008; Dib-Hajj et al., 2009; Griswold et al., 1999). A Nav channel inhibiting activity, as observed for the PnCs peptides, will contribute to a reduced Na⁺ current and thus hereby induce an antinociceptive effect in a model of inflammatory pain. Therefore, it is no surprise that PnCs1, PnCs1[W4K], PnCs1[R6E] and PnCs1[W7Y] induce antinociception in a PGE₂ induced model of pain. Indeed, the antinociceptive effect seen for these peptides can be explained by inhibition of Nav1.3 (PnCs1), Nav1.7 (PnCs1, PnCs1[W4K], PnCs1[W7Y]) and Nav1.9 (PnCs1). Furthermore, the inhibition of Nav1.1 (PnCs1, PnCs1[W4K], PnCs1[W7Y]) and Nav1.6 (PnCs1, PnCs1[W4K], PnCs1[W7Y]) might contribute as well, although the involvement of these channels in pain pathways still remains less understood and thus caution is needed in interpreting these results. Furthermore, it might very well be that PnCs1[W4K] and PnCs1[W7Y] inhibit Nav1.3 and Nav1.9 channels. Further electrophysiological experiments are needed to verify the activity of the 4th generation peptides on these channels. Ideally, future *in vivo* experiments, using a model in which pain is induced by administration of a specific Nav channel activator, will help to explain which channels these PnCs1 peptides inhibit in order to

exert their nociceptive activity. Previous research has shown that intraplantar injection of the scorpion toxin OD1, a selective Nav1.7 activator, caused spontaneous pain behaviours, which were reversed by co-injection with Nav1.7 inhibitors (Deuis et al., 2016). It would be very interesting to test the analgesic activity of PnCs1, PnCs1[W4K], PnCs1[W7Y] in a model of Nav1.7-mediated pain based on intraplantar injection of OD1.

Rather unexpected was the observation that PnCs1[R6E] seems to be equally active as the other peptides. Based on the available electrophysiological data in *X. laevis* oocytes, this peptide has a reduced affinity for Nav1.1, Nav1.2, Nav1.4-Nav1.8. It thus can be speculated that PnCs1[R6E] acts with strong potency on Nav1.3 or Nav1.9 channels. Further experiments are needed to confirm if PnCs1[R6E] indeed shows interesting activity on these channels. Moreover, these peptides need to be tested on other ion channels and receptors as well in order to exclude that the observed nociceptive effect is a resultant of off-target activity on other nociceptors such as for example Cav, TRP channels or opioid and cannabinoid receptors. Unfortunately, these experiments could not be performed within the timeframe of this thesis.

6. General Discussion and Conclusion

It has been well recognized that Nav channels play a crucial role in inherited diseases, such as cardiovascular arrhythmias, central nervous system disorders and pain syndromes. This knowledge highlights Nav channel isoforms as targets of novel compounds that will hopefully fulfil the unmet therapeutic need to successfully treat these disorders (Peigneur et al., 2014b). Therefore, molecules capable of selective targeting and modulation of Nav channel isoforms represent attractive pharmacological tools, either to identify the specific isoform involved in different channelopathies or as potential therapeutics. Over the last few decades, a vast number of studies have focussed on characterising peptide toxins with promising pharmacological activity from venomous animals. Undeniable, exploring venoms for novel ligands remains indispensable in order to identify novel lead compounds with therapeutic potential. This has been, once again, evidenced by the discovery of an insulin-like peptide in the venom from the cone snail *Conus geographus* (Menting et al., 2016). This Conus insulin peptide differs significantly in structure from human insulin and shows great potential as a template for the design of fast-acting insulins for human use (Menting et al., 2016; Norton, 2017).

Several peptide toxins have entered clinical trials or have been approved as drugs (Norton, 2017; Pennington et al., 2018). Notwithstanding herewith, an even greater number of peptide toxins failed clinical progression in recent years (Harvey, 2014). Therefore, it is suggested that different strategies need to be employed in order to ensure that the great potential of peptide toxins is successfully translated into useful therapeutics (Pennington et al., 2018). Rather than following the classical approach of venom-based drug discovery, which requires labour-intensive and high-risk mining of venoms for novel ligands on any possible target, this project aimed at peptide engineering of previously in-depth characterized toxins with an interesting

pharmacological profile. As a start, we looked at potentially interesting peptide toxins already identified from the venom of the spider *Phoneutria nigriventer*.

6.1. PnTx2-1

The characterization of PnTx2-1 as a Nav channel modulator adds to the expanding knowledge on the *Phoneutria nigriventer* venom. A better understanding of the mechanism of action of its composing venom peptides is important for an effective treatment of *Phoneutria nigriventer* envenomation. This work reports for the first time, the activity of a toxin isolated from the venom fraction 2 on insect Nav channels and hereby indicating that this fraction indeed is to be considered as a source of insecticidal peptides. From a therapeutic point of view, the obtained results show that PnTx2-1 does not display an interesting subtype selectivity since a similar affinity was found for Nav1.1 and Nav1.5 channels. Nav1.1 has recently emerged as an important player in acute and mechanical pain. Therefore, a high affinity ligand for Nav1.1 channels is of potential interest to study these channels and their involvement in mechanical nociception. However, the activity of PnTx2-1 on Nav1.5 channels will undoubtedly result in unwarranted side effects. Therefore, further structure-function studies comprising Ala-walk combined with site-directed mutagenesis experiments are needed. Such studies might provide insight in which residues are responsible for Nav1.1 recognition and which residues are determining for Nav1.5 channel activity. Depending on the outcome of these structure-function studies, it might be feasible to design a peptide with a higher selectivity for Nav1.1 channels over other Nav channels. Nevertheless, ample peptide toxins with similar pharmacological activity but higher potency and selectivity have been described previously. For example, the spider toxin Hm1a, isolated from the venom of the spider *Heteroscodra maculata*, also modulates Nav channels, causing an inhibition of inactivation. Hm1a is not only highly selective for Nav1.1 over Nav1.2–Nav1.8 but also displays an EC₅₀ value of 6.7 ± 0.1 nM for

Nav1.1 channels (Osteen et al., 2016; Osteen et al., 2017; Richards et al., 2018). Furthermore, Hm1a is constituted of 35 amino acid residues of which 6 cysteine residues. Compared with PnTx2-1, with its 53 residues and 5 disulphide bridges, Hm1a is smaller peptide and easier to synthesize (Ren et al., 2001). Hm1a is currently under investigation for the treatment of Dravet syndrome. It was found that selective Nav1.1 activation rescues Dravet syndrome mice from seizures and premature death (Ren et al., 2001). Nevertheless, despite its limited therapeutic potential, PnTx2-1 might be an interesting tool to study the involvement of specific Nav channels in channelopathies. Together, it can be concluded that PnTx2-1 is an interesting insecticidal peptide but it does not represent a promising lead compound for the development of novel Nav channel ligands with therapeutic potential.

6.2. PnTx1 & Pn peptides

After verifying PnTx1 as a peptide with an interesting activity on Nav channels, we grafted its pharmacophore into the scaffold of the μ -KIIIA. μ -KIIIA was considered as an ideal template based on the observation that this is the smallest μ -conotoxin identified up to date; it is easy to synthesize and to fold correctly; it is intensively studied for its activity on Nav channels; μ -KIIIA is one of the few μ -conotoxins with a preference for neuronal over muscle Nav channels. The obtained results have shown that it is possible to define peptide toxins targeting Nav channels to a minimal pharmacophore and that cyclization of these minimized peptides can greatly enhance their biopharmaceutical properties without influencing activity. The PnCs peptides represent a promising template for further design of lead compounds in the development of novel therapeutic agents for treatment of Nav channel related diseases.

Drugs currently used in humans can roughly be divided in either small molecules or large biologics, including antibodies. Whereas small organic molecules tend to display the desirable physicochemical property of oral bioavailability, due to their size, small molecule drugs may

suffer from reduced target selectivity that often ultimately manifests in unwanted side effects. An interesting example of a low molecular weight compound targeting Nav channels is TTX. Despite being characterized as a Nav channel blocker for over years, TTX is still one of the most efficient Nav channel inhibitors known to date. TTX is selective for Nav channels, has a preference for TTX-sensitive Nav channels over the cardiac Nav1.5 channel and importantly, does not cross the blood-brain barrier. Not surprising, TTX is under investigation for development of analgesic therapeutics as evidenced by the existing 76 patents related to TTX application (Melnikova et al., 2018). Indeed, in animal studies using different pain models and in human clinical trials, TTX showed promising activity in both neuropathic and nociceptive pain (Nieto et al., 2012). Nevertheless, several hurdles are to be taken before TTX can be further developed in druggable compound. Clinical trials on TTX revealed several occurring side effects, mainly due to toxicity upon systemic distribution of TTX and analogs. Among the most severe side effects reported were ataxia, aspiration pneumonia, hypertension and nausea (Hagen et al., 2017; Melnikova et al., 2018; Nieto et al., 2012). This demonstrates the difficulties and challenges that are involved in the development of Nav channel inhibitors into usable therapeutics.

Large biologics on the other hand, tend to be exquisitely specific for their targets due to their larger surface area. However, this usually comes at the cost of low bioavailability, poor membrane permeability, and metabolic instability (Bhardwaj et al., 2016; Craik et al., 2013). Peptides have emerged with the promise to bridge the gap between small molecules and large biologics, and the field of drug development is now refocusing its efforts to pursue peptides as lead molecules that fit between these two molecular weight extremes and at the same time, exhibit the advantageous characteristics of both (Craik et al., 2013). Indeed, molecules combining advantages of small molecules (cost, conformational restriction, membrane permeability, metabolic stability, oral bioavailability) with those of large biologics (natural

components, target specificity, high potency) might represent the novel tools to overcome the hurdles experienced today in drug discovery (Craik et al., 2013). It is within this philosophy of combining the better of two worlds that we decided to combine the sophisticated evolutionary peptide chemistry of cone snails and spiders in order to design small, cyclic and bioactive peptides. The resulting peptides do represent the first and the smallest (ten residues) cyclic Nav modulators to date. These peptides are unique pharmacological tools to investigate disease pathways including, but limited to, neuropathic and nociceptive pain. Moreover, they represent promising starting scaffolds for further development of peptide-based therapeutics. Notwithstanding, a major challenge in developing these cyclic Pn peptides in therapeutics will be creating ligands that target a single Nav channel subtype. So far, a peptide that (highly) selectively targets a single subtype has not been discovered. However, nature has shown that it is possible to generate peptides with a selectivity window large enough to use these molecules as target specific ligands. Nevertheless, pharmacological interactions of the cyclic Pn peptides with membrane receptors and ion channels other than their Nav channel target cannot be underestimated and should be investigated in order to validate the therapeutic effectiveness of these peptides.

7. References

- Abdelsayed, M., Sokolov, S., 2013. Voltage-gated sodium channels: pharmaceutical targets via anticonvulsants to treat epileptic syndromes. *Channels (Austin)* 7, 146-152.
- Ahern, C.A., Payandeh, J., Bosmans, F., Chanda, B., 2016. The hitchhiker's guide to the voltage-gated sodium channel galaxy. *The Journal of general physiology* 147, 1-24.
- Akondi, K.B., Muttenthaler, M., Dutertre, S., Kaas, Q., Craik, D.J., Lewis, R.J., Alewood, P.F., 2014. Discovery, synthesis, and structure-activity relationships of conotoxins. *Chemical reviews* 114, 5815-5847.
- Alewood, D., Birinyi-Strachan, L.C., Pallaghy, P.K., Norton, R.S., Nicholson, G.M., Alewood, P.F., 2003. Synthesis and characterization of delta-atracotoxin-Ar1a, the lethal neurotoxin from venom of the Sydney funnel-web spider (*Atrax robustus*). *Biochemistry* 42, 12933-12940.
- Aley, K.O., Levine, J.D., 1999. Role of protein kinase A in the maintenance of inflammatory pain. *The Journal of neuroscience : the official journal of the Society for Neuroscience* 19, 2181-2186.
- Almeida, A.P., Andrade, A.B., Ferreira, A.J., Pires, A.C.G., Damasceno, D.D., Alves, M.N.M., Gomes, E.R.M., Kushmerick, C., Lima, R.F., Prado, M.A.M., Prado, V.F., Richardson, M., Cordeiro, M.N., Guatimosim, S., Gomez, M., 2011. Antiarrhythmogenic effects of a neurotoxin from the spider *Phoneutria nigriventer*. *Toxicon : official journal of the International Society on Toxinology* 57, 217-224.
- Anand, P., O'Neil, A., Lin, E., Douglas, T., Holford, M., 2015. Tailored delivery of analgesic ziconotide across a blood brain barrier model using viral nanocontainers. *Scientific reports* 5, 12497.
- Araujo, D.A., Cordeiro, M.N., Diniz, C.R., Beirao, P.S., 1993. Effects of a toxic fraction, PhTx2, from the spider *Phoneutria nigriventer* on the sodium current. *Naunyn Schmiedeberg's Arch Pharmacol* 347, 205-208.
- Baden, D.G., Bourdelais, A.J., Jacocks, H., Michelliza, S., Naar, J., 2005. Natural and derivative brevetoxins: historical background, multiplicity, and effects. *Environmental health perspectives* 113, 621-625.
- Becker, S., Prusak-Sochaczewski, E., Zamponi, G., Beck-Sickinger, A.G., Gordon, R.D., French, R.J., 1992. Action of derivatives of mu-conotoxin GIIIA on sodium channels. Single amino acid substitutions in the toxin separately affect association and dissociation rates. *Biochemistry* 31, 8229-8238.
- Bende, N.S., Dziemborowicz, S., Mobli, M., Herzig, V., Gilchrist, J., Wagner, J., Nicholson, G.M., King, G.F., Bosmans, F., 2014. A distinct sodium channel voltage-sensor locus determines insect selectivity of the spider toxin Dc1a. *Nat Commun* 5, 4350.
- Bennett, D.L., Clark, A.J., Huang, J., Waxman, S.G., Dib-Hajj, S.D., 2019. The Role of Voltage-Gated Sodium Channels in Pain Signaling. *Physiological reviews* 99, 1079-1151.
- Bezanilla, F., 2000. The voltage sensor in voltage-dependent ion channels. *Physiological reviews* 80, 555-592.
- Bhardwaj, G., Mulligan, V.K., Bahl, C.D., Gilmore, J.M., Harvey, P.J., Cheneval, O., Buchko, G.W., Pulavarti, S.V., Kaas, Q., Eletsy, A., Huang, P.S., Johnsen, W.A., Greisen, P.J., Rocklin, G.J., Song, Y., Linsky, T.W., Watkins, A., Rettie, S.A., Xu, X., Carter, L.P., Bonneau, R., Olson, J.M., Coutsiyas, E., Correnti, C.E., Szyperski, T., Craik, D.J., Baker, D., 2016. Accurate de novo design of hyperstable constrained peptides. *Nature* 538, 329-335.
- Binshtok, A.M., Wang, H., Zimmermann, K., Amaya, F., Vardeh, D., Shi, L., Brenner, G.J., Ji, R.R., Bean, B.P., Woolf, C.J., Samad, T.A., 2008. Nociceptors are interleukin-1beta sensors. *The Journal of neuroscience : the official journal of the Society for Neuroscience* 28, 14062-14073.

- Black, J.A., Liu, S., Tanaka, M., Cummins, T.R., Waxman, S.G., 2004. Changes in the expression of tetrodotoxin-sensitive sodium channels within dorsal root ganglia neurons in inflammatory pain. *Pain* 108, 237-247.
- Bosmans, F., Tytgat, J., 2007. Sea anemone venom as a source of insecticidal peptides acting on voltage-gated Na⁺ channels. *Toxicon : official journal of the International Society on Toxinology* 49, 550-560.
- Brady, R.M., Zhang, M., Gable, R., Norton, R.S., Baell, J.B., 2013. De novo design and synthesis of a mu-conotoxin KIIIA peptidomimetic. *Bioorganic & medicinal chemistry letters* 23, 4892-4895.
- Bucarechi, F., Mello, S.M., Vieira, R.J., Mamoni, R.L., Blotta, M.H.S.L., Antunes, E., Hyslop, S., 2008. Systemic envenomation caused by the wandering spider *Phoneutria nigriventer*, with quantification of circulating venom. *Clin Toxicol (Phila)* 46, 885-889.
- Bucherl, W., 1953. [Comparison of the action of gland extracts and pure venom of *Phoneutria nigriventer* Keyserling 1891]. *Memorias do Instituto Butantan* 25, 1-21.
- Bucherl, W., 1969. Biology and venoms of the most important South American spiders of the genera *Phoneutria*, *Loxosceles*, *Lycosa*, and *Latrodectus*. *American zoologist* 9, 157-159.
- Bulaj, G., DeLaCruz, R., Azimi-Zonooz, A., West, P., Watkins, M., Yoshikami, D., Olivera, B.M., 2001. Delta-conotoxin structure/function through a cladistic analysis. *Biochemistry* 40, 13201-13208.
- Bulaj, G., West, P.J., Garrett, J.E., Watkins, M., Zhang, M.M., Norton, R.S., Smith, B.J., Yoshikami, D., Olivera, B.M., 2005. Novel conotoxins from *Conus striatus* and *Conus kinoshitai* selectively block TTX-resistant sodium channels. *Biochemistry* 44, 7259-7265.
- Caldwell, J.H., Schaller, K.L., Lasher, R.S., Peles, E., Levinson, S.R., 2000. Sodium channel Na(v)1.6 is localized at nodes of ranvier, dendrites, and synapses. *Proceedings of the National Academy of Sciences of the United States of America* 97, 5616-5620.
- Campos, F.V., Chanda, B., Beirao, P.S., Bezanilla, F., 2008. Alpha-scorpion toxin impairs a conformational change that leads to fast inactivation of muscle sodium channels. *The Journal of general physiology* 132, 251-263.
- Cao, Z., Gerwick, W.H., Murray, T.F., 2010. Antillatoxin is a sodium channel activator that displays unique efficacy in heterologously expressed rNav1.2, rNav1.4 and rNav1.5 alpha subunits. *BMC neuroscience* 11, 154.
- Cardoso, F.C., Lewis, R.J., 2017. Sodium channels and pain: from toxins to therapies. *Br J Pharmacol*.
- Cardoso, F.C., Lewis, R.J., 2018. Sodium channels and pain: from toxins to therapies. *British journal of pharmacology* 175, 2138-2157.
- Cassola, A.C., Jaffe, H., Fales, H.M., Afeche, S.C., Magnoli, F., Cipolla-Neto, J., 1998. omega-Phonetoxin-IIA: a calcium channel blocker from the spider *Phoneutria nigriventer*. *Pflugers Arch* 436, 545-552.
- Catterall, W.A., 2000. From ionic currents to molecular mechanisms: the structure and function of voltage-gated sodium channels. *Neuron* 26, 13-25.
- Catterall, W.A., 2012a. Sodium Channel Mutations and Epilepsy, in: th, Noebels, J.L., Avoli, M., Rogawski, M.A., Olsen, R.W., Delgado-Escueta, A.V. (Eds.), *Jasper's Basic Mechanisms of the Epilepsies*, Bethesda (MD).
- Catterall, W.A., 2012b. Voltage-gated sodium channels at 60: structure, function and pathophysiology. *The Journal of physiology* 590, 2577-2589.
- Catterall, W.A., Cestele, S., Yarov-Yarovoy, V., Yu, F.H., Konoki, K., Scheuer, T., 2007. Voltage-gated ion channels and gating modifier toxins. *Toxicon : official journal of the International Society on Toxinology* 49, 124-141.
- Cervenka, R., Zarrabi, T., Lukacs, P., Todt, H., 2010. The outer vestibule of the Na⁺ channel-toxin receptor and modulator of permeation as well as gating. *Marine drugs* 8, 1373-1393.

Cestele, S., Scheuer, T., Mantegazza, M., Rochat, H., Catterall, W.A., 2001. Neutralization of gating charges in domain II of the sodium channel alpha subunit enhances voltage-sensor trapping by a beta-scorpion toxin. *The Journal of general physiology* 118, 291-302.

Cestele, S., Yarov-Yarovoy, V., Qu, Y., Sampieri, F., Scheuer, T., Catterall, W.A., 2006. Structure and function of the voltage sensor of sodium channels probed by a beta-scorpion toxin. *The Journal of biological chemistry* 281, 21332-21344.

Chahine, M., George, A.L., Jr., Zhou, M., Ji, S., Sun, W., Barchi, R.L., Horn, R., 1994. Sodium channel mutations in paramyotonia congenita uncouple inactivation from activation. *Neuron* 12, 281-294.

Chan, L.Y., Gunasekera, S., Henriques, S.T., Worth, N.F., Le, S.J., Clark, R.J., Campbell, J.H., Craik, D.J., Daly, N.L., 2011. Engineering pro-angiogenic peptides using stable, disulfide-rich cyclic scaffolds. *Blood* 118, 6709-6717.

Chanda, B., Bezanilla, F., 2002. Tracking voltage-dependent conformational changes in skeletal muscle sodium channel during activation. *The Journal of general physiology* 120, 629-645.

Chassagnon, I.R., McCarthy, C.A., Chin, Y.K., Pineda, S.S., Keramidas, A., Mobli, M., Pham, V., De Silva, T.M., Lynch, J.W., Widdop, R.E., Rash, L.D., King, G.F., 2017. Potent neuroprotection after stroke afforded by a double-knot spider-venom peptide that inhibits acid-sensing ion channel 1a. *Proceedings of the National Academy of Sciences of the United States of America* 114, 3750-3755.

Chau, R., Kalaitzis, J.A., Neilan, B.A., 2011. On the origins and biosynthesis of tetrodotoxin. *Aquat Toxicol* 104, 61-72.

Cheng, Y., 2018. Single-particle cryo-EM-How did it get here and where will it go. *Science* 361, 876-880.

Cohen, L., Troub, Y., Turkov, M., Gilles, N., Ilan, N., Benveniste, M., Gordon, D., Gurevitz, M., 2007. Mammalian skeletal muscle voltage-gated sodium channels are affected by scorpion depressant "insect-selective" toxins when preconditioned. *Molecular pharmacology* 72, 1220-1227.

Cordeiro, M.d.N., de Figueiredo, S.G., Valentim, A.d.C., Diniz, C.R., von Eickstedt, V.R., Gilroy, J., Richardson, M., 1993. Purification and amino acid sequences of six Tx3 type neurotoxins from the venom of the Brazilian 'armed' spider *Phoneutria nigriventer* (Keys). *Toxicon : official journal of the International Society on Toxinology* 31, 35-42.

Cordeiro Mdo, N., Diniz, C.R., Valentim Ado, C., von Eickstedt, V.R., Gilroy, J., Richardson, M., 1992. The purification and amino acid sequences of four Tx2 neurotoxins from the venom of the Brazilian 'armed' spider *Phoneutria nigriventer* (Keys). *FEBS letters* 310, 153-156.

Craik, D.J., Fairlie, D.P., Liras, S., Price, D., 2013. The future of peptide-based drugs. *Chemical biology & drug design* 81, 136-147.

Cruz, L.J., Gray, W.R., Olivera, B.M., Zeikus, R.D., Kerr, L., Yoshikami, D., Moczydlowski, E., 1985. Conus geographus toxins that discriminate between neuronal and muscle sodium channels. *The Journal of biological chemistry* 260, 9280-9288.

Cummins, T.R., Black, J.A., Dib-Hajj, S.D., Waxman, S.G., 2000. Glial-derived neurotrophic factor upregulates expression of functional SNS and NaN sodium channels and their currents in axotomized dorsal root ganglion neurons. *The Journal of neuroscience : the official journal of the Society for Neuroscience* 20, 8754-8761.

da Fonseca Pacheco, D., Freitas, A.C.N., Pimenta, A.M.C., Duarte, I.D.G., de Lima, M.E., 2016. A spider derived peptide, PnPP-19, induces central antinociception mediated by opioid and cannabinoid systems. *J Venom Anim Toxins Incl Trop Dis* 22, 34.

Dalmolin, G.D., Bannister, K., Goncalves, L., Sikandar, S., Patel, R., Cordeiro, M.d.N., Gomez, M.V., Ferreira, J., Dickenson, A.H., 2017. Effect of the spider toxin Tx3-3 on spinal processing

of sensory information in naive and neuropathic rats: an in vivo electrophysiological study. *Pain Rep* 2, e610.

Davis, I.W., Leaver-Fay, A., Chen, V.B., Block, J.N., Kapral, G.J., Wang, X., Murray, L.W., Arendall, W.B., 3rd, Snoeyink, J., Richardson, J.S., Richardson, D.C., 2007. MolProbity: all-atom contacts and structure validation for proteins and nucleic acids. *Nucleic acids research* 35, W375-383.

de Dianous, S., Hoarau, F., Rochat, H., 1987. Re-examination of the specificity of the scorpion *Androctonus australis hector* insect toxin towards arthropods. *Toxicon : official journal of the International Society on Toxinology* 25, 411-417.

de Figueiredo, S.G., de Lima, M.E., Nascimento Cordeiro, M., Diniz, C.R., Patten, D., Halliwell, R.F., Gilroy, J., Richardson, M., 2001. Purification and amino acid sequence of a highly insecticidal toxin from the venom of the brazilian spider *Phoneutria nigriventer* which inhibits NMDA-evoked currents in rat hippocampal neurones. *Toxicon : official journal of the International Society on Toxinology* 39, 309-317.

de la Vega, R.C., Possani, L.D., 2007. Novel paradigms on scorpion toxins that affects the activating mechanism of sodium channels. *Toxicon : official journal of the International Society on Toxinology* 49, 171-180.

de Lera Ruiz, M., Kraus, R.L., 2015. Voltage-Gated Sodium Channels: Structure, Function, Pharmacology, and Clinical Indications. *Journal of medicinal chemistry* 58, 7093-7118.

De Lima, M.E., Figueiredo, S.G., Pimenta, A.M.C., Santos, D.M., Borges, M.H., Cordeiro, M.N., Richardson, M., Oliveira, L.C., Stankiewicz, M., Pelhate, M., 2007. Peptides of arachnid venoms with insecticidal activity targeting sodium channels. *Comp Biochem Phys C* 146, 264-279.

de Lima, M.E., Figueiredo, S.G., Matavel, A., Nunes, K.P., da Silva, C.N., Almeida, F.M., Diniz, M.R.V., Cordeiro, M.N., Stankiewicz, M., Beirao, P.S., 2016. *Phoneutria nigriventer* Venom and Toxins: A review, in: Gopalkrishnakone, P. (Ed.), *Spider Venoms*, Toxinology. Springer, pp. 71-99.

De Lima, M.E., Martin, M.F., Diniz, C.R., Rochat, H., 1986. *Tityus serrulatus* toxin VII bears pharmacological properties of both beta-toxin and insect toxin from scorpion venoms. *Biochemical and biophysical research communications* 139, 296-302.

de Lima, M.E., Stankiewicz, M., Hamon, A., de Figueiredo, S.G., Cordeiro, M.N., Diniz, C.R., Martin-Eauclaire, M., Pelhate, M., 2002a. The toxin Tx4(6-1) from the spider *Phoneutria nigriventer* slows down Na⁽⁺⁾ current inactivation in insect CNS via binding to receptor site 3. *Journal of insect physiology* 48, 53-61.

De Marco Almeida, F., de Castro Pimenta, A.M., Oliveira, M.C., De Lima, M.E., 2015. Venoms, toxins and derivatives from the Brazilian fauna: valuable sources for drug discovery. *Sheng li xue bao : [Acta physiologica Sinica]* 67, 261-270.

Deuis, J.R., Mueller, A., Israel, M.R., Vetter, I., 2017. The pharmacology of voltage-gated sodium channel activators. *Neuropharmacology* 127, 87-108.

Deuis, J.R., Wingerd, J.S., Winter, Z., Durek, T., Dekan, Z., Sousa, S.R., Zimmermann, K., Hoffmann, T., Weidner, C., Nassar, M.A., Alewood, P.F., Lewis, R.J., Vetter, I., 2016. Analgesic Effects of GpTx-1, PF-04856264 and CNV1014802 in a Mouse Model of NaV1.7-Mediated Pain. *Toxins* 8.

Dib-Hajj, S.D., Binshtok, A.M., Cummins, T.R., Jarvis, M.F., Samad, T., Zimmermann, K., 2009. Voltage-gated sodium channels in pain states: role in pathophysiology and targets for treatment. *Brain Res Rev* 60, 65-83.

Dib-Hajj, S.D., Black, J.A., Waxman, S.G., 2015. NaV1.9: a sodium channel linked to human pain. *Nature reviews. Neuroscience* 16, 511-519.

Diniz, C., 1963. Separation of proteins and characterization of active substances in the venom of the Brazilian spiders. *An Acad Bras Cienc.* 35, 283-291.

- Diniz, C.R., Cordeiro Mdo, N., Junor, L.R., Kelly, P., Fischer, S., Reimann, F., Oliveira, E.B., Richardson, M., 1990. The purification and amino acid sequence of the lethal neurotoxin Tx1 from the venom of the Brazilian 'armed' spider *Phoneutria nigriventer*. *FEBS letters* 263, 251-253.
- Diniz, M.R., Paine, M.J., Diniz, C.R., Theakston, R.D., Crampton, J.M., 1993. Sequence of the cDNA coding for the lethal neurotoxin Tx1 from the Brazilian "armed" spider *Phoneutria nigriventer* predicts the synthesis and processing of a preprotoxin. *The Journal of biological chemistry* 268, 15340-15342.
- Diniz, M.R.V., Paiva, A.L.B., Guerra-Duarte, C., Nishiyama, M.Y., Jr., Mudadu, M.A., Oliveira, U., Borges, M.H., Yates, J.R., Junqueira-de-Azevedo, I.L., 2018. An overview of *Phoneutria nigriventer* spider venom using combined transcriptomic and proteomic approaches. *PloS one* 13, e0200628.
- Diniz, M.R.V., Theakston, R.D.G., Crampton, J.M., Nascimento Cordeiro, M.d., Pimenta, A.M.C., De Lima, M.E., Diniz, C.R., 2006. Functional expression and purification of recombinant Tx1, a sodium channel blocker neurotoxin from the venom of the Brazilian "armed" spider, *Phoneutria nigriventer*. *Protein Expr Purif* 50, 18-24.
- Dong, K., 2007. Insect sodium channels and insecticide resistance. *Invertebrate neuroscience : IN* 7, 17-30.
- Dos Santos, R.G., Van Renterghem, C., Martin-Moutot, N., Mansuelle, P., Cordeiro, M.N., Diniz, C.R., Mori, Y., De Lima, M.E., Seagar, M., 2002. *Phoneutria nigriventer* omega-phonetoxin IIA blocks the Cav2 family of calcium channels and interacts with omega-conotoxin-binding sites. *The Journal of biological chemistry* 277, 13856-13862.
- Du, Y., Garden, D.P., Wang, L., Zhorov, B.S., Dong, K., 2011. Identification of new batrachotoxin-sensing residues in segment IIIS6 of the sodium channel. *The Journal of biological chemistry* 286, 13151-13160.
- Dumbacher, J.P., Spande, T.F., Daly, J.W., 2000. Batrachotoxin alkaloids from passerine birds: a second toxic bird genus (*Ifrita kowaldi*) from New Guinea. *Proceedings of the National Academy of Sciences of the United States of America* 97, 12970-12975.
- Eitan, M., Fowler, E., Herrmann, R., Duval, A., Pelhate, M., Zlotkin, E., 1990. A scorpion venom neurotoxin paralytic to insects that affects sodium current inactivation: purification, primary structure, and mode of action. *Biochemistry* 29, 5941-5947.
- Emerich, B.L., Ferreira, R.C.M., Cordeiro, M.N., Borges, M.H., Pimenta, A.M.C., Figueiredo, S.G., Duarte, I.D.G., de Lima, M.E., 2016. delta-Ctenitoxin-Pn1a, a Peptide from *Phoneutria nigriventer* Spider Venom, Shows Antinociceptive Effect Involving Opioid and Cannabinoid Systems, in Rats. *Toxins* 8.
- Escoubas, P., 2006. Mass spectrometry in toxinology: a 21st-century technology for the study of biopolymers from venoms. *Toxicon : official journal of the International Society on Toxinology* 47, 609-613.
- Fainzilber, M., Kofman, O., Zlotkin, E., Gordon, D., 1994. A new neurotoxin receptor site on sodium channels is identified by a conotoxin that affects sodium channel inactivation in molluscs and acts as an antagonist in rat brain. *The Journal of biological chemistry* 269, 2574-2580.
- Figueiredo, S.G., Garcia, M.E., Valentim, A.C., Cordeiro, M.N., Diniz, C.R., Richardson, M., 1995. Purification and amino acid sequence of the insecticidal neurotoxin Tx4(6-1) from the venom of the 'armed' spider *Phoneutria nigriventer* (Keys). *Toxicon : official journal of the International Society on Toxinology* 33, 83-93.
- Fitches, E.C., Pyati, P., King, G.F., Gatehouse, J.A., 2012. Fusion to snowdrop lectin magnifies the oral activity of insecticidal omega-Hexatoxin-Hv1a peptide by enabling its delivery to the central nervous system. *PloS one* 7, e39389.

Fitzgerald, E.M., Okuse, K., Wood, J.N., Dolphin, A.C., Moss, S.J., 1999. cAMP-dependent phosphorylation of the tetrodotoxin-resistant voltage-dependent sodium channel SNS. *The Journal of physiology* 516 (Pt 2), 433-446.

Freitas, A.C.N., Pacheco, D.F., Machado, M.F.M., Carmona, A.K., Duarte, I.D.G., de Lima, M.E., 2016. PnPP-19, a spider toxin peptide, induces peripheral antinociception through opioid and cannabinoid receptors and inhibition of neutral endopeptidase. *Br J Pharmacol* 173, 1491-1501.

Freitas, A.C.N., Peigneur, S., Macedo, F.H.P., Menezes-Filho, J.E., Millns, P., Medeiros, L.F., Arruda, M.A., Cruz, J., Holliday, N.D., Tytgat, J., Hathway, G., de Lima, M.E., 2018. The Peptide PnPP-19, a Spider Toxin Derivative, Activates mu-Opioid Receptors and Modulates Calcium Channels. *Toxins* 10.

French, R.J., Yoshikami, D., Sheets, M.F., Olivera, B.M., 2010. The tetrodotoxin receptor of voltage-gated sodium channels--perspectives from interactions with micro-conotoxins. *Mar Drugs* 8, 2153-2161.

Gajewiak, J., Azam, L., Imperial, J., Walewska, A., Green, B.R., Bandyopadhyay, P.K., Raghuraman, S., Ueberheide, B., Bern, M., Zhou, H.M., Minassian, N.A., Hagan, R.H., Flinspach, M., Liu, Y., Bulaj, G., Wickenden, A.D., Olivera, B.M., Yoshikami, D., Zhang, M.M., 2014. A disulfide tether stabilizes the block of sodium channels by the conotoxin muO section sign-GVIII. *Proceedings of the National Academy of Sciences of the United States of America* 111, 2758-2763.

Garry, E.M., Delaney, A., Anderson, H.A., Sirinathsinghji, E.C., Clapp, R.H., Martin, W.J., Kinchington, P.R., Krah, D.L., Abbadie, C., Fleetwood-Walker, S.M., 2005. Varicella zoster virus induces neuropathic changes in rat dorsal root ganglia and behavioral reflex sensitisation that is attenuated by gabapentin or sodium channel blocking drugs. *Pain* 118, 97-111.

Gawley, R.E., Rein, K.S., Jeglitsch, G., Adams, D.J., Theodorakis, E.A., Tiebes, J., Nicolaou, K.C., Baden, D.G., 1995. The relationship of brevetoxin 'length' and A-ring functionality to binding and activity in neuronal sodium channels. *Chemistry & biology* 2, 533-541.

Gilles, N., Harrison, G., Karbat, I., Gurevitz, M., Nicholson, G.M., Gordon, D., 2002. Variations in receptor site-3 on rat brain and insect sodium channels highlighted by binding of a funnel-web spider delta-atracotoxin. *European journal of biochemistry* 269, 1500-1510.

Gold, M.S., Levine, J.D., Correa, A.M., 1998. Modulation of TTX-R INa by PKC and PKA and their role in PGE2-induced sensitization of rat sensory neurons in vitro. *The Journal of neuroscience : the official journal of the Society for Neuroscience* 18, 10345-10355.

Gold, M.S., Weinreich, D., Kim, C.S., Wang, R., Treanor, J., Porreca, F., Lai, J., 2003. Redistribution of Na(V)1.8 in uninjured axons enables neuropathic pain. *The Journal of neuroscience : the official journal of the Society for Neuroscience* 23, 158-166.

Goldin, A.L., 1999. Diversity of mammalian voltage-gated sodium channels. *Annals of the New York Academy of Sciences* 868, 38-50.

Goldin, A.L., 2001. Resurgence of sodium channel research. *Annual review of physiology* 63, 871-894.

Goldin, A.L., Barchi, R.L., Caldwell, J.H., Hofmann, F., Howe, J.R., Hunter, J.C., Kallen, R.G., Mandel, G., Meisler, M.H., Netter, Y.B., Noda, M., Tamkun, M.M., Waxman, S.G., Wood, J.N., Catterall, W.A., 2000. Nomenclature of voltage-gated sodium channels. *Neuron* 28, 365-368.

Gomes, P.C., de Souza, B.M., Dias, N.B., Cesar-Tognoli, L.M.M., Silva, L.C., Tormena, C.F., Rittner, R., Richardson, M., Cordeiro, M.N., Palma, M.S., 2011. Nigriventrine: A low molecular mass neuroactive compound from the venom of the spider *Phoneutria nigriventer*. *Toxicon : official journal of the International Society on Toxinology* 57, 266-274.

Gomez, M.V., Kalapothakis, E., Guatimosim, C., Prado, M.A.M., 2002. *Phoneutria nigriventer* venom: a cocktail of toxins that affect ion channels. *Cell Mol Neurobiol* 22, 579-588.

Goral, R.O., Leipold, E., Nematian-Ardestani, E., Heinemann, S.H., 2015. Heterologous expression of NaV1.9 chimeras in various cell systems. *Pflugers Archiv : European journal of physiology* 467, 2423-2435.

Gordon, D., Gurevitz, M., 2003. The selectivity of scorpion alpha-toxins for sodium channel subtypes is determined by subtle variations at the interacting surface. *Toxicon : official journal of the International Society on Toxinology* 41, 125-128.

Gordon, D., Martin-Eauclaire, M.F., Cestele, S., Kopeyan, C., Carlier, E., Khalifa, R.B., Pelhate, M., Rochat, H., 1996. Scorpion toxins affecting sodium current inactivation bind to distinct homologous receptor sites on rat brain and insect sodium channels. *The Journal of biological chemistry* 271, 8034-8045.

Green, B.R., Bulaj, G., Norton, R.S., 2014. Structure and function of mu-conotoxins, peptide-based sodium channel blockers with analgesic activity. *Future medicinal chemistry* 6, 1677-1698.

Green, B.R., Olivera, B.M., 2016. Venom Peptides From Cone Snails: Pharmacological Probes for Voltage-Gated Sodium Channels. *Current topics in membranes* 78, 65-86.

Griswold, D.E., Douglas, S.A., Martin, L.D., Davis, T.G., Davis, L., Ao, Z., Luttmann, M.A., Pullen, M., Nambi, P., Hay, D.W., Ohlstein, E.H., 1999. Endothelin B receptor modulates inflammatory pain and cutaneous inflammation. *Molecular pharmacology* 56, 807-812.

Guatimosim, C., Romano-Silva, M.A., Cruz, J.S., Beirao, P.S., Kalapothakis, E., Moraes-Santos, T., Cordeiro, M.N., Diniz, C.R., Gomez, M.V., Prado, M.A., 1997. A toxin from the spider *Phoneutria nigriventer* that blocks calcium channels coupled to exocytosis. *Br J Pharmacol* 122, 591-597.

Gunning, S.J., Chong, Y., Khalife, A.A., Hains, P.G., Broady, K.W., Nicholson, G.M., 2003. Isolation of delta-missulenatoxin-Mb1a, the major vertebrate-active spider delta-toxin from the venom of *Missulena bradleyi* (Actinopodidae). *FEBS letters* 554, 211-218.

Gurevitz, M., Karbat, I., Cohen, L., Ilan, N., Kahn, R., Turkov, M., Stankiewicz, M., Stuhmer, W., Dong, K., Gordon, D., 2007. The insecticidal potential of scorpion beta-toxins. *Toxicon : official journal of the International Society on Toxinology* 49, 473-489.

Hagen, N.A., Cantin, L., Constant, J., Haller, T., Blaise, G., Ong-Lam, M., du Souich, P., Korz, W., Lapointe, B., 2017. Tetrodotoxin for Moderate to Severe Cancer-Related Pain: A Multicentre, Randomized, Double-Blind, Placebo-Controlled, Parallel-Design Trial. *Pain Res Manag* 2017, 7212713.

Hamon, A., Gilles, N., Sautiere, P., Martinage, A., Kopeyan, C., Ulens, C., Tytgat, J., Lancelin, J.M., Gordon, D., 2002. Characterization of scorpion alpha-like toxin group using two new toxins from the scorpion *Leiurus quinquestriatus hebraeus*. *European journal of biochemistry* 269, 3920-3933.

Han, T.S., Zhang, M.M., Walewska, A., Gruszczynski, P., Robertson, C.R., Cheatham, T.E., 3rd, Yoshikami, D., Olivera, B.M., Bulaj, G., 2009. Structurally minimized mu-conotoxin analogues as sodium channel blockers: implications for designing conopeptide-based therapeutics. *ChemMedChem* 4, 406-414.

Harvey, A.L., 2014. Toxins and drug discovery. *Toxicon : official journal of the International Society on Toxinology* 92, 193-200.

Hauke, T.J., Herzig, V., 2017. Dangerous arachnids-Fake news or reality? *Toxicon : official journal of the International Society on Toxinology* 138, 173-183.

Herzig, V., John Ward, R., Ferreira dos Santos, W., 2002. Intersexual variations in the venom of the Brazilian 'armed' spider *Phoneutria nigriventer* (Keyserling, 1891). *Toxicon : official journal of the International Society on Toxinology* 40, 1399-1406.

Herzig, V., King, G.F., 2015. The Cystine Knot Is Responsible for the Exceptional Stability of the Insecticidal Spider Toxin omega-Hexatoxin-Hv1a. *Toxins* 7, 4366-4380.

Herzig, V., Wood, D.L., Newell, F., Chaumeil, P.A., Kaas, Q., Binford, G.J., Nicholson, G.M., Gorse, D., King, G.F., 2011. ArachnoServer 2.0, an updated online resource for spider toxin sequences and structures. *Nucleic acids research* 39, D653-657.

Holford, M., Zhang, M.M., Gowd, K.H., Azam, L., Green, B.R., Watkins, M., Ownby, J.P., Yoshikami, D., Bulaj, G., Olivera, B.M., 2009. Pruning nature: Biodiversity-derived discovery of novel sodium channel blocking conotoxins from *Conus bullatus*. *Toxicon : official journal of the International Society on Toxinology* 53, 90-98.

Honma, T., Shiomi, K., 2006. Peptide toxins in sea anemones: structural and functional aspects. *Mar Biotechnol (NY)* 8, 1-10.

Huang, X., Li, G.C., Yin, L., Zhang, Z.H., Liang, Y.X., Chen, H.B., 2015. [The effective parts of liangxue tongyu prescription on cooling-blood and activating-blood and analysis of chemical constituents by HPLC-MS and GC-MS]. *Yao xue xue bao = Acta pharmaceutica Sinica* 50, 86-93.

Hucho, T., Levine, J.D., 2007. Signaling pathways in sensitization: toward a nociceptor cell biology. *Neuron* 55, 365-376.

Hwang, T.L., Shaka, A.J., 1998. Multiple-pulse mixing sequences that selectively enhance chemical exchange or cross-relaxation peaks in high-resolution NMR spectra. *J Magn Reson* 135, 280-287.

Israel, M.R., Tay, B., Deus, J.R., Vetter, I., 2017'. Sodium Channels and Venom Peptide Pharmacology. *Adv Pharmacol* 79, 67-116.

Jeglitsch, G., Rein, K., Baden, D.G., Adams, D.J., 1998. Brevetoxin-3 (PbTx-3) and its derivatives modulate single tetrodotoxin-sensitive sodium channels in rat sensory neurons. *The Journal of pharmacology and experimental therapeutics* 284, 516-525.

Jover, E., Martin-Moutot, N., Couraud, F., Rochat, H., 1978. Scorpion toxin: specific binding to rat synaptosomes. *Biochemical and biophysical research communications* 85, 377-382.

Kaas, Q., Westermann, J.C., Craik, D.J., 2010. Conopeptide characterization and classifications: an analysis using ConoServer. *Toxicon : official journal of the International Society on Toxinology* 55, 1491-1509.

Kaas, Q., Yu, R., Jin, A.H., Dutertre, S., Craik, D.J., 2012. ConoServer: updated content, knowledge, and discovery tools in the conopeptide database. *Nucleic acids research* 40, D325-330.

Kalapothakis, E., Penaforte, C.L., Beirao, P.S., Romano-Silva, M.A., Cruz, J.S., Prado, M.A., Guimaraes, P.E., Gomez, M.V., Prado, V.F., 1998. Cloning of cDNAs encoding neurotoxic peptides from the spider *Phoneutria nigriventer*. *Toxicon : official journal of the International Society on Toxinology* 36, 1843-1850.

Karbat, I., Kahn, R., Cohen, L., Ilan, N., Gilles, N., Corzo, G., Froy, O., Gur, M., Albrecht, G., Heinemann, S.H., Gordon, D., Gurevitz, M., 2007. The unique pharmacology of the scorpion alpha-like toxin Lqh3 is associated with its flexible C-tail. *The FEBS journal* 274, 1918-1931.

Kawabata, A., Nishimura, Y., Takagi, H., 1992. L-leucyl-L-arginine, naltrindole and D-arginine block antinociception elicited by L-arginine in mice with carrageenin-induced hyperalgesia. *British journal of pharmacology* 107, 1096-1101.

Khoo, K.K., Feng, Z.P., Smith, B.J., Zhang, M.M., Yoshikami, D., Olivera, B.M., Bulaj, G., Norton, R.S., 2009. Structure of the analgesic mu-conotoxin KIIIA and effects on the structure and function of disulfide deletion. *Biochemistry* 48, 1210-1219.

Khoo, K.K., Gupta, K., Green, B.R., Zhang, M.M., Watkins, M., Olivera, B.M., Balaram, P., Yoshikami, D., Bulaj, G., Norton, R.S., 2012. Distinct disulfide isomers of mu-conotoxins KIIIA and KIIB block voltage-gated sodium channels. *Biochemistry* 51, 9826-9835.

Khoo, K.K., Wilson, M.J., Smith, B.J., Zhang, M.M., Gulyas, J., Yoshikami, D., Rivier, J.E., Bulaj, G., Norton, R.S., 2011. Lactam-stabilized helical analogues of the analgesic mu-conotoxin KIIIA. *Journal of medicinal chemistry* 54, 7558-7566.

Kilkenny, C., Browne, W., Cuthill, I.C., Emerson, M., Altman, D.G., 2010. Animal research: reporting in vivo experiments: the ARRIVE guidelines. *British journal of pharmacology* 160, 1577-1579.

King, G.F., Gentz, M.C., Escoubas, P., Nicholson, G.M., 2008. A rational nomenclature for naming peptide toxins from spiders and other venomous animals. *Toxicon : official journal of the International Society on Toxinology* 52, 264-276.

King, G.F., Hardy, M.C., 2013. Spider-venom peptides: structure, pharmacology, and potential for control of insect pests. *Annual review of entomology* 58, 475-496.

King, G.F., Vetter, I., 2014. No gain, no pain: NaV1.7 as an analgesic target. *ACS chemical neuroscience* 5, 749-751.

Kline, A.D., Wuthrich, K., 1986. Complete sequence-specific ¹H nuclear magnetic resonance assignments for the alpha-amylase polypeptide inhibitor tendamistat from *Streptomyces tendae*. *Journal of molecular biology* 192, 869-890.

Klint, J.K., Senff, S., Rupasinghe, D.B., Er, S.Y., Herzig, V., Nicholson, G.M., King, G.F., 2012. Spider-venom peptides that target voltage-gated sodium channels: pharmacological tools and potential therapeutic leads. *Toxicon : official journal of the International Society on Toxinology* 60, 478-491.

Koishi, R., Xu, H., Ren, D., Navarro, B., Spiller, B.W., Shi, Q., Clapham, D.E., 2004. A superfamily of voltage-gated sodium channels in bacteria. *The Journal of biological chemistry* 279, 9532-9538.

Koradi, R., Billeter, M., Wuthrich, K., 1996. MOLMOL: a program for display and analysis of macromolecular structures. *Journal of molecular graphics* 14, 51-55, 29-32.

Kushmerick, C., Kalapothakis, E., Beirao, P.S., Penaforte, C.L., Prado, V.F., Cruz, J.S., Diniz, C.R., Cordeiro, M.N., Gomez, M.V., Romano-Silva, M.A., Prado, M.A., 1999. Phoneutria nigriventer toxin Tx3-1 blocks A-type K⁺ currents controlling Ca²⁺ oscillation frequency in GH3 cells. *J Neurochem* 72, 1472-1481.

Leao, R.M., Cruz, J.S., Diniz, C.R., Cordeiro, M.N., Beirao, P.S., 2000. Inhibition of neuronal high-voltage activated calcium channels by the omega-phoneutria nigriventer Tx3-3 peptide toxin. *Neuropharmacology* 39, 1756-1767.

Lebbe, E.K., Peigneur, S., Brullot, W., Verbiest, T., Tytgat, J., 2014. Ala-7, His-10 and Arg-12 are crucial amino acids for activity of a synthetically engineered mu-conotoxin. *Peptides* 53, 300-306.

Leipold, E., Borges, A., Heinemann, S.H., 2012. Scorpion beta-toxin interference with NaV channel voltage sensor gives rise to excitatory and depressant modes. *The Journal of general physiology* 139, 305-319.

Leipold, E., Hansel, A., Borges, A., Heinemann, S.H., 2006. Subtype specificity of scorpion beta-toxin Tz1 interaction with voltage-gated sodium channels is determined by the pore loop of domain 3. *Molecular pharmacology* 70, 340-347.

Leipold, E., Markgraf, R., Miloslavina, A., Kijas, M., Schirmeyer, J., Imhof, D., Heinemann, S.H., 2011. Molecular determinants for the subtype specificity of mu-conotoxin SIIIA targeting neuronal voltage-gated sodium channels. *Neuropharmacology* 61, 105-111.

Lewis, R.J., Dutertre, S., Vetter, I., Christie, M.J., 2012. Conus venom peptide pharmacology. *Pharmacological reviews* 64, 259-298.

Lewis, R.J., Schroeder, C.I., Ekberg, J., Nielsen, K.J., Loughnan, M., Thomas, L., Adams, D.A., Drinkwater, R., Adams, D.J., Alewood, P.F., 2007. Isolation and structure-activity of mu-conotoxin TIIIA, a potent inhibitor of tetrodotoxin-sensitive voltage-gated sodium channels. *Molecular pharmacology* 71, 676-685.

Li, R.A., Tomaselli, G.F., 2004. Using the deadly mu-conotoxins as probes of voltage-gated sodium channels. *Toxicon : official journal of the International Society on Toxinology* 44, 117-122.

Lipkind, G.M., Fozzard, H.A., 2000. KcsA crystal structure as framework for a molecular model of the Na(+) channel pore. *Biochemistry* 39, 8161-8170.

Liu, M., Wood, J.N., 2011. The roles of sodium channels in nociception: implications for mechanisms of neuropathic pain. *Pain Med* 12 Suppl 3, S93-99.

Lolignier, S., Bonnet, C., Gaudioso, C., Noel, J., Ruel, J., Amsalem, M., Ferrier, J., Rodat-Despoix, L., Bouvier, V., Aissouni, Y., Prival, L., Chapuy, E., Padilla, F., Eschalier, A., Delmas, P., Busserolles, J., 2015. The Nav1.9 channel is a key determinant of cold pain sensation and cold allodynia. *Cell reports* 11, 1067-1078.

Luiz, A.P., Wood, J.N., 2016. Sodium Channels in Pain and Cancer: New Therapeutic Opportunities. *Adv Pharmacol* 75, 153-178.

Mafra, R.A., Figueiredo, S.G., Diniz, C.R., Cordeiro, M.N., Cruz, J.D., De Lima, M.E., 1999. PhTx4, a new class of toxins from *Phoneutria nigriventer* spider venom, inhibits the glutamate uptake in rat brain synaptosomes. *Brain Res* 831, 297-300.

Martin, M.F., Garcia y Perez, L.G., el Ayeb, M., Kopeyan, C., Bechis, G., Jover, E., Rochat, H., 1987. Purification and chemical and biological characterizations of seven toxins from the Mexican scorpion, *Centruroides suffusus suffusus*. *The Journal of biological chemistry* 262, 4452-4459.

Martin-Eauclaire, M.F., Bougis, P.E., de Lima, M.E., 2018. Ts1 from the Brazilian scorpion *Tityus serrulatus*: A half-century of studies on a multifunctional beta like-toxin. *Toxicon : official journal of the International Society on Toxinology* 152, 106-120.

Martin-Moutot, N., Mansuelle, P., Alcaraz, G., Dos Santos, R.G., Cordeiro, M.N., De Lima, M.E., Seagar, M., Van Renterghem, C., 2006. *Phoneutria nigriventer* toxin 1: a novel, state-dependent inhibitor of neuronal sodium channels that interacts with micro conotoxin binding sites. *Molecular pharmacology* 69, 1931-1937.

Matavel, A., Cruz, J.S., Penaforte, C.L., Araujo, D.A.M., Kalapothakis, E., Prado, V.F., Diniz, C.R., Cordeiro, M.N., Beirao, P.S.L., 2002. Electrophysiological characterization and molecular identification of the *Phoneutria nigriventer* peptide toxin PnTx2-6. *FEBS Lett* 523, 219-223.

Matavel, A., Fleury, C., Oliveira, L.C., Molina, F., de Lima, M.E., Cruz, J.S., Cordeiro, M.N., Richardson, M., Ramos, C.H., Beirao, P.S., 2009. Structure and activity analysis of two spider toxins that alter sodium channel inactivation kinetics. *Biochemistry* 48, 3078-3088.

McArthur, J.R., Singh, G., McMaster, D., Winkfein, R., Tieleman, D.P., French, R.J., 2011. Interactions of key charged residues contributing to selective block of neuronal sodium channels by mu-conotoxin KIIIA. *Molecular pharmacology* 80, 573-584.

McDowell, G.C., 2nd, Pope, J.E., 2016. Intrathecal Ziconotide: Dosing and Administration Strategies in Patients With Refractory Chronic Pain. *Neuromodulation : journal of the International Neuromodulation Society* 19, 522-532.

McGrath, J.C., Lilley, E., 2015. Implementing guidelines on reporting research using animals (ARRIVE etc.): new requirements for publication in BJP. *British journal of pharmacology* 172, 3189-3193.

Melnikova, D.I., Khotimchenko, Y.S., Magarlamov, T.Y., 2018. Addressing the Issue of Tetrodotoxin Targeting. *Marine drugs* 16.

Menting, J.G., Gajewiak, J., MacRaild, C.A., Chou, D.H., Disotuar, M.M., Smith, N.A., Miller, C., Erchegeyi, J., Rivier, J.E., Olivera, B.M., Forbes, B.E., Smith, B.J., Norton, R.S., Safavi-Hemami, H., Lawrence, M.C., 2016. A minimized human insulin-receptor-binding motif revealed in a *Conus geographus* venom insulin. *Nat Struct Mol Biol* 23, 916-920.

Miranda, D.M., Romano-Silva, M.A., Kalapothakis, E., Diniz, C.R., Cordeiro, M.N., Moraes-Santos, T., De Marco, L., Prado, M.A., Gomez, M.V., 2001. Spider neurotoxins block the beta scorpion toxin-induced calcium uptake in rat brain cortical synaptosomes. *Brain Res Bull* 54, 533-536.

Moczydlowski, E., Olivera, B.M., Gray, W.R., Strichartz, G.R., 1986. Discrimination of muscle and neuronal Na-channel subtypes by binding competition between [3H]saxitoxin and muconotoxins. *Proceedings of the National Academy of Sciences of the United States of America* 83, 5321-5325.

Munasinghe, N.R., Christie, M.J., 2015. Conotoxins That Could Provide Analgesia through Voltage Gated Sodium Channel Inhibition. *Toxins* 7, 5386-5407.

Narahashi, T., 2008. Tetrodotoxin: a brief history. *Proceedings of the Japan Academy. Series B, Physical and biological sciences* 84, 147-154.

Newman, D.J., Cragg, G.M., 2016. Natural Products as Sources of New Drugs from 1981 to 2014. *Journal of natural products* 79, 629-661.

Nicholson, G.M., 2007. Insect-selective spider toxins targeting voltage-gated sodium channels. *Toxicon : official journal of the International Society on Toxinology* 49, 490-512.

Nicholson, G.M., Little, M.J., Birinyi-Strachan, L.C., 2004. Structure and function of delta-atracotoxins: lethal neurotoxins targeting the voltage-gated sodium channel. *Toxicon : official journal of the International Society on Toxinology* 43, 587-599.

Nicholson, G.M., Little, M.J., Tyler, M., Narahashi, T., 1996. Selective alteration of sodium channel gating by Australian funnel-web spider toxins. *Toxicon : official journal of the International Society on Toxinology* 34, 1443-1453.

Nicholson, G.M., Willow, M., Howden, M.E., Narahashi, T., 1994. Modification of sodium channel gating and kinetics by versutoxin from the Australian funnel-web spider *Hadronyche versuta*. *Pflugers Archiv : European journal of physiology* 428, 400-409.

Nielsen, K.J., Watson, M., Adams, D.J., Hammarstrom, A.K., Gage, P.W., Hill, J.M., Craik, D.J., Thomas, L., Adams, D., Alewood, P.F., Lewis, R.J., 2002. Solution structure of muconotoxin PIIIA, a preferential inhibitor of persistent tetrodotoxin-sensitive sodium channels. *The Journal of biological chemistry* 277, 27247-27255.

Nieto, F.R., Cobos, E.J., Tejada, M.A., Sanchez-Fernandez, C., Gonzalez-Cano, R., Cendan, C.M., 2012. Tetrodotoxin (TTX) as a therapeutic agent for pain. *Marine drugs* 10, 281-305.

Norton, R.S., 1990. Nuclear magnetic resonance (NMR) spectroscopy: applications to protein structure and engineering. *Australian journal of biotechnology* 4, 114-120.

Norton, R.S., 2017. Enhancing the therapeutic potential of peptide toxins. *Expert Opin Drug Discov* 12, 611-623.

Nunes, K.P., Cordeiro, M.N., Richardson, M., Borges, M.N., Diniz, S.O.F., Cardoso, V.N., Tostes, R., De Lima, M.E., Webb, R.C., Leite, R., 2010. Nitric oxide-induced vasorelaxation in response to PnTx2-6 toxin from *Phoneutria nigriventer* spider in rat cavernosal tissue. *J Sex Med* 7, 3879-3888.

Nunes, K.P., Costa-Goncalves, A., Lanza, L.F., Cortes, S.F., Cordeiro, M.N., Richardson, M., Pimenta, A.M.C., Webb, R.C., Leite, R., De Lima, M.E., 2008. Tx2-6 toxin of the *Phoneutria nigriventer* spider potentiates rat erectile function. *Toxicon : official journal of the International Society on Toxinology* 51, 1197-1206.

Nunes, K.P., Toque, H.A., Borges, M.H., Richardson, M., Webb, R.C., de Lima, M.E., 2012a. Erectile function is improved in aged rats by PnTx2-6, a toxin from *Phoneutria nigriventer* spider venom. *J Sex Med* 9, 2574-2581.

Nunes, K.P., Torres, F.S., Borges, M.H., Matavel, A., Pimenta, A.M., De Lima, M.E., 2013. New insights on arthropod toxins that potentiate erectile function. *Toxicon : official journal of the International Society on Toxinology* 69, 152-159.

Nunes, K.P., Wynne, B.M., Cordeiro, M.N., Borges, M.H., Richardson, M., Leite, R., DeLima, M.E., Webb, R.C., 2012b. Increased cavernosal relaxation by *Phoneutria nigriventer* toxin, PnTx2-6, via activation at NO/cGMP signaling. *Int J Impot Res* 24, 69-76.

Oliveira, L.C., De Lima, M.E., Pimenta, A.M.C., Mansuelle, P., Rochat, H., Cordeiro, M.N., Richardson, M., Figueiredo, S.G., 2003. PnTx4-3, a new insect toxin from *Phoneutria*

nigriventer venom elicits the glutamate uptake inhibition exhibited by PhTx4 toxic fraction. *Toxicon* : official journal of the International Society on Toxinology 42, 793-800.

Oliveira, S.M., Silva, C.R., Trevisan, G., Villarinho, J.G., Cordeiro, M.N., Richardson, M., Borges, M.H., Castro, C.J., Jr., Gomez, M.V., Ferreira, J., 2016. Antinociceptive effect of a novel armed spider peptide Tx3-5 in pathological pain models in mice. *Pflugers Arch* 468, 881-894.

Olivera, B.M., 1997. E.E. Just Lecture, 1996. Conus venom peptides, receptor and ion channel targets, and drug design: 50 million years of neuropharmacology. *Molecular biology of the cell* 8, 2101-2109.

Osteen, J.D., Herzig, V., Gilchrist, J., Emrick, J.J., Zhang, C., Wang, X., Castro, J., Garcia-Caraballo, S., Grundy, L., Rychkov, G.Y., Weyer, A.D., Dekan, Z., Undheim, E.A., Alewood, P., Stucky, C.L., Brierley, S.M., Basbaum, A.I., Bosmans, F., King, G.F., Julius, D., 2016. Selective spider toxins reveal a role for the Nav1.1 channel in mechanical pain. *Nature* 534, 494-499.

Osteen, J.D., Sampson, K., Iyer, V., Julius, D., Bosmans, F., 2017. Pharmacology of the Nav1.1 domain IV voltage sensor reveals coupling between inactivation gating processes. *Proceedings of the National Academy of Sciences of the United States of America* 114, 6836-6841.

Paiva, A.L., Matavel, A., Peigneur, S., Cordeiro, M.N., Tytgat, J., Diniz, M.R., de Lima, M.E., 2016. Differential effects of the recombinant toxin PnTx4(5-5) from the spider *Phoneutria nigriventer* on mammalian and insect sodium channels. *Biochimie* 121, 326-335.

Palhares, M.R., Silva, J.F., Rezende, M.J.S., Santos, D.C., Silva-Junior, C.A., Borges, M.H., Ferreira, J., Gomez, M.V., Castro-Junior, C.J., 2017. Synergistic antinociceptive effect of a calcium channel blocker and a TRPV1 blocker in an acute pain model in mice. *Life Sci* 182, 122-128.

Pan, X., Li, Z., Zhou, Q., Shen, H., Wu, K., Huang, X., Chen, J., Zhang, J., Zhu, X., Lei, J., Xiong, W., Gong, H., Xiao, B., Yan, N., 2018. Structure of the human voltage-gated sodium channel Nav1.4 in complex with beta1. *Science* 362.

Payandeh, J., Gamal El-Din, T.M., Scheuer, T., Zheng, N., Catterall, W.A., 2012. Crystal structure of a voltage-gated sodium channel in two potentially inactivated states. *Nature* 486, 135-139.

Payandeh, J., Scheuer, T., Zheng, N., Catterall, W.A., 2011. The crystal structure of a voltage-gated sodium channel. *Nature* 475, 353-358.

Peigneur, S., Cologna, C.T., Cremonez, C.M., Mille, B.G., Pucca, M.B., Cuypers, E., Arantes, E.C., Tytgat, J., 2015. A gamut of undiscovered electrophysiological effects produced by *Tityus serrulatus* toxin 1 on NaV-type isoforms. *Neuropharmacology* 95, 269-277.

Peigneur, S., de Lima, M.E., Tytgat, J., 2018. *Phoneutria nigriventer* venom: A pharmacological treasure. *Toxicon* : official journal of the International Society on Toxinology 151, 96-110.

Peigneur, S., Paolini-Bertrand, M., Gaertner, H., Biass, D., Violette, A., Stocklin, R., Favreau, P., Tytgat, J., Hartley, O., 2014a. delta-Conotoxins synthesized using an acid-cleavable solubility tag approach reveal key structural determinants for NaV subtype selectivity. *The Journal of biological chemistry* 289, 35341-35350.

Peigneur, S., Sevcik, C., Tytgat, J., Castillo, C., D'Suze, G., 2012. Subtype specificity interaction of bactridines with mammalian, insect and bacterial sodium channels under voltage clamp conditions. *The FEBS journal* 279, 4025-4038.

Peigneur, S., Zula, A., Zidar, N., Chan-Porter, F., Kirby, R., Madge, D., Ilas, J., Kikelj, D., Tytgat, J., 2014b. Action of clathrocin and analogues on voltage-gated sodium channels. *Marine drugs* 12, 2132-2143.

Pennington, M.W., Czerwinski, A., Norton, R.S., 2018. Peptide therapeutics from venom: Current status and potential. *Bioorg Med Chem* 26, 2738-2758.

Pereira, A., Cao, Z., Murray, T.F., Gerwick, W.H., 2009. Hoiamide a, a sodium channel activator of unusual architecture from a consortium of two papua new Guinea cyanobacteria. *Chemistry & biology* 16, 893-906.

Pimenta, A.M.C., Rates, B., Bloch, C., Gomes, P.C., Santoro, M.M., de Lima, M.E., Richardson, M., Cordeiro, M.D., 2005. Electrospray ionization quadrupole time-of-flight and matrix-assisted laser desorption/ionization tandem time-of-flight mass spectrometric analyses to solve micro-heterogeneity in post-translationally modified peptides from *Phoneutria nigriventer* (Aranea, Ctenidae) venom. *Rapid Commun Mass Sp* 19, 31-37.

Pineda, S.S., Chaumeil, P.A., Kunert, A., Kaas, Q., Thang, M.W.C., Le, L., Nuhn, M., Herzig, V., Saez, N.J., Cristofori-Armstrong, B., Anangi, R., Senff, S., Gorse, D., King, G.F., 2018. ArachnoServer 3.0: an online resource for automated discovery, analysis and annotation of spider toxins. *Bioinformatics* 34, 1074-1076.

Pineda, S.S., Chaumeil, P.A., Kunert, A., Kaas, Q., Thang, M.W.C., Li, L., Nuhn, M., Herzig, V., Saez, N.J., Cristofori-Armstrong, B., Anangi, R., Senff, S., Gorse, D., King, G.F., 2017. ArachnoServer 3.0: an online resource for automated discovery, analysis and annotation of spider toxins. *Bioinformatics*.

Pineda, S.S., Undheim, E.A., Rupasinghe, D.B., Ikonopoulou, M.P., King, G.F., 2014. Spider venomics: implications for drug discovery. *Future medicinal chemistry* 6, 1699-1714.

Pope, J.E., Deer, T.R., 2013. Ziconotide: a clinical update and pharmacologic review. *Expert opinion on pharmacotherapy* 14, 957-966.

Possani, L.D., Becerril, B., Delepierre, M., Tytgat, J., 1999. Scorpion toxins specific for Na⁺-channels. *European journal of biochemistry* 264, 287-300.

Prado, M.A., Guatimosim, C., Gomez, M.V., Diniz, C.R., Cordeiro, M.N., Romano-Silva, M.A., 1996. A novel tool for the investigation of glutamate release from rat cerebrocortical synaptosomes: the toxin Tx3-3 from the venom of the spider *Phoneutria nigriventer*. *Biochem J* 314 (Pt 1), 145-150.

Prashanth, J.R., Dutertre, S., Lewis, R.J., 2017. Pharmacology of predatory and defensive venom peptides in cone snails. *Molecular bioSystems* 13, 2453-2465.

Priest, B.T., Murphy, B.A., Lindia, J.A., Diaz, C., Abbadie, C., Ritter, A.M., Liberator, P., Iyer, L.M., Kash, S.F., Kohler, M.G., Kaczorowski, G.J., MacIntyre, D.E., Martin, W.J., 2005. Contribution of the tetrodotoxin-resistant voltage-gated sodium channel Nav1.9 to sensory transmission and nociceptive behavior. *Proceedings of the National Academy of Sciences of the United States of America* 102, 9382-9387.

Puillandre, N., Duda, T.F., Meyer, C., Olivera, B.M., Bouchet, P., 2015. One, four or 100 genera? A new classification of the cone snails. *The Journal of molluscan studies* 81, 1-23.

Purkerson-Parker, S.L., Fieber, L.A., Rein, K.S., Podona, T., Baden, D.G., 2000. Brevetoxin derivatives that inhibit toxin activity. *Chemistry & biology* 7, 385-393.

Qiu, F., Jiang, Y., Zhang, H., Liu, Y., Mi, W., 2012. Increased expression of tetrodotoxin-resistant sodium channels Nav1.8 and Nav1.9 within dorsal root ganglia in a rat model of bone cancer pain. *Neuroscience letters* 512, 61-66.

Randall, L.O., Selitto, J.J., 1957. A method for measurement of analgesic activity on inflamed tissue. *Arch Int Pharmacodyn Ther* 111, 409-419.

Raposo, C., Bjorklund, U., Kalapothakis, E., Biber, B., Alice da Cruz-Hofling, M., Hansson, E., 2016. Neuropharmacological effects of *Phoneutria nigriventer* venom on astrocytes. *Neurochem Int* 96, 13-23.

Rash, L.D., Birinyi-Strachan, L.C., Nicholson, G.M., Hodgson, W.C., 2000. Neurotoxic activity of venom from the Australian eastern mouse spider (*Missulena bradleyi*) involves modulation of sodium channel gating. *British journal of pharmacology* 130, 1817-1824.

Ravelli, K.G., Ramos, A.d.T., Goncalves, L.B., Magnoli, F.C., Troncione, L.R.P., 2017. Phoneutria nigriventer spider toxin Tx2-6 induces priapism in mice even after cavernosal denervation. *Toxicon : official journal of the International Society on Toxinology* 130, 29-34.

Ren, D., Navarro, B., Xu, H., Yue, L., Shi, Q., Clapham, D.E., 2001. A prokaryotic voltage-gated sodium channel. *Science* 294, 2372-2375.

Rezende Junior, L., Cordeiro, M.N., Oliveira, E.B., Diniz, C.R., 1991. Isolation of neurotoxic peptides from the venom of the 'armed' spider *Phoneutria nigriventer*. *Toxicon : official journal of the International Society on Toxinology* 29, 1225-1233.

Richards, K.L., Milligan, C.J., Richardson, R.J., Jancovski, N., Grunnet, M., Jacobson, L.H., Undheim, E.A.B., Mobli, M., Chow, C.Y., Herzig, V., Csoti, A., Panyi, G., Reid, C.A., King, G.F., Petrou, S., 2018. Selective NaV1.1 activation rescues Dravet syndrome mice from seizures and premature death. *Proceedings of the National Academy of Sciences of the United States of America* 115, E8077-E8085.

Richardson, M., Pimenta, A.M., Bemquerer, M.P., Santoro, M.M., Beirao, P.S., Lima, M.E., Figueiredo, S.G., Bloch, C., Jr., Vasconcelos, E.A., Campos, F.A., Gomes, P.C., Cordeiro, M.N., 2006. Comparison of the partial proteomes of the venoms of Brazilian spiders of the genus *Phoneutria*. *Comp Biochem Physiol C Toxicol Pharmacol* 142, 173-187.

Rigo, F.K., Rossato, M.F., Trevisan, G., De Pra, S.D.-T., Ineu, R.P., Duarte, M.B., de Castro Junior, C.J., Ferreira, J., Gomez, M.V., 2017. PhKv a toxin isolated from the spider venom induces antinociception by inhibition of cholinesterase activating cholinergic system. *Scand J Pain* 17, 203-210.

Robinson, S.D., Undheim, E.A.B., Ueberheide, B., King, G.F., 2017. Venom peptides as therapeutics: advances, challenges and the future of venom-peptide discovery. *Expert review of proteomics* 14, 931-939.

Rogers, J.C., Qu, Y., Tanada, T.N., Scheuer, T., Catterall, W.A., 1996. Molecular determinants of high affinity binding of alpha-scorpion toxin and sea anemone toxin in the S3-S4 extracellular loop in domain IV of the Na⁺ channel alpha subunit. *The Journal of biological chemistry* 271, 15950-15962.

Saez, N.J., Senff, S., Jensen, J.E., Er, S.Y., Herzig, V., Rash, L.D., King, G.F., 2010. Spider-venom peptides as therapeutics. *Toxins* 2, 2851-2871.

Safavi-Hemami, H., Brogan, S.E., Olivera, B.M., 2018. Pain therapeutics from cone snail venoms: From Ziconotide to novel non-opioid pathways. *Journal of proteomics*.

Safavi-Hemami, H., Brogan, S.E., Olivera, B.M., 2019. Pain therapeutics from cone snail venoms: From Ziconotide to novel non-opioid pathways. *Journal of proteomics* 190, 12-20.

Santos, R.G., Diniz, C.R., Cordeiro, M.N., De Lima, M.E., 1999. Binding sites and actions of Tx1, a neurotoxin from the venom of the spider *Phoneutria nigriventer*, in guinea pig ileum. *Braz J Med Biol Res* 32, 1565-1569.

Sato, K., Ishida, Y., Wakamatsu, K., Kato, R., Honda, H., Ohizumi, Y., Nakamura, H., Ohya, M., Lancelin, J.M., Kohda, D., et al., 1991. Active site of mu-conotoxin GIIIA, a peptide blocker of muscle sodium channels. *The Journal of biological chemistry* 266, 16989-16991.

Sautiere, P., Cestele, S., Kopeyan, C., Martinage, A., Drobecq, H., Doljansky, Y., Gordon, D., 1998. New toxins acting on sodium channels from the scorpion *Leiurus quinquestriatus hebraeus* suggest a clue to mammalian vs insect selectivity. *Toxicon : official journal of the International Society on Toxinology* 36, 1141-1154.

Schenberg, S., Lima, F.A., 1966. Pharmacology of the polypeptides from the venom of the spider *Phoneutria fera*. *Memorias do Instituto Butantan* 33, 627-638.

Schiavon, E., Stevens, M., Zaharenko, A.J., Konno, K., Tytgat, J., Wanke, E., 2010. Voltage-gated sodium channel isoform-specific effects of pompilidotoxins. *The FEBS journal* 277, 918-930.

Schreibmayer, W., Jeglitsch, G., 1992. The sodium channel activator Brevetoxin-3 uncovers a multiplicity of different open states of the cardiac sodium channel. *Biochimica et biophysica acta* 1104, 233-242.

Schroeder, C.I., Adams, D., Thomas, L., Alewood, P.F., Lewis, R.J., 2012. N- and C-terminal extensions of mu-conotoxins increase potency and selectivity for neuronal sodium channels. *Biopolymers* 98, 161-165.

Sheets, M.F., Hanck, D.A., 1995. Voltage-dependent open-state inactivation of cardiac sodium channels: gating current studies with Anthopleurin-A toxin. *The Journal of general physiology* 106, 617-640.

Shen, H., Li, Z., Jiang, Y., Pan, X., Wu, J., Cristofori-Armstrong, B., Smith, J.J., Chin, Y.K.Y., Lei, J., Zhou, Q., King, G.F., Yan, N., 2018. Structural basis for the modulation of voltage-gated sodium channels by animal toxins. *Science* 362.

Shen, H., Zhou, Q., Pan, X., Li, Z., Wu, J., Yan, N., 2017. Structure of a eukaryotic voltage-gated sodium channel at near-atomic resolution. *Science* 355.

Shiomi, K., 2009. Novel peptide toxins recently isolated from sea anemones. *Toxicon : official journal of the International Society on Toxinology* 54, 1112-1118.

Shon, K.J., Hasson, A., Spira, M.E., Cruz, L.J., Gray, W.R., Olivera, B.M., 1994. Delta-conotoxin GmVIA, a novel peptide from the venom of *Conus gloriamaris*. *Biochemistry* 33, 11420-11425.

Shon, K.J., Olivera, B.M., Watkins, M., Jacobsen, R.B., Gray, W.R., Floresca, C.Z., Cruz, L.J., Hillyard, D.R., Brink, A., Terlau, H., Yoshikami, D., 1998. mu-Conotoxin PIIIA, a new peptide for discriminating among tetrodotoxin-sensitive Na channel subtypes. *The Journal of neuroscience : the official journal of the Society for Neuroscience* 18, 4473-4481.

Silva, A.O., Peigneur, S., Diniz, M.R.V., Tytgat, J., Beirao, P.S.L., 2012. Inhibitory effect of the recombinant Phoneutria nigriventer Tx1 toxin on voltage-gated sodium channels. *Biochimie* 94, 2756-2763.

Silva, C.N., Nunes, K.P., Torres, F.S., Cassoli, J.S., Santos, D.M., Almeida Fde, M., Matavel, A., Cruz, J.S., Santos-Miranda, A., Nunes, A.D., Castro, C.H., Machado de Avila, R.A., Chavez-Olortegui, C., Lumar, S.S., Felicori, L., Resende, J.M., Camargos, E.R., Borges, M.H., Cordeiro, M.N., Peigneur, S., Tytgat, J., de Lima, M.E., 2015. PnPP-19, a Synthetic and Nontoxic Peptide Designed from a Phoneutria nigriventer Toxin, Potentiates Erectile Function via NO/cGMP. *The Journal of urology* 194, 1481-1490.

Sleeper, A.A., Cummins, T.R., Dib-Hajj, S.D., Hormuzdiar, W., Tyrrell, L., Waxman, S.G., Black, J.A., 2000. Changes in expression of two tetrodotoxin-resistant sodium channels and their currents in dorsal root ganglion neurons after sciatic nerve injury but not rhizotomy. *The Journal of neuroscience : the official journal of the Society for Neuroscience* 20, 7279-7289.

Souza, A.H., Ferreira, J., Cordeiro, M.d.N., Vieira, L.B., De Castro, C.J., Trevisan, G., Reis, H., Souza, I.A., Richardson, M., Prado, M.A.M., Prado, V.F., Gomez, M.V., 2008. Analgesic effect in rodents of native and recombinant Ph alpha 1beta toxin, a high-voltage-activated calcium channel blocker isolated from armed spider venom. *Pain* 140, 115-126.

Spronk, C.A., Linge, J.P., Hilbers, C.W., Vuister, G.W., 2002. Improving the quality of protein structures derived by NMR spectroscopy. *Journal of biomolecular NMR* 22, 281-289.

Stephan, M.M., Potts, J.F., Agnew, W.S., 1994. The microI skeletal muscle sodium channel: mutation E403Q eliminates sensitivity to tetrodotoxin but not to mu-conotoxins GIIIA and GIIIB. *The Journal of membrane biology* 137, 1-8.

Stevens, M., Peigneur, S., Dyubankova, N., Lescrinier, E., Herdewijn, P., Tytgat, J., 2012. Design of bioactive peptides from naturally occurring mu-conotoxin structures. *The Journal of biological chemistry* 287, 31382-31392.

Stevens, M., Peigneur, S., Tytgat, J., 2011. Neurotoxins and their binding areas on voltage-gated sodium channels. *Frontiers in pharmacology* 2, 71.

Strugatsky, D., Zilberberg, N., Stankiewicz, M., Ilan, N., Turkov, M., Cohen, L., Pelhate, M., Gilles, N., Gordon, D., Gurevitz, M., 2005. Genetic polymorphism and expression of a highly potent scorpion depressant toxin enable refinement of the effects on insect Na channels and illuminate the key role of Asn-58. *Biochemistry* 44, 9179-9187.

Sun, H.Y., Zhu, H.F., Ji, Y.H., 2003. BmK I, an alpha-like scorpion neurotoxin, specifically modulates isolated rat cardiac mechanical and electrical activity. *Sheng li xue bao : [Acta physiologica Sinica]* 55, 530-534.

Tanaka, B.S., Zhao, P., Dib-Hajj, F.B., Morisset, V., Tate, S., Waxman, S.G., Dib-Hajj, S.D., 2016. A gain-of-function mutation in Nav1.6 in a case of trigeminal neuralgia. *Mol Med* 22, 338-348.

Tejedor, F.J., Catterall, W.A., 1988. Site of covalent attachment of alpha-scorpion toxin derivatives in domain I of the sodium channel alpha subunit. *Proceedings of the National Academy of Sciences of the United States of America* 85, 8742-8746.

Thomsen, W.J., Catterall, W.A., 1989. Localization of the receptor site for alpha-scorpion toxins by antibody mapping: implications for sodium channel topology. *Proceedings of the National Academy of Sciences of the United States of America* 86, 10161-10165.

Tietze, A.A., Tietze, D., Ohlenschlager, O., Leipold, E., Ullrich, F., Kuhl, T., Mischo, A., Buntkowsky, G., Gorkach, M., Heinemann, S.H., Imhof, D., 2012. Structurally diverse muconotoxin PIIIA isomers block sodium channel NaV 1.4. *Angew Chem Int Ed Engl* 51, 4058-4061.

Tikhonov, D.B., Zhorov, B.S., 2005. Sodium channel activators: model of binding inside the pore and a possible mechanism of action. *FEBS letters* 579, 4207-4212.

Tonello, R., Fusi, C., Materazzi, S., Marone, I.M., De Logu, F., Benemei, S., Goncalves, M.C., Coppi, E., Castro-Junior, C.J., Gomez, M.V., Geppetti, P., Ferreira, J., Nassini, R., 2017. The peptide Phalalpha1beta, from spider venom, acts as a TRPA1 channel antagonist with antinociceptive effects in mice. *Br J Pharmacol* 174, 57-69.

Tonello, R., Rigo, F., Gewehr, C., Trevisan, G., Pereira, E.M.R., Gomez, M.V., Ferreira, J., 2014. Action of Phalalpha1beta, a peptide from the venom of the spider *Phoneutria nigriventer*, on the analgesic and adverse effects caused by morphine in mice. *J Pain* 15, 619-631.

Torres, F.S., Silva, C.N., Lanza, L.F., Santos, A.V., Pimenta, A.M.C., De Lima, M.E., Diniz, M.R.V., 2010. Functional expression of a recombinant toxin - rPnTx2-6 - active in erectile function in rat. *Toxicon : official journal of the International Society on Toxinology* 56, 1172-1180.

Tosti, E., Boni, R., Gallo, A., 2017. micro-Conotoxins Modulating Sodium Currents in Pain Perception and Transmission: A Therapeutic Potential. *Marine drugs* 15.

Trainer, V.L., Baden, D.G., Catterall, W.A., 1994. Identification of peptide components of the brevetoxin receptor site of rat brain sodium channels. *The Journal of biological chemistry* 269, 19904-19909.

Treede, R.D., Rief, W., Barke, A., Aziz, Q., Bennett, M.I., Benoliel, R., Cohen, M., Evers, S., Finnerup, N.B., First, M.B., Giamberardino, M.A., Kaasa, S., Kosek, E., Lavand'homme, P., Nicholas, M., Perrot, S., Scholz, J., Schug, S., Smith, B.H., Svensson, P., Vlaeyen, J.W., Wang, S.J., 2015. A classification of chronic pain for ICD-11. *Pain* 156, 1003-1007.

Troncone, L.R.P., Georgiou, J., Hua, S.-Y., Elrick, D., Lebrun, I., Magnoli, F., Charlton, M.P., 2003. Promiscuous and reversible blocker of presynaptic calcium channels in frog and crayfish neuromuscular junctions from *Phoneutria nigriventer* spider venom. *J Neurophysiol* 90, 3529-3537.

Van Der Haegen, A., Peigneur, S., Tytgat, J., 2011. Importance of position 8 in mu-conotoxin KIIIA for voltage-gated sodium channel selectivity. *The FEBS journal* 278, 3408-3418.

Vieira, L.B., Kushmerick, C., Hildebrand, M.E., Garcia, E., Stea, A., Cordeiro, M.N., Richardson, M., Gomez, M.V., Snutch, T.P., 2005. Inhibition of high voltage-activated calcium channels by spider toxin PnTx3-6. *J Pharmacol Exp Ther* 314, 1370-1377.

Vijverberg, H.P., Lazdunski, M., 1984. A new scorpion toxin with a very high affinity for sodium channels. An electrophysiological study. *Journal de physiologie* 79, 275-279.

Villanova, F.E., Andrade, E., Leal, E., Andrade, P.M., Borra, R.C., Troncone, L.R.P., Magalhaes, L., Leite, K.R.M., Paranhos, M., Claro, J., Srougi, M., 2009. Erection induced by Tx2-6 toxin of *Phoneutria nigriventer* spider: expression profile of genes in the nitric oxide pathway of penile tissue of mice. *Toxicon : official journal of the International Society on Toxinology* 54, 793-801.

Wang, L., Donald, B.R., 2004. Analysis of a systematic search-based algorithm for determining protein backbone structure from a minimum number of residual dipolar couplings. *Proceedings. IEEE Computational Systems Bioinformatics Conference*, 319-330.

Wanke, E., Zaharenko, A.J., Redaelli, E., Schiavon, E., 2009. Actions of sea anemone type 1 neurotoxins on voltage-gated sodium channel isoforms. *Toxicon : official journal of the International Society on Toxinology* 54, 1102-1111.

Waxman, S.G., Kocsis, J.D., Black, J.A., 1994. Type III sodium channel mRNA is expressed in embryonic but not adult spinal sensory neurons, and is reexpressed following axotomy. *Journal of neurophysiology* 72, 466-470.

Webster, L.R., 2015. The Relationship Between the Mechanisms of Action and Safety Profiles of Intrathecal Morphine and Ziconotide: A Review of the Literature. *Pain Med* 16, 1265-1277.

West, P.J., Bulaj, G., Garrett, J.E., Olivera, B.M., Yoshikami, D., 2002. Mu-conotoxin SmIIIa, a potent inhibitor of tetrodotoxin-resistant sodium channels in amphibian sympathetic and sensory neurons. *Biochemistry* 41, 15388-15393.

Wilson, M.J., Yoshikami, D., Azam, L., Gajewiak, J., Olivera, B.M., Bulaj, G., Zhang, M.M., 2011. mu-Conotoxins that differentially block sodium channels NaV1.1 through 1.8 identify those responsible for action potentials in sciatic nerve. *Proceedings of the National Academy of Sciences of the United States of America* 108, 10302-10307.

Yan, Z., Zhou, Q., Wang, L., Wu, J., Zhao, Y., Huang, G., Peng, W., Shen, H., Lei, J., Yan, N., 2017. Structure of the Nav1.4-beta1 Complex from Electric Eel. *Cell* 170, 470-482 e411.

Yanagawa, Y., Abe, T., Satake, M., 1987. Mu-conotoxins share a common binding site with tetrodotoxin/saxitoxin on eel electroplax Na channels. *The Journal of neuroscience : the official journal of the Society for Neuroscience* 7, 1498-1502.

Yao, S., Zhang, M.M., Yoshikami, D., Azam, L., Olivera, B.M., Bulaj, G., Norton, R.S., 2008. Structure, dynamics, and selectivity of the sodium channel blocker mu-conotoxin SIIIa. *Biochemistry* 47, 10940-10949.

Yonamine, C.M., Troncone, L.R.P., Camillo, M.A.P., 2004. Blockade of neuronal nitric oxide synthase abolishes the toxic effects of Tx2-5, a lethal *Phoneutria nigriventer* spider toxin. *Toxicon : official journal of the International Society on Toxinology* 44, 169-172.

Yu, F.H., Catterall, W.A., 2003. Overview of the voltage-gated sodium channel family. *Genome biology* 4, 207.

Zhang, M.M., Green, B.R., Catlin, P., Fiedler, B., Azam, L., Chadwick, A., Terlau, H., McArthur, J.R., French, R.J., Gulyas, J., Rivier, J.E., Smith, B.J., Norton, R.S., Olivera, B.M., Yoshikami, D., Bulaj, G., 2007. Structure/function characterization of micro-conotoxin KIIIa, an analgesic, nearly irreversible blocker of mammalian neuronal sodium channels. *The Journal of biological chemistry* 282, 30699-30706.

Zhang, M.M., Han, T.S., Olivera, B.M., Bulaj, G., Yoshikami, D., 2010. mu-conotoxin KIIIa derivatives with divergent affinities versus efficacies in blocking voltage-gated sodium channels. *Biochemistry* 49, 4804-4812.

Zhang, M.M., McArthur, J.R., Azam, L., Bulaj, G., Olivera, B.M., French, R.J., Yoshikami, D., 2009. Synergistic and antagonistic interactions between tetrodotoxin and mu-conotoxin in blocking voltage-gated sodium channels. *Channels (Austin)* 3, 32-38.

Zhang, M.M., Wilson, M.J., Azam, L., Gajewiak, J., Rivier, J.E., Bulaj, G., Olivera, B.M., Yoshikami, D., 2013. Co-expression of Na(V)beta subunits alters the kinetics of inhibition of voltage-gated sodium channels by pore-blocking mu-conotoxins. *British journal of pharmacology* 168, 1597-1610.

Zhang, X., Ren, W., DeCaen, P., Yan, C., Tao, X., Tang, L., Wang, J., Hasegawa, K., Kumasaka, T., He, J., Clapham, D.E., Yan, N., 2012. Crystal structure of an orthologue of the NaChBac voltage-gated sodium channel. *Nature* 486, 130-134.

Zhu, S., Peigneur, S., Gao, B., Lu, X., Cao, C., Tytgat, J., 2012. Evolutionary diversification of Mesobuthus alpha-scorpion toxins affecting sodium channels. *Mol Cell Proteomics* 11, M111.012054.

Zlotkin, E., Eitan, M., Bindokas, V.P., Adams, M.E., Moyer, M., Burkhart, W., Fowler, E., 1991. Functional duality and structural uniqueness of depressant insect-selective neurotoxins. *Biochemistry* 30, 4814-4821.

8. Annex Publications



Phoneutria nigriventer venom: A pharmacological treasure

Steve Peigneur^{a,b}, Maria Elena de Lima^{b,c,*}, Jan Tytgat^{a,**}

^a Toxicology and Pharmacology, University of Leuven (KU Leuven), Campus Gasthuisberg, PO Box 922, Herestraat 49, 3000 Leuven, Belgium

^b Laboratório de Venenos e Toxinas Animais, Dept de Bioquímica e Imunologia, Instituto de Ciências Biológicas, Universidade Federal de Minas Gerais, 31270-901, Belo Horizonte, MG, Brazil

^c Programa de Pós-graduação em Ciências da Saúde, Biomedicina e Medicina, Instituto de Ensino e Pesquisa da Santa Casa de Belo Horizonte, Grupo Santa Casa de Belo Horizonte, Belo Horizonte, MG, Brazil



ABSTRACT

In millions of years, spiders have optimized their venoms in order to assure successful prey capture and defence against predators. Spider venoms have become unique cocktails of biological active components enabling potentially interesting application for drug discovery or for agricultural purposes. The venom of *Phoneutria nigriventer* has been studied for over 60 years. This spider is responsible for a high number of envenomations with severe clinical manifestations in humans, which necessitates a comprehensive knowledge of its venom composition. With over 40 different neurotoxic peptides characterized so far and still many more awaiting identification, this venom is undoubtedly a pharmacological treasure. This review provides an overview of the *Phoneutria nigriventer* toxins known today and describes their mechanism of action at a molecular level. We critically discuss the potential of the *Phoneutria nigriventer* venom peptides as pharmaceutical tools or lead compounds for drug development.

1. Spider venom as a source of drug discovery

Spiders can be considered as one of the most successful venomous animals ever to inhabit the planet. So far over 47000 species have been characterized (Pineda et al., 2014). According to ArachnoServer, only of approximately 100 species the venom has been studied. This has resulted in 1427 characterized spider venom peptides (Herzig et al., 2011; Pineda et al., 2017). Since it is believed that spider venoms contain over 10 million biologically active peptides, no more than 0.01% of spider peptides have thus been studied so far (Escoubas, 2006; Klint et al., 2012). Therefore, spider venom can be considered as untapped treasure of biological active compounds that are potentially interesting for drug discovery as well as for the development of bio-insecticides to control pests. Up to date, no spider peptide-based drug has been approved by the Food and Drug Administration. However, one should take into account the small number of spider venom peptides investigated so far. This is a significant lower number compared for instance with scorpion or snake venom components. Several spider venom peptides have been characterized as insecticidal peptides with a strong preference for insect over mammalian targets. Illustrative hereof is the spider toxin ω/κ -HXTV-Hv1a. This peptide, isolated from the venom of *Hadronyche versuta*, is a potent inhibitor of insect voltage-gated calcium (Cav) channels devoid of activity on mammalian Cav

channels. A modified synthetic version of this toxin is the basis of the approved insecticidal agent SPEAR[®] (Fitches et al., 2012; Herzig and King, 2015; King and Hardy, 2013). Recently, exciting research has also highlighted the potential of spider venom-based drug discovery. Hi1a, a toxin isolated from the Australian funnel-web spider *Hadronyche infensa*, was found to be highly neuroprotective in acid-mediated neuronal injuries. This toxin inhibits acid-sensing ion channel 1a and hereby strongly attenuates for instance brain damage after stroke (Chassagnon et al., 2017). Hi1a is thus considered as a lead for development of therapeutics to protect the brain from ischemic injury.

2. *Phoneutria nigriventer*

The spiders of the genus *Phoneutria* are members of the family Ctenidae, suborder Labidognatha, and order Araneidae. They inhabit forests of the neotropical region from Southern Central America (Costa Rica) throughout South America, from the East of the Andes to the North of Argentina. The *Phoneutria* spiders are also known as the “armed spider” because of the characteristic posture they adopt when threatened. When in defence position, the *Phoneutria* will stand on his hind legs while typically raising four frontal legs up high, resulting in an “armed position” (Fig. 1). Another popular name is the “banana spider” which relates to their preference for hiding in banana bunches.

* Corresponding author. Programa de Pós-graduação em Ciências da Saúde, Biomedicina e Medicina, Instituto de Ensino e Pesquisa da Santa Casa de Belo Horizonte, Grupo Santa Casa de Belo Horizonte, Belo Horizonte, MG, Brazil.

** Corresponding author. Toxicology and Pharmacology, University of Leuven (KU Leuven), Campus Gasthuisberg, PO Box 922, Herestraat 49, 3000 Leuven, Belgium.

E-mail addresses: lima.mariaelena@gmail.com (M.E. de Lima), jan.tytgat@kuleuven.be (J. Tytgat).

<https://doi.org/10.1016/j.toxicon.2018.07.008>

Received 28 February 2018; Received in revised form 27 June 2018; Accepted 5 July 2018

Available online 10 July 2018

0041-0101/ © 2018 Elsevier Ltd. All rights reserved.



Fig. 1. *Phoneutria nigriventer*, the “armed spider”. The picture shows the spider assuming the typical defensive or “armed” position. (Photographed by Alcides Sousa, at Fundação Ezequiel Dias, Belo Horizonte, Minas Gerais, Brazil).

The genus *Phoneutria* belongs to the Retrolateral Tibial Apophysis (RTA) clade, whose adaptive and evolutionary process is associated with the loss of cribellate silk and prey-capture webs. They only use silk for the production of the sacs in which the eggs hatch or for nursery webs. These are wandering spiders with nocturnal habits. They are active hunters, relying on their fast acting and efficient venom for prey capture and defence. Their natural preys are insects although there are reports of *Phoneutria* hunting on other spiders and small rodents as well (de Lima et al., 2016; Herzig et al., 2002).

Phoneutria nigriventer are very aggressive, solitary spiders. They are synanthropic species, explaining the high number of human accidents occurring with this spider. Human envenomations involving *Phoneutria* spiders occur mainly in Brazil, but there are reports of sporadic cases in Central America and in neighbouring countries (de Lima et al., 2016). More recently, the export of bananas to Europe has resulted in certain cases of *Phoneutria* envenomation in countries such as the United Kingdom and the Netherlands. Most accidents involving humans are mild with only up to 0.5% of severe cases (Hauke and Herzig, 2017). Despite the venom being highly neurotoxic, the amount inoculated through the bite is usually too small to induce lethal effects. However, fatal envenomation usually occurs after a bite by female species. It is reported that females inject a larger amount of venom compared to males. Furthermore, as with most venomous animals, intersexual differences in venom composition have been demonstrated (Herzig et al., 2002). The clinical manifestations of severe systemic intoxication are usually seen in elderly and children. In such cases, the penile erection or priapism is one of the most noted signs of phoneutrism. Other clinical manifestations often reported after a *Phoneutria* bite are convulsions, agitation, somnolence, nausea, profuse sweating and vomiting, lacrimation, excessive salivation, hypertension, tachycardia, tachypnea, tremors and spastic paralysis (de Lima et al., 2016; Raposo et al., 2016). Cases of systemic poisoning in adults are uncommon but may happen. The effects observed in experimental animals after venom injection are

very similar to those observed in humans after the accidents with this spider. An interesting case report is the envenomation of a 52-year-old man who suffered from a neck bite by a female specimen of *Phoneutria nigriventer*. The patient experienced intense local pain, episodes of vomiting, tremors, blurred vision and excessive sweating. After 2 h, the patient was treated with captopril and meperidine because of a strongly elevated blood pressure. This treatment allowed stabilization of blood pressure and heart rate. Nevertheless, tachypnea, gentle shaking, cold extremities, profuse sweating, generalized tremors, and priapism subsisted. Treatment with antivenom resulted in complete recovery within 1 h (Bucaretychi et al., 2008). This case report nicely demonstrated the presence of venom components with a strong neurotoxic activity, and herewith, underlined the potential pharmaceutical applicability of *Phoneutria* venom. It is thus of no surprise that the venom of *P. nigriventer* is considered as a pharmacological treasure for drug discovery for over 60 years now. Indeed, this venom is a complex mixture of proteins and peptides, including neurotoxins, acting on ion channels and chemical receptors of the nervous and muscular systems of insects and mammals (Richardson et al., 2006). Notwithstanding that no *Phoneutria* venom-derived peptide has made it to the drug market, the potential pharmacological applicability of these peptides is evidenced by the ample research studies using these peptides, not only as potent ligands for specific targets, but also as tools to have a better understanding of their physiological function and their involvement in diseases and channelopathies.

The first studies on *P. nigriventer* venom, report the presence of biologically active proteins such as peptides, proteases, and hyaluronidase. Furthermore, other active compounds such as histamine serotonin and some free amino acids were also identified (de Lima et al., 2016; Gomez et al., 2002). Early work indicated that the whole venom exhibits a pronounced neurotoxic activity. Injection of whole or partially fractionized venom caused a myriad of excitatory symptoms in experimental animals (Bucherl, 1953, 1969; Schenberg and Lima, 1966). These observations in animals corroborated well with the reports on human envenomation (Bucaretychi et al., 2008; Diniz et al., 1990). The very first biochemical and pharmacological characterization of an isolated *Phoneutria nigriventer* toxin was performed in 1990s by Dr. Diniz and colleagues (Rezende et al., 1991) at Fundação Ezequiel Dias (Belo Horizonte, MG, Brazil). Almost 30 years before, Diniz has been the pioneer in studying this venom (Diniz, 1963). Nowadays *P. nigriventer* venom has been extensively studied making it one of the most studied spider venoms in the world. Besides some non-protein low-molecular-mass compounds, 41 neurotoxins have been identified from the crude venom up to date (Tables 1 and 2) (Herzig et al., 2011; Pineda et al., 2017). The *P. nigriventer* venom (PNV) has also been studied for its potential ability to cross the blood-brain barrier. This has recently been very nicely reviewed (Cruz-Hofling et al., 2016). This review shows that certain components of the PNV cause activation in multiple brain areas and upregulate the expression of vascular endothelial growth factor (VEGF) and its receptors Fms-like tyrosine kinase1 (Flt-1) and fetal liver kinase 1 (Flk-1). The authors suggested that these data of the PNV mechanism in the CNS can contribute to improving the treatment in cases of phoneutrism and, in addition, that PNV could be a potential tool for studies on drug permeability across the BBB.

3. Nomenclature of *Phoneutria nigriventer* toxins

The nomenclature of *Phoneutria nigriventer* toxins is rather confusing and problematic. Over time, often several names have been given to the same peptide. Historically, the *Phoneutria* toxins are annotated based on their occurrence in the venom when following the venom purification methods used in the first studies (Diniz et al., 1990), i.e. based on a particular chromatographic step and in the order of elution of the toxin, in this step. In an attempt to solve the confusing nomenclature of peptides of spiders and of other animal venoms, King et al. (2008) have proposed a rational nomenclature, which considers the molecular target

Table 1
 Overview for the toxins isolated from the venom of *P. nigriventer* from the fractions PhTx1–PhTx4. The toxins are ordered numerically according to the original name. AA: number of amino acid residues; P: protein level; NA: nucleic acid level. Average masses are shown. Data was obtained from Arachnoserver and Uniprot.

Name	Alternative Name	Rational Nomenclature	Evidence Level	Uniprot	Mass	AA	Fraction	In vivo Activity	Molecular Target & Mode of Action	Reference
PhTx1	Toxin Tx1, PNTx1, PhTx1	μ-ctenitoxin-Pn1a	P & NA	P17727	8597.7	78	PhTx1	LD50 = 5.5 pmol/g (mice)	Nav channels, Antagonist	Diniz et al., 1990
PhTx2-1	Tx2-1, Tx2-1, PNTx2-1	U2-ctenitoxin-Pn1a	P & NA	P29423	5841.7	53	PhTx2	Lethal to mice (0.02 pmol/g)	Unknown	Cordeiro et al., 1992
PhTx2-1A	Pn2-1A, U3-ctenitoxin-Pn1a, Pn2-1A	U2-ctenitoxin-Pn1b	P & NA	O76198	6070.0	54	PhTx2	n.a.	Unknown	Kalapothis et al., 1998a,b
PhTx2-5	Tx2-5, PNTx2-5, U4-ctenitoxin-Pn1a	δ-ctenitoxin-Pn2b	P	P29424	5100.9	49	PhTx3	Lethal to mice (2.4 pmol/g)	Nav channels, Agonist	Rezende et al., 1991
PhTx2-5A	Pn2-5A, U4-ctenitoxin-Pn1b	δ-ctenitoxin-Pn2c	NA	O76199	5112.8	48	PhTx2	n.a.	Unknown	Kalapothis et al., 1998a,b
PhTx2-6	Tx2-6, PNTx2-6	δ-ctenitoxin-Pn2a	P & NA	P29425	5288.2	48	PhTx2	Lethal to mice (7.5 pmol/g)	Nav channels, Agonist	Cordeiro et al., 1992
PhTx2-9	Neurotoxin Tx2-9, Tx2-9, PNTx2-9	U5-ctenitoxin-Pn1a	P	P29426	3736.5	32	PhTx2	n.a.	Unknown	Cordeiro et al., 1992
PhTx3	U26-ctenitoxin-Pn1a, Tx3	U7-ctenitoxin-Pn1b	P	P31010	unknown	n.a.	PhTx3	LD50 = 21.9 pmol/g (mice) ED50 = 6.4 pmol/g (mice)	Unknown	Rezende et al., 1991
PhTx3A	Pn3A	U6-ctenitoxin-Pn1a	P & NA	P81793	3771.4	34	PhTx3	n.a.	Unknown	Cardoso et al., 2003
PhTx3-1	Tx3-1, PNTx3-1	κ-ctenitoxin-Pn1a	P & NA	O76200	4575.2	40	PhTx3	Paralysis in mice (0.07 pmol/g)	K+ channels, Agonist	Cordeiro et al., 1993
PhTx3-2	Tx3-2, PNTx3-2	ω-ctenitoxin-Pn1a	P & NA	O76201	3533.2	34	PhTx3	Paralysis in mice (0.08 pmol/g)	L-type Cav channels, Antagonist	Cordeiro et al., 1993
PhTx3-3	Tx3-3, PNTx3-3, Omega-PhTx3-3	ω-ctenitoxin-Pn2a	P	P81789	unknown	n.a.	PhTx3	Lethal to mice (0.07 pmol/g)	L-, P/Q- and R-type Cav channels, Antagonist	Cordeiro et al., 1993
PhTx3-3A	Pn3-3A	U9-ctenitoxin-Pn1a	NA	P0C256	3873.3	36	PhTx3	n.a.	Unknown	Kalapothis et al., 1998a,b
PhTx3-4	PNTx3-4	ω-ctenitoxin-Pn3a	P & NA	P81789	8449.6	76	PhTx3	Lethal to mice (5 μg/mouse)	N-, P/Q- and R-type Cav channels, Antagonist	Cordeiro et al., 1993
PhTx3-4	PNTx3-4 isoform, Pn3-4A, U8-ctenitoxin-Pn1a	ω-ctenitoxin-Pn3b	P	P81789	8332.5	70	PhTx3	n.a.	N-, P/Q- and R-type Cav channels	Cardoso et al., 2003
PhTx3-4	PNTx3-4 isoform, ω-Phonetoxin 2A	ω-ctenitoxin-Pn3c	P	P81789	8362.5	70	PhTx3	n.a.	N-, P/Q- and R-type Cav channels	Cassola et al., 1998
PhTx3-4	PNTx3-4 isoform, ω-neutritoxin 3-4	ω-ctenitoxin-Pn3d	P	P81789	8458.5	70	PhTx3	n.a.	N-, P/Q- and R-type Cav channels	Cordeiro et al., 1993
PhTx3-5	PNTx3-5, Tx3-5, PNTx3-5	U7-ctenitoxin-Pn1a	P & NA	P81791	4145.8	45	PhTx3	Paralysis in mice (0.07 pmol/g)	L-type Cav channels	Cordeiro et al., 1993
PhTx3-6	Tx3-6, PNTx3-6, Phα-1β toxin	ω-ctenitoxin-Pn4a	P & NA	P81792	6032.9	55	PhTx3	Paralysis in mice (0.05 pmol/g)	N-, P/Q- and L-type Cav channels	Cordeiro et al., 1993
PhTx4-3	PNTx4-3	δ-ctenitoxin-Pn1b	P	P84034	5199.9	48	PhTx4	Non-toxic to mice (288.5 pmol/g) LD50 = 192.3 pmol/g (house fly)	Unknown	Oliveira et al., 2003
PhTx4 (5-5)	Tx4 (5-5), Pn4A, PNTx4 (5-5)	Γ-ctenitoxin-Pn1a	P & NA	P59367	5174.8	47	PhTx4	Non-toxic to mice (290 pmol/g)	NMDAR (Antagonist), Nav channels (Agonist)	Penaforte et al., 2000
PhTx4 (6-1)	PNTx4 (6-1), Tx4 (6-1)	δ-ctenitoxin-Pn1a	P & NA	P59368	5241.1	48	PhTx4	LD50 = 9.3 ng/house fly Non-toxic to mice (286.2 pmol/g) ED50 = 36.3 pmol/g (house fly)	Nav channels, Agonist	Figueiredo et al., 1995

Table 2

Overview for the toxins isolated from the venom of *P. nigriventer* from the fractions PhTx5. The toxins are ordered numerically according to the original name. AA: number of amino acid residues; P: protein level; NA: nucleic acid level. Average masses are shown. PhM refers to the original name given to PhTx5Data was obtained from Arachnoserver and Uniprot.

Name	Alternative Name	Rational Nomenclature	Evidence Level	Uniprot	Mass	AA	In vivo Activity	Reference
Pn3-5A		U10-ctenitoxin-Pn1a	NA	P0C2S9	4705.3	39	n.a.	Cardoso et al., 2003
Pn3-6A		U11-ctenitoxin-Pn1a	NA	P0C2S7	6589.4	58	n.a.	Cardoso et al., 2003
PNTx22C3		U11-ctenitoxin-Pn1b	P	P84011	6571.3	58	Non-toxic to mice	Richardson et al., 2006
Pn3-6B		U12-ctenitoxin-Pn1a	NA	P0C2S8	6370.3	58	n.a.	Cardoso et al., 2003
PNTx13C3		U13-ctenitoxin-Pn1a	P	P83894	3552.1	32	n.a.	Richardson et al., 2006
PNTx24A0C3		U13-ctenitoxin-Pn1b	P	P84017	3481.0	31	n.a.	Richardson et al., 2006
PNTx24A0C4		U13-ctenitoxin-Pn1c	P	P84018	3679.3	33	n.a.	Richardson et al., 2006
PNTx22A0C1		U14-ctenitoxin-Pn1a	P	P83998	4079.9	35	Non-toxic to mice and housefly	Richardson et al., 2006
PNTx27C4		U17-ctenitoxin-Pn1a	P	P83996	4062.8	36	Lethal in mice (3.0 µg/mouse)	Richardson et al., 2006
PNTx30C3		U18-ctenitoxin-Pn1a	P	P83999	7876.6	n.a.	Lethal in mice (3.0 µg/mouse)	Richardson et al., 2006
PNTx16C1		U19-ctenitoxin-Pn1a	P	P83997	7577.4	68	n.a.	Richardson et al., 2006
Pn4B		U1-ctenitoxin-Pn1a	NA	P61229	5815.4	47	n.a.	Penaforte et al., 2000
PNTx22C5		U20-ctenitoxin-Pn1a	P	P84093	8855.0	80	Lethal in mice (3.0 µg/mouse)	Richardson et al., 2006
PN47		U21-ctenitoxin-Pn1a	P	P84033	22089.0	245	n.a.	Richardson et al., 2006
PN10C5		U23-ctenitoxin-Pn1a	P	P84015	3672.7	33	n.a.	Richardson et al., 2006
PN16C3		U24-ctenitoxin-Pn1a	P	P84032	14775.7	128	n.a.	Richardson et al., 2006
PnV2		U27-ctenitoxin-Pn1a	P	Q9TWR5	unknown	n.a.	n.a.	Marangoni et al., 1993
PnV1		U28-ctenitoxin-Pn1a	P	Q7M3P1	unknown	n.a.	n.a.	Richardson et al., 2006
PnTkP-I	tachykinin peptide-I	U29-ctenitoxin-Pn1a	P	P86298	872.0	7	n.a.	Pimenta et al., 2005
PnTkP-II	tachykinin peptide-II	U29-ctenitoxin-Pn1b	P	P86299	1000.0	8	n.a.	Pimenta et al., 2005
PnTkP-III	tachykinin peptide-III	U29-ctenitoxin-Pn1c	P	P86300	1028.0	8	n.a.	Pimenta et al., 2005
PnTkP-IV	tachykinin peptide-IV	U29-ctenitoxin-Pn1d	P	P86301	1147.3	9	n.a.	Pimenta et al., 2005
PnTkP-V	tachykinin peptide-V	U29-ctenitoxin-Pn1e	P	P86302	1175.4	8	n.a.	Pimenta et al., 2005
PnTkP-VI	tachykinin peptide-VI	U29-ctenitoxin-Pn1f	P	P86303	1217.5	10	n.a.	Pimenta et al., 2005
PnTkP-VII	tachykinin peptide-VII	U29-ctenitoxin-Pn1g	P	P86304	1232.8	10	n.a.	Pimenta et al., 2005
PnTkP-VIII	tachykinin peptide-VIII	U29-ctenitoxin-Pn1h	P	P86305	1337.9	10	n.a.	Pimenta et al., 2005
PnTkP-IX	tachykinin peptide-IX	U29-ctenitoxin-Pn1i	P	P86306	1509.9	12	n.a.	Pimenta et al., 2005
PnTkP-X	tachykinin peptide-X	U29-ctenitoxin-Pn1j	P	P86307	1610.1	13	n.a.	Pimenta et al., 2005
PnTkP-XI	tachykinin peptide-XI	U29-ctenitoxin-Pn1k	P	P86308	1623.9	13	n.a.	Pimenta et al., 2005
PnTkP-XII	tachykinin peptide-XII	U29-ctenitoxin-Pn1l	P	P86309	1626.4	13	n.a.	Pimenta et al., 2005
PnTkP-XIII	tachykinin peptide-XIII	U29-ctenitoxin-Pn1m	P	P86310	1637.9	13	n.a.	Pimenta et al., 2005
PnTkP-XIV	tachykinin peptide-XIV	U29-ctenitoxin-Pn1n	P	P86311	1653.8	13	n.a.	Pimenta et al., 2005
PnTkP-XV	tachykinin peptide-XVI	U29-ctenitoxin-Pn1o	P	P86297	1653.9	14	n.a.	Pimenta et al., 2005
PhM1	tachykinin peptide PhM1	U29-ctenitoxin-Pn1p	P	n.a.	1346.6	11	n.a.	Pimenta et al., 2005

(including sub-types) of the toxin and also the family, genus and species of the animal from which the toxin was obtained. As an example, the toxin originally named Tx2-6/PnTx2-6 from *P. nigriventer*, is also annotated, following the new nomenclature as: δ -CNTX-Pn2a (delta meaning its modulating activity on Nav inactivation, CNTX = Ctenitoxin from Ctenidae family; Pn = *Phoneutria nigriventer*, = isoform). Some efforts have been done to adopt the new nomenclature of King. However, in general with *Phoneutria* venom peptides, the name given to the toxin in the first publication has become the common used name of the toxin. Therefore, in this review we adopted the name as found in the respective publications. The corresponding names suggested by King's nomenclature can be easily consulted in Arachoserver and in Tables 1 and 2. Since the venom is a complex mixture, an efficient purification method was needed. Therefore, an activity-guided purification and fractionation procedure, using gel filtration and reversed-phase chromatography had to be developed (Diniz et al., 1990). Following this procedure typically generated five distinct venom fractions. Each fraction showed different activity when assayed in mammals and/or insects, suggesting the presence of toxins with different pharmacological properties (Figueiredo et al., 1995; Rezende et al., 1991). For most of the initial studies, toxicity was evaluated *in vivo* by intracerebral (i.c.) or intrathoracic injections in mice and insects, respectively, and *in vitro* by smooth muscle assays using guinea pig ileum, besides some assays in synaptosomes from rat brain. Using this activity guided purification method, four distinct venom fractions, named PhTx1, PhTx2, PhTx3, and PhTx4 were identified. PhTx1, PhTx2, and PhTx3 are active on mammals and differ in their lethality and effects in mice (Rezende et al., 1991). PhTx4 produces marked stimulatory effects in insects and is more toxic to insects than to mammals (Figueiredo et al., 1995). More recently, it was shown that some toxins from the PhTx4 fraction,

besides acting on insect sodium channels (de Lima et al., 2002), also can act on mammal sodium channels (Paiva et al., 2016; Silva et al., 2015a), although no apparent toxicity was observed when injecting (i.c.) these molecules in rat brain. The fifth fraction (PhM), apparently not toxic to mammals, is active on smooth muscle, causing contraction (Rezende et al., 1991). The average LD₅₀ by i.c. injection in mice for the whole venom, PhTx1, PhTx2, PhTx3, and PhTx4, was 47, 45, 1.7, 137, and 480 µg/kg, respectively (Rezende et al., 1991). PhTx2 is the fraction which displayed the strongest neurotoxic activity while PhTx5 or PhM (15 mg/kg, i.v. injection) has no lethal effect in mice (Rezende et al., 1991). Fig. 2 shows a flow diagram describing the purification of *Phoneutria nigriventer* venom fractions.

4. PhTx1

The fraction PhTx1 is constituted by just one peptide, initially called Toxin 1 or Tx1. Afterwards, it was given the name *Phoneutria nigriventer* Toxin 1 or PnTx1. This peptide represents 0.45% of the whole venom protein content and it was the first purified and sequenced neurotoxin from *P. nigriventer* venom (Diniz et al., 1990). PnTx1 has a molecular mass of 8594.6 Da and is constituted of 78 amino acid residues, 14 of which are cysteines (Fig. 3). It is thus a fairly large peptide with a complex disulfide bridge pattern that remains undetermined till today.

Early research indicated that PnTx1 induces excitation and spastic paralysis in mice upon i.c. injection (Rezende et al., 1991). PnTx1 is lethal to rodents and has an astonishing LD₅₀ of 5.5 pmol/g in mice (Diniz et al., 1993, 2006; Klint et al., 2012). Nevertheless, the exact molecular target of this toxin remained unknown for many years. Initially, it was suggested that PnTx1 could act on calcium channels because radio-iodinated ¹²⁵I-PnTx1 showed partial competition with the

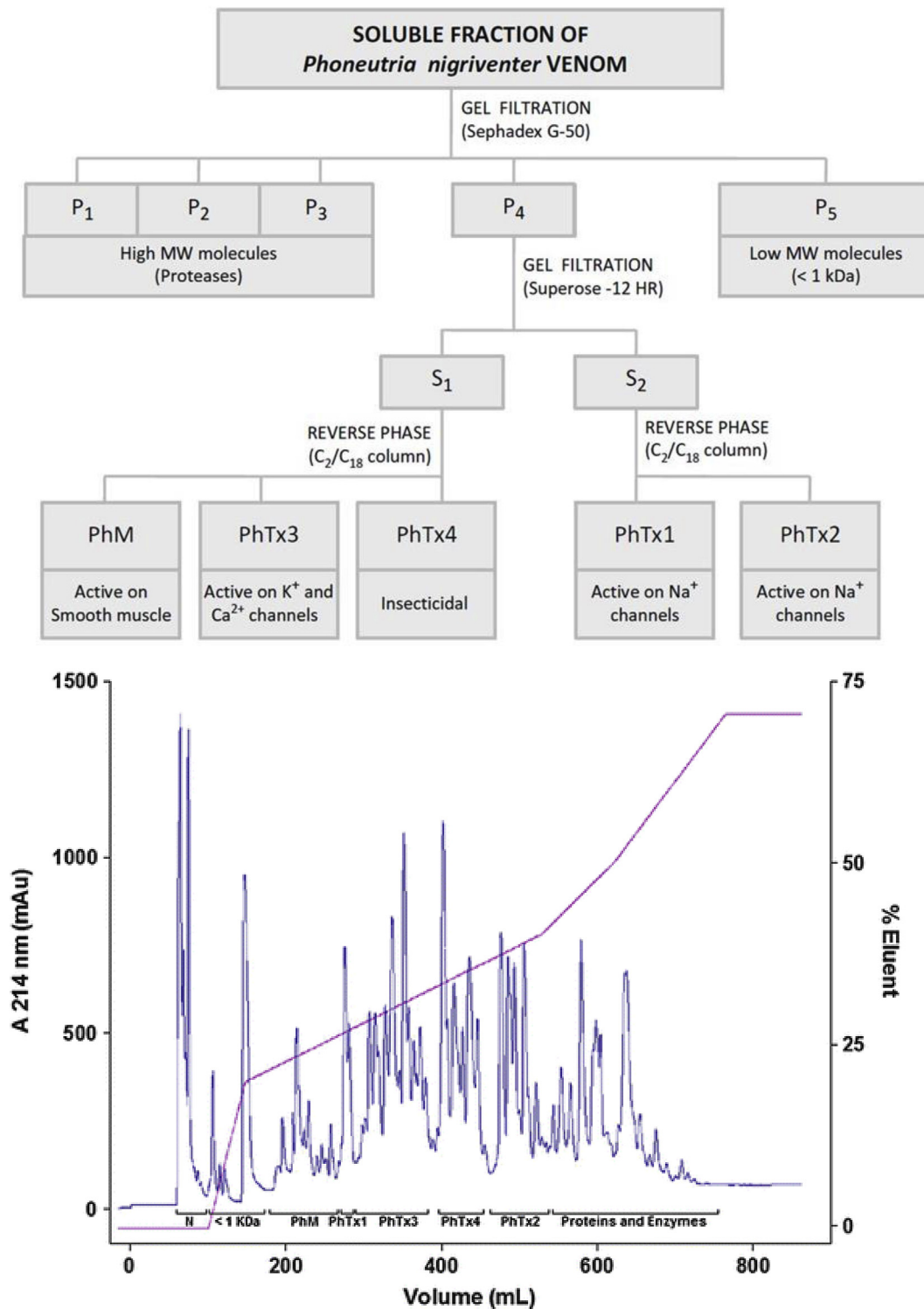


Fig. 2. Upper panel: Flowchart showing the purification procedure of *Phoneutria nigriventer* venom fractions. Adapted from de Lima et al., 2016). Lower panel: Elution profile of reversed-phase (RP-HPLC) fractionation of *Phoneutria nigriventer* venom. Venom sample was loaded on a preparative Vydac C4 column (2.2 × 25 cm). Column was eluted at a flow rate of 5 mL/min, monitored at 214 nm, under a gradient of acetonitrile (Richardson et al., 2006). The solid bars indicate the eluted fractions and (N) nigriventrine. Figure adapted from de Lima et al., 2016.

1 10 20 30 40 50 60 70
AELTSCFPVGH**EC****GD****AS****NC****NC****CG****DD****VY****CG****CG****WGR****WN****CK****CK****VAD****Q****S****Y****A****Y****G****I****CK****DK****VN****CP****NR****HL****W****PA****K****V****CK****PK****PC****RR****NC****GG**

Fig. 3. Sequence of PnTx1. Cysteines are indicated in red. (For interpretation of the references to colour in this figure legend, the reader is referred to the Web version of this article.)

fraction PhTx3, which contains several calcium channel modulating peptides. However, labeled PnTx1 did not compete with ω -conotoxin GVIA, a calcium channel inhibiting toxin isolated from cone snail venom (Santos et al., 1999). This rather contrary result was later attributed to the presence of a small contamination with PnTx3-3. PnTx3-3 is a well-characterized toxin that potently inhibits high-voltage-activated Cav channels, but not low-voltage-activated Cav channels (Leao et al., 2000). This contamination could explain the partial competition for Cav channel inhibition (Martin-Moutot et al., 2006). However, the question whether or not PnTx1 interacts with Cav channels can still not be answered unambiguously. Experiments using a highly purified PnTx1 showed that this toxin partially displaced the calcium-antagonist dihydropyridine derivative 3H-PN200-110 in GH3 cell membranes. Furthermore, a 50% inhibition of the calcium influx in GH3 cells was observed after application of 1 μ M PnTx1 (Santos et al., 1999). On the other hand, experiments with the recombinant PnTx1 (rPnTx1) showed no modification in the calcium currents of dorsal root ganglia (DRG) neurons (Silva et al., 2012). One explanation for these seeming contradictory observations could be that PnTx1 does interact with Cav channels but only selectively with a certain specific subtype of Cav channels. Nonetheless, PnTx1 awaits further investigation in order to elucidate its Cav channel interaction.

Using similar competitive binding experiments it was shown that 125 I-PnTx1 partially blocked the PhTx2 induced activity in myenteric plexus-longitudinal muscle preparations (Santos et al., 1999). Since PhTx2 is the fraction that contains mainly sodium channel toxins, this observation hinted towards an activity of PnTx1 on Nav channels. Interestingly, 125 I-PnTx1 did not compete with PnTx2-6, a toxin that modulates the inactivation process of Nav channels (Silva et al., 2015a). The authors consequently concluded that PnTx1 might be interacting with Nav channels via another binding site on the Nav channel (Santos et al., 1999). Later on, these conclusions were shown to be correct when it was demonstrated that PnTx1 competes with μ -conotoxin GIIIA (Martin-Moutot et al., 2006). μ -conotoxins are small peptides isolated from cone snail venom that inhibit Nav channels with great potency and selectivity (Green et al., 2014; Green and Olivera, 2016; Prashanth et al., 2014). They are known to bind a micro site within the neurotoxin binding site 1 of the Nav channel (French et al., 2010). It is interesting to note that PnTx1 competes with μ -conotoxins for site 1 but not with the small compound Nav channel inhibitor tetrodotoxin (TTX). Using the patch-clamp technique and Chinese hamster ovary cells expressing Nav1.2 channels, PnTx1 was characterized as a state-dependent channel inhibitor, preferring to interact with the Nav channels in the open state (Martin-Moutot et al., 2006).

The recombinant PnTx1 was expressed in a bacterial heterologous system and inhibited a variety of sodium channel isoforms expressed in *Xenopus laevis* oocytes (Fig. 4) and native sodium channels in DRG neurons (Silva et al., 2012). Surprisingly, recombinant toxin displayed a 3-fold lower IC_{50} value compared to native peptide. This could possibly be explained by the presence of three additional amino acids in the sequence of the recombinant produced toxin, namely alanine and methionine at the N-terminus and a glycine at the C-terminus. The recombinant toxin, rPnTx1, inhibited mammalian Nav channel isoforms with the following order of potency: rNav1.2 > rNav1.7 rNav1.4 rNav1.3 > mNav1.6 hNav1.8 with no effect on Nav1.5 (Silva et al., 2012). Accordingly, rPnTx1 was less effective on TTX-resistant sodium channels in DRG neurons (Silva et al., 2012). From a drug development point of view, it is interesting to note that PnTx1 does not inhibit the cardiac isoform Nav1.5. Indeed, such a significant selectivity towards neuronal sodium channels is considered appealing as this avoids unwanted cardiovascular side effects. Inhibition of Nav channels occurred without modification of the biophysical properties of the channels since no alterations of the voltage dependence of activation and steady-state inactivation were noted (Martin-Moutot et al., 2006; Silva et al., 2012). Competitive binding studies have shown that PnTx1 does not compete with toxins acting on site 2, 3, 4, 5. Nor does PnTx1 bind to the

interaction site for local anesthetics or for pyrethroids (Martin-Moutot et al., 2006). Furthermore, using mutated Nav1.2 channels devoid of fast inactivation, it was shown that PnTx1 does not stabilize the channels in the inactivated state (Silva et al., 2012). It thus can be concluded that the PnTx1 induced sodium current inhibition is not a result of modified gating and open time probability but rather from a physical obstruction of the sodium ion pathway through the Nav channel. The result of PnTx1 binding is thus a reduction of the single channel conductance.

PnTx1 does not inhibit insect Nav channels. Even at higher concentrations, PnTx1 failed to decrease the current peak amplitude of arthropod Nav channel isoforms such as from the fruit fly *Drosophila melanogaster* (DmNav1), the cockroach *Blattella germanica* (BgNav1.1) and the mite *Varroa destructor* (VdNav1). This inactivity on arthropod Nav channels corroborates well with previous studies showing a lack of insecticidal activity of venom fraction PhTx1, when injected in insects (Santos et al., 1999).

Curiously, both native and recombinant toxins were not able to block 100% of the Nav1.2 currents, reaching a maximal inhibition of approximately 85% of the sodium peak current, even at saturating conditions. Subsequent addition of TTX results in completely inhibited sodium channels indicating that TTX can still reach and bind its site of interaction, independent of the presence of PnTx1 (Silva et al., 2012). Since these experiments were performed in *Xenopus* oocytes heterologously expressing Nav channels it was concluded that PnTx1 incompletely inhibits the sodium conductance through the channel, a phenomenon shared with the μ -conotoxins (French et al., 2010; Silva et al., 2012).

Moreover, an interesting sequence comparison can be made between a central segment of PnTx1 and μ -conotoxins such as GIIIA and KIIIA. In this way, the amino acids W33, R35 and K39 of PnTx1 can be aligned with the similar amino acids W8, R10 and R14, present in the μ -conotoxin KIIIA (Khoo et al., 2011; Silva et al., 2012; Zhang et al., 2010). μ -conotoxins have been intensively studied and for several of them are the key residues determined (Prashanth et al., 2014; Zhang et al., 2010). Single mutations can alter significantly the selectivity of a toxin. The substitution of tryptophan at position 8 by arginine decreased affinity of μ -conotoxin KIIIA for Nav1.2 subtype, making it more selective to Nav1.4 (Van Der Haegen et al., 2011). There are three basic amino acids conserved in μ -conotoxin GIIIA that are putative key residues for the interaction with Nav channels: R13, K16, and K19. PnTx1 has basic residues in two correspondent positions, R35 (instead K16) and K39 (corresponding to K19). However, PnTx1 lacks the first arginine (R13) and has a glycine (G32) in the corresponding position. Arginine-13 was postulated to be a general residue for μ -conotoxins to interact with the receptor site of sodium channels. This residue is particularly critical, since it is believed to compete with the guanidinium group of TTX or STX for the binding site 1. The toxin binding sites of sodium channels were classified based on their ability to compete with other toxins in binding experiments. Site 1 is the binding site of TTX and STX and toxins that can displace them, such as μ -conotoxin GIIIA. Since PnTx1 competes with μ -conotoxin GIIIA but not with TTX, it would be more appropriate to consider it as a macro site 1 instead (de Lima et al., 2016).

Based on all information to date, one hypothesis is a mechanism of action where PnTx1 binds to the outer mouth of the channel pore, at a site similar or at least partially overlapping with the μ -conotoxin binding site within neurotoxin binding site 1. Upon binding, PnTx1 hinders the flow of sodium ions. Presumably, the inhibition is a result of both physical occlusion and repulsion of positive charges, similar to what has been proposed for the μ -conotoxins (French et al., 2010). Therefore, the likely mechanism of action of PnTx1 would be the reduction of the unitary conductance of the channel, similarly to what is seen for the mutated toxin μ -conotoxin GIIIA (R13Q) (Becker et al., 1992).

Spider venom peptides targeting Nav channels (NaSpTxS) have been

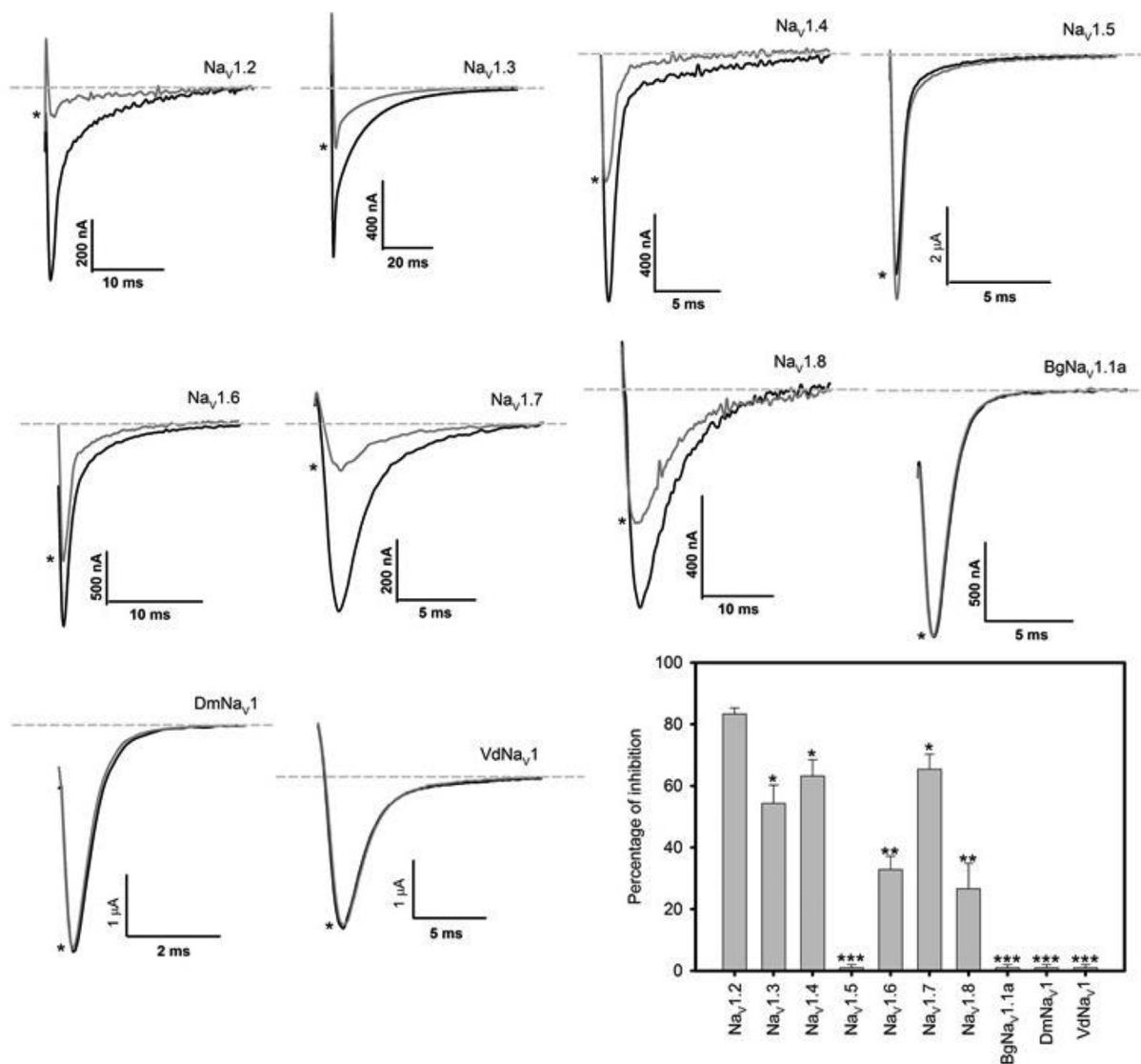


Fig. 4. Effect of rPnTx1 on different subtypes of sodium channels expressed in oocytes. Representative records of Na⁺ currents before (black line) and after (gray line and *) the addition of 1 μM rPnTx1. Dashed line is the baseline. Holding potential: −90 mV. Test potential: 0 mV. (Inset) Average percentage of Na⁺ current inhibition by rPnTx1 (1 μM) of different sodium channel subtypes expressed in oocytes. Nav1.2 inhibition was significantly higher when compared with Nav1.3, Nav1.4 and Nav1.7 and these were higher when compared with Nav1.6 and Nav1.8. No effect was observed for Nav1.5 and for the arthropod isoforms (DmNav1, BgNav1.1a and VdNav1). The symbols (*), (**) and (***) denote the isoforms on which the toxin effects were not statistically different. (*) indicates that PnTx1 inhibits Nav1.3, Nav1.4 and Nav1.7 with a similar affinity. (**) indicates that Nav1.6 and Nav1.8 are inhibited with a similar affinity. (***) indicates that Nav1.5, DmNav1, BgNav1 and VdNav1 are not inhibited by PnTx1. Figure adapted from [Silva et al. \(2012\)](#).

divided into 12 families based on sequence identity and intercysteine spacing ([Klint et al., 2012](#)). PnTx1 is the representative of family 8 which constitutes the family of the longest NaSpTxS. So far, no structure, or even disulfide bridge pattern for that matter, has been determined for this structural family. Moreover, none of the *Phonetreria nigriventer* peptides has its structure determined so far, emphasizing the challenges, and herewith the opportunities from a structural point of view, to be found in the *Phonetreria* venom. This is mainly due to peptide scarcity since only small amounts can be isolated from the venom and due to the peptide size and complexity. Therefore, many structure-function questions about PnTx1 remain open, which makes it an attractive object for future studies. Elucidation of the structure of PnTx1 would greatly enhance the understanding on how this toxin exerts its interesting pharmacology.

5. PhTx2

The fraction PhTx2 was found to be toxic to both mice and insects ([Figueiredo et al., 1995](#)). Intracerebral injection in mice resulted in priapism, salivation, convulsions and spastic paralysis of the anterior and posterior limbs among other manifestations ([Rezende et al., 1991](#)). Using a frog skeletal muscle preparation, it was shown that fraction PhTx2 alters the Nav channel kinetics. PhTx2 caused a shift in the activation and steady-state inactivation curves, a slowing down of the channel inactivation and a partial inhibition of the sodium peak current. The same experiments indicated that PhTx2 does not affect the potassium current ([Araujo et al., 1993](#)). *Phonetreria*.

Purification of fraction PhTx2 resulted in 9 peptides which were named PnTx2-1 till PnTx2-9 ([Cordeiro et al., 1992](#)). All peptides were investigated for their toxicity by i.c. injection in mice. PnTx2-2, PnTx2-3, PnTx2-4, PnTx2-7, and PnTx2-8 showed low toxicity and these peptides still await justification for their classification as neurotoxin.

	1	10	20	30	40	50
PnTx2-1	A T C A G Q D K P C K E T C D C C G E R G E C V C A L S Y E G K Y R C I C R Q G N F L I A W H K L A S C K					
PnTx2-5	A T C A G Q D Q T C K V T C D C C G E R G E C V C G G P C I C R Q G N F L I A W Y K L A S C K K					
PnTx2-6	A T C A G Q D Q P C K E T C D C C G E R G E C V C G G P C I C R Q G Y F W I A W Y K L A N C K K					
PnTx2-9	S F C I P F K P C K S D E N C C K F K C K T T G I V K L C R W					

Fig. 5. Sequences of the toxins identified in *Phoneutria nigriventer* venom fraction 2. Cysteines are indicated in red. (For interpretation of the references to colour in this figure legend, the reader is referred to the Web version of this article.)

PnTx2-1, PnTx2-5, and PnTx2-6 share up to 77% identity with each other (Fig. 5) and all 3 toxins elicit neurotoxic effects when injected into mice (Table 1) (Cordeiro et al., 1992). Pruritus, lacrimation, increased salivation, sweating, and agitation followed by spastic paralysis of the limbs was observed. PnTx2-9, was much less toxic to mice, causing pruritus, reduction in motility and tail erection. PnTx2-9 differs in sequence from the other peptides of PhTx2. It is a rather short peptide of 32 residues with 3 disulfide bridges. Although annotated as a Nav channel toxin, no functional data is available to justify this classification.

PnTx2-1 remains scarcely studied. The *in vivo* tests in mice and based on the sequence homology with PnTx2-5 and PnTx2-6, it can be assumed that this peptide also targets Nav channels. However, functional studies are required to investigate the subtype selectivity and species specificity of PnTx2-1 (Richardson et al., 2006).

Among all the polypeptides purified from PhTx2 fraction, PnTx2-5 and PnTx2-6 are the most studied toxins. They have high sequence homology, differing only in five amino acid residues (Cordeiro et al., 1992). Both toxins were shown to modulate sodium channel kinetics by slowing down the inactivation process and by shifting the voltage dependence of activation towards more hyperpolarized potentials. Both peptides were found to induce a painful and persistent penile erection, also known as priapism which is a common clinical manifestation upon *Phoneutria nigriventer* envenomation. Interestingly, despite the high homology between both peptides, significant differences in potency have been reported. PnTx2-5 displayed an approximately 6-fold lower potency than PnTx2-6 in electrophysiological assays (Matavel et al., 2002, 2009; Nunes et al., 2010).

Using frog skeletal muscle, an in-depth characterization of PnTx2-6 on a molecular level was performed. PnTx2-6 induces a plethora of modifications of channel kinetics. PnTx2-6 reduces the sodium peak current, slows down the time constant for fast inactivation and causes a hyperpolarizing shift of the voltage dependence of both the activation and steady-state inactivation curves (Matavel et al., 2002). The diversity of channel modulations is intriguing from a biophysical point of view. The slowing down of the inactivation process is similar to the activity of certain scorpion, sea anemone and other spider toxins such as the $\beta/8$ -agatoxins (Cardoso and Lewis, 2017; Deus et al., 2017; Israel et al., 2017; Nicholson, 2007; Wanke et al., 2009). The subtype selectivity for mammalian Nav channel isoforms was determined for PnTx2-6 (Fig. 6) (Silva et al., 2015a). These toxins have been characterized to bind to the so called neurotoxin binding site 3 Nav channels (Catterall et al., 2007). These site 3 toxins slow down sodium channel inactivation and in many cases they induce other channel gating modifications as well (Cardoso and Lewis, 2017; Peigneur et al., 2012; Zhu et al., 2012). Binding experiments in brain synaptosomes showed that PnTx2-6 partially competes with the typical α -scorpion toxin AaHII (from *Androctonus australis Hector*) (Matavel et al., 2009). A shift of the midpoint of activation potential toward more negative potentials together with a reduction in sodium peak current are characteristics of gating alterations often observed for β -scorpion toxins and certain spider toxins (Leipold et al., 2006; Nicholson et al., 2004; Peigneur et al., 2015). However, it was shown that PnTx2-6 does not compete

with the β -scorpion toxin CsslV (from *Centruroides suffusus suffusus*) and it thus seems unlikely that PnTx2-6 binds to same site as β -scorpion toxin (Matavel et al., 2009). As such, structure-function studies are required to pinpoint which toxin-channel interactions are responsible for the PnTx2-6 induced channel modulations.

The effect of PnTx2-6 on spontaneous penile erection is remarkable and opens perspectives for clinical applications. In a first step to further investigate the exact role of PnTx2-6 in erectile function, the toxin was expressed recombinantly in *E. coli* cells (Torres et al., 2010). The recombinant toxin was able to produce erection, similar to native toxin (Torres et al., 2010). The mechanism of action through which PnTx2-5 and PnTx2-6 promote cavernosal relaxation and enhance erectile function is not completely clarified (Nunes et al., 2010, 2012a; Yonamine et al., 2004). However, intensive research in recent years has provided a better understanding on how these toxins influence erectile function (Nunes et al., 2012b). It is suggested that PnTx2-6 intervenes in the nitric oxide (NO)/cyclic GMP pathway by increasing the release of NO in the corpus cavernosum tissue (Nunes et al., 2008). The release of NO from penile endothelial cells or nitrergic nerves is a key regulator in erectile function. Increased NO concentrations, triggered by sexual stimulation, induces relaxation of penile smooth muscle. This relaxation results in an increased blood flow and intracavernosal pressure which leads to penile erection. The PnTx2-6 induced relaxation is neuronal nitric oxide synthase (nNOS) dependent (Nunes et al., 2012b). The activation of nNOS by PnTx2-6 is most likely indirect. Since PnTx2-6 is characterized as a modulator of Nav channel inactivation, the binding of PnTx2-6 to Nav channels will result in an increased sodium influx. This will trigger a cascade of cellular reactions, eventually resulting in an activation of nNOS and consequently stimulation of NO release. This mechanism of action was supported by the observation that ω -conotoxin GVIA, an inhibitor of N-type calcium channels, could block the relaxation induced by PnTx2-6. Additionally, it was shown that the cavernosal relaxation provoked by PnTx2-6 is not dependent on phosphodiesterase-5 (PDE5) inhibition (Nunes et al., 2012b). Furthermore, it was shown that PnTx2-6 induces priapism in mice even after cavernosal denervation, indicating that the toxin might not depend on cavernosal nerves integrity (Ravelli et al., 2017). Investigating the gene expression in mice erectile tissue showed overexpressing of two genes potentially related to PnTx2-6 induced priapism (Villanova et al., 2009). One of these genes is directly involved in the activation of the NO/cGMP pathway.

PnTx2-5 has been less investigated, compared to PnTx2-6, but the results that are available do suggest that this toxin is involved in penile potentiation similar to PnTx2-6 (Villanova et al., 2009). PnTx2-5 also caused penile erection when injected intraperitoneal in male mice. These effects are completely abolished by the nNOS-selective inhibitor 7-nitroindazole, indicating an important involvement of nNOS in this effect as well (Yonamine et al., 2004). Both toxins, PhTx2-5 and PhTx2-6, represent interesting pharmacological tools to study erectile dysfunction. A 19 residues peptide, devoid of disulfide bridges but comprising the pharmacophore of PnTx2-6 was designed. This PnTx2-6-derived peptide, named PnPP-19, was no longer active on Nav channels. The abolishment of Nav channel activity can be considered as an

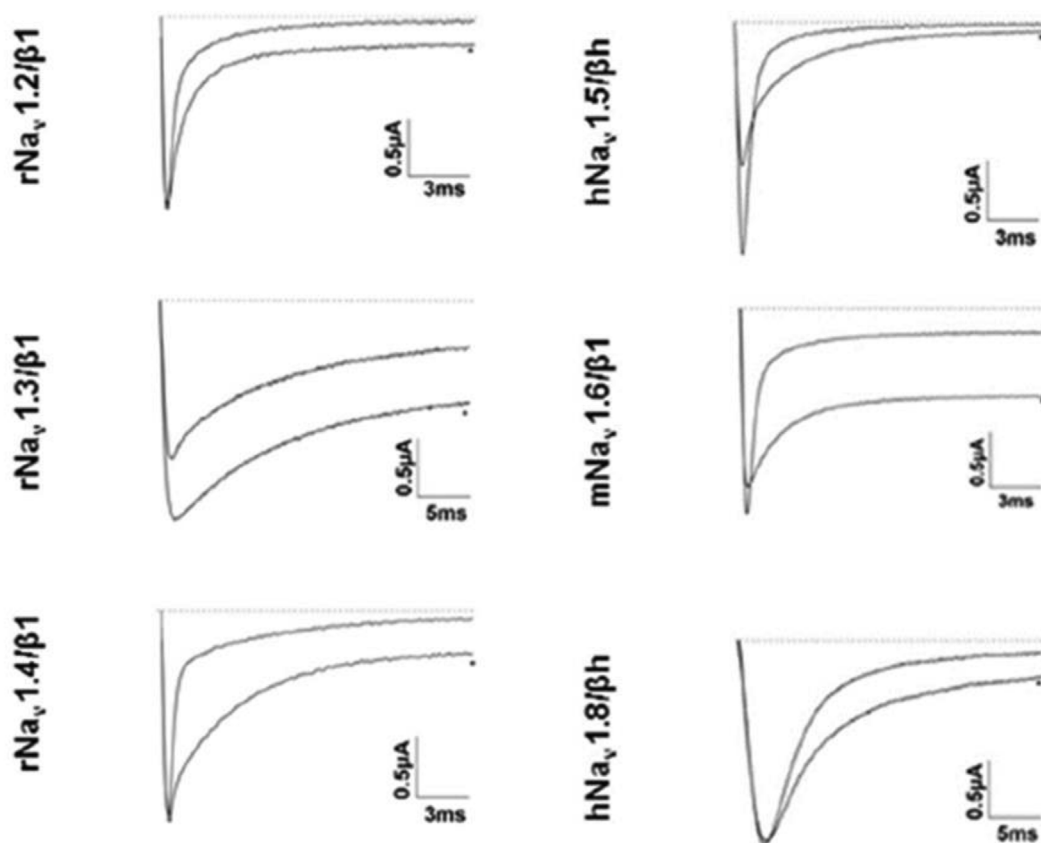


Fig. 6. Representative traces of Nav channel isoforms expressed in *Xenopus* oocytes in control situation and after the application of 3 μ M PnTx2-6. Dotted line indicates zero current level. Asterisk indicates steady state current traces after toxin application. Figure adapted from [Silva et al. \(2015a,b\)](#).

important amenity since this strongly reduces the peptide toxicity and hereby unwanted side effects. Interestingly however, PnPP-19 potentiates penile erection with a similar activity as PnTx2-6 ([Silva et al., 2015a](#)). Therefore, PnPP-19 can be considered as an exciting lead compound for drug development related to the treatment of erectile dysfunction. Moreover, PnPP-19 has also been investigated for its role in both peripheral and central antinociception ([Freitas et al., 2016](#)). It was shown that PnPP-19 inhibits neutral endopeptidase and activates receptors involved in pain pathways such as the cannabinoid receptor 1 and the μ - and δ -opioid receptors ([da Fonseca Pacheco et al., 2016](#); [Freitas et al., 2016](#)). Furthermore, the peripheral antinociceptive effect induced by PnPP-19 is resulting from an activation of the NO-cGMP- K_{ATP} pathway. Hereby, an activation of both endothelial nitric oxide synthase (eNOS) and nNOS by PnPP-19 occurs in rat paw [Freitas et al. \(2017\)](#). PnPP-19 selectively activates μ -opioid receptors inducing indirectly inhibition of calcium channels and hereby impairing calcium influx in dorsal root ganglion (DRG) neurons. Interestingly, notwithstanding the activation of opioid receptors, PnPP-19 does not induce β -arrestin2 recruitment. PnPP-19 is the first spider toxin derivative that, among opioid receptors, selectively activates μ -opioid receptors. The observed lack of β -arrestin2 recruitment highlights the potential of this peptide for the design of new improved opioid agonists ([Freitas et al., 2018](#)). One of the very serious and life-threatening conditions developed following the use of the usual opioid agonist medicines is respiratory paralysis. It has been demonstrated that the induction of respiratory paralysis, as well as other side effects, after the use of opioids may be linked with the recruitment of the β -arrestin pathway, which is stimulated downstream following activation of μ -opioid receptor. Since opioid receptors are still one of the most relevant targets for pain treatment, great effort is being put in the development of new opioid agonists that elicit fewer negative side effects. In this way, the lack of β -

arrestin2 recruitment by PnPP-19 underlines the potential of this peptide as a possible lead compound in the development of improved opioid agonists ([Freitas et al., 2018](#)).

6. PhTx3

Injection in mice of fraction PhTx3 results in a progressive flaccid paralysis of all legs ([Kushmerick et al., 1999](#); [Prado et al., 1996](#); [Rezende et al., 1991](#)). Of all venom fractions, PhTx3 must be the most studied and best characterized fraction. This is a consequence of the pharmacological potential present in this fraction. All of the PhTx3 peptides were found to target voltage-gated calcium (Cav) channels or Kv channels ([Table 1](#)). It is remarkable that up to date only one voltage-gated potassium channel targeting peptide (KSpTx) has been characterized from *Phoneutria* venom while other spiders are known to produce potent and pharmacological interesting KSpTx (Priest et al., 2007; [Swartz, 2007](#)). The genes encoding for all PhTx3 toxins are identified. It was shown that these toxins are encoded as a precursor peptide composed of a signal peptide, an intervening propeptide, and the mature toxin ([Cardoso et al., 2003](#); [Carneiro et al., 2003](#); [Kalapothakis et al., 1998b](#)). Interestingly, certain isoforms identified by molecular cloning have never been purified from the crude venom. However, some of these peptides were functionally expressed in heterologous systems in order to allow functional characterization ([Carneiro et al., 2003](#); [Souza et al., 2008](#)). Many studies have been devoted to the identification of the molecular target of PhTx3. First studies showed that this venom fraction reduces the release of tritiated acetylcholine in the brain indicating a potential target involved in the acetylcholine release in the brain and in the autonomic nervous system. Therefore, the target could be a calcium channel ([de Lima et al., 2016](#); [Gomez et al., 1995](#)). This hypothesis was further supported by the

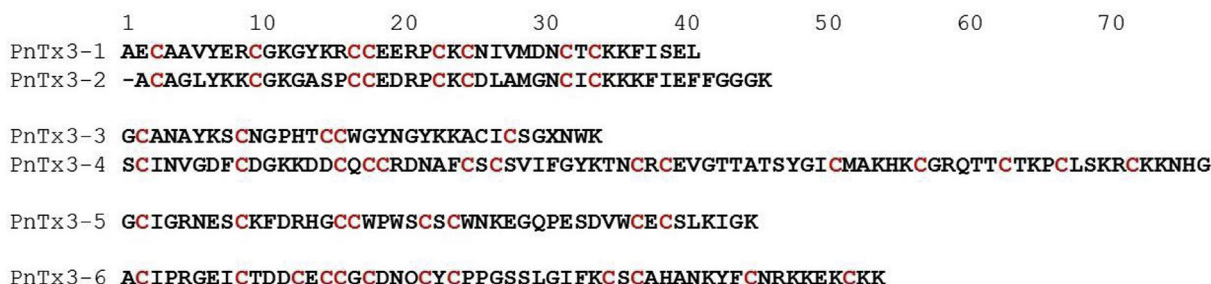


Fig. 7. Sequences of the toxins identified in *Phoneutria nigriventer* venom fraction 3. Cysteines are indicated in red. (For interpretation of the references to colour in this figure legend, the reader is referred to the Web version of this article.)

observation that PhTx3 abolishes calcium-dependent glutamate release in rat brain cortical synaptosomes without influencing the calcium-independent exocytosis. PhTx3 partially inhibited the glutamate release without affecting the glutamate release triggered by intracellular calcium stocks. This hinted towards the presence of toxins in PhTx3 which interfere with the calcium influx in synaptosomes (Prado et al., 1996).

From this fraction six toxins, named PnTx3-1 to PnTx3-6, have been characterized (Fig. 7). PhTx3 is the venom fraction composed of the most heterogeneous group of toxins. The peptides found in PhTx3 share little sequence identity, and therefore, display a wide array of differing pharmacological activities when injected *in vivo*. For example, PnTx3-1, PnTx3-5, and PnTx3-6 induce paralysis of the posterior limbs. PnTx3-2 induces immediate clockwise gyration and flaccid paralysis. PnTx3-3 and PnTx3-4 are the most toxic: at 5 µg/mouse they reproduce the fast flaccid paralysis followed by death observed for the whole PhTx3 fraction (Cordeiro et al., 1993; de Lima et al., 2016). PnTx3-6 also induces analgesia models pain in rodents (Souza et al., 2008).

It was shown that PnTx3-1 increases calcium oscillation in GH3 cells, presumably by blocking potassium currents (Kushmerick et al., 1999). Whole-cell patch clamp experiments showed that PnTx3-1 reversibly and selectively inhibits type-A potassium current (IA) without affecting the delayed or the inward rectifying potassium current. PnTx3-1 has no effect on large conductance calcium sensitive potassium channels. Furthermore, this toxin does not interact with T- and L-type Cav channels. The inhibition of IA favors cell depolarization and Cav channel activation, increasing the frequency of calcium oscillation (Kushmerick et al., 1999). It is important to note that these patch clamp experiments in GH3 cells do not rule out that the observed effects on oscillation frequency are following upon interaction of PnTx3-1 with an unknown target. Further research is required to verify that Tx3-1 is indeed a potassium channel toxin and to determine which potassium channel isoforms this peptide is targeting. In the heart, PnTx3-1 had an anti-arrhythmogenic effect, decreasing the ACh-mediated heart rate by doubling the frequency of spontaneous miniature end plate potential protecting ischemia/reperfusion heart against arrhythmia (Almeida et al., 2011; de Lima et al., 2016). More recently, it was shown that PnTx3-1 causes an antinociception by interfering with the choline esterase activating cholinergic system (Rigo et al., 2017).

PnTx3-2 is characterized as a selective inhibitor of L-type Cav channels (Kalapothakis et al., 1998a). PnTx3-2 does not show affinity for N- or P/Q-type Cav channels since the presence of this toxin did not modify the KCl-evoked glutamate release nor the rise of intracellular calcium in synaptosomes (Prado et al., 1996).

PnTx3-3 is considered as the most potent toxin from the venom fraction PhTx3. Many of the toxic properties of fraction PhTx3 are produced by this toxin (Guatimosim et al., 1997; Prado et al., 1996). PnTx3-3 inhibits P/Q- and R-type Cav channels with high affinity. At higher concentrations, PnTx3-3 also inhibits L- and N-type Cav channels (Leao et al., 2000). Interestingly, PnTx3-3 induces a different profile of behavioral effects compared to the well characterized ω-conotoxin MVIIC which is also an inhibitor of P/Q-type Cav channels.

Ample ω-conotoxins have been identified from cone snail venom (Prashanth et al., 2014). Noteworthy, all studies with PhTx3 peptides acting on Cav channels have used either GVIA or MVIIC ω-conotoxins to compare the analgesic activity. A more recent study investigated the effects of PnTx3-3 on sensory transmission in the spinal cord of rats (Dalmolin et al., 2017). Using *in vivo* electrophysiological recordings, it was shown that PnTx3-3 exerts a prevalent antinociceptive effect mainly by inhibiting R-type Cav channels (Dalmolin et al., 2017).

PnTx3-4 affects the neurotransmission by blocking presynaptic calcium channels associated with exocytosis in mammals, lower vertebrates and arthropods (de Lima et al., 2016; Troncone et al., 2003). PnTx3-4 potentially inhibits high-voltage-activated Cav channels in the sensory neurons of dorsal root. No activity was observed on low-voltage-activated Cav channels (Cassola et al., 1998). Moreover, PnTx3-4 is suggested to act on P/Q-type Cav channels (Miranda et al., 2001). Using heterologous expressed channels in HEK293 cells, it was shown that PnTx3-4 produced a potent and almost irreversible inhibition of P/Q-type Cav2.1 channels and N-type Cav2.2. Only a partial and reversible inhibition of R-type Cav2.3 channels was observed (Dos Santos et al., 2002). Furthermore, this toxin blocked potassium-induced and capsaicin-induced glutamate release from rat brain synaptosomes (Goncaves et al., 2011; Reis et al., 1999). Incubation of synaptosomes with PnTx3-4 in the presence of the calcium chelator EGTA blocked calcium-independent glutamate release, contrasting with the observation that the fraction PhTx3 did not inhibit calcium-independent components of glutamate release (de Lima et al., 2016). This seemingly contradiction could be explained by the low amount of PnTx3-4 present in the venom fraction PhTx3 (de Lima et al., 2016). The fraction PhTx3 exhibits a strong neuroprotective effect against neuronal damage induced by oxygen deprivation and low glucose (ODLG) insults on hippocampal slices (Pinheiro et al., 2006). In an *in vitro* model of retinal ischemia induced by ODLG, the fraction PhTx3 protected approximately 80% of the cells from injury (Agostini et al., 2011). PnTx3-3 and PnTx3-4 were identified as the peptides responsible for this neuroprotective effect. Both toxins were effective in preventing cell death after ischemic injury. It has been shown that ischemic injury induced by ODLG insults in retinal slices leads to increased levels of glutamate. These increased concentrations of glutamate cause retinal cell death. PnTx3-3 and PnTx3-4 exert their neuroprotective effect by indirectly inhibiting the glutamate increase through the inhibition of N and P/Q type Cav channels. PnTx3-4 showed superior protection when compared to PnTx3-3, the fraction PhTx3, or the Cav channel inhibiting cone snail toxins ω-conotoxin GVIA and ω-conotoxin MVIIC (Agostini et al., 2011; Binda et al., 2016; Pinheiro et al., 2009). A similar neuroprotective activity was observed for both toxins in an *in vitro* model of brain ischemia. By using electrophysiology and the glutamate release assay in hippocampal slices, it was observed that both PnTx3-3 and PnTx3-4 blocked the glutamate release (Pinheiro et al., 2009). Furthermore, the neuroprotective effect of PnTx3-4 was also evidenced *in vivo* using a rat model of NMDA-induced injury of the retina (Binda et al., 2016). These results underline the role of PnTx3-4 as a novel

	1	10	20	30	40
PnTx4-3	C GDINA A CKED CD CCGYTT AC DCY W SS SCK CREAA I VI Y TAP KK KL T C				
PnTx4 (5-5)	C AD I NG A CKSD CD CCGDS V TCDCY W SD SCK CRE S N F K I GM A IR K KF - C				
PnTx4 (6-1)	C GDINA A CKED CD CCGYTT AC DCY W SK SCK CREAA I VI Y TAP KK KL T C				

Fig. 8. Sequences of the toxins identified in *Phoneutria nigriventer* venom fraction 4. Cysteines are indicated in red. (For interpretation of the references to colour in this figure legend, the reader is referred to the Web version of this article.)

potential tool to study or treat retinal injury. It is remarkable to note that the complete, correct sequence for PnTx3-4 matching the mass of the native toxin has still not been published despite the growing number of studies using this toxin (Herzig, 2016). As can be seen in Table 1, several PnTx3-4 isoforms have been reported.

The least studied toxin of the venom fraction PhTx3 is the toxin PnTx3-5. However, this peptide is known to potently block L-type Cav channels (Leao et al., 2000). PnTx3-5 demonstrated promising antinociceptive activity in clinically relevant pain models of postoperative, neuropathic and cancer-related pain (Oliveira et al., 2016). Interesting to note is that PnTx3-5 also displayed efficacy in opioid tolerant animals. Indeed, the clinical applicability potential of L-type, as well as N-type, Cav channel inhibitors such as PnTx3-5, can be found in their apparent synergism with morphine. Although the exact mechanism is still under investigation, it is suggested that long-term use of morphine results in an increased expression of L- and N-type Cav channels (Verma et al., 2009). Therefore, inhibitors of L-type Cav channels can induce analgesia but also potentiate the morphine-induced analgesia. This could significantly reduce the consumption of morphine in patients with chronic pain (Oliveira et al., 2016).

The toxin PnTx3-6 (also known as Phc1b) binds to a broad range of high-voltage-activated Cav channels. It inhibits N-, R- and P/Q-type Cav channels with a comparable affinity. At higher concentrations, this toxin also blocks L-type Cav channels. However, PnTx3-6 has no activity on T-type Cav channels (Vieira et al., 2005). More recent, it was discovered that the analgesic activity of PnTx3-6 results, besides of the inhibition of Cav channels, from the interaction with TRPA1 receptors. PnTx3-6 is a potent TRPA1 antagonist while having no affinity for TRPV1 or TRPV4 receptors (Tonello et al., 2017). To overcome scarceness of the native PnTx3-6, a recombinant form of the peptide has been produced. This recombinant peptide, annotated CTK 01512-2, showed similar activity as the native PnTx3-6 (Tonello et al., 2017). PnTx3-6 inhibited potassium-induced calcium-dependent glutamate release by blocking voltage-gated calcium channels, but it was not able to modify the calcium-independent process (de Lima et al., 2016). PnTx3-6 has been investigated for its analgesic proprieties. Using both native and recombinant peptide, it was shown that PnTx3-6 was efficient for the treatment of persistent pathological pain mediated by either glutamate release or capsaicin-induced calcium influx, but not involving capsaicin receptor inhibition (Castro-Junior et al., 2013; Souza et al., 2008). The therapeutic potential of PnTx3-6 was evidenced by the observation that in preclinical models of chronic neuropathic pain, this toxin has a similar efficacy but a higher therapeutic index than the clinically used ziconotide (McGivern, 2007; Tonello et al., 2014). PnTx3-6 was effective in potentiating the analgesic effect of morphine in mice. Furthermore, the same study showed that this peptide reduced the hyperalgesia, tolerance, constipation and withdrawal syndrome induced by repeated morphine injection (Tonello et al., 2014). Similar, PnTx3-6 also potentiates the analgesic action of TRPV1 blockers, underlining the potential of Cav channel inhibitors as adjuvant analgesic agents (Palhares et al., 2017). Because of its action on N- and P/Q-type Cav channels, PnTx3-6 has also been used as a tool to study the involvement of these channels in bladder dysfunctions such as cystitis (Silva et al., 2015b). It should be noted that Cav channel inhibitors, such as the PnTx3 toxins, have not only a potential in antinociception. Because of the relevance of Cav channels in tumor progression, these peptides could also be useful in cancer related studies (Nicoletti et al., 2017).

7. PhTx4

PhTx4 is historically referred to as the insecticidal fraction. It earned this reference based on its high toxicity and lethality toward insects while displaying a minor toxicity when injected in mice. This fraction causes hyperactivity such as cramps, quivering, jerking of the limbs, and violent trembling of the body and the legs, leading to muscle fatigue and therefore causing paralysis in insects (de Lima et al., 2016; Figueiredo et al., 1995). It is suggested that PhTx4 acts on the glutamatergic system of both insects and mammals. Three toxins have been characterized from the venom fraction PhTx4 (Fig. 8 and Table 1). They were named PnTx4 (6-1), PnTx4 (5-5), and PnTx4 (4-3) (de Figueiredo et al., 2001; Figueiredo et al., 1995; Oliveira et al., 2003). These 3 insecticidal toxins share high sequence identity and as such are believed to exhibit similar pharmacological properties.

PnTx4 (4-3) is not very well studied compared to the other toxins in this venom fraction. However, this toxin induces excitatory effects when injected in houseflies and cockroaches. Furthermore, it inhibits the glutamate uptake in rat brain synaptosomes (Oliveira et al., 2003).

PnTx4 (6-1) and PnTx4 (5-5) act on insect sodium channels (de Lima et al., 2007; de Lima et al., 2002). Despite their apparent lack of toxicity to mammals, they have been shown to inhibit glutamate uptake in the mammalian central nervous system and to modulate the inactivation process of mammalian Nav channels (Mafra et al., 1999; Oliveira et al., 2003; Paiva et al., 2016). It was evidenced that PnTx4 (5-5) is a reversible antagonist of NMDA ionotropic glutamate receptor in rat brain neurons (de Figueiredo et al., 2001). Since inhibition of NMDA receptors has been proposed as a therapeutic mechanism of neuroprotection, PnTx4 (5-5) has been investigated for its potential to promote neuronal survival by blocking NMDA receptors. Nevertheless, more research is required to determine the NMDA receptor subtype selectivity of PnTx4 (5-5) (Silva et al., 2016). The activity of PnTx4 (5-5) on insect and mammalian Nav channels was characterized in depth (Paiva et al., 2016). The subtype selectivity among mammalian Nav channels was determined using the *Xenopus* oocyte expression system and recombinant produced PnTx4 (5-5). Among mammalian Nav channels, the toxin caused a delay in the channel inactivation and a reduction of the sodium peak current. This reduction in peak current is the result of a toxin induced shift of the channel activation towards more depolarized membrane potentials. PnTx4 (5-5) has the most pronounced effect on insect Nav channels. Using the cockroach Nav channel BgNav1, it was illustrated that PnTx4 (5-5) has a devastating modulatory effect on these channels (Fig. 9). Upon binding, this toxin causes a complete inhibition of the inactivation of the channel and an increase of the sodium peak amplitude. However, contrary to what was observed for mammalian Nav channels, no shift in the midpoint of activation was noted for insect Nav channels (Fig. 9) (Paiva et al., 2016).

The most active toxin of this fraction is the anti-insect neurotoxin PnTx4 (6-1). A detailed mode of action of PnTx4 (6-1) and PnTx4 (5-5) has been acquired with the double-oil-gap method using axonal preparations of the cockroach *Periplaneta americana* (de Lima et al., 2002). Both toxins induced evoked action potential prolongation in axonal preparations. This effect was stronger after PnTx4 (6-1) administration than after PnTx4 (5-5). Tests performed in a voltage-clamp configuration showed that both PnTx4 (6-1) and PnTx4 (5-5) prolonged the axonal sodium current in a manner similar to toxins binding to neurotoxin site 3 of Nav channels. Similar tests in *Xenopus* oocytes indicated that PnTx4 (6-1) has no effect on Nav1.2 and Nav1.4 channels (de Lima

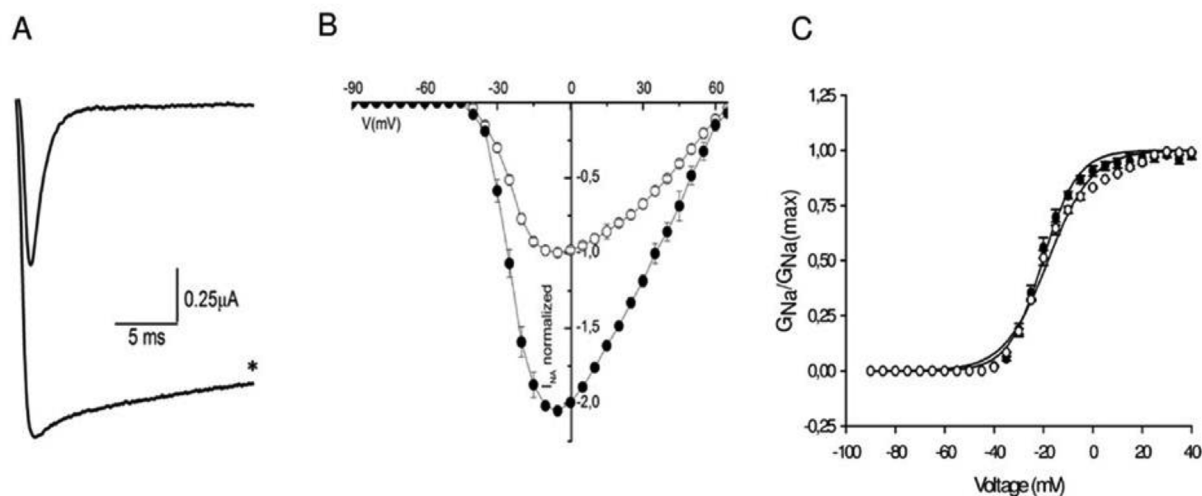


Fig. 9. Effects of PnTx4 (5-5) on the cockroach *B. germanica* sodium channel (BgNav1) expressed in *X. leavis* oocytes. A) Representative whole-cell current traces in control and in presence of 1 μM rPnTx4 (5-5) (*). B) Current–voltage ($I \times V$) relationships in control (○) and in presence of 1 μM rPnTx4 (5-5) (●). C) Activation of the conductance in control (○) and in presence of 1 μM rPnTx4 (5-5) (●), fitted with the Boltzmann equation. Figure adapted from Paiva et al. (2016).

et al., 2016; de Lima et al., 2002).

However, in DUM cells, PnTx4 (6-1) changed the regular spontaneous firing pattern of action potential generation into an irregular activity, evidencing its activity on insect Nav channels. The results obtained with electrophysiological experiments suggested that PnTx4 (6-1) is most likely binding to the neurotoxin binding site 3 of Nav channels. This was later on confirmed with binding assays using Bom IV, an α -like scorpion toxin that binds to receptor site 3 on insect sodium channels. Bom IV was displaced by PnTx4 (6-1) (Figueiredo et al., 1995). More recently, it was found that PnTx4 (6-1) induces antinociception in inflammatory, neuropathic and acute pain models in rats. It is suggested that this antinociceptive effect involves the cannabinoid system, through cannabinoid receptor 1, and the opioid system, through the μ - and δ -opioid subtype receptors (Emerich et al., 2016).

8. PhTx5

The fifth *Phoneutria* venom fraction is also known as fraction PhM (Fig. 2, Table 2). An improved purification method of *P. nigriventer* venom combined with mass spectrometry analysis contributed for the identification of the fraction PhM (Pimenta et al., 2005; Richardson et al., 2006). This fraction was characterized for its activity on smooth muscle. However, the previous described purification method did not allow identification of these peptides because of their low levels in the whole venom and because their N-termini were somehow blocked which prevented sequencing by Edman degradation. It is also probable that some of these small molecules do not represent mature peptides, but are result of precursor processing and/or degradation of mature toxins (Pimenta et al., 2005). PhM consists of a pool of similar isoforms of smaller (< 2 kDa) peptides. The amino acid sequences of 15 of these isoforms (Fig. 10) were determined by mass spectrometry (Pimenta et al., 2005). These muscle-active peptides contain 7–14 amino acid residues and have a common scaffold composed of basic and acid amino acids (PyrKKDKKDX), where x can be either K or R. Since all of these molecules are structurally related to the tachykinin family of neurohormone peptides, which possess N-terminal pyroglutamate residues, they were named *Phoneutria nigriventer* tachykinin peptides PnTkPs (Pimenta et al., 2005). The PnTkPs display a variation of post-translational modifications such as proteolysis, C-terminal amidation, and cyclization (Pimenta et al., 2005). The new procedure also resulted in the discovery of two new structural families of *Phoneutria* peptides (Penaforte et al., 2000; Richardson et al., 2006). The family of 4 kDa

	1	10
PnTkP-I	Q	K
PnTkP-II	Q	K
PnTkP-III	Q	K
PnTkP-IV	Q	K
PnTkP-V	Q	K
PnTkP-VI	Q	K
PnTkP-VII	Q	K
PnTkP-VIII	Q	K
PnTkP-IX	Q	K
PnTkP-X	Q	K
PnTkP-XI	Q	K
PnTkP-XII	Q	K
PnTkP-XIII	Q	K
PnTkP-XIV	Q	K
PnTkP-XV	Q	K

Fig. 10. Amino acid sequences of the tachykinin family identified in the *Phoneutria nigriventer* venom.

toxins targets Cav channels (Lucio et al., 2008). Two different isoforms PnTx27C4 and PnTx26AN0C3 were isolated and characterized. Both peptides share 92% sequence identity. These toxins produce spastic paralysis and death in mice when injected intracerebral. Three very similar peptides, PnTx13C3, PnTx24An0C3 and PnTx24An0C4, were identified in this fraction. These peptides share 79% amino acid sequence identity. Similar to the PhTx4 toxins, these 3.5 kDa toxins are very toxic to houseflies and induce no observable toxic effects in mice by i.c. injection (Richardson et al., 2006).

Two proteases could be identified in the *Phoneutria nigriventer* venom. They were named proteinase PN44 and proteinase PN47. The complete amino acid sequence of the PN47 and the N-terminal sequence of have been determined. Both proteases are serine proteases

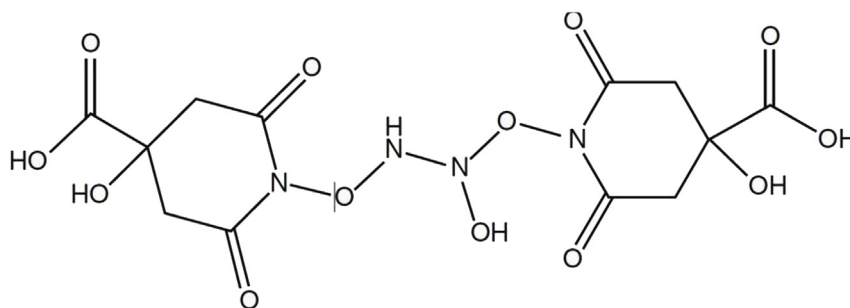


Fig. 11. Proposed structure of nigriventrine (Gomes et al., 2011).

belonging to the peptidase S1 family. It has been suggested that the endogenous proteolytic enzymes in the venom may be responsible for the post-translational modification observed in some of the venom components (de Lima et al., 2016).

9. Non-protein *P. nigriventer* venom components

In addition, a novel non-protein low-molecular-mass neurotoxin named nigriventrine was isolated from the hydrophilic fractions obtained from the venom by RP-HPLC purifications (Gomes et al., 2011). Nigriventrine, a piperidine derivative, has neuroactive properties and causes convulsion when injected in mice, intracerebrally or peripherally by intravenous injection (i.v.). Its structure was determined and it was characterized as a hydroxyl-hydrazydioxipiperidine (Fig. 11) (Gomes et al., 2011).

10. Conclusion and future directions

It is estimated that venom of *P. nigriventer* is complex cocktail of more than 150 peptides/protein components (Richardson et al., 2006). Considering that only about 41 toxins were pharmacologically and/or chemically characterized so far, a wide diversity of new molecules, with possible different biological targets and activities, remains to be discovered in this venom. The studies conducted with *P. nigriventer* venom revealed several toxins acting on sodium, calcium, and TRPA channels, while other showed interesting activity on NMDA, cannabinoid or opioid receptors. Some of them have shown biotechnological and therapeutic potential, for example, by enhancing erectile function, acting as analgesics or insecticides. Although much of the richness and diversity of active peptides of *Phoneutria nigriventer* venom has been revealed many more remains to be discovered. For instance, a comprehensive transcriptomic study of this spider would greatly complement the proteomic work done so far. Furthermore, since at present not a single structure of a *Phoneutria* venom peptide has been elucidated many structural questions remain unanswered. Determination of the structures is a requisite for careful designed mutagenesis studies. Therefore, further exploration of the characterized *Phoneutria* toxins necessitate advancing on the structural knowledge of these peptides. It is interesting that up to now, the venom of *Phoneutria nigriventer* has been intensively investigated for drug discovery but only few studies have focussed on the insecticidal properties of the venom components. It can be anticipated that also within the venom of *Phoneutria nigriventer* peptides can be found with a potential as lead for the development of novel insecticidal agents. It is clear that the complex biochemical and pharmacological diversity of this venom has not yet been unravelled to the fullest and thus it can be expected in the years to come that many new peptides will be characterized as promising pharmacological tools, as lead compounds for drug development and as novel insecticidal agents.

Acknowledgements

M.E. de Lima received grants from Brazilian Agencies FAPEMIG (Fundação de Amparo à Pesquisa do Estado de Minas Gerais), CAPES (Coordenação de Aperfeiçoamento de Pessoal de Nível Superior) and CNPq (Conselho Nacional de Desenvolvimento Científico e Tecnológico).

Transparency document

Transparency document related to this article can be found online at <https://doi.org/10.1016/j.toxicon.2018.07.008>.

References


- Agostini, R.M., do Nascimento Pinheiro, A.C., Binda, N.S., Romano Silva, M.A., do Nascimento Cordeiro, M., Richardson, M., Sena Guimaraes, A.L., Gomez, M.V., 2011. *Phoneutria* spider toxins block ischemia-induced glutamate release and neuronal death of cell layers of the retina. *Retina* 31 (7), 1392–1399 (Philadelphia, Pa.).
- Almeida, A.P., Andrade, A.B., Ferreira, A.J., Pires, A.C.G., Damasceno, D.D., Alves, M.N.M., Gomes, E.R.M., Kushmerick, C., Lima, R.F., Prado, M.A.M., Prado, V.F., Richardson, M., Cordeiro, M.N., Guatimosim, S., Gomez, M., 2011. Antiarrhythmic effects of a neurotoxin from the spider *Phoneutria nigriventer*. *Toxicon* 57 (2), 217–224.
- Araujo, D.A., Cordeiro, M.N., Diniz, C.R., Beirao, P.S., 1993. Effects of a toxic fraction, PhTx2, from the spider *Phoneutria nigriventer* on the sodium current. *N. Schmied. Arch. Pharmacol.* 347 (2), 205–208.
- Becker, S., Prusak-Sochaczewski, E., Zamponi, G., Beck-Sickinger, A.G., Gordon, R.D., French, R.J., 1992. Action of derivatives of μ -conotoxin GIIIA on sodium channels. Single amino acid substitutions in the toxin separately affect association and dissociation rates. *Biochemistry* 31 (35), 8229–8238.
- Binda, N.S., Carayon, C.P.P., Agostini, R.M., Pinheiro, A.C.N., Cordeiro, M.N., Silva, M.A.R., Silva, J.F., Pereira, E.M.R., da Silva Junior, C.A., de Castro Junior, C.J., Guimaraes, A.L.S., Gomez, M.V., 2016. PhTx3-4, a spider toxin calcium channel blocker, reduces NMDA-induced injury of the retina. *Toxins* 8 (3).
- Bucarechi, F., Mello, S.M., Vieira, R.J., Mamoni, R.L., Blotta, M.H.S.L., Antunes, E., Hyslop, S., 2008. Systemic envenomation caused by the wandering spider *Phoneutria nigriventer*, with quantification of circulating venom. *Clin. Toxicol.* 46 (9), 885–889.
- Bucherl, W., 1953. Comparison of the action of gland extracts and pure venom of *Phoneutria nigriventer* Keyserling 1891. *Mem. Inst. Butantan (Sao Paulo)* 25 (2), 1–21.
- Bucherl, W., 1969. Biology and venoms of the most important South American spiders of the genera *Phoneutria*, *Loxosceles*, *Lycosa*, and *Latrodectus*. *Am. Zool.* 9 (1), 157–159.
- Cardoso, F.C., Lewis, R.J., 2018 Jun. Sodium channels and pain: from toxins to therapies. *Br. J. Pharmacol.* 175 (12), 2138–2157.
- Cardoso, F.C., Pacifico, L.G., Carvalho, D.C., Victoria, J.M.N., Neves, A.L.G., Chavez-Olortegui, C., Gomez, M.V., Kalapothakis, E., 2003. Molecular cloning and characterization of *Phoneutria nigriventer* toxins active on calcium channels. *Toxicon* 41 (7), 755–763.
- Carneiro, A.M.D., Kushmerick, C., Koenen, J., Arndt, M.H.L., Cordeiro, M.N., Chavez-Olortegui, C., Diniz, C.R., Gomez, M.V., Kalapothakis, E., Prado, M.A.M., Prado, V.F., 2003. Expression of a functional recombinant *Phoneutria nigriventer* toxin active on Ca^{2+} channels. *Toxicon* 41 (3), 305–313.
- Cassola, A.C., Jaffe, H., Fales, H.M., Afeche, S.C., Magnoli, F., Cipolla-Neto, J., 1998. omega-Phonotoxin-IIA: a calcium channel blocker from the spider *Phoneutria nigriventer*. *Pflueg. Arch. Eur. J. Physiol.* 436 (4), 545–552.
- Castro-Junior, C.J., Milano, J., Souza, A.H., Silva, J.F., Rigo, F.K., Dalmolin, G., Cordeiro, M.N., Richardson, M., Barros, A.G.A., Gomez, R.S., Silva, M.A.R., Kushmerick, C., Ferreira, J., Gomez, M.V., 2013. Phalpa1beta toxin prevents capsaicin-induced nociceptive behavior and mechanical hypersensitivity without acting on TRPV1 channels. *Neuropharmacology* 71, 237–246.
- Catterall, W.A., Cestele, S., Yarov-Yarovoy, V., Yu, F.H., Konoki, K., Scheuer, T., 2007. Voltage-gated ion channels and gating modifier toxins. *Toxicon* 49 (2), 124–141.
- Chassagnon, I.R., McCarthy, C.A., Chin, Y.K., Pineda, S.S., Keramidis, A., Mobli, M., Pham, V., De Silva, T.M., Lynch, J.W., Widdop, R.E., Rash, L.D., King, G.F., 2017. Potent neuroprotection after stroke afforded by a double-knot spider-venom peptide that inhibits acid-sensing ion channel 1a. *Proc. Natl. Acad. Sci. U. S. A.* 114 (14),

- 3750–3755.
- Cordeiro, MdN., de Figueiredo, S.G., Valentim, AdC., Diniz, C.R., von Eickstedt, V.R., Gilroy, J., Richardson, M., 1993. Purification and amino acid sequences of six Tx3 type neurotoxins from the venom of the Brazilian 'armed' spider *Phoneutria nigriventer* (Keys). *Toxicol* 31 (1), 35–42.
- Cordeiro, MdN., Diniz, C.R., Valentim, AdC., von Eickstedt, V.R., Gilroy, J., Richardson, M., 1992. The purification and amino acid sequences of four Tx2 neurotoxins from the venom of the Brazilian 'armed' spider *Phoneutria nigriventer* (Keys). *FEBS Lett.* 310 (2), 153–156.
- Cruz-Hofling, M.A., Tavares, J.C., Rapôso, C., 2016. *Phoneutria nigriventer* venom: action in the central nervous system. In: Gopalakrishnakone, P. (Ed.), *Spider Venoms*, *Toxinology*. Springer, pp. 176–197.
- da Fonseca Pacheco, D., Freitas, A.C.N., Pimenta, A.M.C., Duarte, I.D.G., de Lima, M.E., 2016. A spider derived peptide, PnPP-19, induces central antinociception mediated by opioid and cannabinoid systems. *J. Venom. Anim. Toxins Incl. Trop. Dis.* 22, 34.
- Dalmolin, G.D., Bannister, K., Goncalves, L., Sikandar, S., Patel, R., Cordeiro, MdN., Gomez, M.V., Ferreira, J., Dickenson, A.H., 2017. Effect of the spider toxin Tx3-3 on spinal processing of sensory information in naive and neuropathic rats: an in vivo electrophysiological study. *Pain Rep.* 2 (4), e610.
- de Figueiredo, S.G., de Lima, M.E., Nascimento Cordeiro, M., Diniz, C.R., Patten, D., Halliwell, R.F., Gilroy, J., Richardson, M., 2001. Purification and amino acid sequence of a highly insecticidal toxin from the venom of the Brazilian spider *Phoneutria nigriventer* which inhibits NMDA-evoked currents in rat hippocampal neurons. *Toxicol* 39 (2–3), 309–317.
- De Lima, M.E., Figueiredo, S.G., Pimenta, A.M.C., Santos, D.M., Borges, M.H., Cordeiro, M.N., Richardson, M., Oliveira, L.C., Stankiewicz, M., Pelhate, M., 2007. Peptides of arachnid venoms with insecticidal activity targeting sodium channels. *Comparat. Biochem. Physiol. Toxicol. Pharmacol.* 146 (1–2), 264–279.
- de Lima, M.E., Figueiredo, S.G., Matavel, A., Nunes, K.P., da Silva, C.N., Almeida, F.M., Diniz, M.R.V., Cordeiro, M.N., Stankiewicz, M., Beirao, P.S., 2016. *Phoneutria nigriventer* venom and toxins: a review. In: Gopalakrishnakone, P. (Ed.), *Spider Venoms*, *Toxinology*. Springer, pp. 71–99.
- de Lima, M.E., Stankiewicz, M., Hamon, A., de Figueiredo, S.G., Cordeiro, M.N., Diniz, C.R., Martin-Eauclaire, M.F., Pelhate, M., 2002. The toxin Tx4(6-1) from the spider *Phoneutria nigriventer* slows down Na⁺ current inactivation in insect CNS via binding to receptor site 3. *J. Insect Physiol.* 48 (1), 53–61.
- Deuis, J.R., Mueller, A., Israel, M.R., Vetter, I., 2017. The pharmacology of voltage-gated sodium channel activators. *Neuropharmacology* 127, 87–108.
- Diniz, C., 1963. Separation of proteins and characterization of active substances in the venom of the Brazilian spiders. *An. Acad. Bras. Cienc.* 35, 283–291.
- Diniz, C.R., Cordeiro, MdN., Junior, L.R., Kelly, P., Fischer, S., Reimann, F., Oliveira, E.B., Richardson, M., 1990. The purification and amino acid sequence of the lethal neurotoxin Tx1 from the venom of the Brazilian 'armed' spider *Phoneutria nigriventer*. *FEBS Lett.* 263 (2), 251–253.
- Diniz, M.R., Paine, M.J., Diniz, C.R., Theakston, R.D., Crampton, J.M., 1993. Sequence of the cDNA coding for the lethal neurotoxin Tx1 from the Brazilian "armed" spider *Phoneutria nigriventer* predicts the synthesis and processing of a preprotoxin. *J. Biol. Chem.* 268 (21), 15340–15342.
- Diniz, M.R.V., Theakston, R.D.G., Crampton, J.M., Nascimento Cordeiro, Md, Pimenta, A.M.C., De Lima, M.E., Diniz, C.R., 2006. Functional expression and purification of recombinant Tx1, a sodium channel blocker neurotoxin from the venom of the Brazilian "armed" spider, *Phoneutria nigriventer*. *Protein Expr. Purif.* 50 (1), 18–24.
- Dos Santos, R.G., Van Renterghem, C., Martin-Moutot, N., Mansuelle, P., Cordeiro, M.N., Diniz, C.R., Mori, Y., De Lima, M.E., Seagar, M., 2002. *Phoneutria nigriventer* omega-phosphotoxin IIA blocks the Cav2 family of calcium channels and interacts with omega-conotoxin-binding sites. *J. Biol. Chem.* 277 (16), 13856–13862.
- Emerich, B.L., Ferreira, R.C.M., Cordeiro, M.N., Borges, M.H., Pimenta, A.M.C., Figueiredo, S.G., Duarte, I.D.G., de Lima, M.E., 2016. δ -Ctenitoxin-Pn1a, a peptide from *Phoneutria nigriventer* spider venom, shows antinociceptive effect involving opioid and cannabinoid systems, in rats. *Toxins* 8 (4).
- Escoubas, P., 2006. Molecular diversification in spider venoms: a web of combinatorial peptide libraries. *Mol. Divers.* 10 (4), 545–554.
- Figueiredo, S.G., Garcia, M.E., Valentim, A.C., Cordeiro, M.N., Diniz, C.R., Richardson, M., 1995. Purification and amino acid sequence of the insecticidal neurotoxin Tx4(6-1) from the venom of the 'armed' spider *Phoneutria nigriventer* (Keys). *Toxicol* 33 (1), 83–93.
- Fitches, E.C., Pyati, P., King, G.F., Gatehouse, J.A., 2012. Fusion to snowdrop lectin magnifies the oral activity of insecticidal omega-Hexatoxin-Hv1a peptide by enabling its delivery to the central nervous system. *PLoS One* 7 (6), e39389.
- Freitas, A.C.N., Pacheco, D.F., Machado, M.F.M., Carmona, A.K., Duarte, I.D.G., de Lima, M.E., 2016. PnPP-19, a spider toxin peptide, induces peripheral antinociception through opioid and cannabinoid receptors and inhibition of neutral endopeptidase. *Br. J. Pharmacol.* 173 (9), 1491–1501.
- Freitas, A.C.N., Peigneur, S., Macedo, F.H.P., Menezes-Filho, J.E., Millns, P., Medeiros, L.F., Arruda, M.A., Cruz, J., Holliday, N.D., Tytgat, J., Hathway, G., de Lima, M.E., 2018. The peptide PnPP-19, a spider toxin derivative, activates μ -opioid receptors and modulates calcium channels. *Toxins* 10 (1).
- Freitas, A.C., Silva, G.C., Pacheco, D.F., Pimenta, A.M., Lemos, V.S., Duarte, I.D., de Lima, M.E., 2017 Apr 1. The synthetic peptide PnPP-19 induces peripheral antinociception via activation of NO/cGMP/KATP pathway: role of eNOS and nNOS. *Nitric Oxide* 64, 31–38.
- French, R.J., Yoshikami, D., Sheets, M.F., Olivera, B.M., 2010. The tetrodotoxin receptor of voltage-gated sodium channels—perspectives from interactions with micro-conotoxins. *Mar. Drugs* 8 (7), 2153–2161.
- Gomes, P.C., de Souza, B.M., Dias, N.B., Cesar-Tognoli, L.M.M., Silva, L.C., Tormena, C.F., Rittner, R., Richardson, M., Cordeiro, M.N., Palma, M.S., 2011. Nigriventrine: a low molecular mass neuroactive compound from the venom of the spider *Phoneutria nigriventer*. *Toxicol* 57 (2), 266–274.
- Gomez, M.V., Kalapothakis, E., Guatimosim, C., Prado, M.A.M., 2002. *Phoneutria nigriventer* venom: a cocktail of toxins that affect ion channels. *Cell. Mol. Neurobiol.* 22 (5–6), 579–588.
- Gomez, R.S., Casali, T.A., Romano-Silva, M.A., Cordeiro, M.N., Diniz, C.R., Moraes-Santos, T., Prado, M.A., Gomez, M.V., 1995. The effect of PhTx3 on the release of 3H-acetylcholine induced by tityustoxin and potassium in brain cortical slices and myenteric plexus. *Neurosci. Lett.* 196 (1–2), 131–133.
- Goncaves, J.M., Ferreira, J., Prado, M.A.M., Cordeiro, M.N., Richardson, M., Pinheiro, A.CdN., Silva, M.A.R., Junior, C.JdC., Souza, A.H., Gomez, M.V., 2011. The effect of spider toxin PhTx3-4, omega-conotoxins MVIIA and MVIII on glutamate uptake and on capsaicin-induced glutamate release and [Ca²⁺]_i in spinal cord synaptosomes. *Cell. Mol. Neurobiol.* 31 (2), 277–283.
- Green, B.R., Bulaj, G., Norton, R.S., 2014. Structure and function of mu-conotoxins, peptide-based sodium channel blockers with analgesic activity. *Future Med. Chem.* 6 (15), 1677–1698.
- Green, B.R., Olivera, B.M., 2016. Venom peptides from cone snails: pharmacological probes for voltage-gated sodium channels. *Curr. Top. Membr.* 78, 65–86.
- Guatimosim, C., Romano-Silva, M.A., Cruz, J.S., Beirao, P.S., Kalapothakis, E., Moraes-Santos, T., Cordeiro, M.N., Diniz, C.R., Gomez, M.V., Prado, M.A., 1997. A toxin from the spider *Phoneutria nigriventer* that blocks calcium channels coupled to exocytosis. *Br. J. Pharmacol.* 122 (3), 591–597.
- Hauke, T.J., Herzig, V., 2017. Dangerous arachnids-Fake news or reality? *Toxicol* 138, 173–183.
- Herzig, V., 2016. Create guidelines for characterization of venom peptides. *Toxins* 8 (9).
- Herzig, V., John Ward, R., Ferreira dos Santos, W., 2002. Intersexual variations in the venom of the Brazilian 'armed' spider *Phoneutria nigriventer* (Keyserling, 1891). *Toxicol* 40 (10), 1399–1406.
- Herzig, V., King, G.F., 2015. The cystine knot is responsible for the exceptional stability of the insecticidal spider toxin omega-hexatoxin-hv1a. *Toxins* 7 (10), 4366–4380.
- Herzig, V., Wood, D.L., Newell, F., Chamma, P.A., Kaas, Q., Binford, G.J., Nicholson, G.M., Gorse, D., King, G.F., 2011. ArachnoServer 2.0, an updated online resource for spider toxin sequences and structures. *Nucleic Acids Res.* 39 (Database issue), D653–D657.
- Israel, M.R., Tay, B., Deuis, J.R., Vetter, I., 2017. Sodium channels and venom peptide pharmacology. *Adv. Pharmacol.* 79, 67–116.
- Kalapothakis, E., Penaforte, C.L., Beirao, P.S., Romano-Silva, M.A., Cruz, J.S., Prado, M.A., Guimaraes, P.E., Gomez, M.V., Prado, V.F., 1998a. Cloning of cDNAs encoding neurotoxic peptides from the spider *Phoneutria nigriventer*. *Toxicol* 36 (12), 1843–1850.
- Kalapothakis, E., Penaforte, C.L., Leao, R.M., Cruz, J.S., Prado, V.F., Cordeiro, M.N., Diniz, C.R., Romano-Silva, M.A., Prado, M.A., Gomez, M.V., Beirao, P.S., 1998b. Cloning, cDNA sequence analysis and patch clamp studies of a toxin from the venom of the armed spider (*Phoneutria nigriventer*). *Toxicol* 36 (12), 1971–1980.
- Khoo, K.K., Wilson, M.J., Smith, B.J., Zhang, M.-M., Gulyas, J., Yoshikami, D., Rivier, J.E., Bulaj, G., Norton, R.S., 2011. Lactam-stabilized helical analogues of the analgesic μ -conotoxin KIIIA. *J. Med. Chem.* 54 (21), 7558–7566.
- King, G.F., Hardy, M.C., 2013. Spider-venom peptides: structure, pharmacology, and potential for control of insect pests. *Annu. Rev. Entomol.* 58, 475–496.
- Klint, J.K., Senff, S., Rupasinghe, D.B., Er, S.Y., Herzig, V., Nicholson, G.M., King, G.F., 2012. Spider-venom peptides that target voltage-gated sodium channels: pharmacological tools and potential therapeutic leads. *Toxicol* 60 (4), 478–491.
- Kushmerick, C., Kalapothakis, E., Beirao, P.S., Penaforte, C.L., Prado, V.F., Cruz, J.S., Diniz, C.R., Cordeiro, M.N., Gomez, M.V., Romano-Silva, M.A., Prado, M.A., 1999. *Phoneutria nigriventer* toxin Tx3-1 blocks A-type K⁺ currents controlling Ca²⁺ oscillation frequency in GH3 cells. *J. Neurochem.* 72 (4), 1472–1481.
- King, G.F., Gentz, M.C., Escoubas, P., Nicholson, G.M., 2008 Aug 1. Arational nomenclature for naming peptide toxins from spiders and other venomous animals. *Toxicol* 52 (2), 264–276.
- Leao, R.M., Cruz, J.S., Diniz, C.R., Cordeiro, M.N., Beirao, P.S., 2000. Inhibition of neuronal high-voltage activated calcium channels by the omega-*Phoneutria nigriventer* Tx3-3 peptide toxin. *Neuropharmacology* 39 (10), 1756–1767.
- Leipold, E., Hansel, A., Borges, A., Heinemann, S.H., 2006. Subtype specificity of scorpion β -toxin Tz1 interaction with voltage-gated sodium channels is determined by the pore loop of domain 3. *Mol. Pharmacol.* 70 (1), 340–347.
- Lucio, A.D., Campos, F.V., Richardson, M., Cordeiro, M.N., Mazzoni, M.S.C., de Lima, M.E., Pimenta, A.M.C., Benquerer, M.P., Figueiredo, S.G., Gomes, P.C., Beirao, P.S.L., 2008. A new family of small (4kDa) Neurotoxins from the venoms of spiders of the genus *Phoneutria*. *Protein Pept. Lett.* 15 (7), 700–708.
- Mafrá, R.A., Figueiredo, S.G., Diniz, C.R., Cordeiro, M.N., Cruz, J.D., De Lima, M.E., 1999. PhTx4, a new class of toxins from *Phoneutria nigriventer* spider venom, inhibits the glutamate uptake in rat brain synaptosomes. *Brain Res.* 831 (1–2), 297–300.
- Martin-Moutot, N., Mansuelle, P., Alcaraz, G., Dos Santos, R.G., Cordeiro, M.N., De Lima, M.E., Seagar, M., Van Renterghem, C., 2006. *Phoneutria nigriventer* toxin 1: a novel, state-dependent inhibitor of neuronal sodium channels that interacts with micro-conotoxin binding sites. *Mol. Pharmacol.* 69 (6), 1931–1937.
- Matavel, A., Cruz, J.S., Penaforte, C.L., Araujo, D.A.M., Kalapothakis, E., Prado, V.F., Diniz, C.R., Cordeiro, M.N., Beirao, P.S.L., 2002. Electrophysiological characterization and molecular identification of the *Phoneutria nigriventer* peptide toxin PnTx2-6. *FEBS Lett.* 523 (1–3), 219–223.
- Matavel, A., Fleury, C., Oliveira, L.C., Molina, F., de Lima, M.E., Cruz, J.S., Cordeiro, M.N., Richardson, M., Ramos, C.H., Beirao, P.S., 2009. Structure and activity analysis of two spider toxins that alter sodium channel inactivation kinetics. *Biochemistry* 48 (14), 3078–3088.
- McGivern, J.G., 2007. Ziconotide: a review of its pharmacology and use in the treatment of pain. *Neuropsychiatric Dis. Treat.* 3 (1), 69–85.
- Miranda, D.M., Romano-Silva, M.A., Kalapothakis, E., Diniz, C.R., Cordeiro, M.N., Moraes-Santos, T., De Marco, L., Prado, M.A., Gomez, M.V., 2001. Spider neurotoxins block the beta scorpion toxin-induced calcium uptake in rat brain cortical synaptosomes. *Brain Res. Bull.* 54 (5), 533–536.
- Nicholson, G.M., 2007. Insect-selective spider toxins targeting voltage-gated sodium channels. *Toxicol* 49 (4), 490–512.
- Nicholson, G.M., Little, M.J., Birinyi-Strachan, L.C., 2004. Structure and function of δ -

- atracotoxins: lethal neurotoxins targeting the voltage-gated sodium channel. *Toxicol* 43 (5), 587–599.
- Nicoletti, N.F., Erig, T.C., Zanin, R.F., Roxo, M.R., Ferreira, N.P., Gomez, M.V., Morrone, F.B., Campos, M.M., 2017. Pre-clinical evaluation of voltage-gated calcium channel blockers derived from the spider *P.nigriventer* in glioma progression. *Toxicol* 129, 58–67.
- Nunes, K.P., Cordeiro, M.N., Richardson, M., Borges, M.N., Diniz, S.O.F., Cardoso, V.N., Tostes, R., De Lima, M.E., Webb, R.C., Leite, R., 2010. Nitric oxide-induced vasorelaxation in response to PnTx2-6 toxin from *Phoneutria nigriventer* spider in rat cavernosal tissue. *J. Sex. Med.* 7 (12), 3879–3888.
- Nunes, K.P., Costa-Goncalves, A., Lanza, L.F., Cortes, S.F., Cordeiro, M.N., Richardson, M., Pimenta, A.M.C., Webb, R.C., Leite, R., De Lima, M.E., 2008. Tx2-6 toxin of the *Phoneutria nigriventer* spider potentiates rat erectile function. *Toxicol* 51 (7), 1197–1206.
- Nunes, K.P., Toque, H.A., Borges, M.H., Richardson, M., Webb, R.C., de Lima, M.E., 2012a. Erectile function is improved in aged rats by PnTx2-6, a toxin from *Phoneutria nigriventer* spider venom. *J. Sex. Med.* 9 (10), 2574–2581.
- Nunes, K.P., Wynne, B.M., Cordeiro, M.N., Borges, M.H., Richardson, M., Leite, R., DeLima, M.E., Webb, R.C., 2012b. Increased cavernosal relaxation by *Phoneutria nigriventer* toxin, PnTx2-6, via activation at NO/cGMP signaling. *Int. J. Impot. Res.* 24 (2), 69–76.
- Oliveira, L.C., De Lima, M.E., Pimenta, A.M.C., Mansuelle, P., Rochat, H., Cordeiro, M.N., Richardson, M., Figueiredo, S.G., 2003. PnTx4-3, a new insect toxin from *Phoneutria nigriventer* venom elicits the glutamate uptake inhibition exhibited by PhTx4 toxic fraction. *Toxicol* 42 (7), 793–800.
- Oliveira, S.M., Silva, C.R., Trevisan, G., Villarinho, J.G., Cordeiro, M.N., Richardson, M., Borges, M.H., Castro Jr., C.J., Gomez, M.V., Ferreira, J., 2016. Antinociceptive effect of a novel armed spider peptide Tx3-5 in pathological pain models in mice. *Pflug. Arch. Eur. J. Physiol.* 468 (5), 881–894.
- Paiva, A.L., Matavel, A., Peigneur, S., Cordeiro, M.N., Tytgat, J., Diniz, M.R., de Lima, M.E., 2016. Differential effects of the recombinant toxin PnTx4(5-5) from the spider *Phoneutria nigriventer* on mammalian and insect sodium channels. *Biochimie* 121, 326–335.
- Palhares, M.R., Silva, J.F., Rezende, M.J.S., Santos, D.C., Silva-Junior, C.A., Borges, M.H., Ferreira, J., Gomez, M.V., Castro-Junior, C.J., 2017. Synergistic antinociceptive effect of a calcium channel blocker and a TRPV1 blocker in an acute pain model in mice. *Life Sci.* 182, 122–128.
- Peigneur, S., Cologna, C.T., Cremonese, C.M., Mille, B.G., Pucca, M.B., Cuypers, E., Arantes, E.C., Tytgat, J., 2015. A gamut of undiscovered electrophysiological effects produced by *Tityus serrulatus* toxin 1 on NaV-type isoforms. *Neuropharmacology* 95, 269–277.
- Peigneur, S., Sevcik, C., Tytgat, J., Castillo, C., D'Suze, G., 2012. Subtype specificity interaction of batraches with mammalian, insect and bacterial sodium channels under voltage clamp conditions. *FEBS J.* 279 (21), 4025–4038.
- Penaforte, C.L., Prado, V.F., Prado, M.A., Romano-Silva, M.A., Guimaraes, P.E., De Marco, L., Gomez, M.V., Kalopothakis, E., 2000. Molecular cloning of cDNAs encoding insecticidal neurotoxic peptides from the spider *Phoneutria nigriventer*. *Toxicol* 38 (10), 1443–1449.
- Pimenta, A.M.C., Rates, B., Bloch, C., Gomes, P.C., Santoro, M.M., de Lima, M.E., Richardson, M., Cordeiro, M.D., 2005. Electrospray ionization quadrupole time-of-flight and matrix-assisted laser desorption/ionization tandem time-of-flight mass spectrometric analyses to solve micro-heterogeneity in post-translationally modified peptides from *Phoneutria nigriventer* (Aranea, Tenebrionidae) venom. *Rapid Commun. Mass Spectrom.* 19 (1), 31–37.
- Pineda, S.S., Chaumeil, P.A., Kunert, A., Kaas, Q., Thang, M.W.C., Li, L., Nuhn, M., Herzig, V., Saez, N.J., Cristofori-Armstrong, B., Anangi, R., Senff, S., Gorse, D., King, G.F., 2018 Mar 15. ArachnoServer 3.0: an online resource for automated discovery, analysis and annotation of spider toxins. *Bioinformatics* 34 (6), 1074–1076.
- Pineda, S.S., Undheim, E.A., Rupasinghe, D.B., Ikonomopoulou, M.P., King, G.F., 2014. Spider venomomics: implications for drug discovery. *Future Med. Chem.* 6 (15), 1699–1714.
- Pinheiro, A.C.N., da Silva, A.J., Prado, M.A.M., Cordeiro, M.N., Richardson, M., Batista, M.C., de Castro Junior, C.J., Massensini, A.R., Guatimosim, C., Romano-Silva, M.A., Kushmerick, C., Gomez, M.V., 2009. *Phoneutria* spider toxins block ischemia-induced glutamate release, neuronal death, and loss of neurotransmission in hippocampus. *Hippocampus* 19 (11), 1123–1129.
- Pinheiro, A.C.N., Gomez, R.S., Massensini, A.R., Cordeiro, M.N., Richardson, M., Romano-Silva, M.A., Prado, M.A.M., De Marco, L., Gomez, M.V., 2006. Neuroprotective effect on brain injury by neurotoxins from the spider *Phoneutria nigriventer*. *Neurochem. Int.* 49 (5), 543–547.
- Prado, M.A., Guatimosim, C., Gomez, M.V., Diniz, C.R., Cordeiro, M.N., Romano-Silva, M.A., 1996. A novel tool for the investigation of glutamate release from rat cerebrocortical synaptosomes: the toxin Tx3-3 from the venom of the spider *Phoneutria nigriventer*. *Biochem. J.* 314 (Pt 1), 145–150.
- Prashanth, J.R., Brust, A., Jin, A.-H., Alewood, P.F., Dutertre, S., Lewis, R.J., 2014. Cone snail venomomics: from novel biology to novel therapeutics. *Future Med. Chem.* 6 (15), 1659–1675.
- Raposo, C., Bjorklund, U., Kalopothakis, E., Biber, B., Alice da Cruz-Hofling, M., Hansson, E., 2016. Neuropharmacological effects of *Phoneutria nigriventer* venom on astrocytes. *Neurochem. Int.* 96, 13–23.
- Ravelli, K.G., Ramos, AdT., Goncalves, L.B., Magnoli, F.C., Troncone, L.R.P., 2017. *Phoneutria nigriventer* spider toxin Tx2-6 induces priapism in mice even after cavernosal denervation. *Toxicol* 130, 29–34.
- Reis, H.J., Prado, M.A., Kalopothakis, E., Cordeiro, M.N., Diniz, C.R., De Marco, L.A., Gomez, M.V., Romano-Silva, M.A., 1999. Inhibition of glutamate uptake by a poly-peptide toxin (*Phoneutria* toxin 3-4) from the spider *Phoneutria nigriventer*. *Biochem. J.* 343 (Pt 2), 413–418.
- Rezende Jr., L., Cordeiro, M.N., Oliveira, E.B., Diniz, C.R., 1991. Isolation of neurotoxic peptides from the venom of the 'armed' spider *Phoneutria nigriventer*. *Toxicol* 29 (10), 1225–1233.
- Richardson, M., Pimenta, A.M.C., Bemquerer, M.P., Santoro, M.M., Beirao, P.S.L., Lima, M.E., Figueiredo, S.G., Bloch Jr., C., Vasconcelos, E.A.R., Campos, F.A.P., Gomes, P.C., Cordeiro, M.N., 2006. Comparison of the partial proteomes of the venoms of Brazilian spiders of the genus *Phoneutria*. *Comparat. Biochem. Physiol. Toxicol. Pharmacol.* 142 (3–4), 173–187.
- Rigo, F.K., Rossato, M.F., Trevisan, G., De Pra, S.D.-T., Ineu, R.P., Duarte, M.B., de Castro Junior, C.J., Ferreira, J., Gomez, M.V., 2017. PhKv a toxin isolated from the spider venom induces antinociception by inhibition of cholinesterase activating cholinergic system. *Scandinavian J. Pain* 17, 203–210.
- Santos, R.G., Diniz, C.R., Cordeiro, M.N., De Lima, M.E., 1999. Binding sites and actions of Tx1, a neurotoxin from the venom of the spider *Phoneutria nigriventer*, in Guinea pig ileum. *Braz. J. Med. Biol. Res.* 32 (12), 1565–1569 *Revista brasileira de pesquisas medicas e biologicas*.
- Schenberg, S., Lima, F.A., 1966. Pharmacology of the polypeptides from the venom of the spider *Phoneutria fera*. *Mem. Inst. Butantan (Sao Paulo)* 33 (2), 627–638.
- Silva, A.O., Peigneur, S., Diniz, M.R.V., Tytgat, J., Beirao, P.S.L., 2012. Inhibitory effect of the recombinant *Phoneutria nigriventer* Tx1 toxin on voltage-gated sodium channels. *Biochimie* 94 (12), 2756–2763.
- Silva, C.N., Nunes, K.P., Torres, F.S., Cassoli, J.S., Santos, D.M., Almeida, F.D.M., Matavel, A., Cruz, J.S., Santos-Miranda, A., Nunes, A.D.C., Castro, C.H., Machado de Avila, R.A., Chavez-Olortegui, C., Lauer, S.S., Felicori, L., Resende, J.M., Camargos, ERdS., Borges, M.H., Cordeiro, M.N., Peigneur, S., Tytgat, J., de Lima, M.E., 2015a. PnPP-19, a synthetic and nontoxic peptide designed from a *Phoneutria nigriventer* toxin, potentiates erectile function via no/cGMP. *J. Urol.* 194 (5), 1481–1490.
- Silva, F.R., Batista, E.M.L., Gomez, M.V., Kushmerick, C., Da Silva, J.F., Cordeiro, M.N., Vieira, L.B., Ribeiro, F.M., 2016. The *Phoneutria nigriventer* spider toxin, PnTx4-5-5, promotes neuronal survival by blocking NMDA receptors. *Toxicol* 112, 16–21.
- Silva, R.B.M., Sperotto, N.D.M., Andrade, E.L., Pereira, T.C.B., Leite, C.E., de Souza, A.H., Bogo, M.R., Morrone, F.B., Gomez, M.V., Campos, M.M., 2015b. Spinal blockage of P/Q- or N-type voltage-gated calcium channels modulates functional and symptomatic changes related to haemorrhagic cystitis in mice. *Br. J. Pharmacol.* 172 (3), 924–939.
- Souza, A.H., Ferreira, J., Cordeiro, M.N., Vieira, L.B., De Castro, C.J., Trevisan, G., Reis, H., Souza, I.A., Richardson, M., Prado, M.A.M., Prado, V.F., Gomez, M.V., 2008. Analgesic effect in rodents of native and recombinant Ph α 1 β toxin, a high-voltage-activated calcium channel blocker isolated from armed spider venom. *Pain* 140 (1), 115–126.
- Swartz, K.J., 2007 Feb. Tarantulatotoxins interacting with voltage sensors in potassium channels. *Toxicol* 49 (2), 213–230.
- Tonello, R., Fusi, C., Materazzi, S., Marone, I.M., De Logu, F., Benemei, S., Goncalves, M.C., Coppi, E., Castro-Junior, C.J., Gomez, M.V., Geppetti, P., Ferreira, J., Nassini, R., 2017. The peptide Phalpha1beta, from spider venom, acts as a TRPA1 channel antagonist with antinociceptive effects in mice. *Br. J. Pharmacol.* 174 (1), 57–69.
- Tonello, R., Rigo, F., Gewehr, C., Trevisan, G., Pereira, E.M.R., Gomez, M.V., Ferreira, J., 2014. Action of Phalpha1beta, a peptide from the venom of the spider *Phoneutria nigriventer*, on the analgesic and adverse effects caused by morphine in mice. *J. Pain: Official J. Am. Pain Soc.* 15 (6), 619–631.
- Torres, F.S., Silva, C.N., Lanza, L.F., Santos, A.V., Pimenta, A.M.C., De Lima, M.E., Diniz, M.R.V., 2010. Functional expression of a recombinant toxin - rPnTx2-6 - active in erectile function in rat. *Toxicol* 56 (7), 1172–1180.
- Troncone, L.R.P., Georgiou, J., Hua, S.-Y., Elick, D., Lebrun, I., Magnoli, F., Charlton, M.P., 2003. Promiscuous and reversible blocker of presynaptic calcium channels in frog and crayfish neuromuscular junctions from *Phoneutria nigriventer* spider venom. *J. Neurophysiol.* 90 (5), 3529–3537.
- Van Der Haegen, A., Peigneur, S., Tytgat, J., 2011. Importance of position 8 in μ -conotoxin KIIIA for voltage-gated sodium channel selectivity. *FEBS J.* 278 (18), 3408–3418.
- Verma, D., Gupta, Y.K., Parashar, A., Ray, S.B., 2009. Differential expression of L- and N-type voltage-sensitive calcium channels in the spinal cord of morphine + nimodipine treated rats. *Brain Res.* 1249, 128–134.
- Vieira, L.B., Kushmerick, C., Hildebrand, M.E., Garcia, E., Stea, A., Cordeiro, M.N., Richardson, M., Gomez, M.V., Snutch, T.P., 2005. Inhibition of high voltage-activated calcium channels by spider toxin PnTx3-6. *J. Pharmacol. Exp. Therapeut.* 314 (3), 1370–1377.
- Villanova, F.E., Andrade, E., Leal, E., Andrade, P.M., Borra, R.C., Troncone, L.R.P., Magalhaes, L., Leite, K.R.M., Paranhos, M., Claro, J., Srougi, M., 2009. Erection induced by Tx2-6 toxin of *Phoneutria nigriventer* spider: expression profile of genes in the nitric oxide pathway of penile tissue of mice. *Toxicol* 54 (6), 793–801.
- Wanke, E., Zaharenko, A.J., Redaelli, E., Schiavon, E., 2009. Actions of sea anemone type 1 neurotoxins on voltage-gated sodium channel isoforms. *Toxicol* 54 (8), 1102–1111.
- Yonamine, C.M., Troncone, L.R.P., Camillo, M.A.P., 2004. Blockade of neuronal nitric oxide synthase abolishes the toxic effects of Tx2-5, a lethal *Phoneutria nigriventer* spider toxin. *Toxicol* 44 (2), 169–172.
- Zhang, M.-M., Han, T.S., Olivera, B.M., Bulaj, G., Yoshikami, D., 2010. μ -conotoxin KIIIA derivatives with divergent affinities versus efficacies in blocking voltage-gated sodium channels. *Biochemistry* 49 (23), 4804–4812.
- Zhu, S., Peigneur, S., Gao, B., Lu, X., Cao, C., Tytgat, J., 2012. Evolutionary diversification of Mesobuthus α -scorpion toxins affecting sodium channels. *Mol. Cell. Proteomics: MCP* 11 (1), M111.012054.

Article

Phoneutria nigriventer Spider Toxin PnTx2-1 (δ -Ctenitoxin-Pn1a) Is a Modulator of Sodium Channel Gating

Steve Peigneur^{1,2,*,†} , Ana Luiza B. Paiva^{3,†}, Marta N. Cordeiro³, Márcia H. Borges³, Marcelo R. V. Diniz³, Maria Elena de Lima^{2,4} and Jan Tytgat^{1,*}

¹ Toxicology and Pharmacology, University of Leuven (KU Leuven), Campus Gasthuisberg, P.O. Box 922, Herestraat 49, 3000 Leuven, Belgium

² Laboratório de Venenos e Toxinas Animais, Dept de Bioquímica e Imunologia, Instituto de Ciências Biológicas, Universidade Federal de Minas Gerais (UFMG), Belo Horizonte 31270-901, Brazil; mariaelena@santacasabh.org.br

³ Departamento de Pesquisa e Desenvolvimento, Fundação Ezequiel Dias, Minas Gerais, Belo Horizonte 30510-010, Brazil; analubpaiva@gmail.com (A.L.B.P.); martadonascimento.phoneutria@gmail.com (M.N.C.); mhborgesb@gmail.com (M.H.B.); mdiniz@funed.mg.gov.br (M.R.V.D.)

⁴ Programa de Pós-graduação em Ciências da Saúde, Biomedicina e Medicina, Instituto de Ensino e Pesquisa da Santa Casa de Belo Horizonte, Grupo Santa Casa de Belo Horizonte, Minas Gerais, Belo Horizonte 31270-901, Brazil

* Correspondence: steve.peigneur@kuleuven.be or stevepeigneur@gmail.com (S.P.); jan.tytgat@kuleuven.be (J.T.); Tel.: +321-632-3404 (J.T.)

† These two authors contribute equally to this work.

Received: 26 July 2018; Accepted: 16 August 2018; Published: 21 August 2018



Abstract: Spider venoms are complex mixtures of biologically active components with potentially interesting applications for drug discovery or for agricultural purposes. The spider *Phoneutria nigriventer* is responsible for a number of envenomations with sometimes severe clinical manifestations in humans. A more efficient treatment requires a comprehensive knowledge of the venom composition and of the action mechanism of the constituting components. PnTx2-1 (also called δ -ctenitoxin-Pn1a) is a 53-amino-acid-residue peptide isolated from the venom fraction PhTx2. Although PnTx2-1 is classified as a neurotoxin, its molecular target has remained unknown. This study describes the electrophysiological characterization of PnTx2-1 as a modulator of voltage-gated sodium channels. PnTx2-1 is investigated for its activity on seven mammalian Na_V-channel isoforms, one insect Na_V channel and one arachnid Na_V channel. Furthermore, comparison of the activity of both PnTx2-1 and PnTx2-6 on Na_V1.5 channels reveals that this family of *Phoneutria* toxins modulates the cardiac Na_V channel in a bifunctional manner, resulting in an alteration of the inactivation process and a reduction of the sodium peak current.

Keywords: *Phoneutria nigriventer*; voltage-gated sodium channel; spider; insecticide; peptide toxin PnTx2-1; gating modifier toxin

Key Contribution: *Phoneutria nigriventer* toxin PnTx2-1 modulates both the activation and inactivation gating processes of voltage-gated sodium channels. PnTx2-1 exhibits a strong insecticidal activity.

1. Introduction

Spiders can be considered one of the most successful venomous animals ever to inhabit the planet with over 47,000 species characterized to date [1]. Despite this diversity, no more than 100 spider species

have had their venom investigated [2]. With over ten million estimated biologically active peptides in spider venoms [3], this means that less than 0.01% of spider peptides have been studied [3,4], making spider venom an untapped treasure of biologically active compounds with promising discoveries in drug and bioinsecticide development [1,5,6]. *Phoneutria nigriventer* are very aggressive, solitary spiders. They are active hunters, relying on their fast-acting and efficient venom for prey capture and defense. They prey normally on insects, although there are reports of *Phoneutria* hunting on other spiders and small rodents as well [6,7]. Human envenomation by *Phoneutria nigriventer* is common in Brazil, with 0.5–1% resulting in severe envenomation, with most of these occurring in children [8]. Cysteine-rich peptide toxins with action on ion channels are the most abundant components in its venom [9]. A recent review describes the complexity of this venom [6]. Historically, the *Phoneutria* toxins are annotated based on their occurrence in the venom when following the venom purification methods used in the first studies [10], that is, based on a particular chromatographic step and in the order of elution of the toxin, in this step. However, a new nomenclature has been proposed based on the genus of the spider, the target of the toxin and the isoform [11]. According to this nomenclature, PnTx2-1 is also called δ -ctenitoxin-Pn1a and it can be accessed in the Arachnoserver databank (<http://www.arachnoserver.org>) [2]. In-vivo studies have shown that the PhTx2 fraction is toxic to both mice and insects [12]. Nine peptides could be identified from the PhTx2 fraction. These peptides were named accordingly PnTx2-1 to PnTx2-9. PnTx2-1, PnTx2-5 and PnTx2-6 showed higher toxicity after intracerebral (i.c.) injection in mice [13]. Both PnTx2-5 and PnTx2-6 have been characterized as modulators of the inactivation of voltage-gated sodium (Na_V) channels [14,15]. Toxin PnTx2-1 (5838.8 Da) shares up to 77% identity with PnTx2-5 and PnTx2-6 (Figure 1) [13]. When injected in mice, PnTx2-1 causes pruritus, lacrimation, increased salivation, sweating and agitation followed by spastic paralysis of the limbs [12]. A recent transcriptomic and proteomic investigation of *P. nigriventer* venom showed that PnTx2-1, altogether with its isoforms, is among the most expressed toxins in this venom [9], suggesting that this toxin may play an important role in the envenoming of natural preys. Based on the in-vivo tests in mice and the sequence homology with PnTx2-5 and PnTx2-6, this peptide is classified as a Na_V -channel toxin. However, it has never been tested on any Na_V -channel isoform. Therefore, in this study the Na_V -channel subtype selectivity and species specificity of PnTx2-1 are investigated. Furthermore, comparison of the activity of both PnTx2-1 and PnTx2-6 on $\text{Na}_V1.5$ reveals that this family of *Phoneutria* toxins modulates the cardiac Na_V channel in a bifunctional manner, resulting in an alteration of the inactivation process and a reduction of the sodium peak current.

	1	10	20	30	40	50
PnTx2-1	ATCAGQDKPCKETCDCCGERGECV	CALS	YEGKYRCICRQGNFLIAWHK	CLASCK-		
PnTx2-5	ATCAGQDQTCKVTCDCCGERGECV	CGG	-----PCI	CRQGNFLIAWYK	CLASCKK	
PnTx2-6	ATCAGQDQPCKETCDCCGERGECV	CGG	-----PCI	CRQGYFWIAWYK	LANCKK	

Figure 1. Sequence alignment of PnTx2-1 with Na_V -channel toxins from *Phoneutria nigriventer* venom fraction 2.

2. Results

2.1. Electrophysiological Characterization

2.1.1. Activity of PnTx2-1 on Mammalian Na_V Channels

PnTx2-1 was screened against a panel of seven mammalian Na_V channel isoforms ($\text{Na}_V1.1$ – $\text{Na}_V1.6$ and $\text{Na}_V1.8$), one insect from the cockroach *Blattella germanica* (BgNa_V1) and one arachnid channel from the mite *Varroa destructor* (VdNa_V1) (Figure 2). PnTx2-1 was investigated for its activity on these Na_V channels because of their ability to be effectively expressed in oocytes, and these are the most commonly screened Na_V channels when testing for Na_V channel effects of peptide toxins [16].

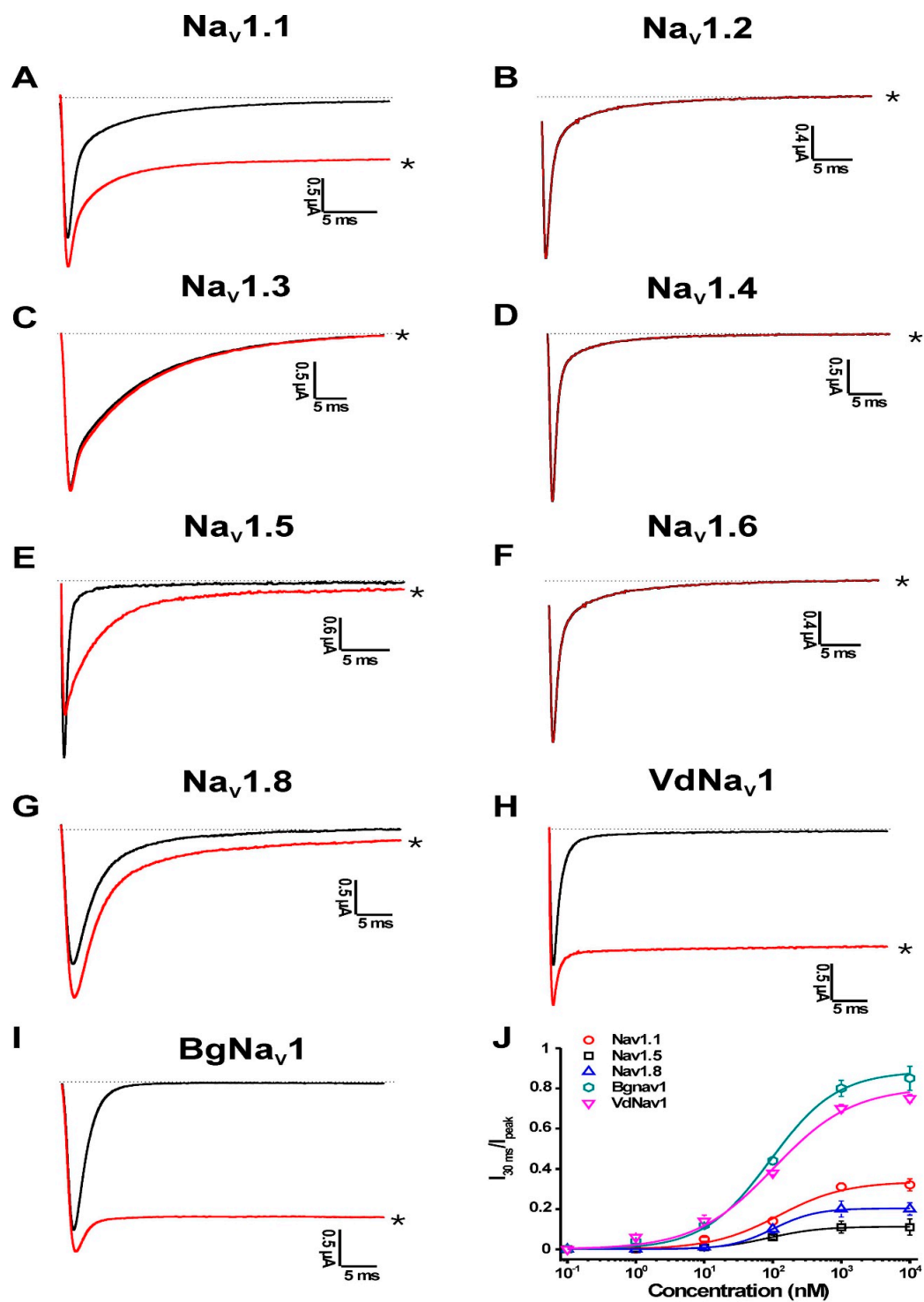


Figure 2. Electrophysiological profiles of PnTx2-1 on Na_vs. Panels show superimposed current traces of 1 μM PnTx2-1. The dotted line indicates zero current level. Black, current trace in control conditions; red, current trace in toxin situation. The asterisk marks steady-state current trace after application of 1 μM peptide. The last panel shows the concentration–response curves for PnTx2-1 on different Na_v channel isoforms.

Among the mammalian isoforms, 1 μM PnTx2-1 slowed the inactivation of Na_v1.1, Na_v1.5 and Na_v1.8. Na_v1.2, Na_v1.3, Na_v1.4 and Na_v1.6 were not affected by PnTx2-1. Interestingly, PnTx2-1 had a profound effect on the inactivation of the insect channel BgNa_v1 and the arachnid channel VdNa_v1.

PnTx2-1 completely inhibited inactivation of BgNa_V1 channels, resulting in sustained non-inactivating currents. Concentration–response curves were constructed to determine the values at which half of the channels were modulated by PnTx2-1. Among the mammalian isoforms, the half-maximal effective concentration (EC₅₀) values yielded 122.1 ± 34.6 nM, 87.0 ± 7.5 nM and 101.1 ± 5.1 nM for Na_V1.1, Na_V1.5 and Na_V1.8, respectively. Activation and steady-state inactivation curves were constructed for Na_V1.1, Na_V1.5 and Na_V1.8 channels (Figure 3A–C, Table 1). In the presence of 1 μM toxin, a significant modulation of gating kinetics was observed for Na_V1.1 and Na_V1.5 (Figure 3A,B, Table 1). For both Na_V1.1 and Na_V1.5 channels, the midpoint of activation shifted towards more depolarized potentials. At the same time, the steady-state inactivation curves shifted towards more hyperpolarized membrane potentials. This resulted in an increased window of open probability for both Na_V1.1 and Na_V1.5. No relevant modulation of the gating kinetics was observed for Na_V1.8-channel isoforms since no significant shift in the half-maximal activation voltage (V_{1/2}) values was noted (Figure 3C, Table 1). No significant change in the reversal potential was observed in the presence of toxin which indicates that the ion selectivity of Na_V channels is not altered. One micromolar PnTx2-1 strongly enhanced the recovery from inactivation for Na_V1.5 channels with τ = 50.2 ± 3.0 ms in control conditions and τ = 22.8 ± 3.2 ms in the presence of the toxin (Figure 3D). To verify whether PnTx2-1 binds to neurotoxin site 1, competitive binding experiments were performed. Application of tetrodotoxin (TTX) at its half-maximal inhibitory concentration (IC₅₀) resulted in a blockage of half of the expressed Na_V1.5 channels. This was observed as a 50% decrease of the sodium current peak amplitude. An additional reduction of the peak amplitude was the result of subsequent and additional application of PnTx2-1 at its EC₅₀ (n = 6) (Figure 3E).

Table 1. V_{1/2} values for the activation and steady-state inactivation curves obtained for Na_V1.1, Na_V1.5, Na_V1.8 and BgNa_V1.

V _{1/2} (mV)	Activation		Inactivation	
	Control	PnTx2-1 (1 μM)	Control	PnTx2-1 (1 μM)
Na _V 1.1	−56.4 ± 0.2	−63.4 ± 0.1	−54.7 ± 0.1	−45.3 ± 0.1
Na _V 1.5	−53.1 ± 0.1	−45.3 ± 0.1	−78.4 ± 0.2	−87.5 ± 0.7
Na _V 1.8	−11.5 ± 0.1	−11.4 ± 0.1	−55.8 ± 0.4	−63.9 ± 0.4
BgNa _V 1	−38.1 ± 0.1	−45.8 ± 0.3	−63.3 ± 0.3	−70.7 ± 0.13

2.1.2. Activity of PnTx2-1 on Insect Na_V-Channel Currents

The EC₅₀ values for BgNa_V1 and VdNa_V1 were determined at 91.9 ± 17.0 nM and 101.8 ± 14.7 nM, respectively. The insect Na_V channel BgNa_V1 was used to further investigate the characteristics of PnTx2-1 in inducing modulation of channel gating (Figure 4). A shift in the midpoint of activation and in the voltage dependence of steady-state inactivation was observed (Table 1). From Figure 4A, it can be seen that the steady-state inactivation became incomplete after toxin addition. A 62.3 ± 3.2% non-inactivating current component of steady-state inactivation can be seen. In addition, we examined the recovery from fast inactivation in the absence or presence of PnTx2-1 and found that 1 μM does not influence the recovery from fast inactivation in BgNa_V1 (Figure 4B). Considering the incomplete steady-state inactivation of BgNa_V1 channels in the presence of PnTx2-1, we decided to determine whether inhibition occurs during the closed or open state of the channel. One micromolar toxin was applied to the bath solution with oocytes clamped at −90 mV, allowing interaction with the membrane for 2 min without depolarizing the membrane. After 2 min, currents were elicited by a depolarizing pulse to 0 mV. The obtained currents in the presence of toxin were normalized to the currents obtained in the same cells in control conditions. A significant slowing down of inactivation was observed when PnTx2-1 was applied to the oocytes without applying depolarizing pulses (Figure 4C). This indicates that there is toxin interaction with the channel in the closed state and suggests that membrane depolarization and hence most likely channel opening is not required to allow the toxin to bind.

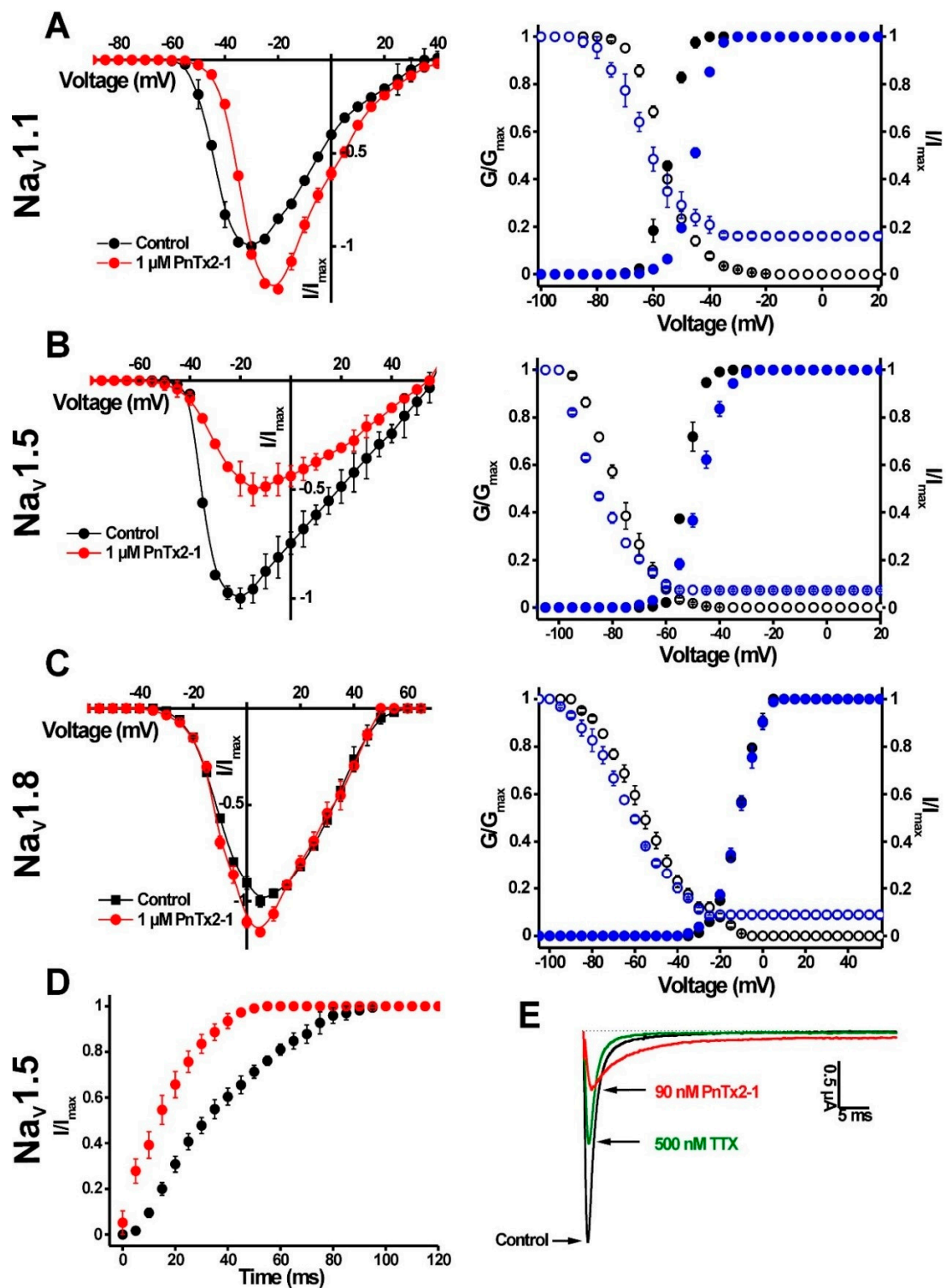


Figure 3. Electrophysiological characterization of PnTx2-1 on mammalian Na_V channels. Left panels show the current voltage relationships and the right panels show the steady-state activation (closed symbols) and inactivation (open symbols) curves in control (black) and toxin conditions (1 μM PnTx2-1, blue) for Na_V1.1 (A), Na_V1.5 (B) and Na_V1.8 (C). (D) Recovery from inactivation for Na_V1.5 channels. Control conditions (black symbols) and in the presence of 1 μM PnTx2-1 (red symbols) are shown. (E) Competitive experiments to indicate that PnTx2-1 does not bind at site 1. Representative traces for Na_V1.5 channels are shown in control; after application of 500 nM tetrodotoxin (TTX) and after subsequent addition of 90 nM PnTx2-1.

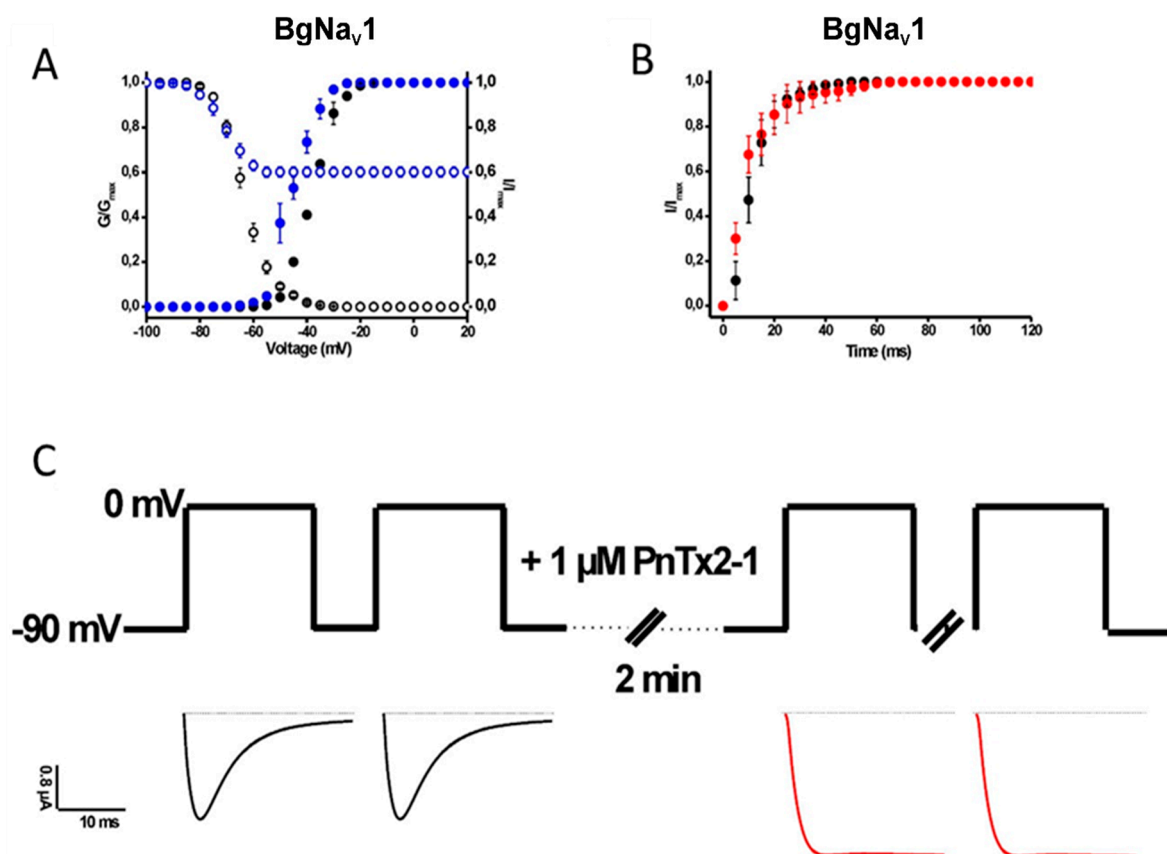


Figure 4. Electrophysiological characterization of PnTx2-1 on insect Na_v channels. (A) Steady-state activation (closed symbols) and inactivation (open symbols) curves in control (black) and toxin conditions (1 μ M PnTx2-1, blue) for BgNa_v1.1. (B) Recovery from inactivation in control (black symbols) and in the presence of 1 μ M PnTx2-1 (red symbols). (C) Investigation of the state-dependence of indicating that an expected degree of channel inactivation inhibition was observed after the 2 min incubation, indicating that the open state is not required for toxin interaction with the channel.

2.1.3. Activity of PnTx2-6 on Na_v1.5-Channel Currents

The pharmacological phenotype induced on Na_v1.5 channels by PnTx2-1 is very similar to what has been reported previously for PnTx2-6 [17]. Therefore, we performed further characterisation of PnTx2-6 on Na_v1.5 channels by investigating the current–voltage relationship in the presence of PnTx2-6. In the presence of 1 μ M PnTx2-6, an inhibition of the sodium peak current and a delay of the inactivation was observed (Figure 5A). The slowing down of inactivation was characterized by an EC₅₀ value of 22.3 ± 3.1 nM (Figure 5B). The voltage–current relationship shows a reduction of the sodium current by $21.3 \pm 2.8\%$ in the presence of 200 nM PnTx2-6 (Figure 5C). Construction of the activation and steady-state inactivation curves indicated that no significant modification of gating processes occurs (Figure 5D).

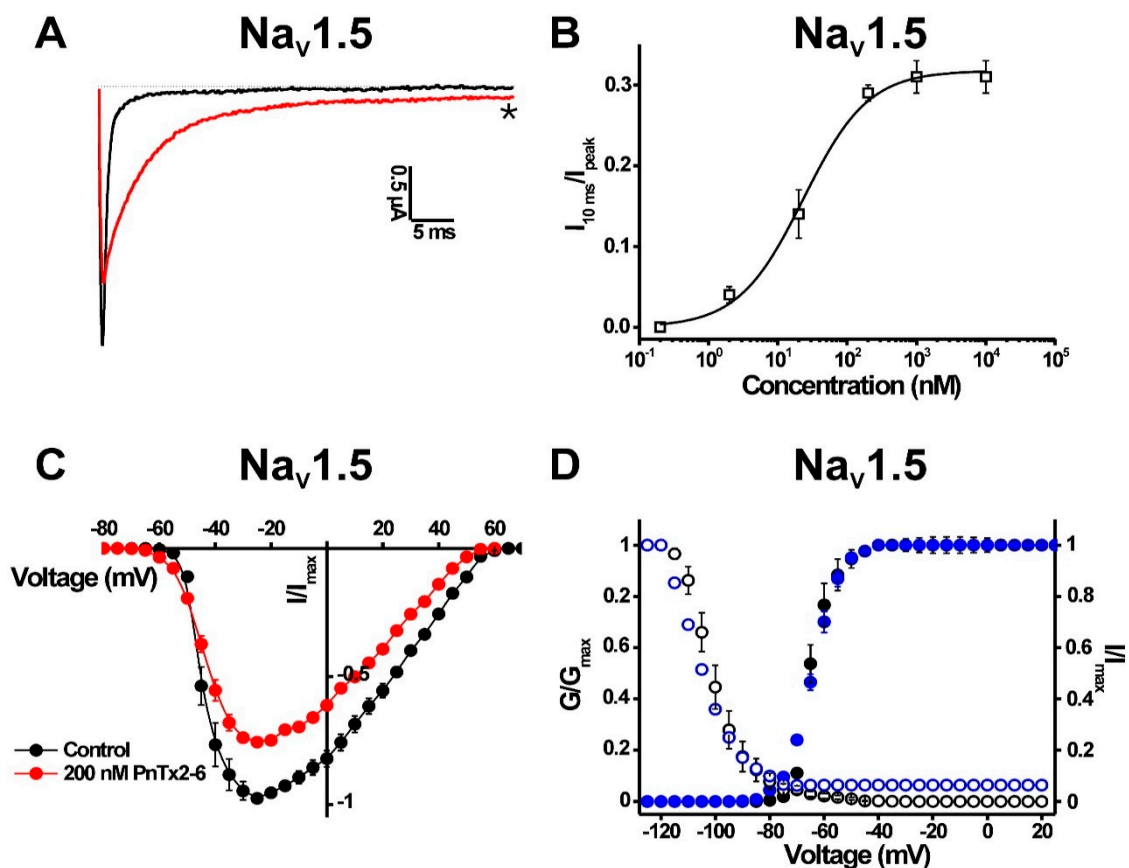


Figure 5. Electrophysiological characterization of PnTx2-6 on Nav_v1.5. (A) Representative whole-cell current traces in control (black) and toxin (red) conditions are shown. The dotted line indicates the zero-current level. The asterisk marks steady-state current trace after application of 1 μM peptide. (B) Concentration–response curve for PnTx2-6 on Nav_v1.5. (C) Current–voltage relationship in control conditions and in the presence of 200 nM PnTx2-6. (D) Steady-state activation (closed symbols) and inactivation (open symbols) curves in control (black) and toxin conditions (1 μM PnTx2-6, blue) for Nav_v1.5 channels.

3. Discussion

PnTx2-1 shares the highest sequence identity with PnTx2-5 and PnTx2-6, which are also isolated from the *Phoneutria nigriventer* venom fraction 2 [13]. PnTx2-5 and PnTx2-6 are the best-characterized toxins from the PhTx2 venom fraction [14,15,17,18]. These two toxins share 90% sequence identity, with only five amino acid residues different (Figure 1). PnTx2-5 and PnTx2-6 are responsible for the painful and persistent penile erection, also known as priapism, a common clinical manifestation observed upon *Phoneutria nigriventer* envenomation [18,19]. Both peptides modulate sodium channel kinetics by slowing down the inactivation process and by shifting the voltage dependence of activation towards more hyperpolarized potentials [14,15]. Interestingly, significant differences in potency have been reported despite the high homology between both peptides. PnTx2-5 displayed an approximately six-fold lower potency than PnTx2-6 on macroscopic sodium currents in patch clamp experiments using GH3 cells [20]. It has been suggested that Tyr41 and Trp43 in PnTx2-6 are involved in the higher potency compared to PnTx2-5 [14]. Interestingly, these residues are also not conserved in PnTx2-1 (Figure 1). Nevertheless, similar EC₅₀ values were found for PnTx2-1 and PnTx2-6 on Nav_v1.5 channels (Figures 2J and 5B). While PnTx2-6 exerts a strong affinity for Nav_v1.2–Nav_v1.4 and Nav_v1.6 channels [17], PnTx2-1 shows no activity on these channels, even at concentrations up to 5 μM (data not shown). It is well established that even minor differences in amino acid composition of peptide toxins can

influence the Na_V channel isoform selectivity [21,22]. Binding experiments in brain synaptosomes indicated a partial competition between the α -scorpion toxin AaHIII (from *Androctonus australis Hector*) and PnTx2-6 [14]. It thus can be hypothesized that PnTx2-1 also acts by binding to a site similar to the site that PnTx2-6 and the typical α -scorpion toxins bind to. β -Scorpion toxins and certain spider toxins modulate Na_V channels by shifting the midpoint of activation towards more negative potentials, often resulting in a reduction in sodium peak current [23–25]. However, the β -scorpion toxin CssIV (from *Centruroides suffusus suffusus*) does not compete with PnTx2-6. Therefore, it seems unlikely that PnTx2-6 shares a binding site with β -scorpion toxins [14]. However, it can be suggested that the PnTx2-1- and PnTx2-6-induced inhibition of the sodium peak current (Figures 2E, 3B and 5A) results from gating modification, rather than physical obstruction of the ion pathway. Scorpion toxins such as Ts1 (from *Tityus serrulatus*) and Tz1 (from *Tityus zulianus*) induce a similar pharmacological phenotype activity on $\text{Na}_V1.5$ channels to that observed for PnTx2-1 [23,25,26]. For these toxins, it was evidenced that by trapping the voltage sensor in the inward position, channels are prevented from opening, which is seen as an inhibition of the sodium current for $\text{Na}_V1.5$ channels [16,23,25,26].

δ -Atracotoxins (δ -ACTX) are a family of Na_V channel-targeting toxins isolated from the venom of Australian funnel-web spiders [24]. They are classified in the Na_V channel-targeting spider toxin (NaSpTx) family 4. This family constitutes six peptides isolated from Australian funnel-web spiders and one peptide from the Asian spider *Macrothele gigas*. They are peptides of 42 amino acid residues including eight conserved cysteine residues which form four disulfide bridges in an inhibitor cysteine-knot (ICK) motif [24,27]. Although very low sequence homology (<25%) can be found between PnTx2-1 and these funnel-web spider toxins, they do seem to modulate the Na_V channels in a similar way. In patch-clamp experiments, it was shown that δ -ACTX interact with TTX-sensitive but not with TTX-resistant sodium currents in dorsal root ganglion (DRG) neurons. To date, no information is available on the Na_V -channel subtype selectivity of δ -ACTX since these peptides have not yet been tested on heterologously expressed Na_V -channel isoforms. However, in DRGs, δ -ACTX produce a selective slowing of Na_V -current inactivation and a reduction in peak sodium current. Moreover, they cause a hyperpolarizing shift in the midpoint of activation, and an increased recovery from inactivation was seen for toxin-bound channels [20,28–30]. Radiolabeled binding assays have determined that the δ -ACTX bind to the neurotoxin site 3 [31]. Several residues have been suggested to be important for the interaction of δ -ACTX with the Na_V channels. However, this family still awaits structure–activity data to elucidate the exact key residues [4,24]. It thus seems that PnTx2-1 and the δ -ACTX exert a comparable complex voltage-dependent modulation of Na_V channel gating.

Although both toxins were insecticidal to the larval and adult forms of the housefly [13], PnTx2-5 and PnTx2-6 have never been evaluated for their insecticidal activity towards insect Na_V channels. In fact, it was always believed that *Phoneutria nigriventer* venom fraction 4 (PhTx4) was the venom fraction with the highest and most specific insecticidal activity [6,32]. However, here we show that peptides of PhTx2 fraction have a similar insecticidal potential, at least regarding Na_V channels. PnTx2-1 is the first member of this spider toxin family to be characterized in depth for its activity on insect Na_V channels. The weak species selectivity of PnTx2-1 challenges the suitability of this peptide for the development of novel insecticidal agents.

4. Conclusions

The characterization of PnTx2-1 as a Na_V -channel modulator adds to the expanding knowledge on the *Phoneutria nigriventer* venom. A better understanding of the mechanism of action of its composing venom peptides is important for an effective treatment of *Phoneutria nigriventer* envenomation. This work reports for the first time the activity of a toxin isolated from the *Phoneutria nigriventer* venom fraction 2 (PhTx2) on insect Na_V channels. This observation indicates that besides venom fraction 4, fraction 2 might also be considered as a source of insecticidal peptides.

5. Materials and Methods

5.1. Toxin Purification

Crude venom from *P. nigriventer* was collected from mature male and female spiders maintained in the Scientific Arachnidium at the Fundacion Ezequiel Dias (FUNED) in Belo Horizonte, Brazil (Sisgen: License for Access to Genetic Patrimony Number 010815/2015-5). Toxin PnTx2-1 was purified as previously described [13].

5.2. Electrophysiology

5.2.1. Heterologous Expression in *Xenopus laevis* oocytes

For expression in *X. laevis* oocytes, the plasmids encoding the α -subunits Nav_V1.1–Nav_V1.6, Nav_V1.8, cockroach *Blattella germanica* BgNav_V1.1, *Varroa destructor* VdNav_V1, and the corresponding β -subunits, r β 1, h β 1 and *Drosophila melanogaster* TipE, were linearized with the respective restriction enzymes, mentioned between parentheses, and transcribed using the T7 or SP6 mMACHINE transcription kit (Ambion, Austin, TX, USA). Stage V and VI oocytes were harvested from anesthetized female *X. laevis* frogs, as described previously [33]. Oocytes were injected with 30–50 nL of 1–3 μ g/ μ L Nav_V-channel cRNA using a microinjector (Drummond Scientific, Broomall, PA, USA). The oocytes were then incubated in ND96 solution (in mM: NaCl 96, KCl 2, MgCl₂ 1, CaCl₂ 1.8, HEPES 5), adjusted to pH 7.5 and supplemented with 50 mg/L of gentamycin sulphate and 90 mg/L theophylline, at 16 °C for 1–5 days, until expression of ion channels.

5.2.2. Electrophysiological Recordings

Electrophysiological recordings were performed as described previously [33]. In brief, whole-cell currents from oocytes were recorded at room temperature (18–22 °C) by the two-electrode voltage clamp technique using a GeneClamp 500 amplifier (Molecular Devices, Sunnyvale, CA, USA) controlled by a pClamp data acquisition system (Molecular Devices). Oocytes were placed in a bath containing ND96 solution. Voltage and current electrodes were filled with 3 M KCl, and the resistances of both electrodes were kept between 0.7 and 1.5 M Ω . The elicited currents were sampled at 20 kHz and filtered at 2 kHz using a four-pole, low-pass Bessel filter. To eliminate the effect of the voltage drop across the bath grounding electrode, the bath potential was actively controlled by a two-electrode bath clamp. Leak subtraction was performed using a $-P/4$ protocol. Whole-cell current traces were evoked every 5 s by a 100-ms depolarization to the voltage corresponding to the maximal activation of the Nav_V subtype in control conditions, starting from a holding potential of -90 mV. The oocyte expressing the specific Nav_V-channel isoform with no toxin added to the bath was considered as control. Concentration–response curves were constructed by adding different toxin concentrations directly to the bath solution. The percentage of Nav_V modulation was plotted against the logarithm of the applied concentrations and fitted with the Hill equation:

$$y = 100/[1 + (IC_{50}/[\text{toxin}])] \times h \quad (1)$$

where y is the amplitude of the toxin-induced effect, IC_{50} is the toxin concentration at half-maximal efficacy, $[\text{toxin}]$ is the toxin concentration and h is the Hill coefficient. The amplitude of the toxin-induced effect is obtained by dividing the current amplitude at 30 ms in steady-state toxin situation by the peak current amplitude in control conditions. To investigate the effects on the voltage dependence of activation, current traces were induced by 100-ms depolarizations from a holding potential of -90 to 65 mV with 5-mV increments. To investigate the effects on the steady-state inactivation process, oocytes were depolarized using a standard two-step protocol. From a holding potential of -90 mV, 100-ms prepulses were generated, ranging from -90 to 65 mV with 5-mV

increments, immediately followed by a 100-ms test pulse to 0 mV. Data were normalized to the maximal Na^+ current amplitude, plotted against prepulse potential and fitted using the Boltzmann equation:

$$I_{\text{Na}}/I_{\text{max}} = [(1 - C)/(1 + \exp((V - V_h)/k))] + C \quad (2)$$

where I_{max} is the maximal I_{Na} , V_h is the voltage corresponding to half-maximal inactivation, V is the test voltage, k is the slope factor, and C is a constant representing a non-inactivating persistent fraction (close to zero in control). All data were tested for normality using a D'Agustino Pearson omnibus normality test. Data following a Gaussian distribution were analyzed for significance using one-way ANOVA and the Bonferroni test. Nonparametric data were analyzed for significance using the Kruskal–Wallis and Dunn tests. All data were analyzed using pClamp Clampfit 10.4 (Molecular Devices®), Downingtown, PA, USA, 2003) and Origin 7.5 software (Originlab®, Northampton, MA, USA, 2003) and are presented as mean \pm standard error (SEM) of at least 3 independent experiments ($n \geq 3$).

Author Contributions: Conceptualization, S.P., A.L.B.P., M.R.V.D., M.E.d.L. and J.T.; Methodology, S.P., A.L.B.P., M.N.C., M.H.B.; Software, S.P.; Formal Analysis, S.P. & A.L.B.P.; Investigation, S.P. & A.L.B.P.; Resources, M.R.V.D., M.E.d.L. and J.T.; Data Curation, S.P. & A.L.B.P.; Writing-Original Draft Preparation, S.P. & A.L.B.P. Writing-Review & Editing, S.P., A.L.B.P., M.R.V.D., M.E.d.L. and J.T.; Visualization, S.P. & A.L.B.P.; Supervision, M.R.V.D., M.N.C., M.H.B., M.E.d.L. and J.T.; Project Administration, M.R.V.D., M.N.C., M.H.B., M.E.d.L. and J.T.; Funding Acquisition, M.R.V.D., M.N.C., M.H.B., M.E.d.L. and J.T.

Funding: This work was supported by the following grants: JT was supported by grant CELSA/17/047–BOF/ISP. SP is a PhD fellow supported by CAPES (Coordenação de Aperfeiçoamento de Pessoal de Nível Superior). ME.d.L. was supported by grants from CAPES (Coordenação de Aperfeiçoamento de Pessoal de Nível Superior), CNPq (Conselho Nacional de Desenvolvimento Científico e Tecnológico) and FAPEMIG (Fundação de Pesquisa do Estado de Minas Gerais).

Acknowledgments: The authors thank John N. Wood (University College London, London, UK) for sharing rNaV1.8; A. L. Goldin (University of California, Irvine, CA, USA) for sharing rNaV1.1, rNaV1.2, rNaV1.3, and mNaV1.6; G. Mandel (State University of New York, Stony Brook, NY, USA) for sharing rNaV1.4; R. G. Kallen (Roche Institute of Molecular Biology, Nutley, NJ, USA) for sharing hNaV1.5; K. Dong (Michigan State University, USA) for sharing the BgNaV1.1 and VdNaV1 clones; S. C. Cannon (University of Texas Southwestern Medical Center, Dallas, TX, USA) for sharing the h β 1 subunit and Martin S. Williamson (Rothamsted Research, Harpenden, UK) for providing the Para and tipE clone.

Conflicts of Interest: The authors declare no conflict of interest.

References

- Pineda, S.S.; Undheim, E.A.; Rupasinghe, D.B.; Ikonopoulou, M.P.; King, G.F. Spider venomics: Implications for drug discovery. *Future Med. Chem.* **2014**, *6*, 1699–1714. [[CrossRef](#)] [[PubMed](#)]
- Pineda, S.S.; Chaumeil, P.A.; Kunert, A.; Kaas, Q.; Thang, M.W.C.; Le, L.; Nuhn, M.; Herzig, V.; Saez, N.J.; Cristofori-Armstrong, B.; et al. ArachnoServer 3.0: An online resource for automated discovery, analysis and annotation of spider toxins. *Bioinformatics* **2018**, *34*, 1074–1076. [[CrossRef](#)] [[PubMed](#)]
- Escoubas, P. Molecular diversification in spider venoms: A web of combinatorial peptide libraries. *Mol. Divers.* **2006**, *10*, 545–554. [[CrossRef](#)] [[PubMed](#)]
- Klint, J.K.; Senff, S.; Rupasinghe, D.B.; Er, S.Y.; Herzig, V.; Nicholson, G.M.; King, G.F. Spider-venom peptides that target voltage-gated sodium channels: Pharmacological tools and potential therapeutic leads. *Toxicon* **2012**, *60*, 478–491. [[CrossRef](#)] [[PubMed](#)]
- King, G.F.; Hardy, M.C. Spider-venom peptides: Structure, pharmacology, and potential for control of insect pests. *Annu. Rev. Entomol.* **2013**, *58*, 475–496. [[CrossRef](#)] [[PubMed](#)]
- Peigneur, S.; de Lima, M.E.; Tytgat, J. *Phoneutria nigriventer* venom: A pharmacological treasure. *Toxicon* **2018**, *151*, 96–110. [[CrossRef](#)] [[PubMed](#)]
- Herzig, V.; John Ward, R.; Ferreira dos Santos, W. Intersexual variations in the venom of the Brazilian ‘armed’ spider *Phoneutria nigriventer* (Keyserling, 1891). *Toxicon* **2002**, *40*, 1399–1406. [[CrossRef](#)]
- Bucarechi, F.; Mello, S.M.; Vieira, R.J.; Mamoni, R.L.; Blotta, M.H.; Antunes, E.; Hyslop, S. Systemic envenomation caused by the wandering spider *Phoneutria nigriventer*, with quantification of circulating venom. *Clin. Toxicol.* **2008**, *46*, 885–889. [[CrossRef](#)] [[PubMed](#)]

9. Diniz, M.R.V.; Paiva, A.L.B.; Guerra-Duarte, C.; Nishiyama, M.Y., Jr.; Mudadu, M.A.; Oliveira, U.; Borges, M.H.; Yates, J.R.; Junqueira-de-Azevedo, I.L. An overview of *Phoneutria nigriventer* spider venom using combined transcriptomic and proteomic approaches. *PLoS ONE* **2018**, *13*, e0200628. [[CrossRef](#)] [[PubMed](#)]
10. Diniz, C.R.; Cordeiro Mdo, N.; Junor, L.R.; Kelly, P.; Fischer, S.; Reimann, F.; Oliveira, E.B.; Richardson, M. The purification and amino acid sequence of the lethal neurotoxin Tx1 from the venom of the Brazilian 'armed' spider *Phoneutria nigriventer*. *FEBS Lett.* **1990**, *263*, 251–253. [[CrossRef](#)]
11. King, G.F.; Gentz, M.C.; Escoubas, P.; Nicholson, G.M. A rational nomenclature for naming peptide toxins from spiders and other venomous animals. *Toxicon* **2008**, *52*, 264–276. [[CrossRef](#)] [[PubMed](#)]
12. Figueiredo, S.G.; Garcia, M.E.; Valentim, A.C.; Cordeiro, M.N.; Diniz, C.R.; Richardson, M. Purification and amino acid sequence of the insecticidal neurotoxin Tx4(6-1) from the venom of the 'armed' spider *Phoneutria nigriventer* (Keys). *Toxicon* **1995**, *33*, 83–93. [[CrossRef](#)]
13. Cordeiro Mdo, N.; Diniz, C.R.; Valentim Ado, C.; von Eickstedt, V.R.; Gilroy, J.; Richardson, M. The purification and amino acid sequences of four Tx2 neurotoxins from the venom of the Brazilian 'armed' spider *Phoneutria nigriventer* (Keys). *FEBS Lett.* **1992**, *310*, 153–156. [[CrossRef](#)]
14. Matavel, A.; Fleury, C.; Oliveira, L.C.; Molina, F.; de Lima, M.E.; Cruz, J.S.; Cordeiro, M.N.; Richardson, M.; Ramos, C.H.; Beirao, P.S. Structure and activity analysis of two spider toxins that alter sodium channel inactivation kinetics. *Biochemistry* **2009**, *48*, 3078–3088. [[CrossRef](#)] [[PubMed](#)]
15. Matavel, A.; Cruz, J.S.; Penaforte, C.L.; Araujo, D.A.; Kalapothakis, E.; Prado, V.F.; Diniz, C.R.; Cordeiro, M.N.; Beirao, P.S. Electrophysiological characterization and molecular identification of the *Phoneutria nigriventer* peptide toxin PnTx2-6. *FEBS Lett.* **2002**, *523*, 219–223. [[CrossRef](#)]
16. Catterall, W.A.; Cestele, S.; Yarov-Yarovoy, V.; Yu, F.H.; Konoki, K.; Scheuer, T. Voltage-gated ion channels and gating modifier toxins. *Toxicon* **2007**, *49*, 124–141. [[CrossRef](#)] [[PubMed](#)]
17. Silva, C.N.; Nunes, K.P.; Torres, F.S.; Cassoli, J.S.; Santos, D.M.; Almeida Fde, M.; Matavel, A.; Cruz, J.S.; Santos-Miranda, A.; Nunes, A.D.; et al. PnPP-19, a Synthetic and Nontoxic Peptide Designed from a *Phoneutria nigriventer* Toxin, Potentiates Erectile Function via NO/cGMP. *J. Urol.* **2015**, *194*, 1481–1490. [[CrossRef](#)] [[PubMed](#)]
18. Nunes, K.P.; Cordeiro, M.N.; Richardson, M.; Borges, M.N.; Diniz, S.O.; Cardoso, V.N.; Tostes, R.; De Lima, M.E.; Webb, R.C.; Leite, R. Nitric oxide-induced vasorelaxation in response to PnTx2-6 toxin from *Phoneutria nigriventer* spider in rat cavernosal tissue. *J. Sex. Med.* **2010**, *7*, 3879–3888. [[CrossRef](#)] [[PubMed](#)]
19. Nunes, K.P.; Torres, F.S.; Borges, M.H.; Matavel, A.; Pimenta, A.M.; De Lima, M.E. New insights on arthropod toxins that potentiate erectile function. *Toxicon* **2013**, *69*, 152–159. [[CrossRef](#)] [[PubMed](#)]
20. Alewood, D.; Birinyi-Strachan, L.C.; Pallaghy, P.K.; Norton, R.S.; Nicholson, G.M.; Alewood, P.F. Synthesis and characterization of delta-atracotoxin-Ar1a, the lethal neurotoxin from venom of the Sydney funnel-web spider (*Atrax robustus*). *Biochemistry* **2003**, *42*, 12933–12940. [[CrossRef](#)] [[PubMed](#)]
21. Deuis, J.R.; Mueller, A.; Israel, M.R.; Vetter, I. The pharmacology of voltage-gated sodium channel activators. *Neuropharmacology* **2017**, *127*, 87–108. [[CrossRef](#)] [[PubMed](#)]
22. Wingerd, J.S.; Mozar, C.A.; Ussing, C.A.; Murali, S.S.; Chin, Y.K.; Cristofori-Armstrong, B.; Durek, T.; Gilchrist, J.; Vaughan, C.W.; Bosmans, F.; et al. The tarantula toxin beta/delta-TRTX-Pre1a highlights the importance of the 12 S-S voltage-sensor region for sodium channel subtype selectivity. *Sci. Rep.* **2017**, *7*, 974. [[CrossRef](#)] [[PubMed](#)]
23. Leipold, E.; Hansel, A.; Borges, A.; Heinemann, S.H. Subtype specificity of scorpion beta-toxin Tz1 interaction with voltage-gated sodium channels is determined by the pore loop of domain 3. *Mol. Pharmacol.* **2006**, *70*, 340–347. [[CrossRef](#)] [[PubMed](#)]
24. Nicholson, G.M.; Little, M.J.; Birinyi-Strachan, L.C. Structure and function of delta-atracotoxins: Lethal neurotoxins targeting the voltage-gated sodium channel. *Toxicon* **2004**, *43*, 587–599. [[CrossRef](#)] [[PubMed](#)]
25. Peigneur, S.; Cologna, C.T.; Cremonez, C.M.; Mille, B.G.; Pucca, M.B.; Cuypers, E.; Arantes, E.C.; Tytgat, J. A gamut of undiscovered electrophysiological effects produced by *Tityus serrulatus* toxin 1 on NaV-type isoforms. *Neuropharmacology* **2015**, *95*, 269–277. [[CrossRef](#)] [[PubMed](#)]
26. Leipold, E.; Borges, A.; Heinemann, S.H. Scorpion beta-toxin interference with NaV channel voltage sensor gives rise to excitatory and depressant modes. *J. Gen. Physiol.* **2012**, *139*, 305–319. [[CrossRef](#)] [[PubMed](#)]

27. Rash, L.D.; Birinyi-Strachan, L.C.; Nicholson, G.M.; Hodgson, W.C. Neurotoxic activity of venom from the Australian eastern mouse spider (*Missulena bradleyi*) involves modulation of sodium channel gating. *Br. J. Pharmacol.* **2000**, *130*, 1817–1824. [[CrossRef](#)] [[PubMed](#)]
28. Gunning, S.J.; Chong, Y.; Khalife, A.A.; Hains, P.G.; Broady, K.W.; Nicholson, G.M. Isolation of delta-missulenatoxin-Mb1a, the major vertebrate-active spider delta-toxin from the venom of *Missulena bradleyi* (Actinopodidae). *FEBS Lett.* **2003**, *554*, 211–218. [[CrossRef](#)]
29. Nicholson, G.M.; Willow, M.; Howden, M.E.; Narahashi, T. Modification of sodium channel gating and kinetics by versutoxin from the Australian funnel-web spider *Hadronyche versuta*. *Pflugers Arch.* **1994**, *428*, 400–409. [[CrossRef](#)] [[PubMed](#)]
30. Nicholson, G.M.; Little, M.J.; Tyler, M.; Narahashi, T. Selective alteration of sodium channel gating by Australian funnel-web spider toxins. *Toxicon* **1996**, *34*, 1443–1453. [[CrossRef](#)]
31. Gilles, N.; Harrison, G.; Karbat, I.; Gurevitz, M.; Nicholson, G.M.; Gordon, D. Variations in receptor site-3 on rat brain and insect sodium channels highlighted by binding of a funnel-web spider delta-atracotoxin. *Eur. J. Biochem.* **2002**, *269*, 1500–1510. [[CrossRef](#)] [[PubMed](#)]
32. Paiva, A.L.; Mavel, A.; Peigneur, S.; Cordeiro, M.N.; Tytgat, J.; Diniz, M.R.; de Lima, M.E. Differential effects of the recombinant toxin PnTx4(5-5) from the spider *Phoneutria nigriventer* on mammalian and insect sodium channels. *Biochimie* **2016**, *121*, 326–335. [[CrossRef](#)] [[PubMed](#)]
33. Peigneur, S.; Billen, B.; Derua, R.; Waelkens, E.; Debaveye, S.; Beress, L.; Tytgat, J. A bifunctional sea anemone peptide with Kunitz type protease and potassium channel inhibiting properties. *Biochem. Pharmacol.* **2011**, *82*, 81–90. [[CrossRef](#)] [[PubMed](#)]



© 2018 by the authors. Licensee MDPI, Basel, Switzerland. This article is an open access article distributed under the terms and conditions of the Creative Commons Attribution (CC BY) license (<http://creativecommons.org/licenses/by/4.0/>).

Where cone snails and spiders meet: design of small cyclic sodium-channel inhibitors

Steve Peigneur,^{*,†} Olivier Cheneval,[‡] Mohitosh Maiti,[§] Enrico Leipold,^{¶,1} Stefan H. Heinemann,[¶] Eveline Lescrinier,[§] Piet Herdewijn,[§] Maria Elena De Lima,^{†,||} David J. Craik,[‡] Christina I. Schroeder,^{‡,2} and Jan Tytgat^{*,3}

^{*}Toxicology and Pharmacology, Katholieke Universiteit (KU) Leuven, Campus Gasthuisberg, Leuven, Belgium; [†]Department de Bioquímica e Imunologia, Laboratório de Venenos e Toxinas Animais, Instituto de Ciências Biológicas, Universidade Federal de Minas Gerais, Belo Horizonte, Brazil; [‡]Institute for Molecular Bioscience, The University of Queensland, Brisbane, Queensland, Australia; [§]Laboratory of Medicinal Chemistry, Rega Institute for Medical Research, KU Leuven, Leuven, Belgium; [¶]Department of Biophysics, Center for Molecular Biomedicine, Jena University Hospital, Friedrich Schiller University Jena, Germany; and ^{||}Programa de Pós-Graduação em Ciências da Saúde, Biomedicina e Medicina, Instituto de Ensino e Pesquisa da Santa Casa de Belo Horizonte, Grupo Santa Casa de Belo Horizonte, Belo Horizonte, Brazil

ABSTRACT: A 13 aa residue voltage-gated sodium channel (Na_v) inhibitor peptide, Pn, containing 2 disulfide bridges was designed by using a chimeric approach. This approach was based on a common pharmacophore deduced from sequence and secondary structural homology of 2 Na_v inhibitors: *Conus kinoshitai* toxin IIIA, a 14 residue cone snail peptide with 3 disulfide bonds, and *Phoneutria nigriventer* toxin 1, a 78 residue spider toxin with 7 disulfide bonds. As with the parent peptides, this novel Na_v channel inhibitor was active on Na_v1.2. Through the generation of 3 series of peptide mutants, we investigated the role of key residues and cyclization and their influence on Na_v inhibition and subtype selectivity. Cyclic PnCS1, a 10 residue peptide cyclized *via* a disulfide bond, exhibited increased inhibitory activity toward therapeutically relevant Na_v channel subtypes, including Na_v1.7 and Na_v1.9, while displaying remarkable serum stability. These peptides represent the first and the smallest cyclic peptide Na_v modulators to date and are promising templates for the development of toxin-based therapeutic agents.—Peigneur, S., Cheneval, O., Maiti, M., Leipold, E., Heinemann, S. H., Lescrinier, E., Herdewijn, P., De Lima, M. E., Craik, D. J., Schroeder, C. I., Tytgat, J. Where cone snails and spiders meet: design of small cyclic sodium-channel inhibitors. *FASEB J.* 33, 000–000 (2019). www.fasebj.org

KEY WORDS: voltage-gated sodium channel · peptide cyclization · toxin-based therapeutics · peptide toxin

Voltage-gated sodium channels (Na_v) are integral membrane glycoproteins responsible for the generation and propagation of action potentials in excitable cells. Mutations in genes encoding these channels can lead to a variety of severe illnesses. Na_v channels are considered as potential drug targets for diseases [including pain syndromes, cardiac disorders, and epilepsy (1, 2)] that require

potent and selective Na_v channel inhibitors. *Phoneutria nigriventer*, also known as the Brazilian wandering spider, produces potent venom that is responsible for many of South Brazil's most severe envenomations in humans (3, 4). *P. nigriventer* toxin 1 [PnTx1 [or Mu-ctenitoxin-Pn1a according to the nomenclature suggested by King *et al.* (5)]] is a 78 aa residue peptide comprising 14 cysteine residues. It has been characterized as a Na_v channel blocker with nanomolar affinities for subtype Na_v1.2 (6–9). Recombinantly produced PnTx1 features selectivity toward neuronal Na_v channels with the following rank: Na_v1.2 > Na_v1.7 ~ Na_v1.4 > Na_v1.3 > Na_v1.6 > Na_v1.8 (10). No significant effect was observed for the cardiac isoform (Na_v1.5) and invertebrate channels. PnTx1's inhibitory activity for the Na_v1.7 channels is particularly important because this Na_v channel subtype is essential for the transmission of acute and inflammatory pain signals (10–12). To the best of our knowledge, despite its interesting pharmacologic profile, PnTx1 has never been explored for its therapeutic potential, most likely because large peptides are hard to administer and normally highly immunogenic.

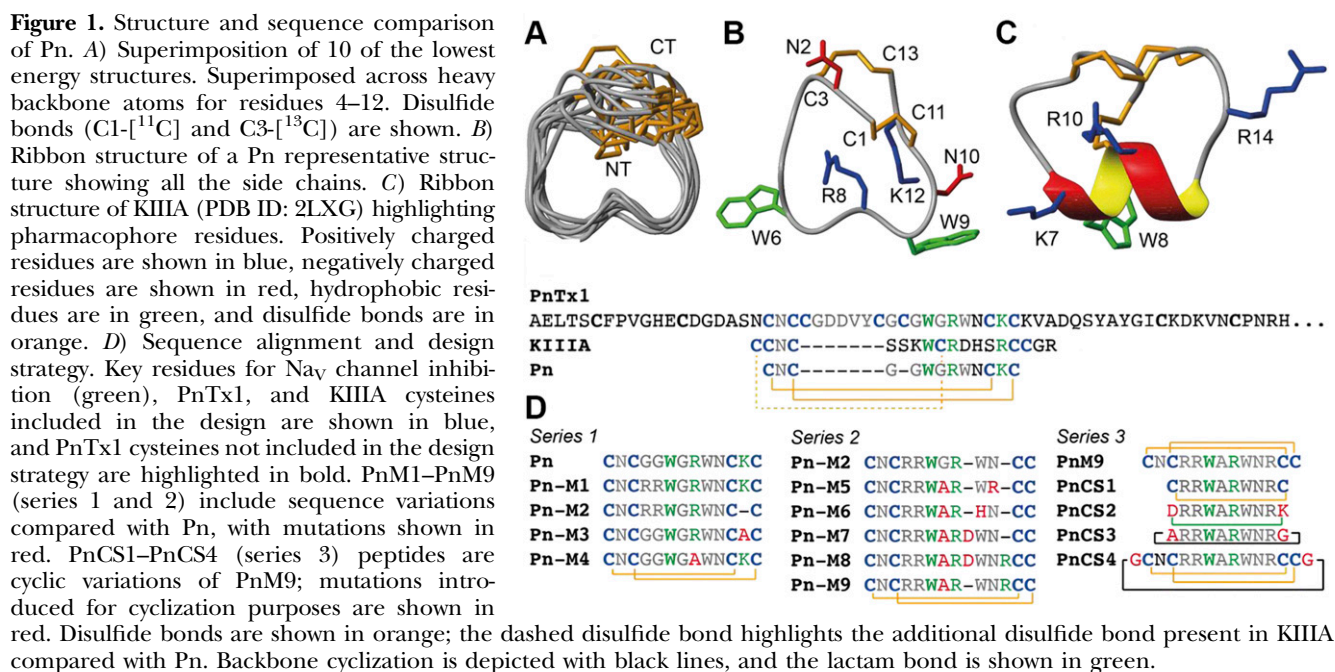
ABBREVIATIONS: 1D, 1-dimensional; 2D, 2-dimensional; DIPEA, *N,N*-diisopropylethylamine; DMF, *N,N*-dimethylformamide; DQF-COSY, double-quantum filtered–correlation spectroscopy; HSQC, heteronuclear single-quantum correlation; KIHA, *Conus kinoshitai* toxin IIIA; Nav, voltage-gated sodium channel; NOE, nuclear Overhauser effect; NOESY, nuclear Overhauser effect spectroscopy; PnTx1, *Phoneutria nigriventer* toxin 1; TOCSY, total correlation spectroscopy; TTX, tetrodotoxin

¹ Current affiliation: Center of Brain, Behavior and Metabolism (CBBM) and Clinic for Anesthesiology and Intensive Care, University of Luebeck, Luebeck, Germany.

² Correspondence: Institute for Molecular Bioscience, The University of Queensland, Brisbane, QLD 4072, Australia. E-mail: c.schroeder@imb.uq.edu.au

³ Correspondence: Toxicology, University of Leuven, Campus Gasthuisberg, PO Box 922, 3000 Leuven, Belgium. E-mail: jan.tytgat@pharm.kuleuven.be

doi: 10.1096/fj.201801909R



an interesting selectivity pattern when screened against a panel of Na_v channel subtypes. A first series of Pn mutants (PnM1–PnM4) and a subsequent second series (PnM5–PnM9) allowed us to pinpoint the key residues important for activity. The remarkable ribbon-shaped and cysteine-stabilized conformation inspired the design of a third series of cyclic peptides incorporating various cyclization strategies, including backbone, lactam bridge, and disulfide bond cyclization, with retained potent activity. These cyclized Na_v channel inhibitor peptides are the smallest cyclic peptides reported to inhibit Na_v channel to date, and they represent promising templates for further development of toxin-based therapeutic agents with improved physiochemical properties.

Design strategy

In the present study, we aimed to design minimized hybrid peptides inhibiting Na_v channels, benefiting from features known to be important for Na_v inhibition of 2 toxins, KIIIA and PnTx1. Alignment of PnTx1 and KIIIA shows that the spacing of key residues of KIIIA (W8, R10, and R14) is conserved in PnTx1 (W33, R35, and K39) (Fig. 1D). Previous research has shown that the first disulfide bridge between Cys1 and Cys9 in KIIIA is removable, almost without affecting the peptides' inhibitory potency on Na_v1.2 and Na_v1.4 (19, 29). Hence, to simplify peptide synthesis, the first disulfide bridge was excluded in our hybrid peptide. This approach resulted in the design of a 13 aa residue peptide with 2 disulfide bridges possessing the central segment of PnTx1 while simultaneously incorporating key residues from KIIIA grafted onto the scaffold of a minimized KIIIA peptide.

Solution structure of Pn

Analysis of 1D and 2D TOCSY, NOESY, DQF-COSY, and ¹H-[¹³C] HSQC NMR spectra shows the formation of a

predominant single set of sharp resonances for the Pn peptide, indicating that it adopts a single conformation in solution. However, additional NOEs were observed for the HE1 protons of the W6 and W9 side chains in the NOESY and TOCSY spectra, albeit with lower intensity, suggesting tryptophan side-chain flexibility and the presence of a minor side-chain conformation.

Resonance assignment was performed by using homonuclear 2D TOCSY, NOESY, and DQF-COSY spectra following the standard assignment protocols as outlined by Wüthrich (30). Assignment of ¹H-[¹³C] HSQC spectra further reconfirmed the homonuclear proton assignments. The geminal methylene protons were not assigned

TABLE 1. Structural statistics for the 20 Pn structures with best MolProbity scores

Structure	MolProbity score
Distance restraint	
Intraresidue	78
Inter-residue	46
Total	124
Dihedral angle restraints	0 (not restrained)
Atomic RMSD (Å) ^a	
Mean global backbone (1–13)	2.89 ± 1.16
Mean global heavy (1–13)	4.35 ± 1.15
Mean global backbone (4–9)	1.41 ± 0.41
Mean global heavy (4–9)	3.31 ± 0.89
MolProbity statistics ^b	
Clash score (>0.4 Å/1000 atoms)	1.61 ± 2.53
Poor rotamers	0.3 ± 0.47
Ramachandran outliers (%)	11.82 ± 7.86
Ramachandran favored (%)	54.09 ± 11.61
MolProbity score	1.91 ± 0.53
MolProbity percentile ^c	75.60 ± 24.16

^aRoot mean square deviation (RMSD). Number ranges between brackets indicate amino acid residue ranges (46). ^bMolProbity (47). ^cOne-hundredth percentile is the best among structures of comparable resolution; 0 percentile is the worst.

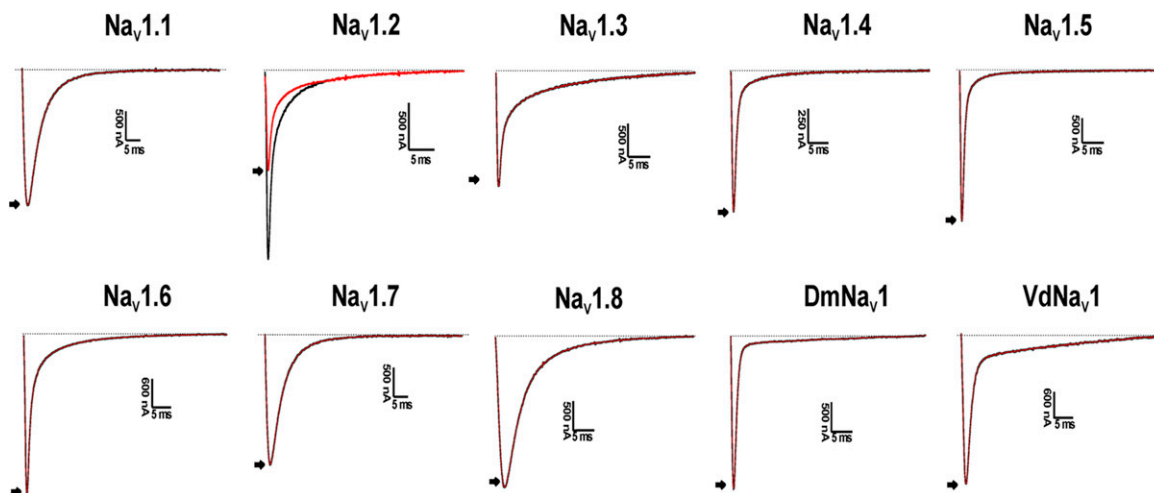


Figure 2. Electrophysiological profile of Pn on Na_Vs. Superimposed current traces for the indicated Na_V isoforms before (black) and after application of 50 μM Pn. Currents were elicited by depolarizing pulses to 0 mV. The arrow indicates the peak current level in the presence of toxin; the dotted line indicates 0 current level.

stereospecifically, and the NOE distance restraints involving these protons were used ambiguously during structure calculation. The solution structure of Pn was calculated by using 124 distance (78 intra-residue and 46 inter-residue) restraints derived from NOESY spectra, including 2 disulfide (C1-[¹³C], C3-[¹³C]) bond restraints. All ³J_{HN-Hα} coupling constant values were between 5.5 and 8 Hz, indicating angular averaging across the Φ dihedrals, reflecting flexibility in the peptide backbone. Therefore, no dihedral restraints were included during structure calculation. Moreover, temperature coefficients (Δδ/ΔT) derived from the chemical shifts of backbone amide protons were -3 to -8 ppb/K, with the one exception being residue [¹³C] with a value of -1 ppb/K. Typically, residues with temperature coefficients less than -4.6 ppb/K are considered shielded and potentially involved in a hydrogen bond. No hydrogen bond acceptors were identified during structure calculations, and thus no hydrogen bond restraints were included in the structure calculations.

Statistical analysis was performed on the final ensemble of 20 lowest energy structures (Fig. 1A and Table 1) of synthetic peptide Pn. The final 20 structures are very flexible, with a backbone and heavy atomic root mean square deviation of 2.89 ± 1.16 and 4.35 ± 1.15, respectively, calculated by using the Molmol program (ETH Zurich,

Zurich, Switzerland). Evaluation of the structure with Procheck (The European Bioinformatics Institute) revealed no bad nonbonded contacts, and the majority of the backbone dihedral angles were within the allowed regions of the Ramachandran plot (3.1% in the disallowed region). A closer assessment of the Pn structures reveals that the peptide backbone adopts a flexible, cyclical ribbon-shaped conformation, having a main disordered loop that is closed by 2 disulfide bonds (C1-[¹³C] and C3-[¹³C]). The structure is devoid of any α-helical or β-turn secondary structural elements. Side-chain orientations for all residues vary considerably within different defined domains.

PnCS1–PnCS4 peptides were analyzed by using 1D ¹H and 2D TOCSY and NOESY spectra. All peptides displayed 1 single conformation evident from 1 set of resonances present for each peptide.

Electrophysiological characterization of Pn and mutants

When screened against a panel of 10 different Na_V channel isoforms (Na_V1.1–1.8, and Na_V insect channels BgNa_V1.1, VNa_V1), 50 μM of Pn selectively inhibited 44.6 ± 2.4% (*n* ≥ 9) of the Na_V1.2 channel (Fig. 2), and a concentration–response

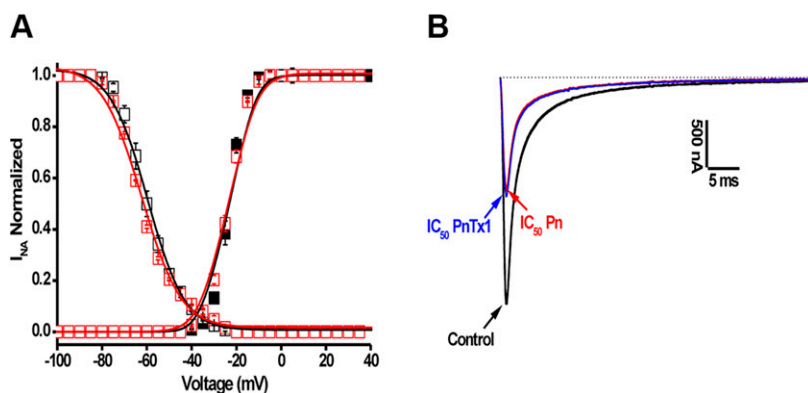


Figure 3. Electrophysiological characterization of Pn on Na_V1.2 channels. A) Steady-state activation and inactivation curves in control (closed symbols) and toxin conditions (50 μM Pn, open symbols). B) Competitive experiments to indicate that Pn binds at site 1. Representative traces are shown in control (1), after application of 35 nM PnTx1 and after subsequent addition of 50 μM Pn.

curve produced an IC_{50} value of $53.7 \pm 3.2 \mu\text{M}$. No shift in the voltage dependence of activation or steady-state inactivation was observed after the addition of $50 \mu\text{M}$ Pn (Fig. 3A). For activation, the observed $V_{1/2}$ values were $-23.4 \pm 0.03 \text{ mV}$ in control conditions and $-23.6 \pm 0.1 \text{ mV}$ after the application of Pn peptide. The steady-state inactivation curves were characterized with $V_{1/2}$ values of $-59.7 \pm 0.4 \text{ mV}$ in control and $-60.3 \pm 0.6 \text{ mV}$ in the presence of Pn. To verify that Pn binds to neurotoxin site 1, competitive binding experiments were performed by using both mother molecules, KIIIA or PnTx1, as competitors. Application of PnTx1 at its IC_{50} value of 35 nM (10) resulted in $48.7 \pm 4.3\%$ ($n \geq 8$) inhibition of the Na^+ peak current. Subsequent addition of IC_{50} concentrations of Pn resulted in no further inhibition (Fig. 3B). Similar experiments, in which the first IC_{50} concentration of KIIIA [60 nM (31)] was applied, followed by subsequent addition of IC_{50} of Pn, also resulted in no additional current reduction (data not shown); these findings indicate that Pn binds to site 1, similar to its parent peptides PnTx1 and KIIIA.

To improve the potency of Pn, we designed a first series of mutants (Series 1) using data available from structure–function studies on KIIIA and other μ -conotoxins (Fig. 1D) (19, 20, 32–36). From this first series of mutants, PnM2 showed the most promising increase in activity when tested on $\text{Na}_V1.2$ – $\text{Na}_V1.6$ (Table 2). Compared with Pn, PnM2 has the G4 and G5 replaced by arginines, and the lysine between the 2 last cysteines has been removed, shortening the peptide by 1 residue. The second series of mutants (series 2) was designed based on the PnM2 sequence. Of these mutants, PnM9 was the most potent (Table 2). In PnM9, Gly7 was replaced by an alanine because a glycine at this position is reportedly unfavorable for Na_V channel activity ($\text{Na}_V1.1$ – $\text{Na}_V1.7$) (37). Furthermore, an extra positive charge in the form of Arg11 was introduced before the C-terminal cysteine. Although PnM9 increased in potency at $\text{Na}_V1.2$ compared with Pn and PnM2, it was less selective and also inhibited the current through $\text{Na}_V1.4$ channels, while being inactive against $\text{Na}_V1.5$ and $\text{Na}_V1.6$ channels (Fig. 4A and Table 2). PnM9 displayed an IC_{50} value for $\text{Na}_V1.2$ channels of $312.4 \pm 12.8 \text{ nM}$ (Fig. 4B).

Considering the close proximity of the N-terminus and the C-terminus in the NMR structure of Pn (Fig. 1A), and the improved potency of PnM9 compared with Pn, a third series of peptides (PnCS1–PnCS4) was designed (Series 3) (Fig. 1D). In PnCS1, the second disulfide bond was removed, and the peptide was cyclized *via* its N- and C-terminal Cys residues, resulting in a 10 aa residue peptide. In PnCS2, the peptide was also shortened with respect to PnM9, and the N- and C-terminal Cys residues were replaced with an Asp and a Lys residue, respectively, and cyclized *via* a lactam bridge; the result was a 10 aa residue peptide. Both PnCS1 and PnCS2 included a C-terminal amidation. PnCS3 was backbone cyclized following the replacement of the N- and C-terminal Cys residues with Ala and Gly, respectively, again leading to a 10 residue peptide, whereas in PnCS4, an additional Gly was introduced in both the N- and the C-terminal and the peptide was backbone cyclized *via* an amide bond, resulting in a 15 residue peptide. Peptides PnCS1–PnCS4 were tested for

TABLE 2. Table with IC_{50} values obtained for PnMI–9 on Na_V channel isoforms included in this study

Peptide	$\text{Na}_V1.2$			$\text{Na}_V1.4$			$\text{Na}_V1.5$			$\text{Na}_V1.6$		
	IC_{50} (μM)	Hill coefficient	Inhibition (%)	IC_{50} (μM)	Hill coefficient	Inhibition (%)	NA	Hill coefficient	Inhibition (%)	IC_{50} (μM)	Hill coefficient	Inhibition (%)
Pn	53.7 ± 3.2	0.9 ± 0.1	85 ± 4	NA	ND	ND	NA	ND	ND	NA	ND	ND
PnM1	6.4 ± 0.2	1.2 ± 0.4	56 ± 5	>100	ND	ND	5.3 ± 0.6	1.3 ± 0.4	74 ± 3	2.2 ± 1.1	1.1 ± 0.2	90 ± 2
PnM2	1.8 ± 0.5	0.9 ± 0.1	90 ± 3	NA	ND	ND	10.4 ± 2.1	$0.9 \pm 0.$	93 ± 3	12.3 ± 1.8	0.8 ± 0.2	84 ± 5
PnM3	NA	NA	NA	NA	NA	NA	NA	NA	NA	NA	NA	NA
PnM4	NA	NA	NA	NA	NA	NA	NA	NA	NA	NA	NA	NA
PnM5	4.2 ± 0.4	1.0 ± 0.1	87 ± 3	8.3 ± 0.8	1.4 ± 0.3	91 ± 3	9.8 ± 1.1	0.9 ± 0.1	84 ± 3	27.4 ± 0.6	1.1 ± 0.1	81 ± 4
PnM6	31.7 ± 2.1	1.3 ± 0.4	68 ± 6	32.4 ± 2.1	0.8 ± 0.1	74 ± 4	>100	ND	ND	>100	ND	ND
PnM7	7.2 ± 0.1	1.0 ± 0.3	88 ± 5	3.1 ± 0.2	1.1 ± 0.2	73 ± 4	8.3 ± 2.1	1.1 ± 0.2	92 ± 2	ND	ND	ND
PnM8	3.7 ± 0.2	0.9 ± 0.3	52 ± 4	2.4 ± 0.1	0.9 ± 0.3	44 ± 2	>100	ND	ND	ND	ND	n.d.
PnM9	0.3 ± 0.01	0.8 ± 0.1	96 ± 2	0.3 ± 0.1	1.0 ± 0.1	95 ± 2	>100	ND	ND	56.3 ± 4.6	1.1 ± 0.1	92 ± 4

IC_{50} values of series 1 mutants on several Na_V channel isoforms. NA, no activity (at $100 \mu\text{M}$), >100 = IC_{50} value estimated >100 μM ; ND, not determined.

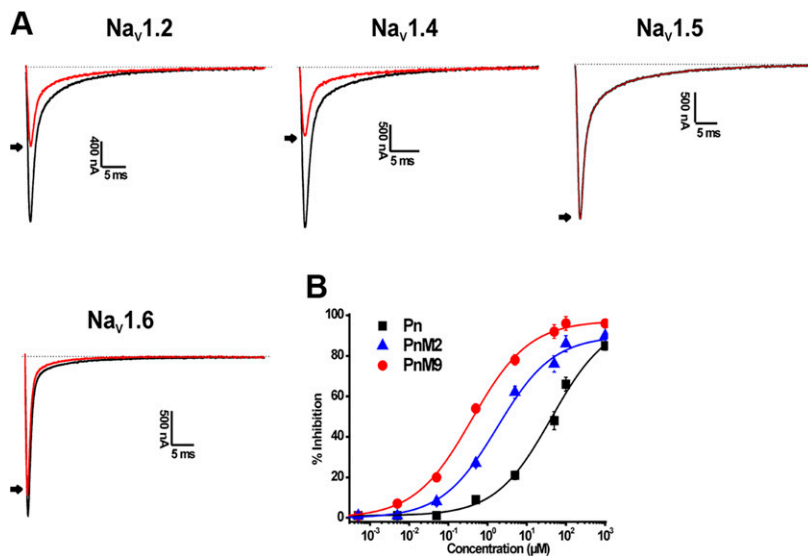


Figure 4. Electrophysiological characterization of PnM9. A) Activity profile of PnM9 on Na_V channel isoforms. Representative whole-cell current traces in control and toxin conditions are shown. The dotted line indicates the 0 current level. The arrow marks steady-state current traces after application of 400 nM peptide. B) Concentration–response curves for $\text{Na}_V1.2$ channels indicating the concentration dependence of the Pn-, PnM2-, and PnM9-induced decrease of the Na^+ peak current.

their activity against 9 vertebrate Na_V channels ($\text{Na}_V1.1$ - $\text{Na}_V1.9_C4$) and 3 invertebrate Na_V channel subtypes ($\text{BgNa}_V1.1$, VdNa_V1 and DmNa_V1) (Fig. 5).

The concentration-dependent inhibitory effect of the PnCS peptides on Na_V channels and IC_{50} values for the 4 cyclic variants are shown in Table 3. Both PnCS2 and PnCS3 exhibited a strong reduction in potency, whereas

PnCS1 and PnCS4 were active, with IC_{50} values in an ~ 3 -fold higher range. PnCS1 was used to further investigate the mechanism by which these cyclic peptides interact with their target. PnCS1, at a concentration of 1 μM , significantly inhibited the current through TTX-sensitive channels ($\text{Na}_V1.1$ - $\text{Na}_V1.4$, $\text{Na}_V1.6$, and $\text{Na}_V1.7$), whereas the TTX-resistant isoforms were less sensitive

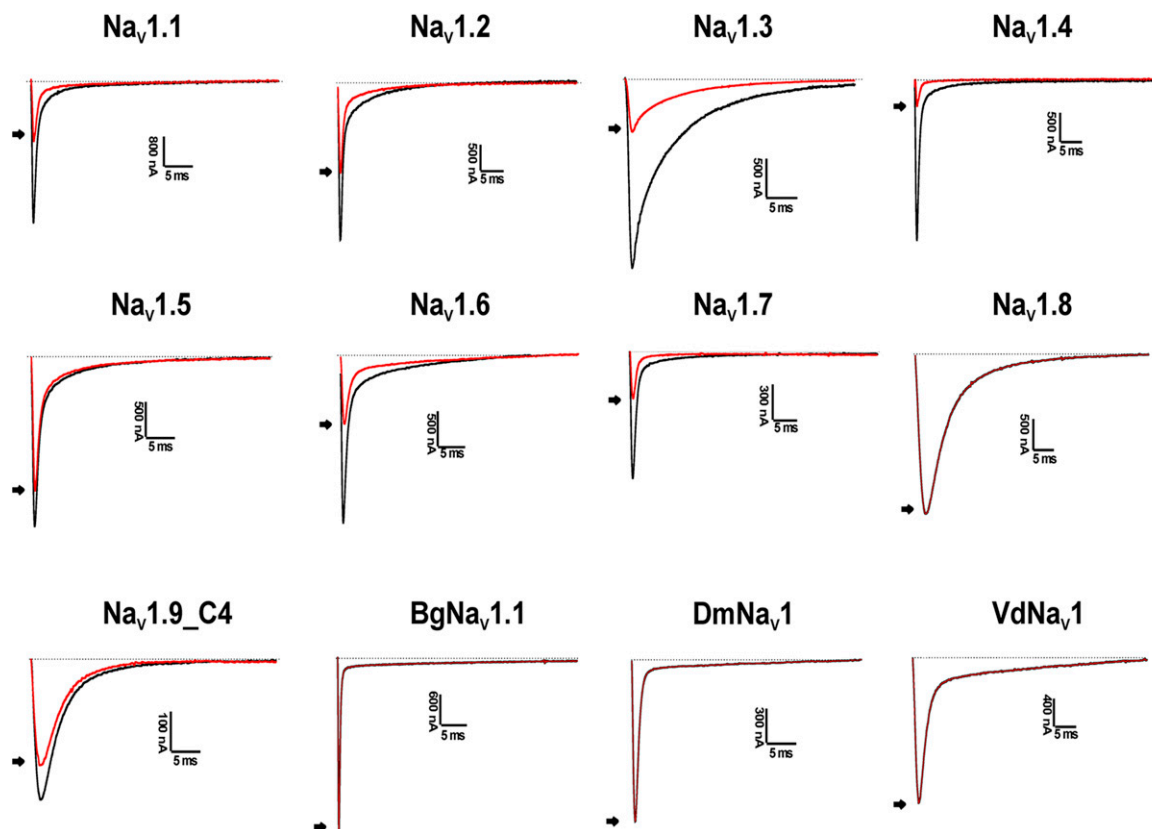


Figure 5. Electrophysiological characterization of PnCS peptides. Activity profile of PnCS1 on Na_V channels. Representative whole-cell current traces in control and toxin conditions are shown. The dotted line indicates the 0 current level. The arrow marks steady-state current traces after application of 1 μM peptide. Black, current trace in control conditions; red, current trace in toxin situation.

TABLE 3. Table with IC₅₀ values obtained for PnCSI-4 on Nav channel isoforms included in this study

Nav channel	PnCSI			PnCS2			PnCS3			PnCS4		
	IC ₅₀ (μM)	Hill coefficient	Inhibition (%)	IC ₅₀ (μM)	Hill coefficient	Inhibition (%)	IC ₅₀ (μM)	Hill coefficient	Inhibition (%)	IC ₅₀ (μM)	Hill coefficient	Inhibition (%)
Nav1.1	0.8 ± 0.1	0.9 ± 0.1	94 ± 3	>100	ND	ND	4.9 ± 0.4	1.2 ± 0.1	89 ± 6	1.1 ± 0.2	1.3 ± 0.14	96 ± 2
Nav1.2	1.0 ± 0.1	0.9 ± 0.2	95 ± 2	>100	ND	ND	5.3 ± 0.3	0.8 ± 0.1	92 ± 1	0.8 ± 0.1	1.0 ± 0.1	93 ± 5
Nav1.3	1.1 ± 0.2	1.1 ± 0.1	94 ± 3	23 ± 1.6	1.4 ± 0.3	48 ± 6	5.4 ± 0.1	0.9 ± 0.2	90 ± 3	2.1 ± 0.6	0.9 ± 0.1	91 ± 3
Nav1.4	0.6 ± 0.2	1.2 ± 0.1	94 ± 2	14.3 ± 1.4	1.1 ± 0.3	62 ± 3	10.7 ± 0.7	1.4 ± 0.2	81 ± 3	0.9 ± 0.2	0.8 ± 0.4	92 ± 5
Nav1.5	2.8 ± 0.6	0.9 ± 0.4	91 ± 4	>100	ND	ND	30.4 ± 4.5	0.8 ± 0.1	64 ± 4	4.5 ± 0.4	1.18 ± 0.2	91 ± 1
Nav1.6	0.7 ± 0.2	0.9 ± 0.3	96 ± 1	>100	ND	ND	4.5 ± 0.7	1.2 ± 0.3	82 ± 4	4.1 ± 0.6	1.10 ± 0.3	93 ± 4
Nav1.7	0.9 ± 0.1	1.1 ± 0.2	90 ± 3	>100	ND	ND	5.7 ± 0.2	0.8 ± 0.3	76 ± 2	3.1 ± 0.2	0.8 ± 0.6	90 ± 2
Nav1.8	>100	ND	ND	>100	ND	ND	>100	ND	ND	>100	ND	ND
Nav1.9_C4	4.5 ± 0.4	0.9 ± 0.1	78 ± 4	>100	ND	ND	23.8 ± 3.5	0.9 ± 0.3	73 ± 4	6.3 ± 0.4	1.4 ± 0.3	64 ± 5
BgNav1.1	NA	NA	NA	NA	NA	NA	NA	NA	NA	NA	NA	NA
VdNav1	NA	NA	NA	NA	NA	NA	NA	NA	NA	NA	NA	NA
DmNav1	NA	NA	NA	NA	NA	NA	NA	NA	NA	NA	NA	NA

Inhibition %, maximum percentage inhibition observed in the presence of 100 μM peptide; NA, not active; ND, not determined.

(Nav1.5 and Nav1.9_C4) or not sensitive (Nav1.8). Nav1.9_C4 is a chimera of Nav1.9, harboring the C-terminus of Nav1.4. Previous research has shown that the C-terminal structure of Nav1.9 limits the heterologous expression in host cells; thus, replacing the C-terminus with the corresponding segment of the Nav1.4 channel allows for functional expression in oocytes (26). Interestingly, this chimera retains the same sensitivity for site 1 blockers as Nav1.9. Nav1.4 channels were used to further characterize the interaction of 1 μM PnCS1 with the channel. Steady-state activation and inactivation curves show that no modulation of Nav channels occurs upon peptide binding (Fig. 6A, B). The midpoint of activation for Nav1.4 did not shift significantly because the V_{1/2} values of activation yielded -27.4 ± 0.1 mV in control and -28.6 ± 0.3 mV in the presence of PnCS1. For the inactivation curves, the V_{1/2} shifted from -59.4 ± 0.6 mV to -57.9 ± 1.4 mV in control and toxin situations, respectively. PnCS1 did not significantly enhance the recovery from inactivation (Fig. 6C). PnCS1 inhibition was found to be voltage independent because no difference in the degree of inhibition was observed over a range of test potentials (Fig. 6D). To investigate the state dependence of inhibition, the following protocol was used. As control, a series of depolarizing pulses was applied to an oocyte expressing Nav1.4 channels. Thereafter, 0.5 μM PnCS1 was added and no pulsing performed for 2 min. This method was followed by a similar series of pulses. A strong degree of delay of inactivation was observed after the 2 min incubation, indicating that the open state is not required for toxin interaction with the channel (Fig. 6E).

Serum stability test

To evaluate whether the designed cyclic peptides acquire increased stability compared with the noncyclized peptides, linear and folded noncyclic peptides (Pn and PnM9) and cyclic peptides (PnCS1-4) were incubated in human serum, and the remaining peptide was quantified by using analytical HPLC (Fig. 7). Linear Pn and PnM9 were fully degraded by proteases in serum within 1 h. The oxidized peptides exhibited higher stability than linear peptides. Nevertheless, after 24 h, folded Pn was completely degraded, whereas only 16% of PnM9 remained. In contrast, the cyclic peptides PnCS1-CS4 were stable in human serum, with 100% of peptide remaining after 24 h.

DISCUSSION

The initial goal of the present study was to identify small cyclic inhibitors for Nav subtypes. We therefore grafted the proposed pharmacophore of PnTx1, a potent Nav channel inhibitor peptide toxin from the Brazilian wandering spider, into the scaffold of KI1A, a potent Nav channel inhibiting peptide isolated from the venom of a cone snail. The resulting peptide, Pn, was investigated for Nav channel inhibition. Competitive binding experiments suggest that Pn competes with its parent peptides, PnTx1 and KI1A, for the same binding site on the Nav channel. It

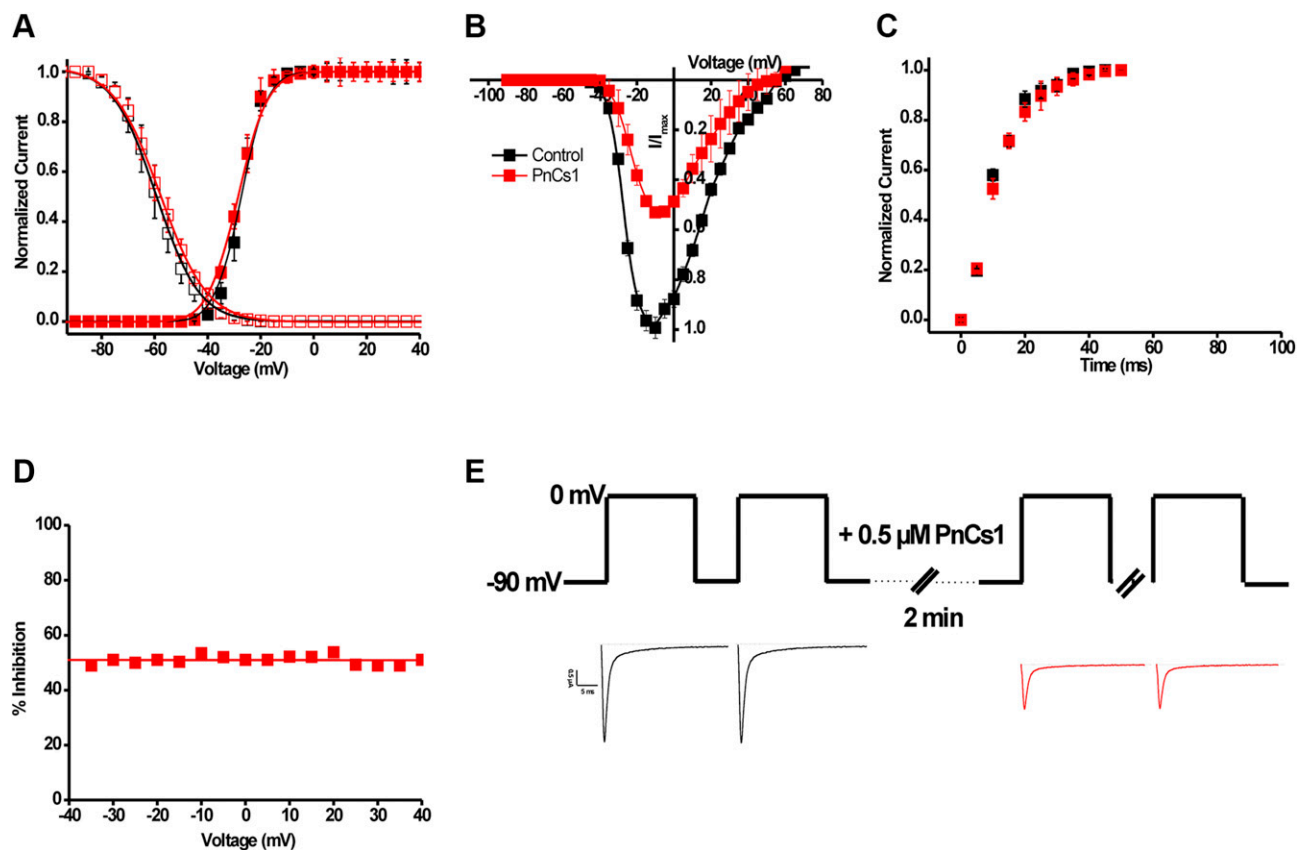


Figure 6. Electrophysiological characterization of PnCS1 on $\text{Na}_V1.4$ channels. *A*) Steady-state activation and inactivation curves in control (black symbols) and toxin ($0.5 \mu\text{M}$ PnCS1, red symbols) conditions. No significant alteration of activation was noted. *B*) Normalized voltage–current relationship. *C*) Recovery from inactivation in control (closed symbols) and in the presence of $0.5 \mu\text{M}$ PnCS1 (open symbols). *D*) Voltage dependence of PnCS1 inhibition. No difference in the degree of inhibition was observed over a range of test potentials. *E*) Investigation of the state dependence of inhibition was performed, and an expected degree of inhibition was observed after the 2-min incubation, indicating that the open state is not required for toxin interaction with the channel.

can thus be assumed that Pn and analogues obstruct the ion flow by binding at the extracellular channel vestibule rather than acting as voltage-sensor modifiers. These results corroborate well with previous studies indicating that PnTx1 and μ -conotoxins compete for the same site as well (6). The solution structure of the Pn peptide was determined by using NMR displaying a highly flexible backbone, and a minor set of peaks were observed for the

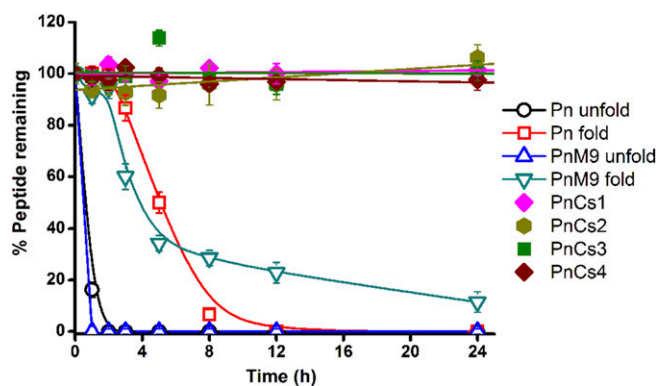


Figure 7. Serum stability assay results. Percentage of peptide remaining in human serum in function of incubation time is shown.

HE1 protons of both Trp residues in the 1D proton NMR spectra, suggesting the presence of a minor conformation.

Next, 2 series of peptide mutants were designed to increase the potency of Pn, resulting first in PnM2 and subsequently in PnM9, the latter displaying nanomolar inhibition at Na_V channel subtypes $\text{Na}_V1.2$ and $\text{Na}_V1.4$. A third series of peptides was designed with the aim to further minimize the peptide scaffold as well as to introduce improved stability of the peptides through various methods of cyclization, including disulfide and lactam bond as well as backbone cyclization. Within the third series of peptides, PnCS1 retained inhibition at submicromolar potency while losing selectivity for $\text{Na}_V1.2$. Cyclization of PnCS1–PnCS4 rendered these peptides highly stable toward degradation when incubated in human serum, compared with linear or oxidized, but not cyclized, peptides in this study, indicating a substantial improvement in their biopharmaceutical properties. However, due to the lack of selectivity for this series of peptides, future structure–function studies are required to obtain peptides with a Na_V channel subtype selective activity. Interestingly, PnCS1, PnCS3, and PnCS4 showed inhibition of $\text{Na}_V1.9_C4$ (albeit in a low μM range), which is an understudied Na_V channel due to difficulties relating to heterologous expression as well as the lack of potent and

- nigriventer predicts the synthesis and processing of a preprotoxin. *J. Biol. Chem.* **268**, 15340–15342
10. Silva, A. O., Peigneur, S., Diniz, M. R., Tytgat, J., and Beirão, P. S. (2012) Inhibitory effect of the recombinant Phoneytria nigriventer Tx1 toxin on voltage-gated sodium channels. *Biochimie* **94**, 2756–2763
 11. Liu, M., and Wood, J. N. (2011) The roles of sodium channels in nociception: implications for mechanisms of neuropathic pain. *Pain Med.* **12**(Suppl 3), S93–S99
 12. King, G. F., and Vetter, I. (2014) No gain, no pain: Nav1.7 as an analgesic target. *ACS Chem. Neurosci.* **5**, 749–751
 13. Tietze, A. A., Tietze, D., Ohlenschläger, O., Leipold, E., Ullrich, F., Kühl, T., Mischo, A., Buntkowsky, G., Görlach, M., Heinemann, S. H., and Imhof, D. (2012) Structurally diverse μ -conotoxin PIIIA isomers block sodium channel Nav 1.4. *Angew. Chem. Int. Ed. Engl.* **51**, 4058–4061
 14. Prashanth, J. R., Dutertre, S., and Lewis, R. J. (2017) Pharmacology of predatory and defensive venom peptides in cone snails. *Mol. Biosyst.* **13**, 2453–2465
 15. Zhang, M. M., Green, B. R., Catlin, P., Fiedler, B., Azam, L., Chadwick, A., Terlau, H., McArthur, J. R., French, R. J., Gulyas, J., Rivier, J. E., Smith, B. J., Norton, R. S., Olivera, B. M., Yoshikami, D., and Bulaj, G. (2007) Structure/function characterization of micro-conotoxin KIIIA, an analgesic, nearly irreversible blocker of mammalian neuronal sodium channels. *J. Biol. Chem.* **282**, 30699–30706
 16. Bulaj, G., West, P. J., Garrett, J. E., Watkins, M., Zhang, M. M., Norton, R. S., Smith, B. J., Yoshikami, D., and Olivera, B. M. (2005) Novel conotoxins from *Conus striatus* and *Conus kinoshitai* selectively block TTX-resistant sodium channels. *Biochemistry* **44**, 7259–7265; erratum: 45, 3116
 17. Zhang, M. M., McArthur, J. R., Azam, L., Bulaj, G., Olivera, B. M., French, R. J., and Yoshikami, D. (2009) Synergistic and antagonistic interactions between tetrodotoxin and μ -conotoxin in blocking voltage-gated sodium channels. *Channels (Austin)* **3**, 32–38
 18. French, R. J., Yoshikami, D., Sheets, M. F., and Olivera, B. M. (2010) The tetrodotoxin receptor of voltage-gated sodium channels—perspectives from interactions with micro-conotoxins. *Mar. Drugs* **8**, 2153–2161
 19. Han, T. S., Zhang, M. M., Walewska, A., Gruszczynski, P., Robertson, C. R., Cheatham III, T. E., Yoshikami, D., Olivera, B. M., and Bulaj, G. (2009) Structurally minimized μ -conotoxin analogues as sodium channel blockers: implications for designing conopeptide-based therapeutics. *ChemMedChem* **4**, 406–414
 20. Khoo, K. K., Feng, Z. P., Smith, B. J., Zhang, M. M., Yoshikami, D., Olivera, B. M., Bulaj, G., and Norton, R. S. (2009) Structure of the analgesic μ -conotoxin KIIIA and effects on the structure and function of disulfide deletion. *Biochemistry* **48**, 1210–1219
 21. Khoo, K. K., Gupta, K., Green, B. R., Zhang, M. M., Watkins, M., Olivera, B. M., Balaram, P., Yoshikami, D., Bulaj, G., and Norton, R. S. (2012) Distinct disulfide isomers of μ -conotoxins KIIIA and KIIIB block voltage-gated sodium channels. *Biochemistry* **51**, 9826–9835
 22. Torres, F. S., Silva, C. N., Lanza, L. F., Santos, A. V., Pimenta, A. M., De Lima, M. E., and Diniz, M. R. (2010) Functional expression of a recombinant toxin - rPnTx2-6 - active in erectile function in rat. *Toxicol* **56**, 1172–1180
 23. Leão, R. M., Cruz, J. S., Diniz, C. R., Cordeiro, M. N., and Beirão, P. S. (2000) Inhibition of neuronal high-voltage activated calcium channels by the omega-phoneytria nigriventer Tx3-3 peptide toxin. *Neuropharmacology* **39**, 1756–1767
 24. Hwang, T. L., and Shaka, A. J. (1998) Multiple-pulse mixing sequences that selectively enhance chemical exchange or cross-relaxation peaks in high-resolution NMR spectra. *J. Magn. Reson.* **135**, 280–287
 25. Spronk, C. A., Linge, J. P., Hilbers, C. W., and Vuister, G. W. (2002) Improving the quality of protein structures derived by NMR spectroscopy. *J. Biomol. NMR* **22**, 281–289
 26. Goral, R. O., Leipold, E., Nematian-Ardestani, E., and Heinemann, S. H. (2015) Heterologous expression of Nav1.9 chimeras in various cell systems. *Pflugers Arch.* **467**, 2423–2435
 27. Liman, E. R., Tytgat, J., and Hess, P. (1992) Subunit stoichiometry of a mammalian K⁺ channel determined by construction of multimeric cDNAs. *Neuron* **9**, 861–871
 28. Chan, L. Y., Gunasekera, S., Henriques, S. T., Worth, N. F., Le, S. J., Clark, R. J., Campbell, J. H., Craik, D. J., and Daly, N. L. (2011) Engineering pro-angiogenic peptides using stable, disulfide-rich cyclic scaffolds. *Blood* **118**, 6709–6717
 29. Stevens, M., Peigneur, S., Dyubankova, N., Lescrinier, E., Herdewijn, P., and Tytgat, J. (2012) Design of bioactive peptides from naturally occurring μ -conotoxin structures. *J. Biol. Chem.* **287**, 31382–31392
 30. Wüthrich, K. (1986) *NMR of Proteins and Nucleic Acids*, Wiley, Chichester, New York
 31. Van Der Haegen, A., Peigneur, S., and Tytgat, J. (2011) Importance of position 8 in μ -conotoxin KIIIA for voltage-gated sodium channel selectivity. *FEBS J.* **278**, 3408–3418
 32. Brady, R. M., Zhang, M., Gable, R., Norton, R. S., and Baell, J. B. (2013) De novo design and synthesis of a μ -conotoxin KIIIA peptidomimetic. *Bioorg. Med. Chem. Lett.* **23**, 4892–4895
 33. Walewska, A., Han, T. S., Zhang, M. M., Yoshikami, D., Bulaj, G., and Rolka, K. (2013) Expanding chemical diversity of conotoxins: peptoid-peptide chimeras of the sodium channel blocker μ -KIIIA and its selenopeptide analogues. *Eur. J. Med. Chem.* **65**, 144–150
 34. Schroeder, C. I., Adams, D., Thomas, L., Alewood, P. F., and Lewis, R. J. (2012) N- and C-terminal extensions of μ -conotoxins increase potency and selectivity for neuronal sodium channels. *Biopolymers* **98**, 161–165
 35. Walewska, A., Skalicky, J. J., Davis, D. R., Zhang, M. M., Lopez-Vera, E., Watkins, M., Han, T. S., Yoshikami, D., Olivera, B. M., and Bulaj, G. (2008) NMR-based mapping of disulfide bridges in cysteine-rich peptides: application to the μ -conotoxin SxIIIA. *J. Am. Chem. Soc.* **130**, 14280–14286
 36. Zhang, M. M., Gruszczynski, P., Walewska, A., Bulaj, G., Olivera, B. M., and Yoshikami, D. (2010) Cooccupancy of the outer vestibule of voltage-gated sodium channels by micro-conotoxin KIIIA and saxitoxin or tetrodotoxin. *J. Neurophysiol.* **104**, 88–97
 37. Lebbe, E. K., Peigneur, S., Brulot, W., Verbiest, T., and Tytgat, J. (2014) Ala-7, His-10 and Arg-12 are crucial amino acids for activity of a synthetically engineered μ -conotoxin. *Peptides* **53**, 300–306
 38. Dib-Hajj, S. D., Black, J. A., and Waxman, S. G. (2015) Nav1.9: a sodium channel linked to human pain. *Nat. Rev. Neurosci.* **16**, 511–519
 39. Leipold, E., Markgraf, R., Miloslavina, A., Kijas, M., Schirmeyer, J., Imhof, D., and Heinemann, S. H. (2011) Molecular determinants for the subtype specificity of μ -conotoxin SIIIA targeting neuronal voltage-gated sodium channels. *Neuropharmacology* **61**, 105–111
 40. Lewis, R. J., Dutertre, S., Vetter, I., and Christie, M. J. (2012) *Conus* venom peptide pharmacology. *Pharmacol. Rev.* **64**, 259–298
 41. Markgraf, R., Leipold, E., Schirmeyer, J., Paolini-Bertrand, M., Hartley, O., and Heinemann, S. H. (2012) Mechanism and molecular basis for the sodium channel subtype specificity of μ -conopeptide CnIIIC. *Br. J. Pharmacol.* **167**, 576–586
 42. Green, B. R., Bulaj, G., and Norton, R. S. (2014) Structure and function of μ -conotoxins, peptide-based sodium channel blockers with analgesic activity. *Future Med. Chem.* **6**, 1677–1698
 43. Akondi, K. B., Muttenthaler, M., Dutertre, S., Kaas, Q., Craik, D. J., Lewis, R. J., and Alewood, P. F. (2014) Discovery, synthesis, and structure-activity relationships of conotoxins. *Chem. Rev.* **114**, 5815–5847
 44. Craik, D. J., Fairlie, D. P., Liras, S., and Price, D. (2013) The future of peptide-based drugs. *Chem. Biol. Drug Des.* **81**, 136–147
 45. Bhardwaj, G., Mulligan, V. K., Bahl, C. D., Gilmore, J. M., Harvey, P. J., Cheneval, O., Buchko, G. W., Pulavarti, S. V., Kaas, Q., Eletsky, A., Huang, P. S., Johnsen, W. A., Greisen, P. J., Rocklin, G. J., Song, Y., Linsky, T. W., Watkins, A., Rettie, S. A., Xu, X., Carter, L. P., Bonneau, R., Olson, J. M., Coutsias, E., Correnti, C. E., Szyperski, T., Craik, D. J., and Baker, D. (2016) Accurate de novo design of hyperstable constrained peptides. *Nature* **538**, 329–335
 46. Koradi, R., Billeter, M., and Wüthrich, K. (1996) MOLMOL: a program for display and analysis of macromolecular structures. *J. Mol. Graph.* **14**, 51–55, 29–32
 47. Davis, I. W., Leaver-Fay, A., Chen, V. B., Block, J. N., Kapral, G. J., Wang, X., Murray, L. W., Arendall III, W. B., Snoeyink, J., Richardson, J. S., and Richardson, D. C. (2007) MolProbity: all-atom contacts and structure validation for proteins and nucleic acids. *Nucleic Acids Res.* **35**, W375–W383

Received for publication September 7, 2018.
Accepted for publication October 22, 2018.